FINAL REPORT

Evaluating the Use of Spatially Explicit Population Models to Predict Conservation Reliant Species in Nonanalogue Future Environments on DoD Lands

SERDP Project RC-2512

AUGUST 2020

Brian Hudgens
Jessica Abbott
Institute for Wildlife Studies

Nick Haddad
Institute for Wildlife Studies
Kellogg Biological Station, Michigan State University

Elsita Kiekebusch
Institute for Wildlife Studies
Kellogg Biological Station, Michigan State University
North Carolina State University

Allison Louthan
Institute for Wildlife Studies
Duke University, Durham, NC
Kansas State University

William Morris
Duke University

Lynne Stenzel
Point Blue Conservation Science

Jeffrey Walters
Virginia Tech

SERDP
DOD · EPA · DOE

REPORT DOCUMENTATION PAGE

Form Approved
OMB No. 0704-0188

Public reporting burden for this collection of information is estimated to average 1 hour per response, including the time for reviewing instructions, searching existing data sources, gathering and maintaining the data needed, and completing and reviewing this collection of information. Send comments regarding this burden estimate or any other aspect of this collection of information, including suggestions for reducing this burden to Department of Defense, Washington Headquarters Services, Directorate for Information Operations and Reports (0704-0188), 1215 Jefferson Davis Highway, Suite 1204, Arlington, VA 22202-4302. Respondents should be aware that notwithstanding any other provision of law, no person shall be subject to any penalty for failing to comply with a collection of information if it does not display a currently valid OMB control number. **PLEASE DO NOT RETURN YOUR FORM TO THE ABOVE ADDRESS.**

1. REPORT DATE *(DD-MM-YYYY)*	2. REPORT TYPE	3. DATES COVERED *(From - To)*
21-08-2020	SERDP Final Report	June 2015 – August 2020

4. TITLE AND SUBTITLE

Evaluating the Use of Spatially Explicit Population Models to Predict Conservation Reliant Species in Nonanalogue Future Environments on DoD

5a. CONTRACT NUMBER
W912HQ-15-C-0051

5b. GRANT NUMBER
RC-2512

5c. PROGRAM ELEMENT NUMBER

6. AUTHOR(S)

Hudgens, Brian; Abbott, Jessica; Haddad, Nick; Kiekebusch, Elsita; Louthan, Allison;
Morris, William; Stenzel, Lynne; Walters, Jeffrey

5d. PROJECT NUMBER   RC-2512

5e. TASK NUMBER

5f. WORK UNIT NUMBER

7. PERFORMING ORGANIZATION NAME(S) AND ADDRESS(ES)

Institute for Wildlife Studies

8. PERFORMING ORGANIZATION REPORT NUMBER

RC-2512

9. SPONSORING / MONITORING AGENCY NAME(S) AND ADDRESS(ES)

Strategic Environmental Research and Development Program
4800 Mark Center Drive, Suite 16F16
Alexandria, VA 22350-3605

10. SPONSOR/MONITOR'S ACRONYM(S)

SERDP

11. SPONSOR/MONITOR'S REPORT NUMBER(S)

RC-2512

12. DISTRIBUTION / AVAILABILITY STATEMENT

DISTRIBUTION STATEMENT A. Approved for public release: distribution unlimited.

13. SUPPLEMENTARY NOTES

14. ABSTRACT

Predicting which species will need ongoing management is valuable for planning and prioritizing natural resource management needs on Department of Defense managed lands. We developed and tested an empirical protocol and theoretical framework for determining if target species are likely to become conservation reliant because of changing climatic conditions. We used time series, space-for-time studies and experimental manipulations to determine climate drivers of demographic rates for seven focal species. We used these relationships and downscaled global climate change models to predict population level changes for each species under future climate scenarios, and developed a process for identifying the importance of different aspects of a species life history in shaping population responses. Three of the 49 populations evaluated across all seven species were projected to respond negatively to projected changes in local climate conditions. Populations most at risk for becoming conservation reliant were those in the warmest parts of the species ranges, while populations in the coolest parts of species ranges tended to benefit from projected changes in climate. The demographic rate most responsible for shaping population responses to projected climate change varied among species and among populations within a species.

15. SUBJECT TERMS

Climate change, conservation, demographic rates, demographic models, non-analogue environmental conditions, mark-recapture, conservation-reliant species

16. SECURITY CLASSIFICATION OF: U			17. LIMITATION OF ABSTRACT	18. NUMBER OF	19a. NAME OF RESPONSIBLE PERSON
a. REPORT U	**b. ABSTRACT** U	**c. THIS PAGE** U	UU	179	Brian Hudgens
					19b. TELEPHONE NUMBER *(include area code)* 707-496-4725

Standard Form 298 (Rev. 8-98)
Prescribed by ANSI Std. Z39.18

Table of Contents

List of Tables

List of Figures

List of Appendices

models. While many of the temperature measures performed similarly or even very slightly better than the intercept only model, the p-values for temperature were always greater than 0.1.

Appendix 8.11 Model selection table for analyses of the effects of climate variable and site differences on hydaspe fritillary adult survival. The climate variables tested include: average daily minimum, maximum, and mean temperature recorded between sample occasions, and total annual (water year) precipitation.

Appendix 8.12 Table showing model results from tadpole survival analysis in the canopy cover experiment.

Appendix 8.13 Non-climate drivers of demographic rates. For fixed effect categorical variables, indicate the coefficient for each categorical variable (note that the missing categorical variable's coefficient is estimated at zero), and for fixed effect numeric variables, we indicate the magnitude of the coefficient. For random effects, we show the standard deviation of the random effect. All numeric predictor variables are scaled, such that the magnitudes of the coefficients are comparable.

List of Acronyms
AIC: Akaike information criterion
AICc: Corrected Akaike information criterion
CCI: Climate contribution index
CI: 95% confidence interval
CJS: Cormack-Jolly-Seber
CRLF: California red-legged frog
CV: Coefficient of variatio
DACS: Duration-amplified cold scores
DIC: Deviance information criterion
DoD: Department of Defense
DPS: Distinct population segment
ED: Environmentally driven
FRI: Fire return interval
GCM: General circulation model
GDD: Growing degree days
IMP: Integral projection model
IUCN: International Union for Conservation of Nature
JBER: Joint Base Elmendorf Richardson
MACA: Multivariate Adapted Constructed Analogs
MODIS: Moderate Resolution Imaging Spectroradiometer
NFS: National Forest Service
NRLF: Northern red-legged frog
PG&E: Pacific Gas and Electric
QAICc: Quasi-binomial corrected Akaike information criterion
SEED: Spatially explicit environmental driver
SERDP: Strategic Environmental Research and Development Program
SNAP: Scenarios Network for Alaska and Arctic Planning group
SVL: snout-vent length
USACE: United States Army Corps of Engineers

UTM: Universal transverse mercator
VIE: Visible implant elastomer

Keywords
Climate change, conservation, demographic rates, demographic models, non-analogue environmental conditions, mark-recapture models, conservation-reliant species

1   Abstract

Introduction and objectives: The Department of Defense (DoD) is responsible for managing threatened, endangered, and rare species inhabiting its properties. Predicting which of these species will need ongoing management due to changing climate conditions is valuable for planning and prioritizing natural resource management needs. We developed and tested an empirical protocol and theoretical framework for determining if target species are likely to become conservation reliant in the future.

Technical approach: We tested the empirical protocol using seven species: hydaspe fritillary butterfly (*Speyeria hydaspe*), Appalachian brown butterfly (*Satyrodes Appalachia*, western snowy plovers (*Charadrius nivosus nivosus*), red-legged frogs (*Rana aurora* and *R. draytonii*), Alaskan doug*lasia* (*Douglasia alaskana*), Venus flytraps (*Dionaea muscipula*) and red-cockaded woodpeckers (*Dryobates borealis*). These species are either special status species or closely related surrogates for special status species managed on or near DoD properties. We used time series or space-for-time data and experimental manipulations to determine how climate influences the demographic rates of each species. We then used these relationships and downscaled global climate change models to build Spatially Explicit Environmental Driver (SEED) models to predict population level changes for each species under future climate scenarios. We also developed another tool, the Climate Contribution Index (CCI) that identifies the relative importance of different aspects of a species life history in shaping population responses to climate change.

Results: Climate influenced demographic rates in numerous and complex ways. In many cases, demographic rates were affected by multiple climate variables, and it was not uncommon for the same climate variable to have opposing effects on different demographic rates. We found that projected population growth rates for our seven study species were typically either unaffected or positively influenced by future climate change. Only three of the 49 populations evaluated across all seven species were projected to have decreasing growth rates under future climate conditions. The populations most at risk for becoming conservation reliant due to climate change were those in the warmest parts of the species ranges. On the other hand, populations in the coolest parts of species ranges tended to benefit the most from projected changes in climate. Like the responses themselves, the demographic rate most responsible for shaping population responses to projected climate change varied among species and among populations within a species.

Benefits: This project provides three main benefits to the DoD and other federal and nonfederal land managers. First, we identified many of the obstacles that need to be overcome when determining if a species is likely to be negatively (or positively) affected by projected changes in climate. Second, we developed and demonstrated the use of two tools to overcome those challenges. Both SEED models and CCI incorporate climate-demographic relationships throughout a species' life cycle to: 1) predict how a species will respond to non-analogue climate conditions, and 2) to provide insight into which stages of the life cycle play shape that response. These tools can be used to prioritize future species management needs and evaluate potential mitigation actions. Third, we identified that many North American species will likely not require more intensive conservation efforts due to climate change. Management priorities aimed at existing threats, such as mitigating habitat destruction or invasive species are recommended. However, populations on the warmer edges of species ranges, particularly species with a large latitudinal or altitudinal range, are at greater risk, and thus should be evaluated more carefully.

2 Executive Summary

2.1 Introduction

In recent decades, climate change has had a negative impact on many species through changes in phenology (Walther et al. 2002, Parmesan and Yohe 2003, Chen et al. 2011) and demographic rates (Saether et al. 2000, Radchuk et al. 2013, Urban et al. 2016). The magnitude and multitude of changes associated with climate change pose several challenges to long term planning for wildlife management and endangered species conservation. Many species are currently conservation reliant, requiring ongoing, intensive management to persist. Even those that currently need only minimal or one-time management may become conservation reliant in the future (Scott et al. 2010). Long-term planning would benefit from knowing which species will be influenced by climate change and which species will require more, or less, intensive management given future environmental conditions.

The difficulty in this challenge is that not all species will respond to climate change in the same way, as specific demographic rates (e.g. survival to reproductive age/stage classes, fecundity) have different optimal environmental conditions, which could result in little, or even positive, change to population growth with changing conditions (Deutsch et al. 2008). Furthermore, relationships between climate variables and demographic rates may be nonlinear (Doak and Morris 2010). Thus, predicting how populations will be affected by non-analogue future climate conditions is particularly difficult based on field observations alone. Instead, such predictions generally require population models to integrate changes in multiple demographic rates. Determining the overall impact of climate change on population growth requires integrating the effects of changing temperatures (and other climate drivers) over all life stages in an environmentally driven (ED) population model. Relationships between climate variables and demographic rates are typically measured using three possible approaches: 1) time series: using annual variation in climate and long-term demographic data from a single location, 2) space-for-time: measuring demographic rates across populations currently experiencing different climates (requires fewer years of data), and 3) experimental: measuring demographic rates under a range of controlled climate conditions.

In addition to integrating climate-demographic rate relationships across a species' life cycle, predictive models need to account for one or more spatial processes. First, projected climate variables used to determine demographic rates of different populations of a species are specific to the locations occupied by those populations. Second, for many species, migration or dispersal among different locations is a relevant factor influencing the modeled population(s), and the resulting redistribution of individuals in space must be tracked within the model. Consequently, models should be Spatially Explicit (SE). We developed Spatially Explicit Environmental Driver (SEED) models for a range of species. SEED models are a powerful tool because they: 1) allow researchers to explore combinations of environmental variables not currently seen but likely to be encountered in the future (non-analogue environments); 2) can include numerous scenarios to account for uncertainty in future environmental conditions; 3) accommodate influences of both local environmental conditions and surrounding landscape features; and 4) can be evaluated at multiple time steps to inform predictions about transient dynamics in a non-stationary world.

2.2 Objectives

The goal of this project was to develop and test an empirical protocol and theoretical framework for determining if target species are likely to become conservation reliant as global

climate change creates novel environments in and around DoD lands. Specifically, we: 1) used downscaled global climate change models (GCMs) to predict plausible temperature and water regimes faced by managed species on military lands; 2) used time series or space-for-time data and experimentally created non-analogue environments to determine how demographic rates for a suite of species are expected to change given future predicted temperature and precipitation regimes; 3) built Spatially Explicit Environmental Driver (SEED) models to predict population level changes expected to occur under non-analogue environmental conditions predicted to be present in the future; and 4) compared SEED model population dynamic predictions across species to explore characteristics that might make species or populations more likely to be negatively impacted by climate change. In addition, we developed a metric integrating both the sensitivity of demographic rates to projected changes in climate conditions and influence of those same demographic rates on population growth rates, the Climate Contribution Index (CCI) to measure the contribution of different life stages to population response to climate change.

2.3   Technical Approach

We studied seven species of animals and plants: hydaspe fritillary butterfly (*Speyeria hydaspe*), Appalachian brown butterfly (*Satyrodes Appalachia*), western snowy plovers (*Charadrius nivosus nivosus*), red-legged frogs (*Rana aurora* and *R. draytonii*), Alaskan douglasia (*Douglasia alaskana*), Venus flytraps (*Dionaea muscipula*) and red-cockaded woodpeckers (*Dryobates borealis*). For the butterfly, frog, and plant species we collected demographic data from populations that varied in current climate conditions (space-for-time approach). For the two bird species we used previously collected demographic data from long term (>20 yrs) studies (time series approach). For the two butterfly species and the frogs we also conducted controlled experiments where we pushed climate conditions beyond those currently experienced at our field sites. These experiments allowed us to compare results in a controlled manipulation to those from the field in order to validate our field results. We also manipulated non-climate related variables for some species in order to examine the potential impacts of habitat and antagonistic interactions with other species on climate responses by our focal species. For each animal species we evaluated: the influence of climate on the following vital rates: fecundity, egg hatch rates, larval/juvenile survival, and adult survival. For the two plants we evaluated: seed production, germination rate, and size specific survival and growth rates. Study locations for each species can be found in Figure 2.3-1.

For each species we used our measured climate-demographic rate relationships in combination with climate projection models to develop SEED models. SEED Models can project how populations would be impacted by predicted changes in local climates. These SEED models are defined by two salient characteristics. First, year to year changes in population size are predicted from a set of equations describing the relationship between demographic rates and relevant climate variables. In each future year, the predicted demographic rates change with the projected values of the climate variables on which they depend. Second, the models are spatially explicit. Projected climate variables used to determine demographic rates of different populations of a species are specific to the locations occupied by those populations. If migration or dispersal among different locations is a relevant factor influencing the modeled population(s), the resulting redistribution of individuals in space is tracked within the model.
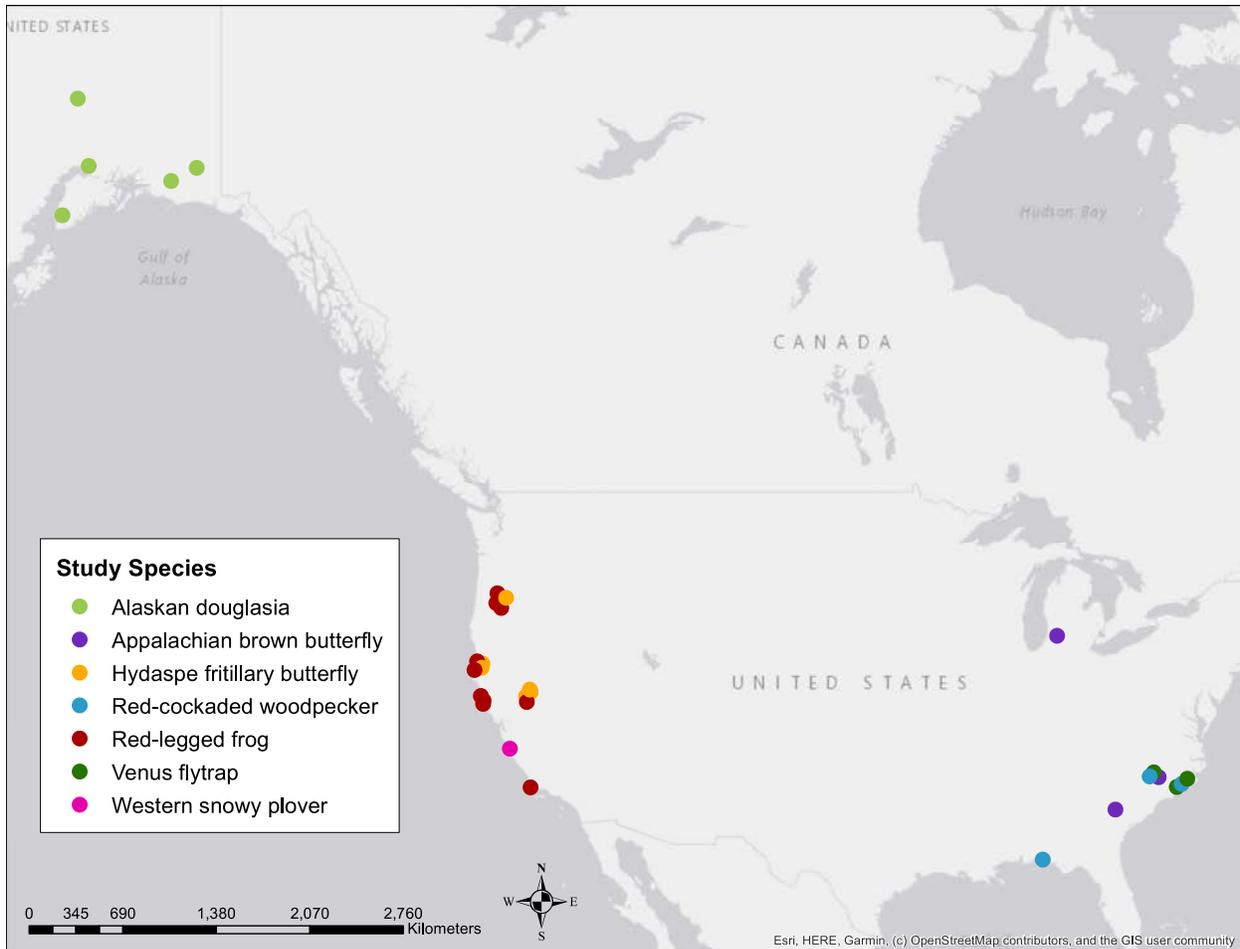
Figure 2.3-1. Locations of study populations for each species. Circles mark population locations and are color-coded by species.

Each SEED model includes six primary components. The first component is the location of each modeled population in the landscape, which allows each population to be linked with the proper downscaled climate projections. This also allows inter-site distances to be calculated for distance-based estimates of dispersal and/or migration probabilities. If there are non-climate related site-specific differences in demographic rates, this information is included in the landscape information. The second component is the relevant downscaled climate projection data. For populations outside of Alaska, we used projections that employed the Multivariate Adaptive Constructed Analogs (MACA) (Abatzoglou, Brown, 2011) method to downscale projections from the RCP8.5 Emissions Scenario for 20 global climate models to a 4 km^2 resolution. For populations of Alaskan douglasia, we used estimates of monthly temperature and precipitation for Emissions Scenario RCP8.5 from the CMIP5/AR5 models from the Scenarios Network for Alaska and Arctic Planning group (SNAP). The third component is the set of functions used to calculate all demographic rates expected for each population during each time step given its location and projected climate conditions. This step varies substantially from model to model, depending on each species' life history and how it is influenced by different climate variables. The fourth component is the integration of demographic rates across the life cycle to calculate changes in population size from year to year in each population. The fifth component is dispersal and/or migration as appropriate. This component is intertwined with the

5

previous component, with the timing of spatial redistribution due to dispersal/migration relative to other demographic rates dependent on each species' life history. The final component is SEED model output, which is a record of the numbers of individuals at each population in each stage during each time step.

2.4   Results and Discussion

Most species we studied were affected by multiple climate drivers, with strong nonlinear effects in some cases (Figure 2.4-1). Our study species with the most complex life histories had no fewer than nine different climate variables impacting demographic rates. Only Appalachian brown butterflies were influenced by a single climate variable (mean temperature during the life-stage), but there was a threshold effect in both egg hatch rates and larval survival. In fact, without experimentally elevating temperatures above those experienced at Fort Bragg during our study, we would not have detected these thresholds. As a consequence, we would have not been able to predict the reduction in egg or larval survival in the non-analogue climate conditions projected to be the new normal within the next decade.
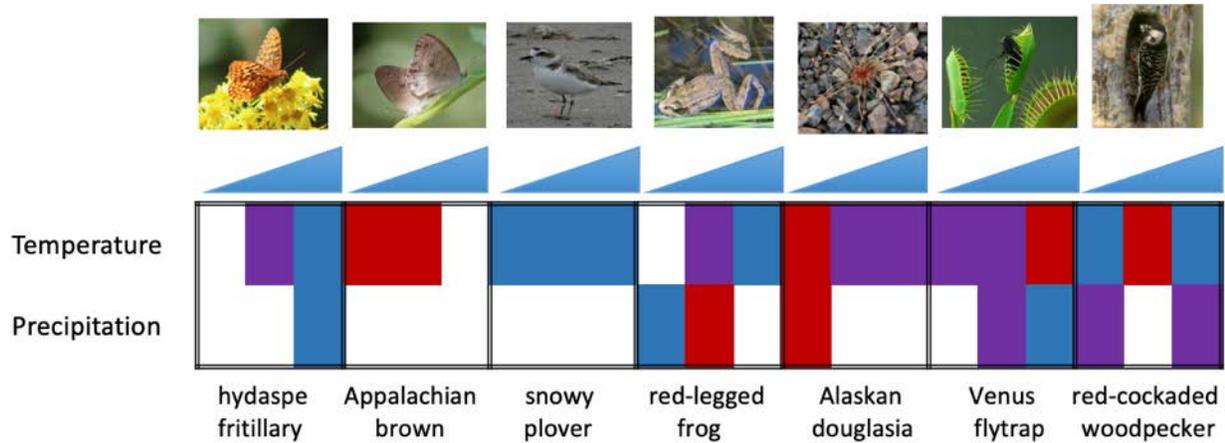
Figure 2.4-1. Summary of temperature and precipitation effects on demographic rates of the seven study species. Color coding shows positive (blue), negative (red) and mixed (purple) effects of increasing either temperature or precipitation on egg production and survival (left-most column for each species), larval survival or plant growth (middle column for each species) and adult survival (right-most column for each species). Mixed effects include quadratic nonlinear terms, different effects during different times of year and different effects on different demographic rates aggregated to these summary life stages (e.g., small tadpole survival, large tadpole survival, and froglet survival all contribute to red-legged frog juvenile survival in this figure).

We found contrasting effects of climate across different life stages for most our study species. Only for the Appalachian brown butterfly and western snowy plover were the effects of climate on demographic rates all in the same direction. Opposing effects of climate across demographic rates may serve as a buffer, reducing the overall impacts of climate change on population growth rates (Doak and Morris 2010). This buffering effect likely contributed to the lack of effects of climate on population growth rates in some of our study species. For example, in red-cockaded woodpeckers increasing temperatures decreased post-fledging survival but increased adult survival. Likewise, in Alaskan douglasia increasing temperatures negatively affected reproductive demographic rates but increased survival and growth.

We found temperature to be a factor in every demographic rate that was sensitive to climate except for the clutch size of the first nest and probability of double brooding in red-cockaded woodpeckers and fecundity in re-legged frogs. In general, we found more negative

6

impacts of warming on early life stages. Warming reduced post-fledging survival in red-cockaded woodpeckers, and in Appalachian brown butterflies the only demographic rate not negatively impacted by temperature was adult survival. With the exception of the Venus flytrap, survival of the adult/plant life stage of all the species we studied either benefited or was unaffected by increased temperatures. Temperature-driven phenological shifts also acted to buffer the effects of climate change. For the Appalachian brown butterfly this shift led to an additional generation. Adding this generation into our SEED models improved population growth rates, although not enough to prevent future population declines.

Most projected population growth rates in our study were unaffected or positively influenced by future climate change (Figure 2.4-2). Of the 49 different populations we evaluated, only 3 (6.1%) are projected to have lower future population growth rates due to climate change. Positive effects of climate change on growth rates may seem unexpected, but this result is consistent with predictions for ectotherms in temperate regions, where species typically have broad thermal tolerances and often experience temperatures that are below their thermal optimum. Warming is generally expected to increase fitness of ectotherms living at higher latitudes, while for ectotherms living near their thermal optimum at lower latitudes, even moderate warming could have negative impacts on population growth rates as fitness typically drops steeply at temperatures above the thermal optimum (Deutsch et al. 2008, Angilletta 2009). This suggests that populations closer to the southern periphery of their range would be most at risk from warming temperatures, which is what we observed. All three populations projected to be adversely affected by climate change, Appalachian brown butterflies at Fort Bragg, NC and the two California red-legged frog populations at Vandenberg Air Force Base, are at the southern end of their species ranges (Figure 2.4-2). Among the remaining populations, there was a general trend for populations at warmer locations to respond less favorably to projected warming conditions than populations at cooler locations. This pattern held true not only for the ectotherm animals in our study, but also for snowy plovers. It is not obvious for Alaskan douglasia whether the southern or northern population currently experiences warmer conditions, because the northern population is closer to the coast and buffered from temperature extremes.
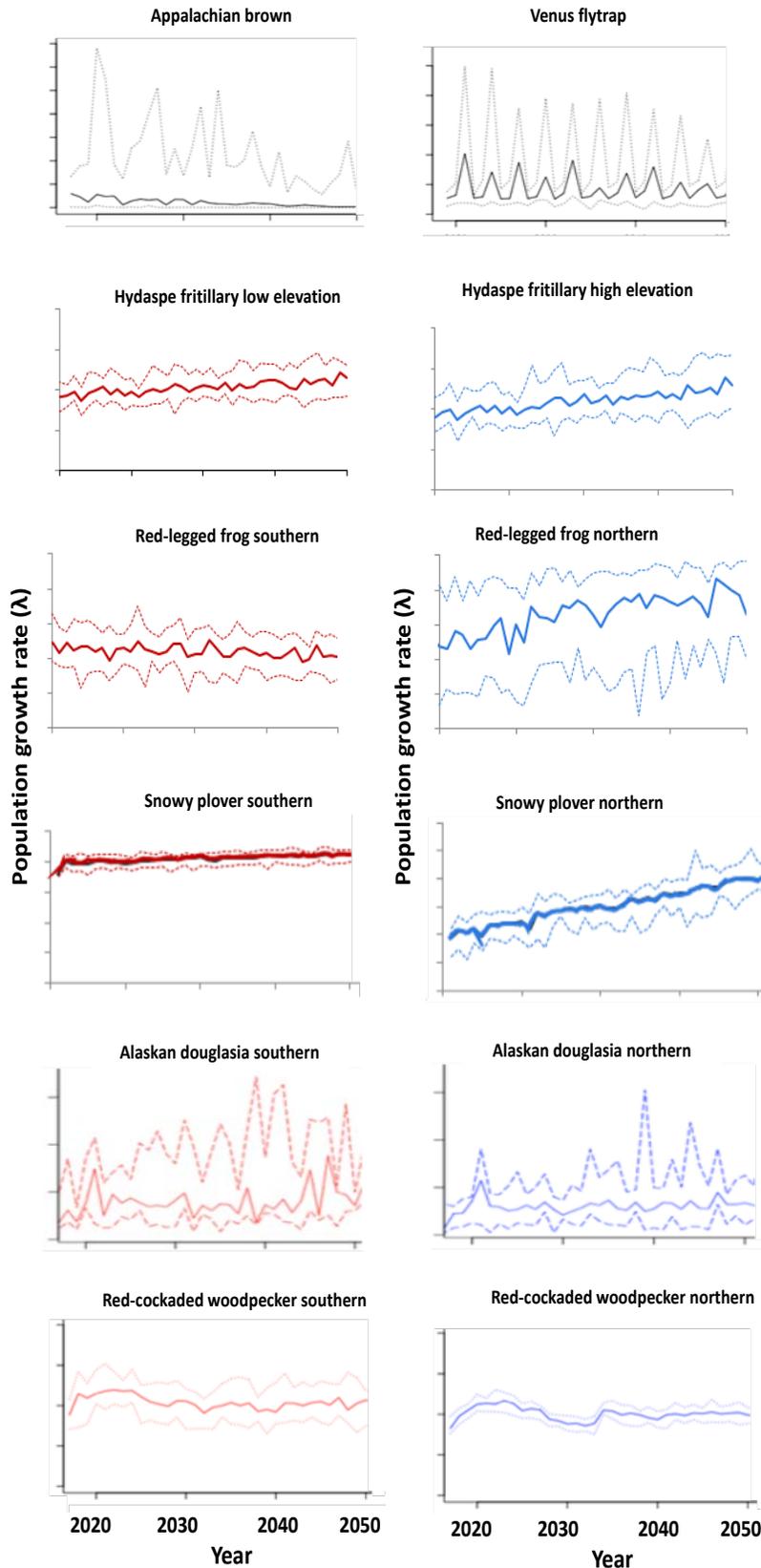
Figure 2.4-2. SEED model projections for annual discrete population growth rates (λ) for all study species. Dark solid lines show the median projected annual growth rate from SEED model runs linked to projected climate data from 5-20 downscaled global climate models. Dashed light lines show the 5th (bottom) and 95th (top) percentile of projected annual growth rates. For the Appalachian brown butterfly and Venus flytrap we ran a single model based on data from all populations on Fort Bragg. For the other species we created at least two models from different populations across sites that varied in climate. For species with more than one model we present the results from the most southern and northern (or lowest and highest elevation for the hydaspe fritillary butterfly) populations that we studied. Southern (or low elevation) population growth rate projections are in red and northern (high elevation) are in blue.

Based on our SEED model results, two of our study species appear to be exceptions to this pattern, Venus flytrap and red-cockaded woodpecker. Both of these species occupy a smaller latitudinal range (spanning 10° or less) than the butterflies, red-legged frogs, or snowy plover, each of which have species ranges spanning at least 15° of latitude. The narrow distribution of Venus flytrap and red-cockaded woodpecker is clearly linked to specialized habitat requirements unrelated to climate. While our SEED models suggested little difference between the response of red-cockaded woodpecker populations to climate change in the northern and southern portions of their range, previous work has found evidence that this species may be more susceptible to climate change at the southern end of its range. Garcia 2014 and DeMay and Walters 2019 found that red-cockaded woodpecker productivity was high and increasing in the northeastern portion of the range, but low and decreasing in the southwestern portion. Two of the populations we analyzed for the SEED model are located at the northeastern edge of the species' range (Lejeune, Sandhills), and one is located in the southwestern portion of the range (Eglin). Our modeling of relationships of demography to climate in red-cockaded woodpeckers was driven more by the large samples available from the two northern populations than the small samples from the southern one, which may account for the similar projections across populations.

We did not find a general pattern relating climate effects on any particular life stage to climate change effects on future population growth. For example, negative effects of warming temperatures on tadpole survival rates had a strong influence on the coastal California red-legged frog populations, contributing to future declines in projected population growth at these sites. In contrast, reduced tadpole survival in northern red-legged frogs is more than offset by gains in adult survival, leading to increasing projected population growth rates. The demographic rate contributing the most to a population's response to climate change did not necessarily correspond to the rate most heavily affected by differences in climate conditions nor to the rate with the greatest influence population growth rates (Figure 2.4-3). Instead, the demographic rates that tended to be the best predictors of population responses were those that were both relatively sensitive to climate conditions and had a relatively large influence on population dynamics. Identifying these demographic rates *a priori* is problematic, because there is an inherent tradeoff between the demographic rate variability and elasticity (Pfister 1998, Morris and Doak 2004).
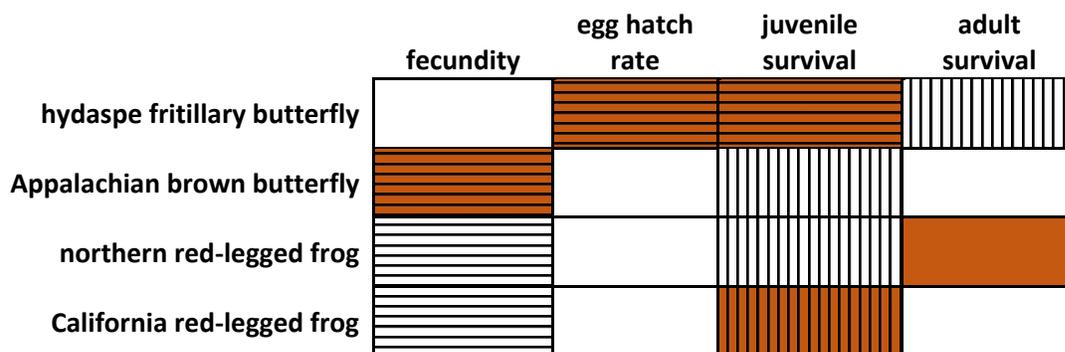
Figure 2.4-3. Demographic rates predicted to change the most due to differences in climate conditions (horizontal lines), have the highest demographic sensitivity (vertical lines) and have the largest CCI score (filled) for two butterfly species and two frog species. For Appalachian brown butterflies the highest climate sensitivity and demographic rate sensitivity are associated with first generation demographic rates while the largest CCI score is associated with fecundity in the second generation. Northern red-legged frog demographic rate elasticities differed from sensitivities with adult survival having the highest elasticity.

We found evidence of indirect effects of climate mediated through interactions with other species. Temperature strongly influence hydaspe fritillary butterfly egg survival by increasing daily egg predation rates by 46% per one °C warming. While we did not measure it directly, we suspect that the quality of both host and nectar plants could influence hydaspe fritillary demographic rates. Nectar availability has been linked to fecundity in related species (Boggs and Ross 1993), and host plant quality likely influences larval survival. Early snow melt can reduce floral resources (Inouye 2008), and violets, the hydaspe fritillary's host plants, require moist conditions and are negatively impacted by droughts. Temperature driven changes in phenology and development rates also have the potential to impact population growth rates through interactions with other species or processes. For example, the increased development rates we found with warming for hydaspe fritillary butterfly and red-legged frog eggs and larvae could reduce predation rates by reducing exposure of vulnerable life stages to predators. In hydaspe fritillary butterflies this reduced exposure time could mitigate some of the effects of warmer temperatures increasing the daily egg predation rates. Red-legged frog breeding phenology and egg/larvae development rates might also interact with canopy cover to affect the amount of shading to which these early life stages are exposed.

2.5   Implications for Future Research and Benefits

SEED models and the Climate Contribution Index are useful tools for predicting whether expected changes in future climate conditions will exacerbate or mitigate threats to special status species managed on DoD lands. These predictions provide useful information for planning future management needs. For example, our study included two military bases, Fort Bragg, NC and Vandenberg Air Force Base, CA, with managed species predicted to have different responses to projected climate change in the coming decades. On Fort Bragg, both red-cockaded woodpeckers and Venus flytrap populations are expected to be buffered from changing climate conditions, whereas warming temperatures are expected to cause Appalachian brown butterfly populations there to switch from sources to sinks. At Vandenberg Air Force Base, snowy plover populations are predicted to benefit from warming spring temperatures and milder winters along the west coast, while California red-legged frogs are predicted to do worse. Looking ahead, what this means is that Fort Bragg may want to plan now for mitigation projects to reduce the impacts of expected warming on Appalachian brown butterflies. Such mitigation may come in the form of habitat restoration focused on providing greater shade coverage while continuing to support robust host-plant coverage, or tactics to reduce predation on eggs and larvae to offset reduced survival during these stages associated with warmer temperatures. For Vandenberg Air Force Base, this means potentially devoting more resources to California red-legged frog protection (e.g., through bullfrog removal at breeding sites). In contrast, future budgeting needs for snowy plovers, or for red-cockaded woodpeckers and Venus flytraps, should be determined by mitigation requirements for non-climate threats. We note here that climate does play a role in critical management issues for all three species, fire frequency for red-cockaded woodpeckers and Venus flytraps and sea-level rise for snowy plovers.

The populations of special status species most likely to be vulnerable to climate change in our study were wide-ranging species at the climatic edges of their ranges (i.e., these are most likely to become conservation reliant because of climate change). We note that climatic edges are not necessarily the same as the geographic periphery of a species range, as is evidenced by multi-directional shifts in avian species ranges in Britain (Gillings et al. 2015) and in presumed bioclimatic envelopes in the United States (Bateman et al. 2016). The mismatch between

climatic edges and geographic periphery may be due to landforms influencing temperatures or precipitation patterns, differences in the latitudinal and longitudinal directionality of temperature and precipitation patterns, and spatial patterns of extreme climate events. Another important climatic edge may be where winter precipitation occurs primarily as snow versus rain. For example, even though red-legged frogs occupy habitats with and without significant snowfall, we found that the relationship between adult survival and temperatures observed in populations without snowfall are not consistent with sustainable populations in places with snowfall. Differences in the timing of breeding between inland and coastal sites likely reflect strategies for avoiding colder winter weather by inland populations; similar patterns have been observed for populations of Ambystoma salamanders breeding in Massachusetts vs North Carolina (Petranka 1989). The transition from winter snow to rain has been shown to increase thermal stress and even to lead to complete reproductive failure in some winter breeding birds (Wingfield et al. 2017, 2011; Shipley et al. 2019). Changes in the timing of snowmelt are also associated with different coping strategies in mammals (Sheriff et al. 2017) and the flowering phenology of nectar plants, and consequently the length of butterfly flight periods (Section 5.1.1).

We were surprised at the rarity of climate-related reductions in population growth rates predicted by our SEED models. Only three of the 49 populations we evaluated from the seven different species included in our study were predicted to do worse because of projected changes in climate over the next few decades. In contrast, seven populations were projected sinks under current climate conditions, not including snowy plover populations without active predator management known to be populations sinks (Colwell 2017) but predicted by our SEED models to be sources given fecundity and survival rates associated with active predator management. We interpret this result to reflect that for temperate special status species, climate-related threats are probably less prevalent than non-climate related threats, such as habitat loss, degradation and fragmentation, altered disturbance regimes, or competition with and predation by invasive species.

3 Objective

Global climate change will play a critical role in shaping future environments, and thus biodiversity. Key climate variables— temperature and precipitation— will shift (Girvetz et al. 2009, IPCC 2013), affecting species ranges, phenologies, abundances and viability (Parmesan et al. 1999, Deutsch et al. 2008, Chen et al. 2011, Urban et al. 2016). In many cases, a changing world climate will lead to future environmental conditions unlike any currently experienced by species managed on DoD lands. As a result, many species will likely become "conservation reliant" requiring active management to prevent local, regional, and even global declines or extinctions. The goal of this project was to develop and test an empirical protocol and theoretical framework for determining which species are likely to become conservation reliant as global climate change creates novel environments in and around DoD lands. We demonstrated these protocols on a suite of species representing the spectrum of conservation reliance. Specifically, we: 1) used global climate change models (GCMs) to predict plausible temperature and precipitation regimes faced by species managed on military lands; 2) for each of demonstration species, used times series, space-for-time substitution, and experimentally created non-analogue environments to determine how demographic rates are expected to change given future predicted temperature and precipitation regimes; 3) built Spatially Explicit Environmental Driver (SEED) models to predict population level changes expected to occur in non-analogue environmental conditions predicted to be present in the future; and 5) compared SEED model population

11

dynamic predictions across those species to determine ecological characteristics of future conservation reliant and adaptive species.

4   Technical Approach

4.1   Background

In recent decades, climate change has had a negative impact on many species through changes in phenology (Walther et al. 2002, Parmesan and Yohe 2003, Chen et al. 2011) and demographic rates (Saether et al. 2000, Radchuk et al. 2013, Urban et al. 2016). The magnitude and multitude of changes associated with climate change pose several challenges to long term planning for wildlife management and endangered species conservation. Many species are currently conservation reliant, requiring ongoing, intensive management to persist, but even species that currently need only minimal or one-time management may become conservation reliant in the future (Scott et al. 2010). Long-term planning would benefit from knowing which species are likely to become conservation reliant, and, for species already managed on DoD lands, which species will require more, or less, intensive management given future environmental conditions.

The difficulty in this challenge is that not all species will respond to climate change in the same way, as specific demographic rates (e.g., survival to reproductive age/stage classes, fecundity) have different optimal environmental conditions. Disparate effects of climate on different demographic rates could result in little, or even positive, change to population growth (Deutsch et al. 2008). Furthermore, relationships between climate variables and demographic rates may be nonlinear (Doak and Morris 2010). Large shifts in climate are more likely to cause dramatic population declines, corresponding to so-called demographic tipping points (Harley and Paine 2009, Doak and Morris 2010). Demographic tipping points may be especially relevant for populations located at species range boundaries, where even relatively small shifts in climate might lead to large effects on demographic rates. Thus, predicting how populations will be affected by future climate change (i.e., non-analogue conditions) is particularly difficult based on field observations alone, and generally requires population models to integrate changes in multiple demographic rates.

Whether or not climate change causes a population to become conservation reliant will often depend on the climate conditions the population currently experiences. Intuitively, because performance (e.g., survival, fecundity) is typically a unimodal function of temperature, temperature increases from a cooler starting point should have a smaller negative effect – or even a positive effect – relative to increases from a warmer starting point. For example, decreasing latitude has been associated with greater extinction risk of California red-legged frogs in southern California– where temperatures are warmer – but not in coastal central California (Davidson et al. 2001) where coastal populations are buffered from warm temperatures by marine influence.

The most common strategy for studying the impacts of climate change on species extinction risk is to correlate a species' current range with current climate conditions and assume that species will go extinct in regions where future climate conditions are no longer represented within the species' current range (e.g., Lawler et al. 2009, Blaustein et al. 2010, Urban 2015). Metapopulation approaches represent an important advance to the correlative approach by accounting for species' dispersal capabilities relative to the spatial scale of shifting climatic conditions (e.g. Anderson et al. 2009, Aiello-Lammens et al. 2011). A parallel recent advance in

assessments of the impacts of climate change on extinction risk is the development of models based on environmental drivers of demographic rates. While it has long been recognized that climatic variables influence demographic rates (Davidson and Andrewartha 1948, Birch 1953), only recently have population models been used to integrate distinct responses of different demographic rates to predict population consequences of climate change. Determining the overall impact of climate change on population growth requires integrating the effects of rising temperatures (and other climate drivers) over all life stages in an environmentally driven (ED) population model.

When ED models are linked into climate projection models (e.g., Jenouvrier et al. 2009), population trajectories can be used to predict whether a population is likely to become more, or less, conservation reliant due to climate change. Populations likely to become more conservation reliant due to climate change are characterized by a declining growth rate over time, particularly if projected growth rates switch from growing or stable trajectories under current climate conditions to declining trajectories under most future projected climate conditions. Likewise, populations projected to have increasing population growth rates under future climate conditions could be interpreted as becoming less conservation reliant (or less likely to become conservation reliant) due to climate change.

In order to predict which species are likely to become more (or less) conservation reliant at the regional or species-wide scale, ED models need to incorporate spatial processes to link populations to the proper climate projections and to account for the potential influence of migration, dispersal-mediated metapopulation processes or population tracking shifting locations of favorable habitat. We developed Spatially Explicit Environmental Driver (SEED) models for a range of species. In SEED models, demographic rates are assumed to be functions of environmental drivers. SEED models provide a particularly powerful tool because they: 1) allow researchers to explore combinations of environmental variables not currently seen but likely to be encountered in the future (non-analogue environments); 2) can include numerous scenarios to account for uncertainty in future environmental conditions; 3) accommodate influences of both local environmental conditions and surrounding landscape features; 4) account for migration and for dispersal limitations that may constrain a species' ability to track spatial shifts in suitable habitat; and 5) can be evaluated at multiple time steps to inform predictions about transient dynamics in a non-stationary world.

Predicting population fates in non-analogue conditions requires extrapolation beyond current conditions. This can be done by using fitted performance curves that go beyond the range of the observational or experimental data. Previous studies have typically taken one of three approaches to obtain fitted performance curves. First, in the space-for-time substitution approach, demographic rates are measured at multiple sites along an environmental gradient. Often the gradient is latitude or elevation, where more equatorial (or lower elevation) sites currently experience warmer conditions (Lawler et al. 2009, Doak and Morris 2010, Picó 2012). While this approach uses realistic data by following individuals in the field, sites may differ in fundamental ways besides climate. The second approach is to exploit temporal variation in environmental conditions across years at a single site to quantify the relationship between demographic rates and environmental drivers. This approach also uses realistic data, but years may differ in other important ways besides climate. The third approach is to experimentally vary one or a few environmental variables outside normal ranges by means of a controlled environment (e.g., Deutsch et al. 2008). This latter approach is particularly well suited to exploring demographic responses to extreme climate conditions, which, due to their rarity, are

difficult to observe in the time frame relevant to most studies. However, controlled environments may not reflect realistic demographic rates. We use all three approaches, by using the two "natural experiment" approaches– space-for-time or time series– to parameterize SEED models, and then using controlled experiments to validate model predictions in extreme conditions.

4.2   Methods

We studied seven species of animals and plants: hydaspe fritillary butterfly (*Speyeria hydaspe*), Appalachian brown butterfly (*Satyrodes appalachia*, western snowy plovers (*Charadrius nivosus nivosus*), red-legged frogs (*Rana aurora* and *R. draytonii*), Alaskan doug*lasia* (*Douglasia alaskana*), Venus flytraps (*Dionaea muscipula*) and red-cockaded woodpeckers (*Dryobates borealis*). For the butterfly, frog, and plant species we collected demographic data from populations that vary in current climate conditions (space-for-time approach), while for the two birds species we used previously collected demographic data from long term (>20 yrs) studies (time series approach). Study locations for each species are presented in Figure 4.2-1. For the two butterfly species, the frogs, and Venus flytraps we also conducted controlled experiments in which we pushed climate variables beyond conditions currently experienced at our field sites. This allowed us to compare results in a controlled experiment to those from the field in order to validate our field results. We also manipulated additional variables likely to be shaped by climate and some non-climate related variables for these species in order to examine the potential impacts of habitat, common management strategies, and antagonistic interactions with other species on climate responses by our focal species. For each animal species, we estimated the following demographic rates: fecundity, egg hatch rates, larval/juvenile survival, and adult survival. For the two plants we estimated: seed production, germination rate, and size specific survival and growth rates. Additional demographic rates, including developmental rates, migration rates, and dispersal were measured for some species as needed to adequately describe a species life history in the SEED model developed for the species.
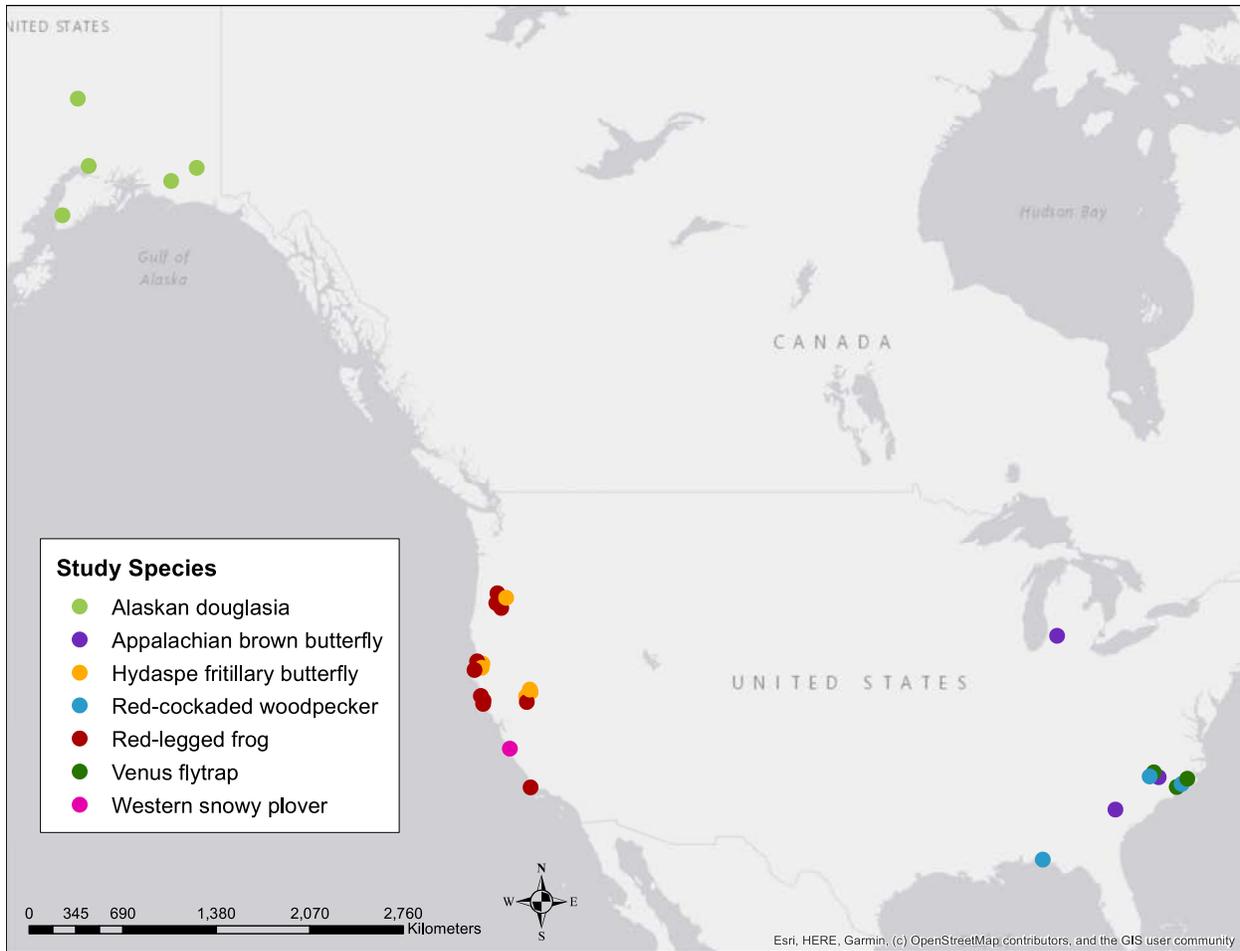
Figure 4.2-1. Locations of study populations for each species. Circles marking population locations are color-coded by species.

4.2.1 Data collection

4.2.1.1 Hydaspe Fritillary Butterfly (*Speyeria hydaspe*)

Study system: Hydaspe fritillary butterflies occur throughout the northwestern US and south through the Sierra Nevada in CA. They are found in moist montane coniferous forest openings and meadows, typically between 1000-2000 m in elevation. They are univoltine with a flight period between June and September. The larvae overwinter as unfed first instars and feed on several species of violets (*Viola spp.*) in the spring (Scott 1986, Robinson et al. 2002). Adults use a variety of nectar plant species. We studied six hydaspe fritillary populations in Northern California and Oregon that varied in elevation from 1085 to 1585 m and spanned a latitudinal range from 39.2 to 44.2° N (Figure 4.2-2). Five sites were in California: three in the Sierra Nevada and two in the Coast Range. One site was in the Cascades in Oregon. Each site included a mix of wooded and open (meadow) habitat, and all sites typically have snow on the ground for some portion of the winter/spring. See Table 4.2-1 for site details. We deployed HOBO Pro data loggers (Onset Computer Corporation, Bourne, MA, USA) at each site to record air temperatures.
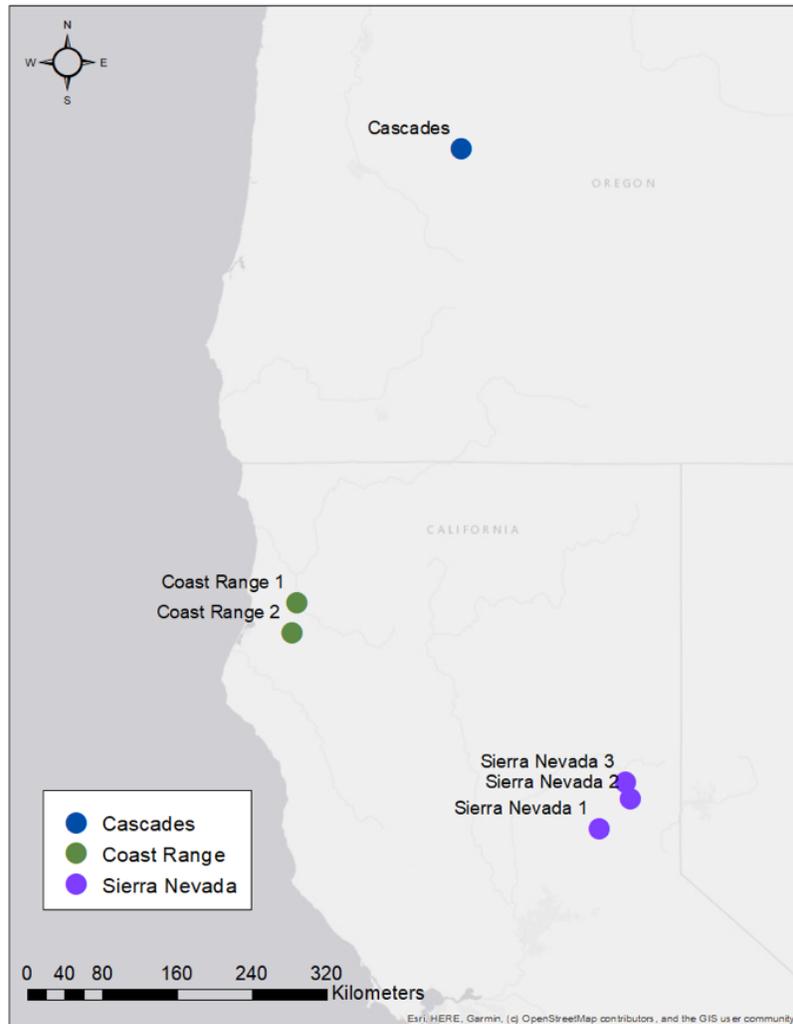
Figure 4.2-2 Hydaspe fritillary butterfly study locations in California and Oregon.

16

Table 4.2-1. Study site locations, elevations, and demographic rates measured at each site each year. Demographic rates: F = Fecundity, E = Egg hatch rates, L = Larval survival, A = Adult survival.

Site	Elevation	2016	2017	2018	2019
Cascades	1320 m	A	F, E, A	F, E, A	L
Coast Range 1	1440 m	A	F, E, A	F, E, A	L
Coast Range 2	1485 m	A	F, E, A	F, E, A	L
Sierra Nevada 1	1085 m		F, E, A	F, E, A	
Sierra Nevada 2	1400 m	A	F, E, A	F, E, A	L
Sierra Nevada 3	1585 m			F, E, A	L

Demographic field methods: We used mark-recapture surveys to estimate adult survival across sites. We surveyed butterflies at each site along four to six transects that could be easily surveyed by a single person in 1-1.5 hours (total time for all transects) (Pollard 1977). We visited each site three to four times a week from prior to the beginning of the flight period in mid to late June through the end of the flight period in August or September. The one exception was Sierra Nevada 3, which we added in 2018 and missed the beginning of the flight period. We surveyed each site for the same amount of time each visit; however, the amount of time spent on a survey varied across sites depending on the survey area but was always between 1-1.5 hours. We marked adults with a unique number using fine-tip Sharpie markers. Getting the butterfly out of the net and marking it typically took about 1-3 minutes, and in order to account for the time spent handling butterflies and not surveying we added 2 minutes to the total survey time for every butterfly we marked (up to a total of 30 extra minutes). For each hydaspe butterfly that we caught, we recorded its age (subjective measure broken into 3 categories), sex, if it was on a nectar plant, and if so what species of nectar plant. We also recorded the GPS location at time of capture for all butterflies that we caught.

In addition to our mark-recapture surveys, during the summers of 2017 and 2018, we recorded the nectar plants that were blooming along our transects at all of the sites every other week. We determined each plant species' blooming progression by assigning them to one of five stages based on the majority of individuals in each section. The six stages were: 1 - no buds present, 2 - buds present, 3 - starting to bloom, 4 - peak bloom, 5 - finishing blooming/starting to go to seed, and 6 - completely done blooming/gone to seed.

We measured the number of eggs laid per female per day (egg laying rate) by placing females that we caught during our surveys into oviposition cages for 1-7 days. The cages were made of plastic flowerpots (~ 20 cm diameter) covered with screen. Inside of each pot we placed violet leaf clippings (larval host plant) in cups of water to prevent wilting. We placed cotton balls or sponges soaked with sugar water in each container with sticks for butterflies to perch on. We checked the cages every 1-3 days and released the female once eggs were laid or after several days with no eggs. If a female laid eggs, we carefully collected and counted all of the eggs. We calculated egg laying rate as the total number of eggs collected for each female divided by the number of days they were in the cage. If a female died while in the cage, we excluded that individual from the analysis.

We measured egg viability using the eggs we collected. We placed a maximum of 10-20 eggs into white plastic 88 ml (3 oz) cups (keeping eggs from different females separate. We covered the cups with fine insect mesh secured with rubber bands. We checked the eggs at least

once a week until all the eggs had hatched, or until 2-3 weeks past the date that the first egg hatched. Any remaining eggs were considered unviable. On rare occasions, we observed larvae that were able to make it through the insect mesh cover on the cups (the openings were not totally uniform). In some cases, the number of unviable eggs left at the end and the number of larvae we observed post hatching did not sum up to the total number of eggs placed in the cups. In these cases, we assumed that the discrepancy was due to larvae escaping the cup, such that the egg hatch rates were calculated as follows: (total at start – unviable at end) / total at start.

We quantified egg predation rates in the field by placing eggs in plastic 88 ml cups buried in the duff and left uncovered. Hydaspe fritillary butterflies lay their eggs singly throughout the understory on twigs, leaves, and other debris in areas where their host plants (*Viola spp.*) grow (Capinera 2008). We placed two eggs in each cup and spread them out by at least 50 cm. We checked the predation cups at least once a week until both eggs were missing or until eggs from that female hatched in our predator-free cups. Because larvae are known to eat the egg husks after hatching and can crawl out of the cups, we only considered eggs to be predated if they went missing at least six days prior to the first observed larvae to hatch from that female. This ensured that we did not incorrectly count eggs as predated that actually hatched.

In the wild, hydaspe larvae overwinter as first instars and bury themselves a few centimeters into the duff prior to going into diapause. To track overwinter survival, we wanted to mimic natural conditions as much as possible while still making it easy to relocate larvae in the spring. To do this, we caged larvae inside modified 88 ml white plastic cups. We modified the cups by cutting off the bottoms and replacing them with insect mesh, so that any rainwater or snow melt could drain through the cup. We filled the cups with pieces of Styrofoam packing peanuts to provide insulation and placed up to 10 larvae in each cup. Each cup contained larvae from a single female. We then covered each cup with insect mesh and buried all cups into the top layer of the duff such that the rim of cup was flush with the ground. We placed large pieces of bark over the cups to shelter them from direct rain. We placed HOBO Pro data loggers in empty cups also placed in the duff to record the temperatures the larvae experienced.

During the spring we monitored snowpack at our field sites and checked the larval overwintering cups shortly after the snow melted in the area they were placed. We counted the number of larvae that survived in each cup, and either placed them directly onto potting violets in larval rearing cages (methods below). If violets had not emerged yet, we placed the larvae back into overwintering cups and replaced them in the duff until violets could be transplanted. We created larval rearing cages by transplanting local violets into 15 cm diameter plastic pots and placing the pots in 30 cm x 30 cm x 30 cm popup mesh cages (Bioquip). We used the species of violet that was must abundant at each site which included three species: *Viola glabella*, *V. lobata*, and *V. sempervirens*. At one site both *V. glabella* and *V. lobata* were abundant and we used both species in the cages (half of the cages for each species). To increase the amount of variation in temperature the larvae were exposed to in the field, we positioned cages across a gradient in sun exposure and used HOBO data loggers to measure temperature differences.

We checked on the cages every three to seven days from when larvae were placed in the cages until all surviving individuals had pupated and most had eclosed. We watered the violets as needed to maintain plant quality and added in new potted violets when vegetation became sparse due to feeding. We examined larval survival during two separate periods: overwinter survival and survival from ending diapause (placement on violets) to eclosion. At some of our sites time constraints required that we stopped checking the cage before a few of the latest pupae had

18

eclosed. We considered these individuals to have survived successfully if the pupae were viable (moved when prodded) during the last check.

Experimental tests of climate effects: We used two methods to increase the range of temperatures experienced by different life stages: 1) we constructed greenhouses and 2) we relocated females (and the eggs they subsequently laid) to a lower elevation site that experiences higher temperatures. We constructed three small greenhouses (1.8 m x 1.2 m x 2.1 m Brighton greenhouses) positioned on a shade gradient and a mesh shade tent (3 m x 3 m x 2.1 m Coleman Instant Screenhouse) on Institute for Wildlife Studies property in Humboldt County, CA. Within each structure we set up shelves with three levels to house eggs, larvae, and adults. In addition to temperature differences among structures there was also a temperature gradient across the shelves in each structure. We deployed HOBO data loggers on each shelf in each structure to record temperature variation.

We measured egg hatch rates in one of the greenhouses with eggs laid by two females from one of our field sites in Humboldt County during the summer of 2018. We also reared larvae on potted violets in the greenhouses and shade tent in 2019. Most of the larvae (85 individuals) we used for this experiment came from our mid-elevation site in the Sierra Nevada and had overwintered in cups at that site. We also had a small sample of nine larvae which came from eggs collected from females at one Coast Range site, which overwintered in the greenhouses. We distributed larvae from the same female randomly across structures and shelves within each structure. We used the same methods as described in the field experiment for rearing larvae in the greenhouses and shade tent.

In 2019 we collected egg laying and egg hatch rate data using adult females (and the eggs they laid) relocated from two of our field sites in the Sierra Nevada down in elevation to Sacramento County, CA, where average daily maximum temperatures experience by females exceeded that of any other site by 2-3 ºC. We used the same methods as in the field to measure egg laying and hatch rates.

Fitting Relationships between demographic rates and climate variables: We used data from both the field and greenhouses to fit climate – demographic rate relationships. Minimum, maximum, and mean daily temperatures are often highly correlated, so for analyses described below we only included one measure of temperature at a time in our models. Because a high number of females laid no eggs (65%), we used zero-inflated negative binomial models, with site as a fixed effect, to examine the relationship between climate variables and fecundity (pscl package in R Studio v1.2.1335, R Studio Team 2018, Jackman 2017). The climate variables we tested were average daily minimum, maximum, and mean temperatures while females were in the cages, and the snow melt date for each site/year. Nectar intake correlates with fecundity in a related fritillary species (*Speyeria mormonia*) (Boggs and Ross 1993), and earlier snow melt dates in this system decreases nectar resources through frost damage (Inouye 2008). Because we believed that butterflies not laying eggs indicated a stress response, we tested climate effects on the count portion of the model only, and not the zero-inflated portion. We considered that butterflies might also "egg-dump", laying an unusually high number of eggs in a short time period, as a stress response. However, we did not observe any indication of this. Eggs were not laid in clusters within the cages, and the frequency distribution of numbers of eggs/day from females that laid eggs had no obvious breaks or secondary peaks indicative of egg dumping. We evaluated the relative performance based on AIC corrected for small sample sizes (AICc) (MuMIn package in R Studio v1.2.1335, R Studio Team 2015, Bartoń 2019).

We used binomial mixed models to test the effects of climate on egg viability and both overwinter and post diapause larval survival (MCMCglmm package in R 3.3.3; Hadfield 2010, R Core Team 2017). For egg viability, we evaluated the influence of the average daily minimum, maximum, and mean temperatures as well as the maximum temperature experienced from when eggs were laid through hatching. We also tested the effects of total precipitation from that water year (October-September) on egg viability. We included female as a random effect and site as a fixed effect in the model. We used generalized linear models to test the effects of temperature on egg development rate, which we measured as the number of days from egg laying to hatching by female.

We evaluated the effects of temperature on the chances of eggs being predated in our field trials using binomial mixed models with female as a random effect and site as a fixed effect (MCMCglmm package in R 3.3.3; Hadfield 2010, R Core Team 2017). We used the average daily minimum, maximum, and mean temperature from the time eggs were placed in predator accessible cups until the trial ended (last survey at least six days prior to first larvae hatching from that female).

Egg predation rates found from our field trials are a function of both the daily predation rates and how long the eggs are exposed to predation. The exposure time is dictated by how quickly the eggs develop, which could be affected by temperature. In order to further explore the effects of temperature on predation probability, we evaluated the effects of temperature on daily egg predation rates using Cox proportional-hazards regression models (survival package in R Studio v1.2.1335, R Studio Team, 2015, Fox 2002). Because we surveyed the egg predation cups at different intervals at each sites, we specified our first survey date to start on day five or later (the earliest date at some sites), and used the average daily minimum, maximum, and mean temperature between each survey period at each site as our predictor variables. Because egg predators are likely to be relatively similar across sites within the same region but differ across regions, we included region in the model as well. The regions included two sites in the Sierra Nevada, (we did not obtain enough eggs for predation trails at Sierra Nevada 1), two sites in the Coast Range, and one site in the Cascades. We right-censored the data by female based on the last survey date at least six days prior to the first egg hatching from that female. We evaluated model performance based on AIC.

For overwinter larval survival we tested the effects of average daily minimum, maximum, and mean temperature from when larvae were placed in the duff until first snow fall, the lowest temperature experienced over the winter, and snow melt date. We included female and overwintering cup as random effects and site as a fixed effect. Because all of our climate measures were correlated with each other, and because there was only one value of each climate variable for each site, we only included one fixed effect at a time in the models. For post-diapause survival we assessed the effects of average daily minimum, maximum, and mean temperatures and maximum temperature experienced from when larvae were placed on violets until the last individual had eclosed at each site. We included female and container as random effects and site as a fixed effect. Because of low sample sizes we excluded larvae from Sierra Nevada 1 from the analyses (only 16 overwintering larvae and two post-diapause larvae), and we considered Coast Range 1 and Coast Range 2 to be one site for this analyses (there were larvae from only one female at Coast Range 1 and all larvae were reared at Coast Range 2). We evaluated relative performance of our models using the model deviance information criterion (DIC). DIC is a Bayesian generalization of the Akaike information criterion (AIC) that is

20

particularly suited to comparing models that use Markov chain Monte Carlo (MCMC) to obtain posterior distributions (Spiegelhalter et al. 2002).

We used generalized linear mixed look for effects of temperature of the development rate for eggs and larvae (MCMCglmm package in R Studio v1.2.1335, R Studio Team, 2015, Hadfield 2010). We measured development rate of eggs as the number of days from when eggs were laid until the first larvae hatched for each female. We tested the average daily minimum, maximum, and mean temperatures during development as fixed effects and included site as a random effect. We measured larval development rate as the number of days from when larvae were placed in cages until adults emerged. We tested average daily minimum, mean, and maximum temperatures and growing degree days (GDD) from when larvae were placed on violets until the last individual had eclosed at each site, as well as GDD for the first 30 and 50 days of development as fixed effects. We included site, female, and cage as random effects. GDD is a measure of heat accumulation that is calculated by taking the daily integral of warmth between minimum and maximum temperature thresholds (D_{min} and D_{max}), which are typically based on the range of temperatures where plant or insect growth are possible. GDD is a common measure used for predicting plant and insect phenology in agriculture (Cross and Zuber 1972, Zalom et. al 1983, Russelle et al. 1984, McMaster and Smika 1988). We calculated GDD based on daily minimum and maximum temperatures using the single sine method (Zalom et al. 1983). We specified D_{min} as 10 °C and D_{max} as 30 °C, which are commonly used thermal thresholds for warm season plants and insects (Dethier and Vittum 1967, Nufio et al. 2010).

We used multi-strata mark-recapture models to evaluate the effects of mean, minimum, and maximum daily temperature between capture occasions and total annual precipitation on adult survival ('RMark' package in R and Program MARK; White and Burnham 1999, R Core team 2017). Each site by year combination was modeled as a separate stratum. We used multi-strata models because we suspected butterflies could disperse between the two Coast Range study sites. When no marked butterflies were observed to move between the two sites in three years we simplified the analysis by setting all transition probabilities to zero. Survival was estimated on a daily time scale. We accounted for occasions when a stratum was not surveyed but other strata were surveyed by modeling capture probability as a function of effort. Effort for a given stratum was set to one on occasions when it was surveyed and zero on occasions when it was not surveyed.

Effects of climate variables on population growth and phenology: In addition to testing the effects of climate on each life stage, we used our survey data to explore how climate influences changes in abundance and flight period phenology. Results from this section were not included in the SEED model for hydaspe fritillary butterflies, but they can provide insight into some of the complexities of how climate change might affect this species. We used the adult mark-recapture data from our surveys to estimate the population size of male butterflies at each site each year. Because we caged a large proportion of the females we caught to obtain eggs, we could only use our mark-recapture data to estimate the population size of males. We used these population size estimates to assess the effects of climate and density dependence on continuous population growth rates using a multivariate form of the Gompertz population growth model (Gompertz 1825):

Equation 4.2-1 $$ln\left(\frac{N_{t+1}}{N_t}\right) = a + b * ln(N_t) + c * C_1 \dots C_i$$

where N_t is the population size estimate in year t and $C_1 \dots C_i$ are climate variables 1 through i. We tested the effects of GDD from snow melt to August 1st in year t and year t+1, snow melt

date in year t and year t+1, and total precipitation from October 1st through September 30th in year t and year t+1 using generalized linear models (stats package in R Studio v1.2.1335, R Studio Team, 2015).

We calculated four response variables related to hydaspe phenology: flight period start date, flight period end date, flight period peak date, and flight period length. We considered the first day we observed adult hydaspe fritillaries at each site/year to be the flight period start date and the last day we observed adults to be the end date. Because we surveyed each site two to three times prior to observing adults and at least three times after we stopped seeing adults each year, we believe our determinations of the beginning and end of the flight period to be fairly accurate. We also estimated the date of the peak abundance of adults during the flight period, because peak abundance is typically influenced less by detectability and variation in sample size (Moussus et al. 2010). To determine the date of peak abundance at each site and year combination we fit curves of our counts of hydaspe adults over time using nonlinear least squares (nls function in R) with a standard three parameter gaussian function:

Equation 4.2-2 $$y = a \times exp(-\frac{1}{2} \times (\frac{(x-b)}{c})^2)$$

The ordinal date of peak abundance corresponds to parameter b in the equation above (a is the amplitude and c is the width of the curve).

We tested the effects of GDD, snow melt date, and region on the hydaspe flight period start, peak, end, and length using generalized linear models (stats package in R Studio v1.2.1335; R Studio Team, 2015). We used region (Sierra, Northern Coast, or Cascades) rather than site in our models because of our limited sample size (16 site/year combinations). The small sample size also preluded the use of mixed models with region or site as a random factor. We used AIC corrected for small sample sizes (AICc) to evaluate relative model performance. We considered there to be support for any model within two AICc of the best performing model. GDD was calculated from snow melt date to July 15th each year for analyses of flight period start date and from snow melt to August 1st for all other measures of abundance and phenology.

Nectar resources can influence butterfly populations by affecting both adult survival and fecundity (Boggs and Ross 1993, Lebeau et al. 2016). Based on personal observations at our sites, we also suspected that nectar plant senescence might influence the timing of the end of the flight period. Our survey data showed that hydaspe fritillary butterflies used nectar plants preferentially, visiting one species a majority of the time (57 to 98% of visits across sites), but that the primary species visited was different at each site (Appendix 8.2). Based on our nectar plant surveys in 2017 and 2018 we determined the date that the primary nectar plant at each site fully senesced (6 on blooming progression scale). We used generalized linear models to test the influence of GDD, snow melt date, total precipitation in the current year, and Region on the timing of senescence. We also looked for a correlation between plant senescence date and the end of the flight period.

4.2.1.2 Appalachian brown butterfly (*Satyrodes appalachia*)

Much of the text in is section and in section 5.1.2 is drawn from Kiekebusch 2020. *Study system:* The Appalachian brown is a satyrine butterfly found in forested wetlands throughout the eastern United States. The range of the Appalachian brown butterfly encompasses a large portion of eastern North America (Cardé et al. 1970) and as far north as southern Quebec, Canada and as far south as the central Gulf States, with a small isolated population in northern Florida (Opler 1994). Appalachian brown butterflies have been observed to complete at least two

22

generations per year in the southeastern US and to overwinter as diapaused early-instar larvae. We carried out the field portion of our study on the US Army installation at Fort Bragg, NC where Appalachian brown butterflies are locally rare in wetland areas. A combination of land-use change, fire suppression, and beaver extirpation at Fort Bragg have altered wetland habitat and reduced the number of early successional *Carex* species (Bartel et al. 2010), including *Carex mitchelliana* that is a known host plant for Appalachian brown butterflies (Kuefler et al. 2008). Although Appalachian brown butterflies have previously been considered bivoltine at this field location (Aschehoug et al. 2015, Sivakoff et al. 2016), recent observations revealed that a portion of the second generation individuals to develop directly into a third generation (Kiekebusch 2020).

Demographic methods: We measured survival rates for all life stages in the field at Fort Bragg, NC using plots that had experimental habitat restoration treatments implemented in 2011 with funding from a previous SERDP award (SI 04-014). The restoration treatments were intended to increase (or not) the abundance of host plants (sedges in the genus *Carex*) and the abundance of butterflies, including Appalachian brown butterflies and the federally endangered Saint Francis' Satyr (*Neonympha mitchellii francisci*, methods in Aschehoug et al. 2015). The restoration treatments were implemented in a factorial design and included a control (no treatment), hardwood removal ("Cut"), dam installation ("Dam"; intended to increase soils moisture to favor sedges) and Cut + Dam. The restoration plots were 30 m x 30 m and there were a total of 16 plots across three sites (three control and Dam plots and five Cut and Cut + Dam plots). The ambient temperature varied across restoration treatments due primarily to differences in canopy cover, etc.

We evaluated the effects of temperature on egg and larval survival in the field within the 30 m x 30 m restoration plots. In addition to ambient temperature differences among restoration treatments, we used warming/cooling arenas within each plot to increase the range of temperatures experienced by eggs and larvae. For this experiment, we selected three plots in each of the three field sites, including one Cut plot and two Cut + Dam plots. We ignored uncut plots because the warming arenas relied on solar warming to increase temperatures.

To manipulate temperatures, we created three experimental arenas within each of the plots. Each arena consisted of a 208 L polyethylene drum cut into a ring 37 cm high and 57 cm in diameter. We established arenas around naturally occurring wetland plants including *C. mitchelliana* by burying them 10 cm deep in the ground. We planted extra sedges where necessary to maintain a similar amount of live sedge within each arena. We removed all visible predators from inside the arenas and excluded predators by enclosing arenas within no-see-um netting (Skeeta©). Within each plot, we randomly assigned each arena to one of three temperature treatments: 1) Control, 2) Shade and 3) Open-top warming. We shaded arenas by covering them with Coolaroo© shade fabric (84-90% UV Block) cut into 1.8 x 1.8 m squares and hung by the corners from PVC pipes at 1.5 m above the ground, such that the arena was centered beneath the shade fabric. We constructed open-top warming chambers using Sun-Lite© pre-fabricated solar glazing panels (Solar Components Corporation, New Hampshire USA). We cut the panels into 2.4 m x 0.9 m rectangles, rolled them into cylinders and fastened them with screws. The resulting cylinders were 0.9 m high with a circumference of 2.1 m, and each was placed over one arena per plot. Inside each arena, we placed a Maxim iButton temperature logger within the foliage of *C. mitchelliana*, shielded from direct sunlight under a plastic cup covered in reflective foil, and at an approximate height of 30 cm above the ground (typical height of naturally occurring eggs and larvae).

To measure egg survival, we collected eggs from wild-caught Appalachian brown butterfly females that we brought to a greenhouse located at the Endangered Species Branch of the Fort Bragg Army instillation. We placed the famales in a 15 cm high by 10 cm diameter 'oviposition chamber' consisting of a single potted host plant (*Carex mitchelliana*) enclosed within mesh netting. After 48 hours, we removed the netting, released the butterfly and counted the number of eggs laid. We placed entire potted plants with known numbers of eggs into each experimental arena in the field for approximately 48 hours. Afterwards, we removed the plant and counted the remaining viable eggs. Non-viable eggs were identified by their altered color, shape and/or size. This allowed us to estimate daily egg survival. We carried out the egg survival experiments during three generations (first: 5/3 – 6/9/17, second: 7/20-8/12/16, and third: 8/31-9/29/16).

We estimated larval survival using the larvae that hatched from these eggs. We allowed the eggs to hatch at ambient temperatures in the greenhouse. As soon as all larvae hatched, we counted them and placed them back into the same experimental arenas in the field. Once we noticed formation of pupae, we checked the arenas daily for emerged adults. We carried out the larval survival experiments over all three annual generations (first: 5/19 – 7/10/17, second: 7/27-9/25/16, and third: 9/7/16-5/31/17).

To estimate adult survival rates and lifespan, we carried out mark-recapture surveys over a three-week period covering the second adult flight period of 2017 (7/14-8/3). We carried out surveys along transects established within a total of fifteen plots across the three restoration sites. We followed mark-recapture methods as described in Haddad et al. (2008). We carried out surveys on every weekday throughout the flight period. Over the same time period, we placed shielded iButtons into each plot and recorded hourly temperatures.

We estimated egg laying rate by measuring oviposition in artificially warmed enclosures in the greenhouse. We carried out the experiment from 7/12 – 8/31/17. We caught wild females, placed them in oviposition chambers for 40-42 hours, and then counted the number of eggs laid. We manipulated temperature during oviposition by placing chambers under infrared lamps. We used a single iButton placed inside each chamber to record temperatures.

Fitting Relationships between demographic rates and climate variables: To evaluate the effect of field arena temperatures on egg and larval survival rates, we carried out generalized linear mixed effects models using R statistical software (R Core Team, 2016). We used binomial regression analyses to evaluate effects of temperature variables on egg and larval survival. The temperature variables included: 1) the average of the daily mean temperatures, 2) the average of the daily maximum temperatures, and 3) the average of the daily minimum temperatures recorded by the iButtons over the period of time that an individual spent in each life stage in each arena. By design, this was two days for the eggs and the entire larval life stage for larvae. We compared a suite of models that included fixed effects of temperature, warming treatment (Control, Shade, Open-top warming), restoration treatment (Dam or No Dam), generation (first, second, third), and/or the interactions between generation and each of the three temperature variables. All models included a nested random effect of plot in site (block). Because the three temperature variables were highly correlated, we only included one temperature variable at a time in the models. We ranked models using corrected Akaike's Information Criterion (AICc, Hurvich and Tsai 1989) and used the best-supported model in all subsequent analyses.

We analyzed adult survival via a multistate mark-recapture model using the package RMark (Laake, 2013) in R to run the program MARK (White and Burnham 1999). In order to test for effects of temperature on dispersal, we compared five models using covariates of

probability of transition (Psi) between plots that included maximum, minimum, and mean temperatures, distance between plots, and constant dispersal across sites and time. We ranked all models using corrected Akaike's Information Criterion (AICc) and selected the best covariate for use in subsequent analyses. In order to evaluate possible effects on detection, we carried out a second round of model selection and compared two covariates of detection probability (p) that were linked to detection in a prior study (Sivakoff et al. 2016). We tested for plot and restoration (Cut) effects on detection, while holding survival probability (Phi) constant across sites and time. We selected the highest ranked covariate for further use. In order to test for effects of temperature on adult survival probability, we carried out a third round of model selection. We ranked seven models using AICc to compare survival probability covariates that included average daily minimum, maximum, and mean temperature, field site, plot, Dam treatment and constant survival across sites and time. We selected the best supported model for further analyses.

To evaluate temperature effects on daily fecundity, we regressed number of eggs laid per day against temperature variables using a quasipoisson generalized linear model to account for overdispersion. We compared a suite of six egg laying rate models to evaluate effects of mean temperature, average daily maximum temperature, average daily minimum temperature, and the quadratic effects of these variables. We defined the average daily minimum and maximum temperatures as the mean of the daily minima and maxima over the 40-42 hour period that each female was in an artificial warming chamber. We carried out QAICc model ranking using the R package MuMIn (Bartoń 2017) to assess support for each temperature variable. To calculate daily fecundity, we accounted for propagation of females by assuming a 1:1 sex ratio and halving the number of eggs laid per day as fitted by the highest ranked temperature model.

Determining cues for shifting voltinism and phenology: We carried out an experiment to determine the timing of the occurrence of the critical photoperiod cueing the onset of diapause in Appalachian brown butterflies. Individuals exposed to this cue during a sensitive early life stage halt development and initiate diapause through the winter. Warmer temperatures result in earlier annual emergences, shifting the exposure of the offspring of second generation individuals prior to the critical photoperiod and leading to their direct development into an additional third generation.

Over a ten-week period beginning in mid-July, we caught adult female Appalachian brown butterflies that emerged during the second annual flight period. Each week we caught two females and placed each one into a 15 cm high by 10 cm diameter 'oviposition chamber' consisting of a potted host plant (*Carex mitchelliana*) enclosed within mesh netting. After 48 hours, we removed the netting, released the butterflies, and put each potted plant with eggs into a separate netted enclosure. As we could not be sure of the exact date that each egg was laid, we defined the date eggs were laid per clutch as the second day of the 48-hour period. We placed all enclosures onto a bench located at a shaded wetland field site and monitored the larval development over a three-month period. We recorded the proportion of surviving offspring within each clutch that developed directly into adults versus those that initiated diapause. We fit a binomial generalized linear model to the resulting data to understand the relationship between the date that eggs were laid and the likelihood that they developed directly into adults. As has been done in previous studies (e.g. Xue et al. 1997), we considered the critical photoperiod to occur at the point at which 50% of individuals developed directly.

We estimated the timing of annual first emergence of Appalachian brown butterflies in the spring using data from the larval warming experiments and a degree-day model. Our goal

was to quantify Appalachian brown butterfly development as a combination of time and temperature, such that we could later project future emergence ordinal dates using future temperatures. Degree-day models have long been used in the fields of agriculture, biological control, and species distribution modelling under climate change (Moore and Remais 2014). Cumulative growing degree days (GDD) are a more accurate predictor of butterfly emergence timing than the ordinal date (Cayton et al. 2015).

During the warming experiments, we raised diapausing larvae during the winter in enclosures placed at field sites. We recorded hourly temperatures throughout the winter by placing a single Maxim iButton temperature logger in each enclosure. When we observed the formation of pupae in the spring, we began daily monitoring of all enclosures and recorded the exact date of each butterfly's emergence. For each individual, we extracted daily maximum and minimum temperatures during its larval development from recorded temperature data. We calculated GDD using a lower threshold of 10 °C and an upper threshold of 30 °C and applied the single-triangle method to extracted temperatures. These temperature thresholds have been applied to other Satyrinae (Kuefler et al. 2008) as well as many other butterfly species (Crozier and Dwyer 2006, Cayton et al. 2015, Bryant et al. 2002). We began accumulating degree days on March 1st. We identified the lowest accumulated degree days necessary for emergence and used this for further analyses.

Range boundary experiment: We reared eggs collected from adult female Appalachian brown butterfly populations located near the southern (South Carolina) and northern (Michigan) ends of the species geographic range. We collected females during June-August of 2018 when adults are active at both population locations. In South Carolina, we collected female butterflies in a forested wetland area at the Savannah River Site in Jackson, SC located at the approximate latitude of 33 °N. We transported individuals to a greenhouse located on site at the Savannah River Ecology Laboratory for the experiment. In Michigan, we caught females at a forested wetland site managed by the Southwest Michigan Land Conservancy at approximately 42 °N and transported them to a greenhouse located at the Kellogg Biological Station in Hickory Corners, MI.

We brought all wild-caught females to the greenhouses and placed them into oviposition chambers consisting of a single potted host plant (*Carex* sp.) enclosed within mesh netting. We allowed females to lay eggs for approximately 48 hours before releasing them. We created warming enclosures using 27 x 27 x 48 "Pop Up Butterfly Terrariums" (Educational Science©). We placed 100 W 110 V infrared ceramic heating lamps (theBlueStone©) inside the enclosures and manipulated the temperatures emitted by connecting the lamps in series to TT-300H-WH plug-in dimmers (Lutron©). We aimed to increase temperatures by up to 5 °C above ambient greenhouse temperature. We randomly assigned each enclosure to one of three warming treatments: 1) control (no lamps), 2) one lamp set at medium dimmer intensity, 3) two lamps set at high dimmer intensity. We placed a single iButton temperature logger (Maxim©) into each enclosure to record hourly temperatures throughout the experiment.

We removed eggs from oviposition chambers in order to count them and then returned 7-12 eggs to the enclosures on film caps placed next to the potted plants. We estimated egg survival rates based on the proportion of eggs to successfully hatched, and larval survival as the proportion of larvae to successfully eclosed. We estimated the length of time individuals spent in each life stage as the mean number of days it took all individuals within each enclosure to develop from eggs to larvae and from larvae to adults.

We used generalized linear mixed effects models using R statistical software (R Core Team, 2017) to evaluate the effect of temperatures on egg and larval survival rates at the two sites. We combined the data from both sites and used binomial regression analyses to compare a suite of models, which included fixed effects of the site of population origin (i.e., Michigan or South Carolina), average daily mean, maximum, and minimum temperatures experienced by individuals in each enclosure as well as interactions between site and temperature variables. We also included row (location within the greenhouse) as a random effect. We ranked models using corrected Akaike's Information Criterion (AICc, Hurvich and Tsai 1989). Mean temperatures were correlated with maximum and minimum temperatures at $R^2 > 0.5$ and were excluded from candidate models for selection. Maximum and minimum temperatures were less well correlated ($R^2 < 0.5$) so both were included in candidate models.

We used the fitted egg and larval survival curves and projected climate data for the Michigan and South Carolina field sites to estimate future survival rates of these early life stages. We used the temperature variable that emerged as the highest ranked in our model selection process for egg and larval survival and extracted projected future temperatures from the Multivariate Adapted Constructed Analogs (MACA) downscaled climate dataset (Abatzoglou and Brown 2012). We extracted daily temperature data from each of the two 4-km grid cells containing the butterfly population sites for time periods that corresponded to approximate dates during which our egg and larval experiments were carried out (June 1 – July 1 for the egg survival and June 15 – September 1 for larval survival). We used data from 20 General Circulation Models (GCMs) parameterized by the RCP 8.5 ("business as usual") emissions scenario for the years 2018 – 2098 (Appendix 8.1). From the resulting 20 values, we calculated the median and 5 - 95% range and used these values to estimate future juvenile survival rates using the fitted juvenile survival curves.

4.2.1.3   Western snowy plover (*Charadrius nivosus nivosus*)

Study system: The western snowy plover is a temperate breeding shorebird that nests on sand beaches and, less commonly, alkali flats along the Pacific Coast from central Washington State to southern Baja California (Page et al. 2009). In the U.S. western snowy plovers occur on DoD lands from Santa Barbara to San Diego counties and, from 2013-2018, western snowy plovers nesting on DoD lands account for 54-66% of the breeders in those counties and 20-29% of the U.S. portion of the breeding population (USFWS unpublished data). This distinct population segment (DPS) was listed as threatened in 1993, due to documented substantial declines in the number of western snowy plover breeding sites and individuals along the coast, threats from human activity and development on the coast, and the impacts of introduced species in its breeding range (USFWS 2007). Introduced species of special concern at the time of listing included red fox (*Vulpes vulpes*) and invasive beach grasses (*Ammophila arenaria*). Released or escaped from inland fur farming operations, the fox exerted unsustainably high levels of nest and chick predation on western snowy plovers on the coast (USFWS 2007). The beach grass alters natural beach and dune sand dynamics and eliminates the open, lightly vegetated habitat required by the western snowy plover for nesting. Since the time of listing, additional meso-predators, whose populations are augmented by human food and shelter subsidies (e.g., ravens, *Corvus corax*, Burrell and Colwell 2012) have been found to exert a large negative effect on western snowy plover breeding success. There has been a growing awareness of the threat to the western snowy plover's coastal breeding habitat from accelerated sea level rise (Aiello-Lammens et al. 2011).

An extended breeding season is characteristic for the species, with nest initiations underway throughout the range by early April. In the California and Mexico portion of the range nest initiation usually begins in March and very rarely in February. Nest initiations occur only rarely after mid-July (Page et al. 2009, Point Blue Conservation Science unpubl. data). Modal clutch size is three eggs. Western snowy plovers employ a serially polygamous breeding system in which both sexes share incubation, but typically one parent, usually the male, tends chicks to independence. The female normally abandons the brood to the male's care within a few days of the nest hatching and initiates a new nesting attempt with a different male. Males often initiate additional nesting attempts when either failing or succeeding to fledge young before the end of June (Warriner et al. 1986, Stenzel et al. 1994). This breeding system is facilitated by a sex ratio slightly skewed toward males (Stenzel et al. 2011). Incubation and chick-rearing periods are approximately a month long. Because of the lengthy breeding season, females may hatch eggs from three nests and males fledge young from two broods within a breeding season. The individual plovers occupying sites are in flux over the course of a year, with some individuals remaining year-round in the general area in which they bred and others moving variable distance after breeding to winter elsewhere (Warriner et al. 1986, Hudgens et al. 2014).

The longest running intensive study of western snowy plover demographics has been conducted on the shores and alkali flats of Monterey Bay since 1977, with coverage of the entire bay shore starting in 1984 (Warriner et al. 1986, Stenzel et al. 2011). Monterey Bay shoreline, in Monterey and Santa Cruz counties, is in Recovery Unit 4 (RU4), which spans the outer coastline from Monterey to Sonoma counties, California. Annually, the Monterey Bay area has supported 15-20% of the listed distinct population segment breeding within the United States (USFWS unpublished data). Until 2015, Monterey Bay researchers attempted to 1) find all nests laid (or broods, in the few cases each year in which chicks hatched from nests that had previously not been found), 2) identify the individual identity of both parents for each nest, 3) determine the fate of nests (i.e., number of chicks hatched) and broods (i.e., number of chicks fledged) from each nest found, 4) maintain >90% rate of individually-banded breeders and also to individually band a similar proportion of chicks each year, and 5) follow banded individuals during the non-breeding season to determine fidelity to and dispersal from breeding or natal areas (Warriner et al. 1986, Stenzel et al. 1994, Neuman et al. 2003, Stenzel et al. 2007). We modeled demographic rates for this study using the data from Monterey Bay breeders because the study at Monterey Bay was both long-term and intensive, the size of the breeding population was large relative to the U. S. portion of the DPS, and Monterey Bay's location sufficient variability in temperature and precipitation. We focused on modeling annual survival, breeding season length, and the annual number of fledglings per male as key elements through which temperature and precipitation might affect demographic rates.

To measure the effect of local winter weather conditions on annual survival, we fit Cormack-Jolly-Seber (CJS) mark-recapture models to May (our capture occasion) capture and sighting data with program Mark version 9.0. We compared different models within an information-theoretic framework (Burnham and Anderson 2003) using QAICc, the Akaike Information Criterion corrected for overdispersion and small sample size. We estimated over-dispersion using program MARK's median procedure and adjusted model outputs by the estimate. We modeled effects with a logit link function. The CJS mark-recapture model estimates "apparent" survival and cannot differentiate between that die and those that permanently emigrate. However, in these analyses individuals enter the sample after having bred locally during May, a central month of the breeding season. Breeding site fidelity has been

documented to be high among these breeders (mostly > 95% for males, Stenzel et al. 2011). Therefore, we believe these apparent survival estimates to be very close to true survival values.

We examined the sighting histories of banded males and females that bred in the Monterey Bay area during the month of May from 1984 to 2016 and extracted histories for 635 male and 584 female breeders that were found wintering in Recovery Unit 4, from 40 km south to 230 km north of the Monterey Bay area. We compiled encounter histories for those breeders starting with the first year in which they were found breeding in the Monterey Bay area in May and were known to be wintering in RU4.

To characterize conditions for each winter (November - February), we used weather data from Monterey Bay and from Point Reyes, approximately 170 km north. We suspected low temperatures or large storms to be the most likely weather conditions to negatively affect survival. Because the range between the minimum and maximum daily temperature was greater on Monterey Bay and precipitation amounts greater at Point Reyes, we used minimum and maximum daily temperature data from Monterey Bay and precipitation data from Point Reyes. For each year, we calculated the mean minimum daily temperature, mean maximum daily temperature, and mean daily precipitation. Suspecting that extreme events, particularly cold snaps, could have a greater effect than average conditions, we also calculated two versions of a cold score for each winter. The bases for the cold score were daily cold anomalies, consisting of 1) the number of degrees by which the minimum daily temperature did not exceed 2 °C, added to 2) the number of degrees by which the maximum daily temperature did not exceed 10 °C, only for days in which the minimum temperature did not exceed 2 °C. The basic annual cold score (ACS) was the sum of the daily cold anomalies from November through February. To include the effect of the duration of a cold event (as opposed to the same number of low temperature days occurring for only one day's duration), we also calculated a duration-amplified cold scores (DACS), in which we added to each day's cold anomaly one half the previous day's amplified cold anomaly. Each year ACS and DACS were calculated for both Monterey Bay and Point Reyes and the two locations summed for final scores so that cold events better reflected conditions in all of RU4 in winter.

We compared two competing global models in the mark-recapture analysis. Both global models included the following variables: sex, a linear trend through time, mean maximum daily temperature, and mean daily precipitation. We did not include mean minimum temperature to avoid collinearity between independent variables. One global model included the ACS and the other the DACS. With a model weight ~1.5 times higher for the DACS (0.61) than for the ACS (0.39), we proceeded with variable reduction using the DACS global model. We made detection time-dependent for all models.

We assessed how the beginning and end of the breeding season affected the length of the breeding season by examining dates of nest initiations at either end of the season, 1984 - 2016. Since the first nest initiation (date on which the first egg was laid) of a year was sometimes separated from subsequent initiations by as many as 11 days (Point Blue Conservation Science unpubl. data), we considered two dependent variables, the date on which the first nest of the season was initiated (first nest models) and the date of the onset of breeding (breeding onset models). We defined the onset of breeding as the first date on which at least three nests were initiated within a three-day period. We similarly defined the conclusion of nest initiations as the date the last nest was initiated after which there were no more than two nests in any subsequent three-day period. Thus, the onset to the conclusion of nest initiations includes all initiation dates except those we defined as outlying.

We examined all clutch initiation data up to 21 April from 1984-2016 to examine the effects of weather variables during the spring and prior winter on the timing of the breeding season start. We considered 13 predictor variables: the DACS of the previous winter and the mean daily temperature and daily precipitation for the following periods: November through January, February, March, 1-10 March, 11-21 March, and 22-31 March. We used linear regression in R (version 3.6.1, R Core Team 2016) to construct 13 single factor and four global models for each response variable, differing only by including temperature and precipitation for either all of March or one of the three periods in the month, because of generally high (> 0.6) correlations among some of the climate variables for these four periods.

We suspected that males whose first nests were earlier would fledge more young during a breeding season than males whose first nests were initiated later, because they would have more time to renest after failure and to double brood. Further, we suspected that first-time breeders would fledge fewer young in a season than older more experienced males. We explored models predicting the total number of young fledged in a breeding season, summed over all nesting attempts, by 715 known-age males from 1984 to 2016, using a mixed generalized linear model and selected the most parsimonious model by comparing AIC values in R (version 3.6.1, R Core Team 2016). Predictor variables included the clutch initiation date of the male's first nest for that year, the age of the male (0 = first-time breeder, 1 = second-time or older breeder), and random effects male identification and year, to account for differences in the qualities between different males and general differences between years in breeding success. With up to two successful nesting attempts possible for males and a modal clutch size of three eggs, the response variable, number of young fledged, varied between 0 and 6, (mean = 1.43, variance = 1.86, thereby slightly over-dispersed for a Poisson distribution and slightly zero-inflated). Therefore, to assess the most appropriate model structure, we fit models with an intercept and random effects male and year and compared Poisson, zero-inflated Poisson, negative binomial, and zero-inflated negative binomial errors. The best supported structure, zero-inflated Poisson, was used to examine the effect of the first nest date and age of the male.

4.2.1.4   Red-legged frog (*Rana aurora* and *R. draytonii*)

Study system: We combined data from two closely related and ecologically similar species for the purposes of this study, the California red-legged frog (*Rana draytonii*) and the northern red-legged frog (*Rana aurora*). We were particularly interested in California red-legged frogs, which are federally listed as threatened and are endemic to California and northern Baja California, Mexico. In California, their current distribution is primarily restricted the coast ranges from Riverside County to Mendocino County, with a few remnant populations in the Sierra Nevada. This species is managed on Vandenberg Air Force Base, Camp Parks, and Camp San Luis Obispo. However, because we could not quickly get the necessary federal permits to work with California red-legged frogs, we used northern red-legged frogs as a surrogate species, allowing us to collect a more robust data set. Northern red-legged frogs are identified as a Sensitive species in Oregon and a Species of Special Concern in California. They are found throughout the Pacific Northwest form Mendocino County, CA to British Columbia, Canada. There is a narrow zone of overlap in Mendocino County, CA, where breeding pools may support either species, both species, and hybrids of the two species (Shaffer et al. 2004). Both species breed in the still waters of ponds, marshes, and streams and can be found from sea level to about 1200 -1500 m elevation. For this report, we refer to the species complex comprising California red-legged frogs, northern red-legged frogs and hybrids as red-legged frogs.

We studied 11 populations of red-legged frogs at sites that vary in elevation from 2 to 1043 m and span a latitudinal gradient from approximately 34.5 to 44.4° N (Figure 4.2-3) in CA and OR. Of these, six sites support northern red-legged frogs (*R. aurora*), three sites support California red-legged frogs (*R. draytonii*), and two sites potentially support both species and/or hybrids (Shaffer et al. 2004). See Table 4.2-2 for details.
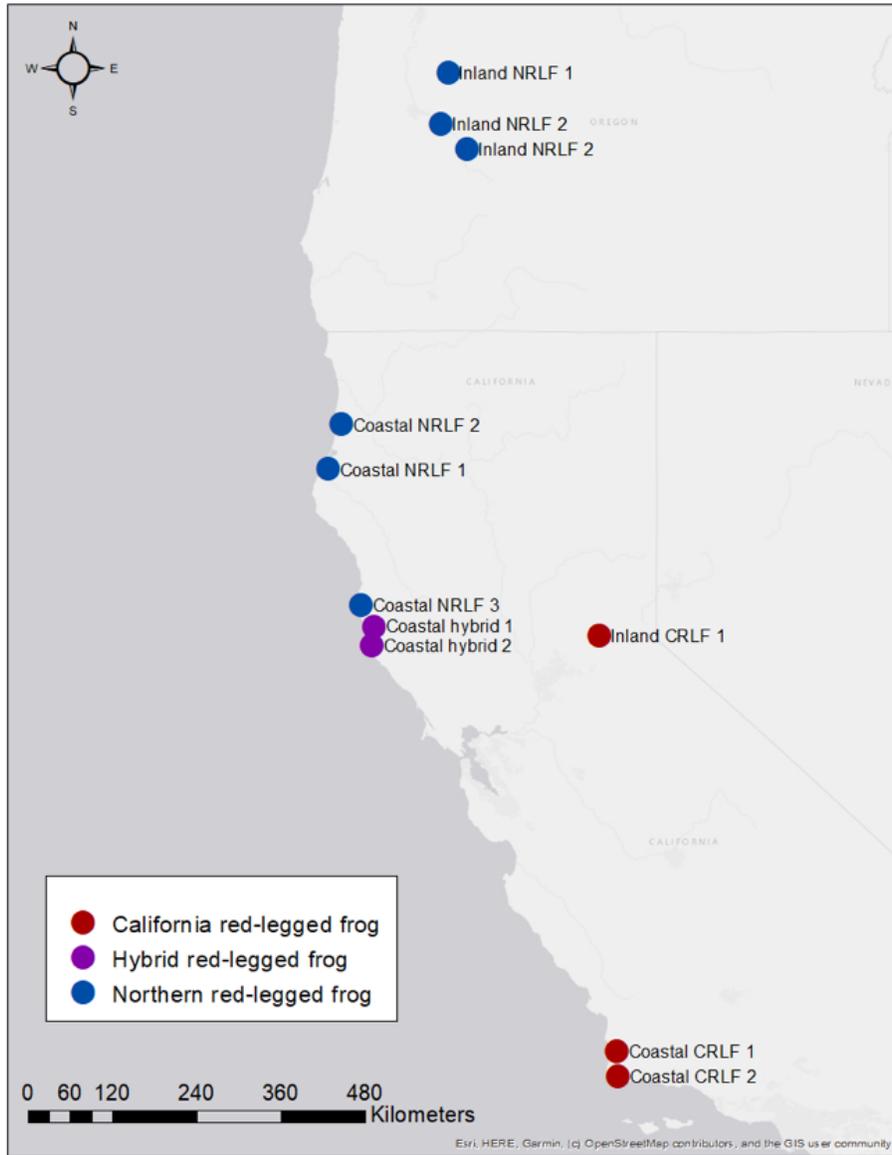
Figure 4.2-3 Red-legged frog study locations in California and Oregon.

Table 4.2-2. Red-legged frog study sites with the species, location, and breeding pool type listed, as well as which demographic rates were measured at each study site each breeding season. Demographic rates: F = Fecundity, E = Egg hatch rates, T = Tadpole survival, FL = Froglet survival, A = Adult survival. Sites are named by whether they were inland or coastal and which species of red-legged frog was there (NRLF = northern red-legged frog, CRLF = California red-legged frog).

Site	Species	Breed site type	2015-2016	2016-2017	2017-2018	2018-2019
Inland NRLF 1	*R. aurora*	Semi-ephemeral pond	F, T	F, E, T		
Inland NRLF 2	*R. aurora*	Ephemeral pond	T,	F, E, T,	E, T	
Inland NRLF 3	*R. aurora*	Semi-ephemeral pond	F, T, FL, A	F, E, T, FL, A	F, E, T, FL, A	A
Coastal NRLF 1	*R. aurora*	Ephemeral pond	F, A	F, E, A	A	F, A
Coastal NRLF 2	*R. aurora*	Ephemeral wetland	F, T, FL	F, E, T, FL A	F, E, T, FL, A	F, E, T, FL, A
Coastal NRLF 3	*R. aurora*	Semi-ephemeral pond	T, FL	F, E, A	F, E, T, FL, A	F, E, A
Coastal hybrid 1	*R. aurora/ R. draytonii*	Permanent ponds (3)		T, FL	E	
Coastal hybrid 2	*R. aurora/ R. draytonii*	Ephemeral pond		FL		
Inland CRLF	*R. draytonii*	Semi-ephemeral Ponds (6)			FL, A	F, FL, A
Coastal CRLF 1	*R. draytonii*	Stream			E	E
Coastal CRLF 2	*R. draytonii*	Stream			E	F, E

Demographic field methods: We estimated fecundity (number of eggs per mass) at each site by photographing a subsample of randomly chosen egg masses (typically >20 masses per site) in shallow containers and then counting the number of eggs in the photographs. To estimate the proportion of eggs that successfully hatched at each site, we placed 20-50 eggs collected from the same mass in predator excluded cages. We used eggs from a different egg mass for each cage and had up to 15 cages per site per year. The cages consisted of a plastic frame with three sides and the bottom covered by a fine (~1mm) fiberglass mesh to allow water flow and a mesh lid covering the top. The cages were attached to stakes within each breeding pond and positioned such that they were at a similar depth in the water column as the egg masses they were collected from. During the course of the 2017 breeding season, at one site we found a high number of eggs missing from containers and noticed that amphipods were able to enter the cages through the mesh sides. We confirmed our assumption that amphipods were preying on the eggs in the closed containers by adding cages with extremely fine mesh that excluded amphipods completely (Hudgens and Harbert 2019). We subsequently conducted plankton tows at all of our other study sites, and in 2018 we deployed amphipod free cages, in addition to the standard cages, at all sites where we observed amphipods.

We checked egg cages every 7-10 days through hatching and recorded the number of viable and non-viable embryos, and the Gosner stage of viable embryos (Gosner 1960). We opened cages once eggs reached stage 21/22 (just prior to hatching) to ensure tadpoles were free to leave the cages once hatched. We determined the proportion of eggs that successfully hatched (egg viability) based on the number of viable embryos observed during the survey when we removed container lids.

We used mark-recapture methods to estimate survival rates for tadpoles, recently metamorphosed froglets, and adults. We used visible implant elastomer (VIE; Northwest Marine Technology, Anholt 1998, Grant 2008) tags to identify individual animals for mark-recapture analyses. The marking procedure involved injecting the fluorescent polymer just under the skin using a 0.3 cc insulin syringe. We also used photos as a secondary method of identification for tadpoles and adults that lost tags (froglets we caught did not have distinct enough markings to use for photo identification). We took photos of every capture and when a recapture was missing one or more tags. We typically visually determined the identity of individuals with missing tags, however in the few cases where the number of possible individuals was large, we used the Interactive Individual Identification System (I^3S) program (Van Teinhoven et al. 2007) to assist with identification.

We marked tadpoles once they reached a total body length >35 mm using unique color combinations of four VIE tags, two on either side of the tail, and also photographed the left side of each tadpole we marked. Prior to tagging, we recorded the total length, body size from the tip of snout to junction of the body and tail at the midline, categorical development stage (hind limb buds, hind legs, front limb buds, front legs) and any injuries or deformities. To reduce the risk of injury during the tagging procedure, we anesthetized tadpoles using a solution of Tricaine methanesulfonate (MS-222; Cecala et al. 2007), in an immersion bath using established protocols (Anholt 1998, USGS National Wildlife Health Center). Tagging methods are descried in further detail in McHarry et al. (2018). Capture-recapture surveys were conducted 1-3 times/week during the time tadpoles were in breeding ponds.

Because recapture rates were extremely low in open ponds, we confined tadpoles to mesocosms maintained within each pond in areas where tadpoles were regularly observed. From 2017-2019, we used 2 m x 4 m mescosms constructed of drift fence, which allowed water to freely pass but prevented tadpole escape. Mesocosms were larger and irregularly shaped in 2016. Most aquatic predatory invertebrates, birds, and snakes could access mesocosms. We left the pond vegetation intact within each mesocosm to provide refugia from predators and surfaces for algae and bacteria (the primary sources of food for tadpoles) to grow on. If pond drying led to water levels in a mesocosm dropping below 10 cm, we lifted the bottom of the drift fence, which was buried or weighted with gravel bags, to allow any tadpoles that had not yet metamorphosed out to swim to deeper waters.

We tagged froglet and adult red-legged frogs on the feet in the webbing between the toes. We used four tags in total, with two on each foot in a unique color combination. We did not anesthetize froglets or adults because we were able to secure them safely for tagging without causing injury and we wanted tot to minimize the risk of anesthesia induced mortality. We also photographed the right inner thigh of each adult, where markings are pronounced, and recorded the snout vent length (SVL) and the presence of injuries or deformities.

Fitting Relationships between demographic rates and climate variables: We assessed the effects of temperature and precipitation on fecundity (number of eggs per mass), egg hatching success, egg development rates, and tadpole survival. We deployed HOBO Pro data loggers (Onset Computer Corporation, Bourne, MA, USA) to record the water and air temperature at each site. Because projections of future water temperatures were not available, we used air temperatures at the site when fitting climate-demographic rate relationships to be used in SEED models. Unless specified otherwise, all temperature data were taken from the HOBO Pro data logger collecting air temperatures. We downloaded precipitation data for each site from the gridMET database (Abatzoglou 2013). Daily minimum, maximum, and mean temperatures are often highly

correlated, so for analyses described below we only included one measure of temperature at a time in our models.

To test the effects of climate on fecundity, we used generalized linear models (stats package in R 3.3.3; R Core Team 2017) to evaluate the effects of total rainfall (mm) for one calendar year prior to the onset of breeding, total rainfall from June 1 to November 30 prior to onset of breeding, total days of measurable rainfall from June 1 to November 30, and total rainfall during the previous breeding season (October 1 to March 31) on the number of eggs per egg mass. All of the precipitation variables were highly correlated, so we only included one in the model at a time. We also included species (*R. aurora* vs. *R draytonii*), and either site or the average snout vent length (SVL) of females at each site in our models. We used SVL data that we collected at all of our sites, except for one site, Coastal CRLF 2, where we did not work with adults. We obtained SVL data for *R. draytonii* on Vandenberg Air Force Base (where Coastal CRLF 2 is located) from biologists at ManTech SRS Technologies, Inc.

We evaluated the effects of climate on egg viability using data from the predator excluded egg cages. We used binomial mixed models, with cage and female as random effects and site as a fixed effect, to test the effects of mean, minimum, and maximum daily water and air temperature from the time eggs were placed in egg cages until they hatched, cumulative season precipitation from September 1 through the time that eggs hatched in each cage, and cumulative precipitation from the prior water year (October 1 to September 30) (MCMCglmm package in R Studio v1.2.1335, R Studio Team, 2018, Hadfield 2010). Using our best performing climate model, we also explored if there were any effects of frog species (*R. aurora* vs. *R. draytonii*) or interactions between species and climate.

We used generalized linear models (stats package in R 3.3.3; R Core Team 2017) to test the effects of water temperature on egg development rates. In this analysis we used water temperature rather than air temperature because egg development rate was not included in our SEED model.We used data from the predator free egg cages and considered development time to be the number of days from being placed in cages to hatching. We excluded any cages were eggs were greater than stage 12 when placed in the cage.

We used ordinal regression models to evaluate the effects of daily mean temperatures and cumulative growing degree days (GDD) on tadpole development rates of marked tadpoles recaptured at least once. The regression models estimated the probability of remaining in the same developmental stage or transitioning one or multiple stages between captures given the number of days between captures, starting stage, number of days since the start of the breeding season, and mean temperature or GDD. We considered all tadpoles to be in one of seven stages based on leg development: no leg buds present, hind leg buds present, hind feet present, hind legs present, front leg buds present, front legs present, or froglet. Even though tadpoles are a fully aquatic life stage, we used air temperatures in these regressions to facilitate using them to link projected air temperatures from global climate models to development rates in our SEED models.

We used Cormack-Jolly Seber models to evaluate the effects of climate variables on tadpole, froglet, and adult survival ('RMark' package in R and Program MARK; White and Burnham 1999, R Core team 2017) of animals marked in 2016 - 2018. We separated animals from different sites or different years into different groups such that each group represented a single site x year combination. For tadpoles, we also put animals in different mesocosms within each site into separate groups, so tadpole groups represented different mesocosm x year combinations. We estimated survival in terms of daily intervals for tadpoles, monthly intervals

for froglets, and quarterly intervals for adults. If there were multiple surveys at a site within the same interval, we combined capture data from the surveys, such that if an animal was captured or recaptured during any survey it was recorded for that interval. In order to account for numerous unmeasured factors potentially effecting animal catchability, we modeled detection probability as a function of the number of animals captured during all occasions sampled during an interval. This resulted in the capture probability for any animal in a group that was not sampled during a given interval being equal to 0, since no animals could have been caught. We evaluated the possible effects of several climate variables on survival for each life stage. For tadpoles we evaluated: daily minimum, mean, and maximum air temperatures, total winter precipitation, and combinations of precipitation and each temperature variable. For froglets we evaluated: the monthly average daily minimum, mean, and maximum temperature, monthly precipitation, cumulative monthly precipitation since April 1, total annual precipitation during the previous water year (October 1 of the previous year through September 30 of the year when a froglet was tracked) and total precipitation during the previous two water years. We also tested each combination of minimum temperature, maximum temperature and the precipitation variables. For adults, we evaluated quarterly mean daily minimum, mean and maximum temperature, quarterly precipitation, and all combinations of one temperature variable plus quarterly precipitation.

Experimental tests of environmental effects: Predicting how changing climate conditions will influence population growth rates of managed species is only the first step to planning future management needs. We conducted a set of experiments with red-legged frogs to address a few of the additional factors that will likely influence future management decisions for this taxon. First, we addressed the issues of how multiple stressors might interact to influence red-legged frogs through two sets of experiments. In the first experiment, we simultaneously varied pool drying rates, the presence of an invasive competitor widely recognized as a threat to red-legged frogs, and temperatures experienced by tadpoles. We used these experiments to evaluate how invasive species might influence responses to climate change and to ask if increased temperatures either mitigated or exacerbated the effects of shortened hydroperiods often associated with warmer spring and summer conditions. In a second experiment, we manipulated canopy cover experienced by tadpoles at several of our study sites to ask if 1) the effect of canopy cover on red-legged frogs varied among sites in a way that indicated a climate influence, and 2) habitat management at breeding pools could have a large enough effect on egg and tadpole survival to influence population growth rates. The results from these experiments were not included in the SEED models for this species.

Hydroperiod, invasive species, and temperature experiment: We used experimental mesocosms to explore the influence of climate and non-climate related stressors on the performance of northern red-legged frog early life stages. We tested direct effects of climate by elevating the air and water temperatures experienced by developing tadpoles and potential indirect effects of climate by shortening hydroperiods. Hydroperiods, or the length of time that an ephemeral breeding pond holds water, can be influenced by a variety of factors including precipitation, temperature, soil characteristics, and emergent vegetation. We also evaluated the effects of an introduced species known to influence red-legged frog populations. American bullfrogs (*Lithobates catesbeiana*) are listed among the top 100 world's most invasive alien species by the IUCN (Lowe et al. 2000) and have been identified as threats to native amphibians worldwide (Kats and Ferrer 2003, Kiesecker 2003). Bullfrogs are invasive in the western U.S. and threaten red-legged frogs through a variety of mechanisms including direct competition and predation,

causing behavioral changes that reduce tadpole foraging efficiency, and increasing the spread of pathogens (Kiesecker and Blaustein 1997, Lawler et al. 1999, Kiesecker et al. 2001, Yap et al. 2018).

We designed a 6 x 3 multi-factorial mesocosm experiment to determine how shortened hydroperiods and bullfrog presence affect northern red-legged frog tadpole survival and froglet size post metamorphosis. We had three bullfrog treatments 1) northern red-legged frog tadpoles only (control) 2) northern red-legged frog and bullfrog tadpoles separated by a permeable divider (signal) or 3) northern red-legged frog and bullfrog tadpoles together without divider (direct). This design allowed the separation of the direct effects of bullfrogs via competition and indirect effects due to behavioral changes in response to bullfrog presence. For each bullfrog treatment we applied six hydroperiod treatments, and we had two replicates of each bullfrog x hydroperiod treatment combination. We implemented the hydroperiod treatments by varying the date at which the mesocosm began drying down, (i.e. all mesocosms dried at the same rate but how soon they began drying varied). We had 12 additional mesocosms with only northern red-legged frog tadpoles that were warmed above ambient temperatures using greenhouse lids. We had two replicates of each of the six hydroperiod treatments with the warming lids, which could be compared to the control mesocosms from the factorial bullfrog experiment to look at the interactive effects of temperature and hydroperiod on northern red-legged frog tadpoles. We deployed two HOBO Pro data loggers in each mesocosm; one in the water near the bottom of the tank to measure water temperature and one attached to the underside of the lid to measure air temperature.

The mesocosms consisted of 150-gallon water stock tanks housed at the Institute for Wildlife Studies' (IWS) property near Fieldbrook, California. Each tank had a capacity of 567 l (approximate dimensions: 99.06 cm x 147.32 cm x 60.96 cm). We arranged the tanks in a 6 x 7 grid, separated by approximately 2 m, and covered each tank with a screen or plastic lid to exclude predators and prevent animals from escaping. Prior to introducing northern red-legged frog egg masses and bullfrog tadpoles, we allowed each tank to fill with rainwater during the fall and winter season and added plant material (dead cattails and grasses) from our Coastal NRLF 2 study site (the egg collection site) to provide refuge and food resources. We measured temperature, pH, dissolved oxygen, nitrites, phosphates, ammonia, and alkalinity in each tank at initial set up and monthly thereafter in order to ensure tadpoles were being kept in a healthy environment based on standard captive amphibian care guidelines (Odum and Zippel 2008). All tanks started the experiment with water depths of 50 cm, and we maintained this water level in each tank until we initiated drying.

We seeded each tank with 80 - 170 northern red-legged frog eggs that came from 10 egg masses collected from our Coastal NRLF 2 study site. We placed eggs in floating cages to maintain thermoregulation and facilitate counting unviable eggs and hatchlings. We released tadpoles into the main tank as they hatched. We constructed refuge cylinders from hard plastic fencing with ½ inch square openings and placed one in each bullfrog tank to allow newly hatched northern red-legged frog tadpoles to enter the cylinder while restricting bullfrog tadpoles access. We added 10 bullfrog tadpoles to each direct and signal treatment 33 days after we seeded the tanks with northern red-legged frog eggs. In the direct treatment, bullfrog tadpoles had access to the whole tank and could interact directly with northern red-legged frog tadpoles. In the signal treatment, bullfrog tadpoles were confined to a mesh cage (35.56 cm x 35.56 cm x 67.31 cm) placed within the tank. The permeable material of the mesh cage allowed for the exchange of water, nutrients, and chemical cues.

We based the drying rate for the hydroperiod treatments on water depth data from the Coastal NRLF 2 site in 2018. We did not completely dry out the tanks, so that any remaining tadpoles that did not metamorphose could be euthanized humanely at the end of experiment. We considered any tadpoles remaining three days after the water level reached 3 cm as mortalities for our survival analyses. The drying rate was constant across the six hydroperiod treatments, but the date of initiation of draw-down varied such that the total number of days from the beginning of the experiment to final drying varied from 87 to 147 days in increments of 10-12 days for each treatment (Figure 4.2-4). The longest hydroperiod treatment (147 days) was designed to completely dry down at the same time of the year that most of pond at Coastal NRLF 2 dried out in 2018 (early July). We maintained the appropriate water level in each tank by drilling holes in standpipes or by adding stored rainwater when to compensate for water lost to evaporation.
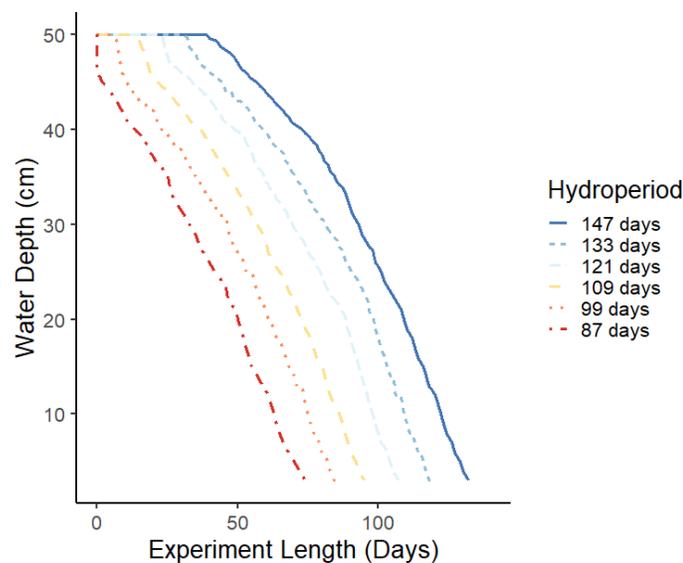
Figure 4.2-4. Hydroperiod treatments for captive experiment. Drying rate is the same across all hydroperiod treatments and shortened by changing the start day of water draw down.

Due to concerns about tadpole size, we began administering algae and spirulina tablets (Aquatic Foods Inc., United States) to all tanks on day 70 of the experiment. We gave half of the tanks twice as many tablets to see if food resource availability affected interactions between northern red-legged frog and bullfrog tadpoles. We randomly assigned the low and high food treatments to all tanks.

We measured two response variables in this experiment: survival through metamorphosis and froglet size post metamorphosis. We considered successfully metamorphosed individuals (froglets) to be any individual with all limbs fully developed, mouth down turned, and tail fully absorbed by the final draw-down date. We measured the froglet's snout vent length (SVL) as measure of body condition. For the analyses related to the bullfrog portion of the experiment, we used data from 29 of the 36 tanks for analyses because seven tanks experienced complete die offs prior to the end of the experiment. The die off occurred in all six of the 121-day hydroperiod treatments, which had the lowest water level at the time of the die off, and one control tank in the 147-day hydroperiod treatment. The die off was likely caused by unusually warm temperatures experienced for three consecutive days in June, which caused water temperatures in the effected

tanks to reach nearly 35 ℃. We conducted analyses related to temperature both with and without the die-off tanks included.

To look for effects of bullfrog treatment, hydroperiod, and food addition on survival through metamorphosis we used logistic regression with a quasibinomial distribution to account for overdispersion (Warton and Hui 2011). The three shortest hydroperiod treatments (87, 99, and 109 days) ended before any tadpoles completed metamorphosis (0% survivorship). With all hydroperiod treatments included there was clearly a strong effect of hydroperiod on survival, but our ability to detect effects of bullfrog treatments or food was hindered by the complete mortality in fast drying tanks. Therefore, we also ran the analysis with a truncated dataset where we excluded the shortest three hydroperiod tanks.

We analyzed the interactive effects of bullfrog treatment, hydroperiod, and food availability on size at metamorphosis (SVL) using linear mixed-effects models with tank as a random variable using the lme4 package in R (Bates et al. 2012). All analyses were performed in R Studio (R Studio Team, 2018). We used the Akaike information criterion (AICc) or overdispersed modification of AICc, QAICc, both corrected for small sample size, to compare models for each analysis (Burnham and Anderson 2002) with the MuMIn package (Bartoń 2019).

To examine the effects of temperature on survival through metamorphosis and size at metamorphosis we used data from the control tanks in the bullfrog experiment and the warming top tanks. We used logistic regression to assess the effects of average daily minimum, maximum, and mean air temperature in each tank over the course of the experiment, the maximum air temperature experienced anytime during the experiment, hydroperiod, and food availability on survival through metamorphosis. We also included a temperature by hydroperiod interaction in our models. Because all of the temperature measures were highly correlated, we only included one measure of temperature at a time in the models. We used air temperature from the tanks because 1) we had found that air temperature was a stronger predictor than water temperature of tadpole survival in the field, and 2) climate models project future air temperatures but not water temperatures. We ran the analysis with and without die off tanks included as well as with and without hydroperiods with zero survival included.

For size at metamorphosis (SVL), we used growing degree days (GDD) as our measure of temperature. There is a long history of using GDD for explaining patterns of growth and development in plants, insects, and other ectotherms (e.g. Seamster 1950, Atkinson 1994, Bonhomme 2000). We calculated GDD using the daily minimum and maximum air temperature recorded in each tank for the first 95 days of the experiment using the single sine method (Zalom et al. 1983) We used two specification of D_{min} and D_{max}: 1) 10 and 30 ℃, 2) 15 and 35 ℃, and tested each to see which performed better in our models. In addition to GDD, we tested the effects of hydroperiod, food availability, and development time (days to metamorphosis) on froglet SVL using mixed-effects models with tank as a random variable in the lme4 package in R (Bates et al. 2012). We also explored the effects of GDD, hydroperiod, and food availability on larval development time (days to metamorphosis) using the same analytical methods.
We performed all analyses in R Studio (R Studio Team, 2019) and used AICc to compare models for each analysis (Burnham and Anderson 2002) with the MuMIn package (Bartoń 2019).

Effects of canopy cover: We conducted a short-term (single breeding season) field experiment to test the effects of canopy cover on egg and tadpole survival. Conservation efforts for pond-breeding amphibians often focus on improving breeding habitat. Habitat modifications have the

potential to influence population growth rates directly and potentially indirectly through interactions with other environmental variables. For example, canopy cover surrounding breeding ponds might influence pond water temperature via shading, and potentially buffer aquatic early life stages from warming air temperatures. Studies have shown that canopy cover can influence tadpole growth and survival in several anuran species, with more open canopy conditions typically benefiting tadpoles (Werner and Glennemeier 1999, Skelly et al 2002, Thurgate and Pechmann 2007). We investigated the effects of canopy cover surrounding breeding ponds on egg viability and tadpole survival rates at five of our northern red-legged frog sites.

To assess the impacts of canopy cover on egg viability we used the same egg cage study design described previously, but placed sets of paired cages in relatively shaded (closed canopy) and relatively open (open canopy) areas of each breeding pond at four sites during the 2017-18 breeding season. We estimated in the amount of average monthly solar exposure the shaded and open portions of the pond received using a Solar Pathfinder™ device (The SolarPathfinder Company, Linden, Tennessee, United States of America). We tested the effects of canopy cover on egg hatching success using logistic regression with a quasibinomial distribution to account for overdispersion (Warton and Hui 2011). We include canopy cover, site, and interactions between site and canopy cover as our explanatory variables. We assessed relative model performance using QAICc, the overdispersed modification of AIC corrected for small sample size (Burnham and Anderson 2002). We used the stats and MuMIn packages in R Studio (R Studio Team, 2018, Bartoń 2013).

For tadpole survival we placed drift fence enclosures (mesocosms) in relatively shaded and relatively open areas of each breeding pond at five of our northern red-legged frog sites during the 2015-16 breeding season. We used the mark-recapture methods described previously to estimate tadpole survival in each canopy treatment. We tested models that assumed that tadpole survival was a function of site, canopy treatment, and temperature. We also tested models with interactions between canopy cover and site, and canopy cover and temperature. We assessed model performance using Akaike information criterion corrected for small sample size (AICc) (Akiake 1973, Burnham and Anderson 2002)

To determine if canopy cover had an effect on discrete population growth rates (λ) through its influence on egg viability or tadpole survivorship, we created pre-breeding stage-based matrices (Lefkovitch 1965). The matrix transition elements were calculated from 10 total parameters (Table 4.2-3). Six of those parameters (proportion of adult females breeding, eggs per mass, egg hatch success rate, tadpole daily survival, tadpole stage length, juvenile survivorship, froglet survival) contributed to a single transition rate describing fecundity and first year survival. The transition elements were either estimated directly from the data in this study or taken from Licht (1974). We created two sets of matrices for each site that had non-overlapping 95% confidence intervals in either egg hatch success or tadpole survivorship between canopy treatments. These matrices differed only in the value of the parameter that was affected by canopy cover at the site. Each set of matrices included one matrix using the best estimate of the demographic rate, and two matrices using associated lower and upper confidence limits, respectively.

To determine the relative contribution of different life stages to population growth, we performed an elasticity analysis (Caswell 2000). We calculated elasticities analytically using eigenvalues and eigenvectors (de Kroon et al. 1986), in the R software program version 3.4.0 (R core team 2017). Elasticities were evaluated using a matrix with the mean value of the combined

early stage transition rate, for the mesocosms/site combinations included in the population growth rate analysis.

Table 4.2-3. Basic matrix showing parameterization for transition rates. The six parameters contributing to the early life stage transition rate are: F_b = proportion of adult females breeding, E_m = eggs per mass, H = egg hatch success rate, S_h = recruitment into tadpole population, S_d = tadpole daily survival, n = tadpole stage length (days), and FL_s = froglet survival. The later life stage transition rates are: $J1_s$ = $J2_s$ = juvenile survivorship, and A_s = adult survivorship

	J1	J2	A
J1	0	0	$(F_b * E_m)* [(H * S_h) * (S_d^n) * FL_s]$
J2	$J1_s$	0	0
A	0	$J2_s$	A_s

4.2.1.5 Alaskan douglasia (*Douglasia alaskana*)

Study system: The Alaskan douglasia is a perennial alpine plant with leaves occurring in one to three rosettes with fruits presented on short (<15 cm) peduncles. Its occurs in alpine scree on ridgelines and mountaintops in Southwest Alaska. Alaskan douglasia populations are typically small, ranging from 4-300 individuals in our study. The species is uncommon, with a very small fraction of seemingly suitable habitat occupied. Individuals drop seeds within 30 cm of the parent plant into unvegetated scree fields. The species is partially semelparous, with most (775/987) individuals dying after reproducing.
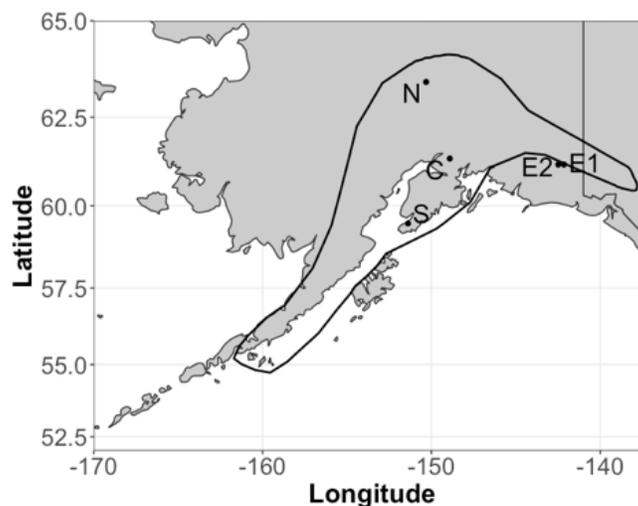
Figure 4.2-5. Map of South Central Alaska in grey, with the approximate range of Alaskan douglasia indicated by the black polygon (Hulten). Populations used in this work are indicated by dots, and the labels of populations correspond to those of other figures. E2 and E1 are offset from one another to allow readability.

Demographic field methods: To quantify response of Alaskan douglasia to climate, we conducted a demographic survey at five populations (Figure 4.2-5) over one transition interval. In 2016, we marked and mapped 56-196 individuals at two populations, measuring size and number of fruits of each individual. We returned in 2017 to score survival and measure size and

number of fruits. In 2017-2018, we repeated these procedures on three additional populations, with 218-383 individuals marked and mapped at each population in 2017. From the 2016-2018 interval, we obtained five population x years of data with 1162 individual x years of data. We derived six demographic rates from these data: annual survival, mean size after one year of growth, variance in size after one year of growth, probability of fruiting, and number of fruits given fruiting. We also estimated seedlings per fruit in the prior year by counting all seedlings within a 15 cm radius the year after an individual fruited at four of these five populations. At each population, we deployed 1-2 temperature loggers (iButtons) to measure local temperature variation over the period of our study. We buried these temperature loggers ~5 cm underground, and used the resulting data to obtain mean monthly temperature for every month (besides July, for which we were missing data from some populations).

Fitting Relationships between demographic rates and climate variables: To estimate the timing of snow-free periods, we combined projections of temperature and precipitation with satellite images of daily snow cover at each of these populations from the Moderate Resolution Imaging Spectroradiometer Dataset (MODIS; Hall and Riggs 2016). Specifically, we estimated months of snowmelt and snowfall using the Daily Snow Cover MODIS dataset for 2007-2018. We used the month of the first observation of zero daily snow cover to estimate month of snowmelt, and the month of the last such observation to estimate month of snowfall. We then obtained downscaled projections of monthly average, minimum, and maximum temperatures for five global circulation models from the CMIP5/AR5 models from the Scenarios Network for Alaska and Arctic Planning group (SNAP). Delta downscaling used CRU CL v. 2.1 climatological datasets from 1961-1990 as the baseline, generating 2 km x 2 km spatial resolution climate projections from 2006-2099 (Scenarios Network for Alaska and Arctic Planning, University of Alaska). We then determined the relationship between timing of snowmelt and snowfall and climate using a model selection approach. We regressed 2007-2018 month of snowfall and 2007-2018 month of snowmelt on total annual precipitation, mean annual monthly temperature, and their interaction, using a model selection approach to select a best-fit model (temperature and precipitation projections were averaged across the five GCM's). We then used this best performing model to predict snowmelt dates and snowfall dates for all subsequent analyses. For all analyses, we defined each year by the August 1 to July 31 interval; for example, to estimate precipitation in 2018, we calculated cumulative precipitation from August 1 2017 - July 31 2018.

We synthesized our iButton temperature and SNAP data into six metrics of 2015-2018 climate at each population: 1. average annual temperature; 2. average snow-free season temperature; 3. average snow-covered season temperature; 4. coldest month temperature; 5. hottest month temperature; 6. annual precipitation. We determined the identity of the coldest and hottest month from the average monthly temperatures across the five GCMs and determined the identity of the snow-free months and snow-covered months using the MODIS regression described above. Recall that we were missing iButton data for July, which was often the hottest month; thus, we used the predictions of the SNAP data for the temperature of the hottest month (averaged across GCMs). We calculated cumulative annual precipitation using the mean predicted annual precipitation across the five GCM's. We determined the identity of the coldest and hottest month from the average monthly temperature across the five GCMs and determined the identity of the snow-free months and snow-covered months using the MODIS regression described above.

We assessed the impact of these climate metrics on demographic rates using a model selection approach. For mean log size after one year of growth, log variance in size after one

year of growth, probability of fruiting, and log number of fruits per size, we tested all possible subsets of a global model with log size in previous time step, average annual temperature, cumulative annual precipitation, and the interaction of average annual temperature and cumulative annual precipitation as predictor variables. We used AICc to select a best performing model, correcting for collinearity as described in the next paragraph. We repeated this process for four other global models: 1) snow-covered season temperature and precipitation, 2) snow-free season temperature and precipitation, and 3) coldest and 4) hottest month temperatures and precipitation, testing the best performing model from each of these five comparisons against each other using AICc. We used the resulting best performing model in subsequent analyses. We used a linear model for all demographic rates besides probability of fruiting, for which we used a general linear model with a binomial distribution.

We modified our model selection approach for probability of survival, which likely depends on both climate variables over the year of interest as well as probability of fruiting in the year prior (which itself depends on the climate conditions the year before the year of interest). Specifically, we tested the same five global models as described above, but also allowed these models to have terms for coldest month temperature and precipitation in the year prior, as well as an interaction between log size in the year prior and coldest month temperature, and between log size in the year prior and coldest month precipitation. Coldest month conditions affected the probability of reproduction; thus, we allowed for lagged effects of these climate variables on probability of survival. Note that climate variables in the year prior were transformed into population-specific climate variables using the differences between SNAP and iButton data. Specifically, the SNAP temperature data could differ from the iButton temperature data due to elevation of the population, insolation, or other microsite characteristics; thus, we converted the prior years' SNAP projections into predictions of local temperature using the population-specific differences between the SNAP and iButton temperature data for the first four metrics of climate.

We ensured our best performing model was robust to collinearity among predictor variables. Freckleton (2011) shows that information theoretic approaches are largely robust to collinearity, with the exception of correlated variables that have quite different effect sizes. For all best performing models with linear predictor variables correlated at $|R| > 0.6$, we ensured that the absolute value of the coefficient estimates of correlated predictor values (a rough estimate of their true effect size) were similar to one another (ratios of coefficients were $<= 3$). If ratios of coefficients differed by more than a factor of three, we replaced the best performing model with the next best model with a coefficient ratio $<= 3$ (or with no correlated predictor variables). Note that the approach outlined here uses conservative cutoffs, according to Freckelton's analysis of simulated data.

4.2.1.6   Venus flytrap (*Dionaea muscipula*)

Study system: Venus flytraps are endemic to North and South Carolina and occur primarily in mesic savannas, usually dominated by longleaf (*Pinus palustris*) or pond pine (*Pinus serotina*). Tree-ring records indicate fire return intervals (FRIs) of one to two years throughout the majority of its range prior to European settlement (Frost 1998). Some of our study populations are currently subjected to prescribed burning, with target FRIs dictated by threatened and endangered species in the area, but FRIs vary widely among our study populations, and likely among all extant populations. Venus flytraps are carnivorous, consuming small insect prey to alleviate nitrogen limitation in the sandy, waterlogged soils in which it grows. They are small in stature relative to most other plants in the community, which likely limits both light and prey acquisition, and could impede access by its insect pollinators (Youngsteadt et al. 2018). They are

42

moderately long-lived, survive fire, and regrow quickly following either fire or mechanical disturbance. Lack of recruitment immediately following a reproductive-season fire demonstrates the absence of a multi-year seed bank.

Demographic field methods: We measured demographic rates at two populations in each of three regions spanning the East-West axis of the historical range of Venus flytraps. The study populations were within 2 km of each other within each region (Figure 4.2-6). In the middle of June in 2015, at each population, we searched exhaustively for all plants within areas of a high density of Venus flytraps. We mapped, marked, and measured ~300 individual plants in each population, measuring number of leaves, length of longest leaf, and number of fruits for each individual. In all subsequent analyses, we use as a metric of plant size ln(number of leaves x length of longest leaf), where number of leaves x length of longest leaf correlates well with total leaf area (Appendix 8.3). In the middle of June each year until 2018, we scored survival of the marked plants and remeasured survivors. To estimate seedlings per fruit (recruitment), we searched exhaustively for all unmarked plants within 25 cm x 25 cm quadrats containing fruiting plants in each population in 2018. We then divided the number of seedlings per area by the number of fruits per area in the previous year to obtain seedlings per fruit. We synthesized our data into six demographic rates: annual survival, mean and variance in plant size after one year of growth, probability of producing fruits, number of fruits given a plant produced fruits, and seedlings per fruit. All demographic rates other than seedlings per fruit were size-dependent.
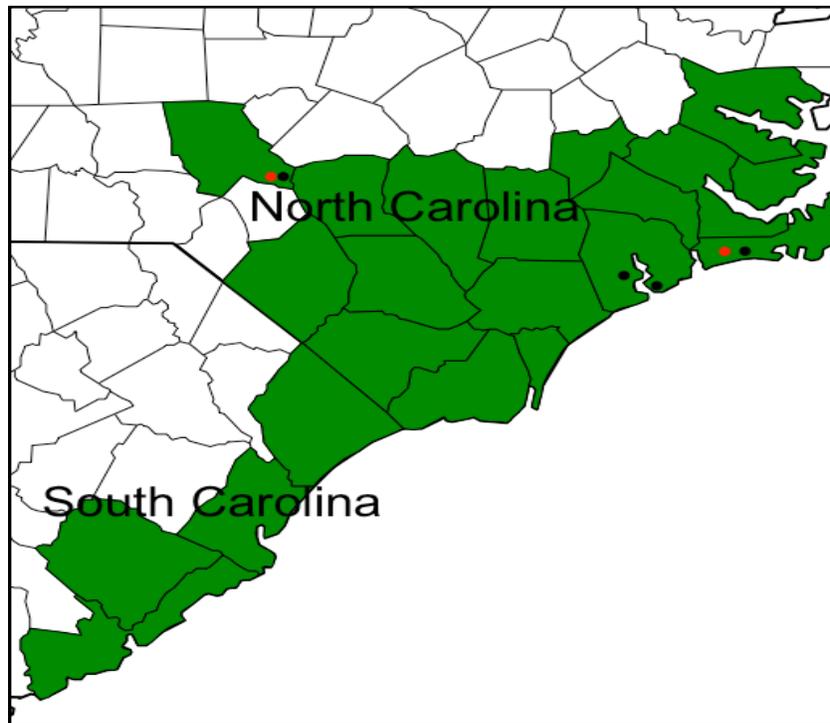
Figure 4.2-6. Counties in North and South Carolina where Venus flytraps were found historically are shown in green (United States Department of Agriculture 2019b). We also show approximate locations of our populations using points; populations indicated by red points included both observational and experimental work, whereas populations in black only included observational work.

In each population and year, we quantified temperature, precipitation, and years since most recent fire. To quantify local soil temperature, at each population we deployed two temperature loggers (iButtons;

https://www.maximintegrated.com/en/products/ibutton/ibuttons/index.cfm) enclosed in a plastic container and buried 5 cm underground immediately adjacent to our marked plots. We also obtained regional estimates of temperature and precipitation from gridMET (Abatzoglou 2013) for each population and year, averaging minimum and maximum daily temperatures to estimate mean daily temperature. We quantified years since most recent burn either by direct observation during our censuses or using records of burn history available from land managers.

Due to iButton failure, we had short time periods of missing local temperature data. To fill these gaps, we regressed mean daily local temperature on mean daily regional temperature and the square of mean daily regional temperature for each population, and then used the fitted regressions to predict any missing local daily data (correlations between local and regional temperature estimates were high and AICc supported a quadratic term). We conducted the same procedure for daily maximum and minimum temperatures.

Experimental tests of fire effects: To parse the role of the three key effects of fire (neighbor removal, ash addition, and tissue damage) on how climate influences fire responses in Venus flytraps, we conducted an experimental manipulation of the first two effects (addition of ash-derived nutrients and removal of competitors) and quantified the effects of an accidental burn (allowing us to see any additional effects of tissue damage). In 2016, at two of our populations (one in the cooler inland region and one in the warmer coastal region; Figure 4.2-6), we marked and measured additional plants in 12 50 x 50 cm quadrats (127 plants in the coastal; 194 in the inland population). We randomly assigned each quadrat to one of three conditions: 1) unmanipulated control; 2) ash addition; or 3) ash addition and neighbor removal. In the latter two treatments, we manually removed above-ground vegetation every year in June, and to the last treatment, we also added enough ash annually, collected from nearby recently burned areas, to mimic the amount of ash deposited during a fire.

We remeasured these plants annually at both populations, repeating these experimental manipulations. Specifically, for both our ash addition conditions, ash was added annually in June at the inland population and in October at the coastal population (a fire just before the June 2016 census at the coastal population had left sufficient ash). At our inland population, we measured demographic rates in 2017 and 2018 and measured recruitment in 2018 using the same protocol outlined above. In 2018, we did not resurvey control plots, so we used demographic rate data from our demography study as the control condition over the 2017-2018 interval. For our coastal population, we measured all demographic rates outlined again in 2017. Fortuitously, at the coastal population, an accidental burn (most likely caused by hunters) occurred over the 2017-2018 interval. To take advantage of this burn as a way to quantify effects of plant damage, we combined our experimental data from 2016-2018 (inland population) or 2016-2017 (coastal population) with our 2017-2018 observational data from the coastal population, coding data from the burn as a fourth condition in our statistical analyses, and used this combined dataset in subsequent analyses.

Fitting Relationships between demographic rates and climate variables: We synthesized climate data for each year x population combination during 2015-2018 into a series of regional and local climate variables, which were estimated across the entire year and over extreme (driest, wettest, coldest, and hottest) months of the year. We identified extreme months using regional temperature and precipitation data from analogous climate data from the historical period (1979-2018). In all analyses, we assume a survey date of June 15, with months beginning and ending on the 15th of each month. We estimated the mean of the daily mean temperatures over the entire year, the maximum of the daily mean temperatures in the hottest month (July 15- August 14), the

44

minimum of daily mean temperatures in the coldest month (January 15- February 14), and the mean of the daily mean temperatures in the driest (December 15- January 14) and the wettest (August 15- September 14) months, for both local temperatures (derived from iButtons) and regional temperatures (derived from gridMET data). We calculated total annual precipitation and total precipitation in the wettest, hottest, and driest months from gridMET data. We also synthesized temperature and precipitation data into two metrics of cumulative water stress. First, climatic water deficit (calculated using Redmond 2019) quantifies the degree to which potential evapotranspiration exceeds actual evapotranspiration. We calculated soil moisture using the soil water capacity at 30 cm depth (United States Department of Agriculture 2019a). Second, we defined water balance as the difference between potential evapotranspiration and precipitation, a metric of potential plant stress from lack of water. We calculated both climatic water deficit and water balance for the whole year and for the hottest, wettest, and driest months, using both local temperatures derived from iButtons and regional temperatures derived from gridMET data. Note that for precipitation, only gridMET data were available.

We used a model selection approach to assess support for three alternative ways (temperature $\times$ precipitation, climatic water deficit, and water balance) to represent interactive effects of temperature and precipitation on Venus flytrap performance (Table 4.2-4). For each demographic rate and each measure of water stress, we fit a suite of models using annual and extreme monthly values of the climate variable as predictors (as well as years since fire). For each suite of models, we compared the performance of climate variables derived from regional and local temperatures, while accounting for collinearity among climate variables (Freckleton 2011, Table 4.2-4). Thus, our analytical approach determined which of six different ways of representing climate at two different time scales (annual and monthly) best predicted demographic rates: 1) local temperature $\times$ precipitation (including main and interactive effects); 2) local climatic water deficit; 3) local water balance; 4) regional temperature $\times$ precipitation (including main and interactive effects); 5) regional climatic water deficit; and 6) regional water balance.

For each of these 12 ways of representing climate, we fit climate-dependent demographic rate functions that included the effect of years since most recent fire. For each demographic rate, climate variable, and time scale, we first fit a global model (Table 4.2-4; either a generalized linear model for binomial responses, or a general linear model for normal responses) using as predictors: size in the previous time step, years since fire, the square of years since fire, population nested in region, annual climate variables, and the square of the annual climate variable. For each climate variable, we used AICc to compare all possible subsets of the global model (using the MuMIn package in R) and selected a best perfoming model. We conducted the same analysis using monthly climate variables, including all three extreme months (and their squares) in the best performing model (Table 4.2-4). We then asked, using AICc, which combination of terms from the best performing monthly and annual models best predicted plant responses, yielding an overall best performing model for each climate variable which could contain both annual and monthly climate effects. Finally, we compared the performance of the six resultant best performing models to one another using AICc and used the best model for each demographic rate to construct our population models. Survival and probability of reproduction were binomial response variables, and mean and variance in plant size, seedlings per fruit, and log-transformed number of fruits given fruiting per unit size were normal response variables.

After each AICc comparison step described above, we ensured our best performing model was robust to collinearity among predictor variables using methods derived from

45

Freckleton's (2011) analysis of simulated data. Freckleton (2011) shows that information theoretic approaches are largely robust to collinearity, with the exception of correlated variables that have quite different effect sizes. For all best-fit models with linear, additive predictor variables correlated at $|R| > 0.6$, we ensured that the absolute value of the coefficient estimates of correlated predictor values (a rough estimate of their true effect size) were similar to one another (ratios of coefficients were $<= 3$). If ratios of coefficients differed by more than a factor of three, we replaced the best performing model with the next best model with a coefficient ratio $<= 3$ (or with no correlated predictor variables). Note that the approach outlined here uses conservative cutoffs, according to Freckleton's analysis (2011).

For seedlings per fruit, we had only one year of data for each population, and thus were unable to test for the effect of climate drivers on seedlings per fruit. Because preliminary data suggested strong effects of fire on seedlings per fruit, we compared using AICc three different (binomial) models for seedlings per fruit: constant seedlings per fruit, years since fire, and whether or not a fire occurred in the year immediately prior (yes/ no). Note that our approach assumes that any variation among populations in seedlings per fruit is due only to burn effects, rather than population-level differences in recruitment. Our experimental analysis of burn effects supports this assumption, in that it also suggests strong effects of fire on recruitment (Appendix 8.4).

Table 4.2-4. Climate variables present in the annual and monthly global models for regional and local water balance, climatic water deficit, and temperature/ precipitation. The terms shown here were present in the global model for each demographic rate x climate variable x annual/monthly time frame, and we then used AICc to determine which subset of the terms best predicted demographic rates, also allowing other terms such as years since fire (both linear and quadratic). The first letter of the subscript indicates the time period of the effect; "a" (annual) represents effects over the entire year, whereas "w" (wettest), "d" (driest), "h" (hottest), "c" (coldest) or indicate characteristics of extreme months. The second subscript for temperature variables indicates whether the variable is regional ("r") or local ("l"). The monthly temperature and precipitation models have terms for temperature (but not precipitation) of the coldest month, but the water balance and climatic water deficient models do not because temperature alone, rather than water stress, likely affects coldest-month performance. Note that for probability of survival or fruiting, we did not include any quadratic precipitation terms (P_w^2, P_d^2), nor terms including temperature in the wettest month (e.g., $T_{w,r}$, $T_{w,r} \times P_w$) and for probability of reproduction, we did not include a quadratic temperature in the coldest month term (e.g., $T_{c,r}^2$) in the monthly temperature and precipitation models, as there were not enough data to reliably fit these terms.

Climate variable	Annual	Monthly
Regional water balance (W)	$W_{a,r} + W_{a,r}^2$	$W_{c,r} + W_{c,r}^2 + W_{w,r} + W_{w,r}^2 + W_{d,r} + W_{d,r}^2$
Regional climatic water deficient (C)	$C_{a,r} + C_{a,r}^2$	$C_{c,r} + C_{c,r}^2 + C_{w,r} + C_{w,r}^2 + C_{d,r} + C_{d,r}^2$
Regional temperature (T) + precipitation (P)	$T_{a,r} + P_a + T_{a,r} \times P_a + T_{a,r}^2 + P_a^2 + T_{a,r}^2 \times P_a^2$	$T_{c,r} + T_{c,r}^2 +$ $T_{w,r} + P_w + T_{w,r} \times P_w + P_w^2$ $T_{d,r} + P_d + T_{d,r} \times P_d + P_d^2$ $T_{h,r} + P_h + T_{h,r} \times P_h + T_{h,r}^2$
Local water balance (W)	$W_{a,l} + W_{a,l}^2$	$W_{c,l} + W_{c,l}^2 + W_{w,l} + W_{w,l}^2 + W_{d,l} + W_{d,l}^2$
Local climatic water deficient (C)	$C_{a,l} + C_{a,l}^2$	$C_{c,l} + C_{c,l}^2 + C_{w,l} + C_{w,l}^2 + C_{d,l} + C_{d,l}^2$
Local temperature (T) + precipitation (P)	$T_{a,l} + P_a + T_{a,l} \times P_a + T_{a,l}^2 + P_a^2 + T_{a,l}^2 \times P_a^2$	$T_{c,l} + T_{c,l}^2 +$ $T_{w,l} + P_w + T_{w,l} \times P_w + P_w^2$ $T_{d,l} + P_d + T_{d,l} \times P_d + P_d^2$ $T_{h,l} + P_h + T_{h,l} \times P_h + T_{h,l}^2$

We fit the same demographic rates described for our observational work (survival, mean and variance in size after one year of growth, probability of fruiting, number of fruits given fruiting, and recruitment) to test for effects of experimental manipulations of burn effects. For each demographic rate, we fit a global model including size, population, condition, year, and the interaction between population and condition. We then compared all possible subsets of the global model using AICc. The functional forms of demographic rates were the same as in our observational work. For recruitment, we simply used the mean recruitment for each condition (because each condition was only represented by one population x year combination).

We used the best performing models from each of these comparisons in our SEED models.

4.2.1.7   Red-cockaded woodpecker (*Dryobates borealis*)

Study system: Red-cockaded woodpeckers are a cavity nesting species that lives in cooperatively breeding, territorial family groups consisting of a breeding pair and zero to six non-breeding adult helpers (Walters and Garcia, 2016). In addition to breeders and helpers, adult ($\geq$ 1 year old) birds can also act as floaters, non-breeding adults not part of a group. The demographic data used in this analysis come from long-term studies at three locations, the Sandhills region in south-central North Carolina, which includes colonies on Fort Bragg Army Base (1980-2015), Marine Corps Base Camp Lejeune on the central coast of North Carolina (1986-2015), and Eglin Air Force Base on the Gulf Coast in the western panhandle of Florida (1996-2015; hereafter, "Sandhills," "Lejeune", and "Eglin", respectively). Sandhills is the largest site, consisting of 716 groups of birds, of which 313 were monitored in 2017. Eglin is also a large population (462 groups in 2017), but only a small sample of groups is monitored there (39 in 2017). Lejeune is a smaller population (115 groups in 2017), but all the groups are monitored there. The data collection methods are much the same at all three sites and are described in detail in Walters et al. (1988); briefly, we conducted complete sampling of populations or subpopulations of marked birds at each site, including censusing of all, individually identifiable adults and monitoring of all nesting attempts during each breeding season (May-June). We base our estimates of survival on a hypothetical census taken on May 1 of each year.

Fitting Relationships between demographic rates and climate variables: We synthesized the demographic data into 11 response variables: 1) annual adult survival (including data from both males and females); 2) survival from fledging to the following breeding season (including data from both males and females, hereafter, "post-fledging survival"); 3) probability of a female breeder attempting a first nest; 4) probability of success of a first nest (given a first nest was attempted; success means at least one egg survived to fledging and failure means no eggs survived to fledging); 5) number of eggs in first nest (given a first nest was attempted and successful; hereafter, clutch size); 6) fraction of eggs surviving to fledging from the first nest (given a first nest was attempted and successful); 7) probability of a female breeder attempting two or more nests (given the first nest was attempted and failed); 8) probability of attempting double brooding (attempting two or more nests, given the first nest was attempted and successful); 9) probability of success of any second and later nests (given first and later nests were attempted); 10) total number of eggs in second and later nests (given first nest was attempted, second or later nests were attempted and at least one of the second and later nests are successful; hereafter, additional clutch size); and 11) total fraction of eggs surviving to fledging from second and later nests (given first nest was attempted, second and later nests were attempted and at least one of the second and later nests were successful). Third nests were too

rare to consider separately from second nests (only 25/10,004 first nesting attempts led to a third nesting attempt).

To obtain functional forms for demographic rates, we used AICc (Hurvich and Tsai 1989) to select a best performing mixed model for each demographic rate, comparing the perfomance of a global model to all possible subsets of this global model. In all of these models, we used site (Sandhills, Lejeune or Eglin) as a random effect to control for systematic differences among sites, such as habitat quality (models did not consistently converge when using individual-level random effects). For adult survival, fixed effects in the global model were: group size, status, age, age^2, and sex; for post-fledging survival, sex was the only fixed effect. For all reproductive demographic rates, fixed effects were: maternal age, paternal age, maternal age^2, paternal age^2, and number of helpers. All demographic rates were fit with a binomial error term using the lme4 package (Bates et al., 2015) in R (version 3.3.2, R Core Team 2016), except for clutch size and additional clutch size, which were fit with a quasi-Poisson variance using the glmmADMB package (Fournier et al. 2012, Skaug et al. 2014). For both first nests and second and later nests, we fit two distinct demographic rates (probability of initiating a nest, and clutch size or additional clutch size given the nest was initiated) because we wanted to determine whether probabilities of initiating nests, clutch size, and additional clutch size were determined by different climate drivers. Fitting two demographic rates is not possible with the commonly employed hurdle model (e.g. Reynolds et al. 2017). Importantly, our final models never predict a mean clutch size or additional clutch size of zero for first nests or for second and later nests, respectively, which would be a biologically impossible scenario (i.e., our models do not predict that a nest was initiated but no eggs were produced). Similarly, we chose to fit two distinct demographic rates (probability of nest success, and fraction of eggs surviving given nest success) to determine whether these two demographic rates were dependent on different climate drivers. We used chi-square tests to ensure that a binomial distribution was a good fit to the fraction of eggs surviving to fledging when only including instances where fraction of eggs surviving was >0 (as was done to fit the models). The predicted fraction of eggs surviving is never zero, for first or second and later nests, indicating that our models never predict that a nest was successful, but no eggs survived (also biologically impossible).

We used the best performing model lacking climate drivers for each demographic rate as a baseline model to look for climate effects. We obtained observed daily climate data (daily maximum and minimum temperatures, precipitation, and wind velocity (daily mean 10 m above the ground surface, hereafter "windspeed") over the period 1979-2016 at a resolution of 4 km^2 from the gridMET dataset (Abatzoglou 2013; Supporting Information). We calculated daily mean temperatures using the average of the maximum and minimum daily temperatures. We then extracted monthly summaries of these climate variables (mean windspeed, cumulative precipitation, and mean of daily minimum, maximum, and mean temperatures) for the 4 km^2 climate grid cell overlaying each territory center. We assumed that all individuals occupying each territory experienced the same climate as the territory center. For each of these five climate variables, we used a sliding window approach (Bailey and van de Pol 2016, van de Pol et al., 2016) to assess support for a series of climate signals varying in timing and duration. We assessed support for each of 78 climate signals spanning the 12-month period from the beginning of a breeding season on May 1 to the following May 1 (where window size ranges from 12 months to one month, in increments of one month), modifying this approach slightly to test for effects of multiple climate signals and interactions among climate signals. This procedure allowed us to include both short-lag (more recent) and long-lag (more distant) climate signals as

demographic rate drivers (short- and long-lag *sensu* van de Pol et al. 2016). For example, both spring maximum temperatures just before a breeding season, a short-lag signal, and summer maximum temperatures just after the previous breeding season, a long-lag signal, might affect survival.

4.2.2   SEED models

We developed several Spatially Explicit Environmentally Driven (SEED) models of population dynamics linked to downscaled future climate projections to project how populations of our study species would be impacted by predicted changes in local climates. These SEED models are defined by two salient characteristics. First, year to year changes in population size are predicted from a set of regression equations describing the relationship between demographic rates and relevant climate (and sometimes non-climate) variables. In each future year, the predicted demographic rates change with changes in the projected values of the climate variables on which they depend. Second, the models are spatially explicit. Projected climate variables used to determine demographic rates of different populations of a species are specific to the locations occupied by those populations. If migration or dispersal among different locations is a relevant factor influencing the modeled population(s), the resulting redistribution of individuals in space is tracked within the model. The models followed a general framework, with modifications made to accommodate differences among the species in their life history and ways in which climate influenced demographic rates. We first describe the general framework shared by all SEED models developed for this project, and then the species-specific modifications. Sample R code for the general framework is provided in Appendix 8.5.

Each SEED model includes six primary components. The first component is to read in the information required to locate each modeled population on the landscape. This information typically includes a site location identifier and UTM coordinates for each modeled population or population segment. The site location identifier allows it to be linked with the proper downscaled climate projections. The UTM coordinates also allow inter-site distances to be calculated for distance-based estimates of dispersal and/or migration probabilities. If there are non-climate related site-specific differences in demographic rates, this information is included in the landscape information read in. The second component is to read in the relevant downscaled climate projection data. We used projections that employed the Multivariate Adaptive Constructed Analogs (MACA) (Abatzoglou and Brown 2011) method to downscale projections from 20 global climate models to a 4 km^2 resolution for all species except Alaskan douglasia, for which we used downscaled projections from the Scenarios Network for Alaska and Arctic Planning (SNAP) as described in section 4.2.2.5. The third component is to define the functions used to calculate all demographic rates expected for each population during each time step given its location and projected climate conditions. This step varies substantially from model to model, depending on each species' life history and how it is influenced by different climate variables. The fourth component is to integrate the different demographic rates to calculate changes in population size from year to year in each population. This step also varies substantially from model to model. For structured populations, the numbers of individuals in each stage class are updated during this step. The fifth component is to incorporate dispersal and/or migration as appropriate. This component is intertwined with the previous component, with the timing of dispersal/migration spatial redistribution relative to other demographic processes dependent on each species' life history. The final component is to record numbers at each population in each stage during each time step. SEED model output comprises these data, which can be summarized in different ways to facilitate their interpretation.

4.2.2.1 Hydaspe Fritillary Butterfly (*Speyeria hydaspe*) SEED model

We modeled hydaspe fritillary butterfly population dynamics at our six study sites. We did not include dispersal in the hydaspe fritillary butterfly model because of the large distances between sites relative to the butterfly's dispersal capabilities.

The hydaspe fritillary butterfly has the simplest life history among the species studied in this project. Unlike the multivoltine Appalachian Brown Butterfly, the hydaspe fritillary butterfly completes one generation per year throughout its range. Throughout their one to three week lifespan, adult female butterflies lay eggs singly on plants, twigs, and other debris in areas near violets, their host plant (Capinera 2008). Eggs hatch after 30-35 days. First-instar larvae remain unfed in the duff after hatching and go into diapause with cooling autumn temperatures. Larvae emerge and begin feeding when violets appear after spring snowmelt. Larvae typically take one to two months to pupate, with the first adults typically eclosing in early July. The relevant demographic rates for hydaspe fritillary butterfly are thus: adult lifespan and eggs laid/day, which together determine fecundity; egg survival rate (a combination of egg viability and predation rates); larval overwinter survival; and larval spring survival.

We incorporated several climate related variables and site-specific non-climate variables that influence hydaspe fritillary butterflies throughout their life cycle into the hydaspe fritillary butterfly SEED model. Adult longevity, and therefore fecundity, was positively influenced by higher total precipitation in the 12 months prior to the flight period, and by warmer daily minimum temperatures during the flight period, which occurs July through September. Hatch rates were negatively influenced by warmer daily minimum temperatures during the flight period and by site-specific egg predation rates. Spring larval survival was positively influenced by warmer daily maximum temperatures during the late instar development period (June-August). Average number of eggs laid per day and larval overwinter survival were unaffected by climate variables and did not vary significantly among sites. Thus, we modeled year to year changes in hydaspe fritillary butterfly populations as:

Equation 4.2-3
$$N_{t+1} = N_t * eggs/day * adult lifespan(precip, min.temp) * hatch.rate(min.temp) * \left(1 - egg.pred(site)\right) * winter.surv * spring.surv(max.temp)$$

where Nt is the number of adult butterflies in year t
The functional forms and parameter values used in equation 4.2-3 are shown in Table 4.2-5 and site specific demographic rates are shown in Table 4.2-6.

Table 4.2-5. Hydaspe fritillary butterfly demographic rates used in the SEED model with functional forms and parameter values.

Demographic rate[1]	Demographic rate symbol	Functional form[5]
eggs/day	**eggs**	see Table 4.2-6
logit transformed adult daily survival[2]	logit.ad.surv	1.2748+0.03961*min.temp+0.000217*precip
adult daily survival[3]	ad.surv	exp(logit.ad.surv)/(1+exp(logit.ad.surv))
lifespan	**lifespan**	1/(1-ad.surv)
logit transformed hatch rate[2,4]	logit.hatch.rate	3.38-0.1703*min.temp
hatch rate	**hatch.rate**	exp(logit.hatch.rate)/(1+exp(logit.hatch.rate))
egg predation rate	**egg.pred**	see Table 4.2-6
larval overwinter survival	**winter.surv**	0.7022
logit transformed larval spring/early summer survival[2]	logit.spring.surv	-5.615+0.147*max.temp
larval spring/early summer survival[3]	**spring.surv**	exp(logit.spring.surv)/(1+exp(logit.spring.surv))

1. Variables appearing in Equation 4.2-3 are bolded. Other non-bolded variables appear in the functional forms of variables appearing Equation 4.2-3.
2. Linear functional forms were fit to logistically transformed data. These variables represent the projected logit transformation of demographic rates used in the model.
3. Inverse-logit transformation of the projected logit transformation of demographic rate calculated from linear equations of climate variables.
4. Alternative functional form was baseline.hatch-0.0655*min.temp. See Table 4.2-6 for site specific values of baseline.hatch
5. Temperature values are in degrees C. Precipitation values are in mm.

Table 4.2-6. Site specific egg predation rates (egg.predation), average number of eggs laid per female per day (eggs), and logit transformed egg viability rates (baseline.hatch).

Site	Egg.predation	Eggs	Baseline.hatch[2]
Cascades	0.7744	9.18	3.8834
Coast Range 1	0.3077	6.82	0.976
Coast Range 2	0.3498	7.65	0.5647
Sierra Nevada 1	0.7245[1]	3.03	1.52927
Sierra Nevada 2	0.8323	17.84	2.3734
Sierra Nevada 3	0.6166	12.86	1.9976

1 Predation not measured at this site, rate listed/used is the average predation rate at the two other Sierra Nevada sites.
2. Because models with and without site differences in baseline hatch rates had similar model support (see Section 5.1), we ran two sets of SEED models; one based on parameter estimates assuming a single baseline hatch rate (Table 4.2-5) and one assuming these (logit transformed) site-specific hatch rates.

4.2.2.2 Appalachian brown Butterfly (*Satyrodes appalachia*) SEED model

We modelled Appalachian brown butterfly population dynamics for the metapopulation of butterflies at Fort Bragg. Two aspects of Appalachian brown butterfly life history at this site added complexity to these SEED models compared to the Hydaspe fritillary butterfly. First, butterflies frequently dispersed among subpopulations, which means that the model had to keep track of how many individuals emigrated out of each patch and how far they dispersed during each butterfly generation. Second, Appalachian brown butterflies go through two to three generations a year, with the fraction of butterflies from the second generation contributing to the third generation determined by the timing of the second flight period, which is affected by climate. Thus, for each growing season, our SEED model kept track of population sizes for each site on each day of all of the flight periods.

To determine emigration rates we used a spatially explicit individual based model (SEIBM) built in Netlogo v.5.2.1 (Wilensky 1999) to simulate the movement of individual female Appalachian brown butterflies over multiple generations within a landscape representative of the real landscape occupied by the species on Fort Bragg. The simulated landscape was composed of 30 m x 30 m grid cells characterized as one of the following habitat types: wetland, riparian forest, upland forest, and open areas (including grasslands and developed areas). Simulated butterflies started in wetland habitat, and at each five second increment moved or rested based on empirical movement data collected as part of an earlier SERDP project (SI 1471) (Kuefler et al. 2010). Movements were characterized by turn angle and distance, with values drawn from empirical data from Appalachian brown butterflies (Keufler et al. 2010). If the resulting move led to the crossing of a habitat boundary, the move was completed or rejected based on empirical boundary-crossing probabilities (Kuefler et al. 2010). If the move was rejected, a new turn angle and distance was drawn until the move resulted in the butterfly staying in the originating habitat. We simulated the movement of 200 butterflies in a single year (two flight periods) for 300 simulations. We simulated movement of butterflies starting in patches of wetland ranging in size from 0.45 ha up to 1.8 ha. For each patch size, we ran simulations under two crossing probability matrices, 1) using the empirical crossing probabilities found in Kuefler et al. 2010, and 2) using a modified version that assumes that any time a butterfly crosses from a less preferred to a more preferred habitat, it will always cross the boundary, but will follow probabilities in Kuefler et al. 2010 if going from more preferred to less preferred habitat.

To determine the distance that emigrating butterflies moved, we drew the distances from a dispersal kernel estimated from mark-recapture data Sivakoff et al. (2016).

We identified occupied and unoccupied sites at Fort Bragg via a species distribution model (Wilson et al. 2013). We distinguished between the two via observation of Appalachian brown butterflies at the sites. We estimated current population sizes at each occupied site using a mark-recapture study (described in the field methods section) and subsequent analysis using the package RMark (White and Burnham 1999, Laake 2013). The study was carried out at three occupied sites (see section 4.2.1.2). We extrapolated the population sizes at the other sites using the ratio of the population size to the area of each site.

We initialized populations at their current sizes and summed population numbers across all sites at Fort Bragg for the results that we present in this report. To determine population size at a given site in a given year, we assumed that the total number of butterfly-days in the first flight period was equivalent to 11.1 (the average lifespan of a butterfly, in days), multiplied by the population size (number of butterflies) in that flight period. We assumed that emergence date of the first flight period was determined by the growing degree days (as outlined in section

5.1.2). We also assumed that the total number of butterfly-days was approximately normally distributed, with a flight period lasting 45 days, such that the maximum number of flying butterflies was observed 22.5 days following the emergence date of the first flight period. We determined the number of eggs laid on each of those 45 days as the product of daily fecundity (a function of climate conditions on that day) multiplied by the number of butterflies flying on that day. We limited the total number of eggs laid per day to 5.3, which is derived from the average maximum number of female eggs counted during dissection of female ovaries (58.457 eggs, Sivakoff et al. 2016), divided by average lifespan (11.1 days). We modeled egg survival to hatching over the next seven days based on daily temperatures over that period. We determined larval survival over the next 48 days by climate during that period, and multiplied the overall larval survival by 0.16 in order to incorporate an estimate of larval predation (Aschehoug et al. 2015). We modeled dispersal, and then negative density dependence, during the flight period but before eggs are laid, such that an egg could be laid in any site to which the butterfly disperses during the flight period. Eggs laid in any one population survived to hatching and developed as a larva in the population in which they were laid.

We modeled adult butterflies as emerging during the second flight period 55 days after they were laid as eggs (seven days to survive as eggs plus 48 days to survive as larvae). In the model, the adults dispersed among populations, underwent density dependence, and laid eggs over their lifespan (the next 11 days). We determined the probability of an egg laid on a given day to going into diapause and overwintering versus developing into a third flight period using a binomial function of day of year; eggs laid before a certain critical photoperiod developed into a third adult generation, but eggs laid after this photoperiod overwintered as larva. If an egg was laid before the critical photoperiod, the resultant adult butterfly again developed over 55 days as an egg and then larvae (the survival of both life stages was dependent on climate over that same time period). After hatching, adult butterflies dispersed, suffered density dependence, and then laid eggs at the same climate-dependent but limited daily fecundities as for previous flight periods. Those eggs survived to hatching over the next seven days (at a rate dependent on climate over that time period) and overwintered as larvae at the climate-dependent overwintering rate we estimated in demographic rate regressions. If an egg was laid after the critical photoperiod during the second flight period, the individual survived to hatching over the next seven days (again, at a rate dependent on climate), and overwintered as a diapaused larva until re-initiating development and emerging as an adult butterfly the following year. We did not estimate overwinter survival rates for butterfly larvae that were offspring of butterflies that only had two generations per year. Instead, we used overwinter survival rates for butterfly larvae that were offspring of butterflies that had three generations to calculate a daily survival probability for the winter, which we then used to calculate overall overwinter survival for the longer time period associated with larvae from two generations per year butterflies.

We carried out two additional modeling exercises to understand how changing climate conditions might affect this species. First, we used a simplified SEED model to determine the potential for a climate-mediated increase in generations per year to offset climate-mediated declines in fecundity and survival. This model used the same parameter values for demographic rate functions but assumed a single start to the second flight period, and that either all larvae from the second generation entered diapause or all larvae from the second generation underwent direct development into a third generation.

4.2.2.3 Western snowy plover (*Charadrius nivosus nivosus*) SEED model

We modeled the 24 western snowy plover breeding sites used by Hudgens et al. 2014. These sites span the United States coastal range of the species. We considered both dispersal and winter migration rates between pairs of populations to depend only on the distance between them. We used dispersal rates among populations from Hudgens et al. 2014 and estimated Migration rates from banded birds breeding at Monterey Bay and observed at coastal locations in the United States. We fit a negative exponential curve to the proportion of migrating birds observed in each western snowy plover recovery unit. We assumed that the distance of each recovery unit to Monterey Bay was equal to the mean distance between of all known breeding sites in the recovery unit and Monterey Bay. There was no evidence that birds from Monterey Bay were more likely to migrate to southern wintering grounds than to northern wintering grounds the same distance away, so we modeled migration as being equally likely in either direction.

The western snowy plover life cycle can be broken down into three stages corresponding to the first three years of their life. Hatch year birds suffer the highest mortality rate as they transition from eggs to nestlings to fledglings and finally independent young. Second year birds have similar survival rates as older birds but may have more limited breeding opportunities. Western snowy plovers are partially migratory, with most birds remaining near their breeding site. Most dispersal takes place during a bird's first winter/spring.

We modeled climate influencing western snowy plover population dynamics through effects on two demographic rates. Warmer early spring temperatures led to longer breeding seasons, which in turn led to greater fecundity. Adult survival was influenced by weather at their wintering grounds. Warmer mean daily maximum temperatures were associated with higher survival, while an effect of cold snaps (DACS; extended periods of days with lows below 2 ⁰C and highs below 10 ⁰C) were associated with higher mortality.

In the absence of dispersal, the year to year changes in a western snowy plover population would be described by:

Equation 4.2-4

$$N1_{t+1} = (N1_t + N2_t) * 0.5 * fecundity\left(\frac{N1_t}{(N1_t + N2_t)}, march.mean.temp\right) * juv.survival$$

$$N2_{t+1} = (N1_t + N2_t) * adult.survival(max.temp, DACS)$$

where $N1_t$ is the number of second year birds, $N2_t$ is the number of after-second year birds at the start of the breeding season in time t, and DACS is an index of the number, length, and severity of cold snaps experienced birds from that population over the previous winter. This climate variable was calculated as a weighted average of the DACS for each potential overwintering site, weighted by the proportion of birds from the breeding site expected to migrate to that overwintering site.

The functional forms and parameter values used in Equation 4.2-4 are shown in Table 4.2-7.

Table 4.2-7. Western snowy plover demographic rates used in the SEED model with functional forms and parameter values.

Demographic rate[1]	Functional form[7]
proportion breeders that migrate[2]	0.163
expected proportion migrating to each potential overwinter site	see Appendix 8.6
nest.season.start[3]	49.18-2.13*mean.March.temp
fecundity	0.37+0.22*p.ASY- 0.004*first.nest.day
juvenile survival	0.67*adult.survival
logit.adult.survival[4,5]	-1.736+0.1759*max.temp-0.00375*DACS
adult.survival[6]	exp(logit.adult.survival)/(1+exp(logit.adult.suvival))

1. Variables appearing in Equation 4.2-4 are bolded. Other non-bolded variables appear in the functional forms of variables appearing Equation 4.2-4.
2. Conversely, the proportion of breeders that are expected to overwinter at their breeding site is 0.837
3. March temperatures are based on where adults overwinter. The value used at a given breeding site is the weighted average of the values calculated for all potential overwintering sites with the weighting factor equal to the expected proportion of the population overwintering at any given overwinter sites.
4. Mean daily maximum temperatures during the winter months (November-February) and Duration Amplified Cold Scores (DACS) are based on where adults overwinter. The value used at a given breeding site is the weighted average of the values calculated for all potential overwintering sites with the weighting factor equal to the expected proportion of the population overwintering at any given overwintering site.
5. Linear functional forms were fit to logistically transformed data. These variables represent the projected logit transformation of demographic rates used in the model.
6. Inverse-logit transformation of the projected logit transformation of demographic rate calculated from linear equations of climate variables.
7. Temperature values are in degrees C.

4.2.2.4   Red-legged frog (*Rana aurora* and *R. draytonii*) SEED model

We modeled red-legged frog populations dynamics at each of our eleven study sites. We did not include dispersal in the red-legged frog model because of the large distances between sites relative to the frog's dispersal capabilities.

The red-legged frog life history is characterized by two phases, an aquatic larval phase and terrestrial post-metamorphic phase. Eggs are laid at different times of year in different parts of the range. Coastal northern red-legged frogs may breed from October through March, depending on local rainfall patterns and hydrology. Inland northern red-legged frogs breed in mid-February, typically after the harshest winter temperatures. Both modelled populations of California red-legged frogs bred in March and April, corresponding to the end of wet season when the streams used as breeding habitat in the coastal populations are less prone to flash flooding, and to warm temperatures and snow melt for the inland population. Eggs hatch after several weeks and the timing is influenced by water temperatures; eggs develop faster in warmer waters. Tadpoles are less than 1 cm long when they emerge from eggs. After two to four months tadpoles have grown to 40 mm— large enough to escape predation by smaller aquatic invertebrates— and begin forming rear leg buds. Tadpoles continue to progress through a gradual metamorphosis, growing rear legs, then front legs, and resorbing their tails, until they become fully metamorphosed into froglets capable of living on land. They remain in this juvenile

terrestrial phase over their first winter, and become reproductive adults during the following breeding season, at age two.

We incorporated several climate related variables and site-specific non-climate variables that influence red-legged frogs throughout their life cycle into the red-legged frog SEED model. We assumed that each breeding female laid a single egg mass each breeding season. The number of eggs per egg mass increased with the average size (snout-vent length) of adult females observed at the site and the amount of precipitation at the breeding pond the previous breeding season. We assumed early tadpole (from hatching to 40 mm length) survival to be constant. Daily survivorship of later-stage tadpoles (from 40 mm to metamorphosis) decreased with warmer temperatures. The length of time required to complete metamorphosis after tadpoles reached 40 mm decreased with warmer temperatures and varied among sites independent of climate (Appendix 8.7). We tracked froglet survival for the final 1-4 months of their first year, with the starting month depending on site-specific breeding times and the combined length of the aquatic stages, which was temperature dependent. Monthly survival rates increased with froglet size and warmer mean daily maximum temperatures and decreased with warmer mean daily minimum temperatures and higher precipitation. We calculated adult survival quarterly to account for seasonal variation in temperature-related mortality; quarterly adult survival rates increased with warmer mean daily minimum temperatures. We calculated annual adult survival from October through the following September as the product of the corresponding four quarterly survival rates. Year to year changes in red-legged frog populations are approximated by:

Equation 4.2-5

$$N1_{t+1} = N2_t * 0.5 * eggs(site, last.breeding.season.precip)$$
$$* hatch.rate(max.temp)$$
$$* small.tadpole.survival$$
$$* lg.tadpole.suvival(mean.temperature, tadpole.period)$$
$$* froglet.survival(size, min.temp, max.temp, precip)$$

$$N2_{t+1} = (N1_t + N2_t) * adult.survival(min.temp)$$

where $N1_t$ is the number of pre-breeding juvenile frogs and $N2_t$ is the number of 2+ year old adult frogs in year t. All climate variables correspond to the time period when the stage is present, except for last.breeding.season precip, which is the precipitation during the previous breeding season.

The functional forms and parameter values used in Equation 4.2-5 are shown in Table 4.2-8 and site specific parameters are shown in Table 4.2-9.

Table 4.2-8. Red-legged frog demographic rates used in the SEED model with functional forms and parameter values.

Demographic rate[1]	Symbol	Functional form[7]
adult.svl	svl	see Table 4.2-9
eggs.per.mass	epm	10760-272.7*svl+1788*svl^2+0.1253*last.breeding.season.precip
		See
baseline.hatch.rate		see Table 4.2-9
logit.hatch.rate[2]		baseline.hatch.rate-0.3607*max.temp
hatch.rate[3]	hatch.rate	exp(logit.hatch.rate)/(1+exp(logit.hatch.rate))
sm.tadpole.surv[4]		0.042
logit.daily.tadpole.surv[2]		3.7-0.05947*mean.temp
daily.tadpole.surv[3]		exp(logit.daily.tadpole.surv)/(1+exp(logit.daily.tadpole.surv))
tadpole.stage.lgth		see Appendix 8.7
lg.tadpole.surv		daily.tadpole.surv^tadpole.stage.lgth
froglet.svl		23.67+0.003699*GDD
Logit.froglet.surv[5]		-1.279+0.32*froglet.svl-0.396*min.temp(month)+0.414*max.temp(month)-0.324*precip(month)
monthly.froglet.surv[5]		exp(logit. froglet.surv)/(1+exp(logit. froglet.surv))
logit.adult.quarterly.surv[6]		-2.2594+0.8561*min.temp
adult.quarterly.surv[6]	QSa1, QSa2, QSa3, QSa4	exp(logit.adult.surv)/(1+exp(logit.adult.surv))
adult.annual.surv		QSa1*QSa2*QSa3*QSa4

1. Variables appearing in Equation 4.2-5 are bolded. Non-bolded variables appear in the functional forms of variables appearing Equation 4.2-5.
2. Linear functional forms were fit to logistically transformed data. These variables represent the projected logit transformation of demographic rates used in the model.
3. Inverse-logit transformation of the projected logit transformation of demographic rate calculated from linear equations of climate variables.
4. From McHarry 2017 and Licht 1974
5. Overall froglet survival was calculated as the product of monthly froglet survival rates from the month of emergence to the following October. The month of emergence was calculated as the breeding month + 3 months + tadpole.stage.lgth/30; rounded to the nearest month. The three months in this calculation accounts for the egg and small tadpole development times.
6. Adult survival was calculated quarterly, with annual adult survival equal to the product of the four quarterly survival rates. Temperatures for each quarter were calculated as the average of the monthly mean daily minimum temperature for the corresponding three months.
6. Temperature values are in degrees C. Precipitation values are in mm.

Table 4.2-9. Red-legged frog primary month when breeding occurs (breed.month), average SVL of females captured (mean.SVL), and the logit transformed egg viability rates (hatch.base) for each site.

Site	Breed.month	Mean.svl	Batch.base
Inland NRLF 1	Feb	74	8.56
Inland NRLF 2	Feb	73	7.07
Inland NRLF 3	Feb	73	6.34
Coastal NRLF 1	Jan	82.5	7.3
Coastal NRLF 2	Dec	71	7.17
Coastal NRLF 3	Nov	72	8.87
Coastal hybrid 1	Dec	71	8.22
Coastal hybrid 2	Mar	71	8.22
Inland CRLF 1	Apr	95	8.02
Coastal CRLF 1	Mar	90	7.35
Coastal CRLF 2	Mar	90	11.1

4.2.2.5 Alaskan douglasia (*Douglasia alaskana*) SEED model

We modeled Alaskan douglasia population dynamics at our five study sites. Note that while we attempted to conduct this work at Joint Base Elmendorf Richardson (JBER), we were unable to obtain reliable temperature data at JBER, and the small number of plants found at this location (four individuals) made it impossible to make robust inferences about population dynamics. Our "Central" site is just adjacent to JBER and population dynamics at this site are likely similar to those at JBER. In addition, we were unable to use the MACA climate projections, but instead used Alaska-specific projections (described in more detail below). We did not include dispersal in the Alaskan douglasia model, because of the large distances among sites relative to the plant's dispersal abilities.

Instead of using the MACA climate projections, we obtained estimates of monthly temperature and precipitation for Emissions Scenario RCP8.5 from the CMIP5/AR5 models from the Scenarios Network for Alaska and Arctic Planning group (SNAP). These projections were downscaled using CRU CL v. 2.1 climatological datasets from 1961-1990 as the baseline, generating 2 km x 2 km spatial resolution climate projections from 2006-2099 (Scenarios Network for Alaska and Arctic Planning, University of Alaska). These data include climate projections from 5 GCMs, rather than the 20 GCM's represented by the MACA data (Appendix 8.1). We corrected our SNAP data to better represent soil temperature data (soil temperature data were derived from iButtons, used to fit demographic rate functions) using population specific differences between SNAP and iButton temperatures. Namely, we only had temperature data from both iButton and SNAP sources for the 2016-2017 or 2017-2018 period, depending on site. For each site, climate variable, and GCM, we calculated a difference between the iButton and SNAP data, and then used this difference to 'correct' all SNAP data used in population projections. Note that we did not measure precipitation at our populations, so all precipitation data used in projections was obtained from SNAP.

For each site, we constructed a standard integral projection model (IPM) with no density dependence using climate projections. We used the demographic rate regressions outlined in section 5.1.5 to construct climate-driven population-specific IPMs for future conditions. We used

SNAP temperature ('corrected' using the iButton data, as described above) and precipitation data to predict demographic rate functions. As in our demographic rate fitting procedure, the identity of hottest and coldest months could vary across years, sites, and GCMs. Our integral projection models used log size as a size variable and had an additional class for seedlings. We initialized projections with the size distribution from the mean 2008-2099 kernel. We used the population-specific estimates of seedlings per fruit in the year prior as an estimate of recruitment (using the across-population average for our S population, for which we were missing recruitment data). Seedlings survived at the average rate across populations, and survivors joined the IPM kernel with a mean and variance in size equivalent to the mean and variance across all populations in our field study. Our integral projection model had 40 mesh points (or size classes), and upper and lower size limits were +/- 10% more than the range of sizes observed during our study. We renormalized predicted size in the next time step to avoid eviction (Williams et al. 2012). To prevent complete eviction below the lower size bound (where all predicted sizes, not just mean size after one year of growth, were below the lower bound of the kernel), we assumed in these cases that all individuals transitioned to the smallest size class (Williams et al. 2012). No complete eviction over the upper limit occurred.

4.2.2.6 Venus flytrap (*Dionaea muscipula*) SEED model

We modeled Venus flytrap metapopulation dynamics at Fort Bragg, NC using a standard integral projection model with no density dependence. We did not include dispersal in the model because of the large distances between sites relative to the plant's dispersal abilities.

We estimated the plant's dispersal abilities by delimiting the geographic extent of three introduced populations in Florida for which we know from herbarium records an approximate establishment date. At each of these three populations, we quantified geographic extent by demarcating the boundaries of the Venus flytrap population; we then assumed that populations were circular and quantified the increase in radius per year since establishment of the populations. The increases in radius per year at the three populations were 0.12, 0.18, and 0.34 m/year. These dispersal estimates are much too low to warrant inclusion of dispersal into our SEED model, given the distances between occupied sites at Fort Bragg.

We identified 35 currently or recently occupied sites at Fort Bragg using data available from managers at Fort Bragg and constructed projections of population growth rate at each of these 35 sites. We initialized population models using the number of plants observed in the most recent census (2014) at each site, which ranged from 1 to 259. We summed the projections of population size across all 35 sites at Fort Bragg to obtain estimates of metapopulation size through time.

We used the best performing demographic rate functions from the regression analysis described in section 4.2.1.6 to construct IPMs (Ellner and Rees 2006) to project metapopulation growth of Venus flytraps at Fort Bragg. We used MACA climate projections for each site to predict site-specific future demographic rates. For the demographic rates for which soil iButton temperatures were included in the best performing models, we used a regression of soil temperatures (derived from iButtons) against the analogous gridMET temperatures for 2015-2018, the years for which we had both types of data. Namely, for each climate variable, we fit a linear regression with the iButton climate variable (e.g., iButton annual mean daily temperature) as the response variable, with population (one of the six monitored populations used to fit demographic rates), the analogous gridMET climate variable (e.g., gridMET annual mean daily temperature), and their interaction as predictor variables. We used the relationship (for the average for Fort Bragg populations) to generate predicted future iButton climate variables. One

climate variable present in the best-fit model for fruit number, local climatic water deficit in the driest month, was not well-correlated with its analogous regional climate variable; therefore, we used the next-best model, which included regional water balance (but not local climatic water deficit) to construct our IPMs.

We used future climate variables for each of the 35 currently occupied sites across Fort Bragg to predict future demographic rates for each occupied site. When demographic rate functions contained a term for population or region, we used the region coefficient for Fort Bragg, and for site effects, we averaged the two Fort Bragg populations' coefficients. Identities of extreme months do not change substantially in a future climate, so we used the same extreme months as the demographic rate function fitting.

We then used these future demographic rates to construct integral projection models (IPMs) that assumed a fire return interval of three years (as usually occurs at Fort Bragg , where all fire is prescribed). In our simulations, a fire always occurred in the first year. We used natural log of plant size [namely, ln(number of leaves x length of longest leaf)] as a metric of size in our IPM. Our kernel had 100 mesh points, and bounds of the kernel were 30% more and 10% less (on the log scale) than the range of sizes observed during our study. We renormalized predicted size in the next time step to ensure that no plants were lost because they grew or shrank to sizes not included in the model (eviction, Williams, Miller, and Ellner 2012). Seedlings entered the kernel with a normal size distribution reflective of the seedling size distribution in 2018 (on the logged scale, mean of 3.38 and variance of 0.33), similarly renormalized to avoid eviction. To prevent complete eviction below the lower size bound (where all predicted sizes, not just mean size after one year of growth, were below the lower bound of the kernel), we assumed in these cases that all individuals transitioned to the smallest size class (Williams et al. 2012). No complete eviction over the upper limit occurred. We initialized integral projection models using the stable size distribution over the mean 2018-2099 IPM kernel.

Because future climate scenarios could result in unrealistic predicted demographic rate values, we bounded demographic rate values to improve realism. First, for each bin in the discretized IPM kernel, we limited fruit number, mean size after one year of growth, and variance in size after one year of growth to be at most 20% more than the range of observed values for that bin (when there were at least five observations at that bin). We allowed survival to vary +/- 20% beyond the range of observed probabilities for that bin (where probabilities were calculated across size class x population x year combinations with at least five observations). For probability of fruiting, we allowed predicted probabilities 30% more than the observed probabilities of that size class (minimum or maximum probabilities, as we used for survival, were unstable due to relatively sparse data).

4.2.2.7   Red-cockaded woodpecker (*Dryobates borealis*) SEED model

We modeled red-cockaded woodpecker population dynamics at our three study sites: Sandhills, Lejeune, and Eglin. At each site, we used an individual-based model in which the 'individuals' were territories; each territory had associated breeders, helpers, and nestlings (with floaters associated only with the site). Our SEED model did not include detailed treatment of dispersal within a site; as described in more detail below, an individual had the same probability of dispersing to a territory 0.1 v. 2 km away. Because reproductive demographic rates depended on both male and female breeder age, we kept track of both males and females in our model. We did not include dispersal in our SEED model, because dispersal probabilities among these three sites were too low to warrant their inclusion (see more details below). In our SEED models, density dependence is present because the number of breeding territories, and thus breeding

pairs, is limited to the number of breeding territories occupied by a breeding pair in the last year of our demographic monitoring (2015); however, the number of nestlings and helpers at each territory is not limited, nor is the number of floaters across the site.

We predicted demographic rates using the average climate in a given year at that site, as well as individual- or territory-specific characteristics such as number of helpers or age. For each year of our simulation, we calculated a weighted average of the MACA predictions for that site, where the weights correspond to the number of territories occupied by a breeding pair in 2015 that are present in each 4 km x 4 km MACA climate grid cell. We used this weighted average to predict demographic rates in each year of our simulations. We used territory- or individual-specific characteristics to predict demographic rates of each individual or territory. For each age, status, and territory combination in each year, we calculated a predicted mean demographic rate (e.g., mean survival) and then sampled from an appropriate distribution to simulate fates of individuals. For example, in the case of simulating survival of a breeding male three years of age, we calculated the predicted mean survival rate for a three year old breeding male using our demographic rate functions, then sampled from a Bernoulli distribution to determine whether that particular three year old male breeder survived. Similarly, for each territory, we calculated a mean probability of initiating a first nest, and then sampled from a Bernoulli distribution with this mean probability to determine whether a first nest actually occurred in that territory. In this way, we incorporate demographic stochasticity in most demographic rates; note that we do not include demographic stochasticity in the case of number of eggs or the fraction surviving to fledging from nests, as occasionally the observed value was predicted to be zero, which is biologically impossible.

To improve biological realism, we limited all adult survival rates to the maximum and minimum observed, across years and sites, for that status and sex. We limited survival during the year of hatching to be no less than the 0.25 quantile of observed values across years and sites, with no upper limit. We imposed similar limits on all reproductive demographic rates; namely, we limited all reproductive demographic rates to the minimum observed across years and sites, with no upper limit. Finally, if a bird happened to live to 18 years of age (the maximum age observed in our dataset), we assumed it did not survive to the next year.

We initialized projections of population growth with the observed sex, age, and status distribution in each territory in each site in 2015. We incorporated the social dynamics of this species using a series of rules that dictated what happened when a breeder died, or when new hatchlings transitioned into the pool of adults (where they could become helpers, floaters, or breeders). We first outline what occurs when male breeders dies, then when female breeders die, and then what happens to nestlings that survive to fledge and become adults. When a male breeder did not survive, the oldest helper at that territory replaced the male breeder (or, if there were no helpers at that territory, we selected a new male breeder randomly from all floating males at that site). If the oldest helper at a given territory replaced the breeding male but was younger than the breeding female at that territory, we assumed that he was her son, so that she left the territory to become a floater. When this scenario occurred, her survival rate was 50% of her predicted survival rate as a breeder (Daniels and Walters 2000). If she survived to the next year, she occupied any female breeding positions that were abandoned or where the breeding female died; the identity of the territory to which she moved was selected randomly. If she survived to the next year but no female breeding positions were available, she transitioned into the floater class. If there were additional unoccupied female breeding positions, we selected randomly from the female floaters at that site to fill the breeding position. If male or female

nestlings were not selected to occupy a breeding position, they became helpers at their natal territory at the average sex-specific nestling-to-helper transition rate observed at that site across all years of our study. Otherwise, they became floaters.

If population numbers declined, some territories became unoccupied. We allowed territories to become occupied by a male (without an associated female breeder), as can happen in the field, but females could not occupy a territory alone (without an associated male breeder). Thus, unoccupied territories were treated as vacant breeding positions for males, but not females. If a female breeder's mate died and was not replaced due to low numbers in the population, we assumed that she left the territory, after which her survival rate was 50% of her predicted survival rate as a breeder (Daniels and Walters 2000). A breeding female that left a territory was preferentially selected to occupy any female breeding positions that were abandoned or where the previous female did not survive (as occurs when a breeding female's son succeeded the breeding male position) or where the female did survive.

We used the observed dispersal events in our demographic data to fit a Weibull distribution (following Kesler et al. 2010). Here, we define dispersal as a bird leaving a territory and relocating to another territory in the next census. The best-fit Weibull distribution had a shape parameter of 0.969 with a scale parameter of 3.421, yielding a cumulative probability of 0.9999999 at 60km. This cumulative probability indicated that birds were unlikely to disperse > 60km (probability= 0.00000001). Further, because this Weibull distribution is fit with data from dispersal distances among largely contiguous longleaf pine habitat, the probability of dispersing between populations that are separated by inhospitable matrix is likely even lower, we did not include dispersal among sites in our SEED model.

4.2.3 Climate Contribution Index (CCI)

We developed a method for measuring the contribution of each life stage to a population's response to climate change that accounts for both the sensitivity of demographic rates to climate drivers and the influence of those demographic rates on population growth. We start with an observation that the change in population growth rates caused by a change in climatic conditions between two time periods can be approximated by the following equation:

Equation 4.2-6

$$\Delta\lambda = \sum_{j=1}^{nv}\sum_{i=1}^{nc}\Delta c_i \frac{\Delta V_j}{\Delta c_i}\frac{\Delta\lambda}{\Delta V_j}$$

The term $\Delta c_i \frac{\Delta V_j}{\Delta c_i}$ describes how much a given demographic rate (v) changes given the difference in climate driver i between the two periods (hereafter, "climate sensitivity"). When summed over all *nc* climate variables, this is the climate sensitivity of the demographic rate. The term $\frac{\Delta\lambda}{\Delta V_j}$ describes how much the population growth rate changes with a small change in the demographic rate v_i, (hereafter, "demographic rate sensitivity"). The total change in a population's growth rate then is described by the sum of the product of the sensitivity of the population growth rate to each demographic rate and the climate sensitivity of that demographic rate over all *nv* demographic rates composing a species' life history. For any given demographic rate, the larger the product of the two sensitivities, the more it will influence how future population growth rates respond to a changing climate. Thus, this product serves as an index of the relative contribution of each demographic rate to a species' response to climate change. We call this index the Climate Contribution Index (CCI).

We calculated the CCI for three of our study species to demonstrate its use in practice and to help inform our interpretation of SEED model results: Appalachian brown butterflies, hydaspe fritillaries butterflies, and red-legged frogs. For the Appalachian brown butterfly, we assumed that the entire population went through three generations each year, so that the annual population growth rate can be described by the equation:

Equation 4.2-7 $$\lambda = f_1 * e_1 * l_1 * f_2 * e_2 * l_2 * f_3 * e_3 * l_3$$

The terms f_i, e_i, and l_i represent fecundity, egg hatch rate, and larval survival in each of the three generations. The fecundity terms are further broken down to: $\frac{1}{1-a} d_i$ where a is the daily survival of adult female butterflies (which does not vary among generations) and d_i is the average number of eggs laid per day in generation i. For the hydaspe fritillary butterfly and red-legged frogs, we used the equations presented in the SEED model methods sections Equation 4.2-3 and Equation 4.2-5, respectively.

We assumed the same climate-demographic rate relationships for each species as were used for their respective SEED models. We calculated climate sensitivities for each demographic rate as the difference between the average value of the parameter during the first 10 years during which SEED models were run (representing the current climate conditions) and the average parameter value over a 10 year period 25-30 years later (representing future climate conditions). Average parameter values for each period were calculated as follows. First, we calculated the projected value of each demographic rate given the climate conditions projected by each of the 20 GCMs used in the SEED models (Appendix 8.1). We then extracted the median value for each demographic rate for each year. Finally, we calculated the mean value over the 10 year period of these median projected values.

We calculated population growth rate sensitivities to demographic rates for each species from Equation 4.2-7 (Appalachian brown butterfly), Equation 4.2-3 (hydaspe fritillary butterfly), and Equation 4.2-5 (red-legged frog) based on the demographic rates in the current period. For each demographic rate, we calculated the sensitivity assuming a change in the average value of the demographic rate during the current period of 0.01 in the direction indicated by its climate sensitivity. We calculated population growth rate sensitivities to demographic rates not projected to change (i.e., with a climate sensitivity equal to 0) assuming a positive change.

We calculated the CCI for Appalachian brown butterflies based on climate conditions at Fort Bragg, NC. Because current climate conditions (and hence, current demographic rates) noticeably varied among hydaspe fritillary butterfly populations, we calculated separate CCIs for each of our study populations. Because we suspect that projected adult survival rates for inland populations of red-legged frogs are biased low due to local adaptation for cold winters (see section 5.2.4 below), we calculated CCIs only for coastal populations.

5   Results and Discussion

5.1   Relationships between demographic rates and climate variables

5.1.1   Hydaspe Fritillary Butterfly (*Speyeria hydaspe*)

We found a complex set of relationships between climate and hydaspe fritillary demographic rates. Some demographic rates were positively affected by warmer temperatures, while others were negatively affected. Some demographic rates were affected by both temperature and precipitation, and some were not influenced by any climate variable we tested.

Egg and larval development rates and the timing of the adult flight period were strongly influenced by climate. Observed population growth rates based on adult mark-recapture data hint at climate-demographic relationships we were unable to capture in the short duration of our field studies.

Demographic rates for SEED models: We found no significant effects of any of the climate variables tested on the number of eggs laid per female per day when site was included in the model (Appendix 8.8). Adding or removing the data from the females held under experimentally elevated temperatures in the greenhouse and Sacramento County did not change the results.

Higher temperatures reduced egg viability, with strong effects of average daily minimum temperature. The best performing model included minimum temperature and site (Table 5.1-1, Figure 5.1-1a). However, models that included only temperature or only site performed nearly the same (Table 5.1-1, Δ DIC < 1). The results presented included eggs that were housed under elevated temperatures in the greenhouses and Sacramento County. The results were the same qualitatively regardless of whether or not the experimental data were included. While the greenhouses reached higher temperatures during the day, the nighttime temperatures were not elevated compared to the butterfly field sites in Humboldt County where the females that laid the eggs came from (natal site), resulting in no difference between the two in minimum temperatures. The Sacramento County eggs experienced temperatures that were over 10 °C warmer for the average daily minimum temperature than the egg's natal site, which was the site with the lowest minimum temperatures. However, the minimum temperatures were still within the range currently experienced at our warmest study site, the lowest elevation Sierra Nevada site. Overall, the minimum temperatures experienced while eggs were developing were fairly consistent within sites but distinct across sites, with warmer sites having lower egg viability, making it difficult to differentiate between site and temperature effects. The negative association we found between temperature and egg viability is likely due to a higher chance of desiccation at higher temperature. We frequently noted desiccation in eggs that did not hatch.

Table 5.1-1. Model selection tables for analyses of the effects of temperature on egg viability and post-diapause (spring) larval survival. Parameter estimates from the top models that were used in the SEED models can be found in Table 4.2-5.

Egg viability models	DIC	Delta DIC	Weight
Site + min temperature	2106.71	0	0.37
Site	2106.86	0.15	0.34
Min temperature	2107.46	0.75	0.25
Intercept (female as random factor)	2111.30	4.59	0.04
Larval survival models			
Site + max temperature	405	0	0.82
Max temperature	409.05	4.05	0.11
Site	409.74	4.74	0.08
Intercept (female and cage as random)	415.25	10.25	0.005

We found that overall egg predation rates during our trials were not influenced by temperature, but did vary across sites (Appendix 8.9). However, we did find an effect of

temperature on daily predation rates. Temperature and region affected daily egg predation rates (Cox proportional hazards model, P< 0.05). Namely, average daily mean temperature increased the hazard ratio ($\beta = 0.38$, $z = 9.72$, $P < 0.0001$), resulting in a 46.4% increase in the daily predation rate per °C of warming. Based on our personal observations, we suspect that ants are significant egg predators at our sites. Ants are known to prey on butterfly eggs in other species (Prysby 2004), and ant foraging behavior is influenced by temperature (Hölldobler and Wilson 1990). In the field, the average egg development time varied from about 16 to 27 days across sites and was strongly influenced by mean daily temperature ($\beta = -1.81$, $P < 0.001$, $R^2 = 0.67$). While the daily egg predation rate increased with temperature, egg development time shortened with warming, leading to reduced exposure to predation. This pattern may explain why we found little influence of temperature on overall predation rates in our trials, but an effect of temperature on daily predation rates. Because we ended our predation trials at least six days prior to eggs hatching, the expected predation rates at each site will actually be slightly higher than what we observed in our trials because of the additional exposure time. To more accurately estimate egg predation rates prior to hatching at each site we used a combination of survival analysis and the mean days to hatching at each site. We used survival analysis to estimate the proportion of eggs expected to survive (S) to the last survey date for each site (survival based on predation only and not egg viability). We then calculated the daily survival probability (S_{daily}) by taking the nth root of the estimated proportion survived: $\sqrt[n]{S}$, where n is the number of days until the last survey date at each site. We then used the daily survival probability (S_{daily}) and the mean days to hatching (N) at each site to estimate the proportion of eggs expected to survive until hatching ($S_{hatch} = S_{daily}^{N}$). The predation rate prior to hatching (P_{hatch}) is then $1 - S_{hatch}$. Estimated predation rates (from laying to hatching) using this method are listed in Table 4.2-6.

Average overwinter larval survival was fairly consistent across sites (0.54 – 0.71), and none of the climate variables we tested influenced overwinter survival (Appendix 8.10). Higher temperatures increased larval survival post diapause, especially higher daily maximum temperatures (Table 5.1-1, Figure 5.1-1b). We present the results for models that included data from larvae reared in greenhouses that elevated the average maximum daily temperatures experienced by as much as 5 °C compared to any of our field sites. Adding in the greenhouse data to our analyses did not change model rankings and did not substantially change parameter estimates. The best performing model for larval survival included both temperature and site effects. Only one site showed any significant difference in baseline larval survival, and the parameter estimates for the effects of temperature were nearly the same regardless of whether site was included in the model or not (0.15 vs. 0.145). To simplify the hydaspe SEED model we used the results from the model without site specific larval survival.

Average daily minimum temperature and total annual (water year) precipitation increased adult survival (Figure 5.1-1c, Appendix 8.11).
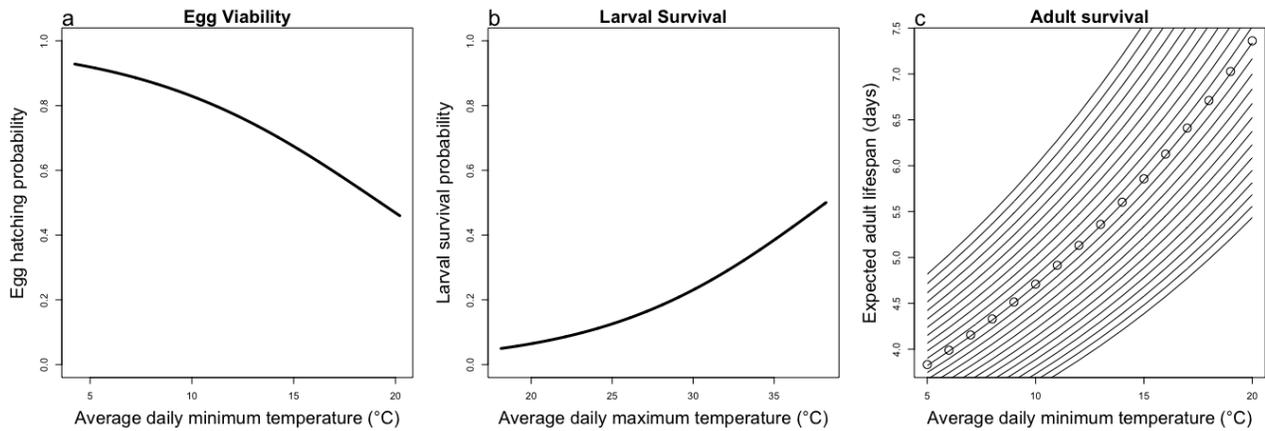
Figure 5.1-1. Predicted relationships between climate variables and demographic rates from the best performing models. Graphs a and b show the relationships we found between temperature and egg viability (a) or spring larval survival (b). Graph c depicts the relationship between average daily minimum temperature and the expected life span of adults based on daily survival estimates from mark recapture analyses (intercept represents the mean of all sites). The points represent the relationship when the annual precipitation total is equal to the mean across sites and years. The lines represent the relationship with different precipitation levels from the lowest to highest experienced at any site/year. Lines are spaced in 100 mm precipitation increments.

Population growth and phenology: We found strong model support for both total precipitation and male population size in year t affecting continuous population growth rates (r) calculated from population size estimates (Δ AICc > 8 compared to next best model). Total precipitation increased r (β= 0.0007, P = 0.002), while population size decreased r, indicating negative density dependent population growth (Figure 5.1-2, Table 5.1-2). Together, precipitation and population size in year t explained about 89% of the variation in population grow rates.
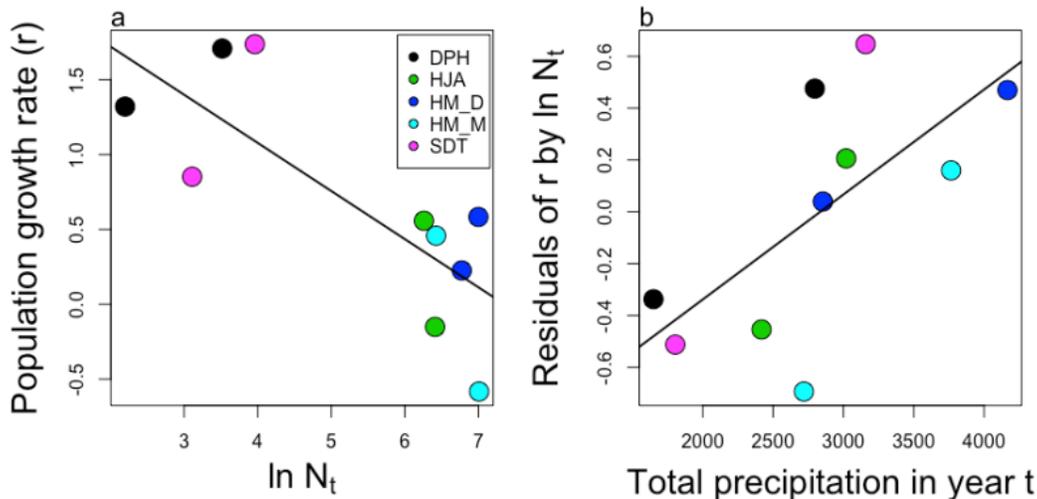
Figure 5.1-2. Effects of male population size and precipitation on continuous population growth rates. a) Relationship between the natural log of the male population size in year t (ln N_t) and growth rate (r). b) Relationship between total precipitation in year t and population growth after accounting for the effects of male population size (residuals of the relationship between ln N_t and r).

The timing of our study may be part of the reason why we saw such strong effects of precipitation and density dependence on population growth rates estimated from observed changes in abundance. Our study started during the tail end of the one of the worst droughts in California's history (2012-2016), which ended in the 2016-2017 water year with the wettest year

on record in northern CA (CA Department of Water Resources). As the furthest south and warmest sites, our sites in the Sierra Nevada were hit hardest by the drought (NOAA 2015). During the first two years of our study, Sierra Nevada 1, the lowest elevation site, had male population size estimates of less than 35 and Sierra Nevada 2 had estimates of less than 55. In contrast the lowest estimate of male population size at any other site in 2016 and 2017 was 523. In 2018, a year after the wettest water year on record, male population size estimates increased more than 450% at Sierra Nevada 1 and 2, while they increased by 58-79% at the more northerly sites.

The best performing models for all of the phenology measures included GDD and all but flight period end also included snow melt date (Table 5.1-2). Region was never included in the top model for any measure of phenology. Higher GDD resulted in earlier flight period start, peak, and end dates (Figure 5.1-3). Melt date also helped explain some variation in flight period start date and peak date between sites and years, however it was in the opposite direction than you might expect; later snow melt dates were associated with earlier flight period starts and peaks. Flight period length was influenced by both GDD and melt date, with greater GDD and earlier snow melt dates leading to shorter flight periods (Figure 5.1-3). While later snow melt dates leading to earlier flight period starts and peaks may seem counterintuitive, early snow melt can have negative effects on plants both directly by leaving plants exposed to frost (Inyouye 2008, Sherwood et al. 2017) and indirectly through freeze thaw cycles affecting soil microbial and fungal communities, and nutrient availability (Feng et al. 2007, Freppaz et al. 2007). Reduced host plant quality or abundance could delay larval development, leading to later flight periods.

Table 5.1-2. Results from generalized linear models testing the effects of climate on population growth rate and phenology measures. Only the best performing model for each phenology measure is presented. For each model the degrees of freedom, Akaike Information Criteria corrected for small (AICc), and difference in AICc between the top and the next best performing are presented. For each parameter in the top model the parameter estimate, standard error, t-value, and p-value are presented. $Precip_t$ = total precipitation in year t, $\ln N_t$ = natural log of the male population size in year t, GDD = growing degree days, melt date = ordinal day of the year when the last snow of the season had completely melted.

Population level results	Estimate	Std. error	t-value	p-value	DF	AICc	Δ AICc from next best model
Population growth rate							
Model: $Precip_t + \ln N_t$					7	13.4	-8.13
$Precip_t$	0.0007	0.0001	4.91	0.002			
$\ln N_t$	-0.51	0.06	-8.54	<0.001			
Flight period start							
Model: GDD + melt date					12	100.3	-5.03
GDD	-0.029	0.0078	-3.80	0.0032			
Melt date	-0.16	0.04	-3.86	0.0023			
Flight period peak							
Model: GDD + melt date					13	99.6	-9.01
GDD	-0.053	0.0052	-10.15	<0.0001			
Melt date	-0.13	0.032	-4.033	0.0014			
Flight period end							
Model: GDD					14	103.7	-3.58
GDD	-0.065	0.0060	-10.99	<0.0001			
Flight period length							
Model: GDD + melt date					12	112.7	-2.37
GDD	-0.039	0.0098	-4.0	0.0018			
Melt date	0.16	0.061	2.61	0.023			

Senescence date of the primary nectar plant was most strongly influenced by GDD (β = -0.06, t value = -6.64, P = <0.0001), with greater GDD being associated with earlier senescence (Figure 5.1-3h). Senescence date was also strongly correlated with the end of the flight period (R^2 = 0.76), although GDD was a better predictor of the flight period end date (R^2 = 0.86, Figure 5.1-3d). However, we only surveyed nectar plant blooming progression every two weeks, and the date recorded as the end of the flight period and the date recorded for full senescence of the primary nectar plant only differed by more than a week on one occasion across all sites and years. This suggests that the effects of temperature on the timing of the end of the flight period may be mediated through the influence of temperature on nectar plant phenology.
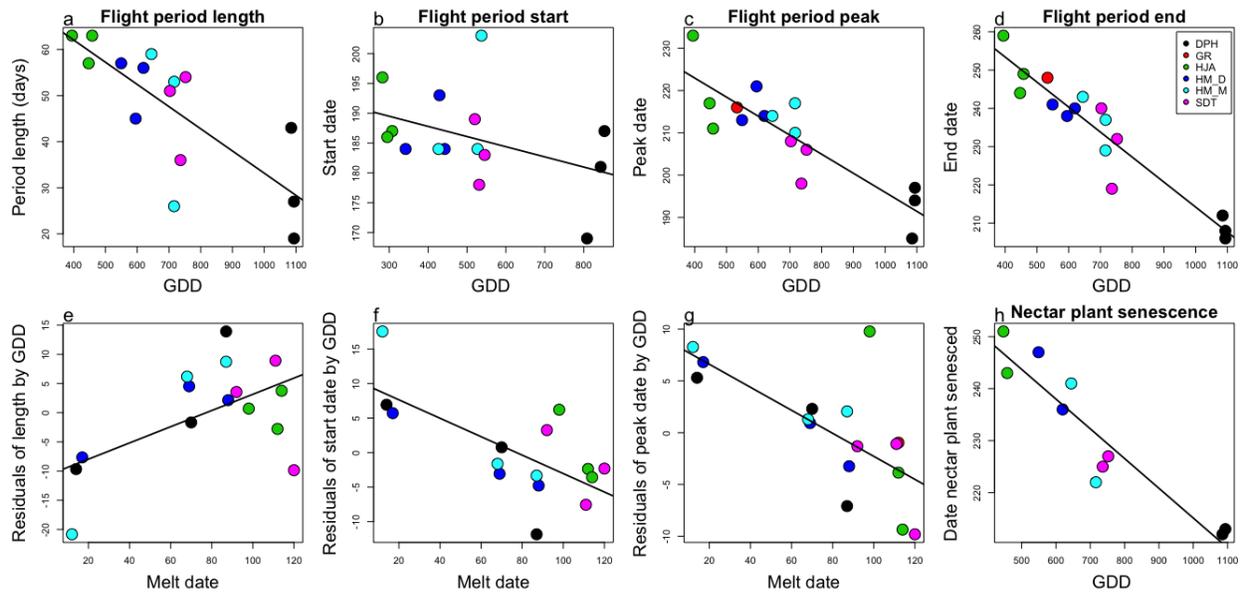
Figure 5.1-3. Relationships between climate variables included in the best performing model and phenology measures (a-g) and between climate and nectar plant senescence date (h). Climate variables include growing degree days (GDD) (a-d,h) and snow melt date (e-g). Phenology measures included the length of the flight period (a,e), the ordinal date that flight period starts (b,f), the ordinal date of the peak (highest adult abundance) of the flight period (c,g), and the ordinal date that the flight period ends (d). Graphs for snow melt date show the relationship between melt date and phenology measure after accounting for the effects of GDD. Nectar plant senescence date is the ordinal date that the hydaspe fritillary's primary nectar plant was fully senesced. Points are color coded by site and the legend for all graphs is in graph d.

5.1.2 Appalachian brown Butterfly (*Satyrodes appalachia*)

We found strong effects of temperature on most of the demographic rates that we tested in Appalachian brown butterflies. Only adult survival was unaffected by temperature. There was generally a negative effect of increasing temperatures on demographic rates, except for the proportion of caterpillars from the second generation undergoing direct development and contributing to a third generation within the same year. Many of the temperature-demographic rate relationships exhibited strong thresholds, where temperature increases below the threshold had little effect, but temperature increases above the threshold resulted in large reductions in the demographic rate.

Demographic rates for SEED models: During the egg survival experiments, average arena temperatures were 18.4-24.3 ℃ in the first generation, 24.9-28.8 ℃ in the second, and 22.1-25.9 ℃ in the third. The highest ranked model included a marginally significant negative effect of maximum temperature on egg daily survival (Table 5.1-3). This model also included a fixed effect of generation (Table 5.1-3, Figure 5.1-4) and a random effect of plot nested within site.

69

Table 5.1-3. Highest ranked generalized linear mixed effect models for egg and larval survival (binomial) and daily fecundity (quasipoisson). Bolded values indicate p <0.05.

Experiment	Fixed Effect	X^2	DF	p-value
Egg Daily Survival	Maximum Temperature	3.2308	1	0.07227
	Generation	5.9118	2	0.05203
Larval Survival	Maximum Temperature	26.468	1	**<0.001**
	Generation	20.807	2	**<0.001**
Daily Fecundity	Maximum Temperature	2.5856	1	0.10784
	Maximum Temperature ^2	3.0760	1	0.07946

During the larval survival experiments, average arena temperatures were 23.4-24.9 ºC, 24.3-26.7 ºC and 12.1-13.9 ºC during the first, second, and third annual generation respectively. The highest ranked model included a significant negative effect of maximum temperature (Table 5.1-3, Figure 5.1-4). The model also included a significant effect of generation (Table 5.1-3, Figure 5.1-4) as well as a random effect of plot nested in site. Larval survival was lower in the third than in the first (p=0.001) or second generations (p<0.001). First and second generation larval survival did not significantly differ.
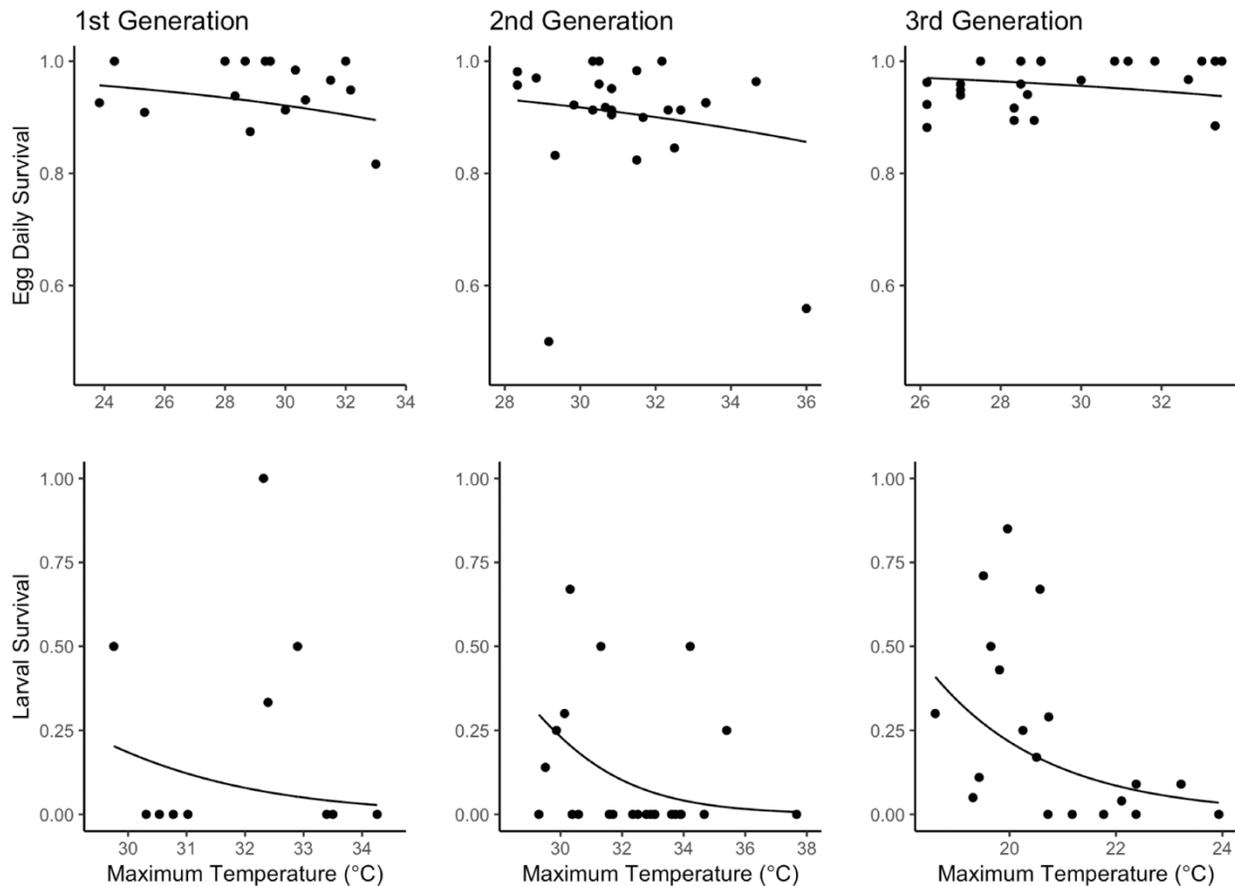
Figure 5.1-4. Daily egg survival and total larval survival by average of daily maximum temperatures during each generation. Lines represent highest ranked model for each life stage.

During the summer generations (1st and 2nd), we increased average temperatures by up to 4 ℃ in the arenas; during the winter generation (3rd), when sunlight was reduced, we increased average temperatures by 2 ℃. The lower value corresponds to predictions for temperature increases in the Southeastern United States under lower emissions scenarios over the 21st Century (Girvetz et al. 2009).

During the time period when we conducted adult mark-recapture studies, plot temperatures varied from 23.6 to 26.7 ℃ on average. In the first round of model selection we tested for effects of temperature on dispersal. We found that distance was the most important covariate affecting probability of moving among patches and that other covariates including mean, maximum, and minimum temperature had little effect. In the second round of model selection, we evaluated two possible covariates of detection probability: plot and restoration (Cut) treatment. We found that restoration treatment was the most important covariate determining detection probability. In the third round of model selection, we used our highest ranked covariate for detection and transition probability from the first two rounds and then compared different covariates of adult survival. We found that adult survival remained constant across plots and time in the highest ranked model. The best performing model estimated a daily adult survival rate of 0.915, which translated to an average adult lifespan of 11.1 days.

In the fecundity experiment, average temperature ranged from 23.2-32.4 ℃. The highest ranked model included a quadratic effect of maximum temperature Table 5.1-3, Figure 5.1-5). At lower temperatures, increasing maximum temperatures increased eggs laid per day, but at higher temperatures this effect was reversed.
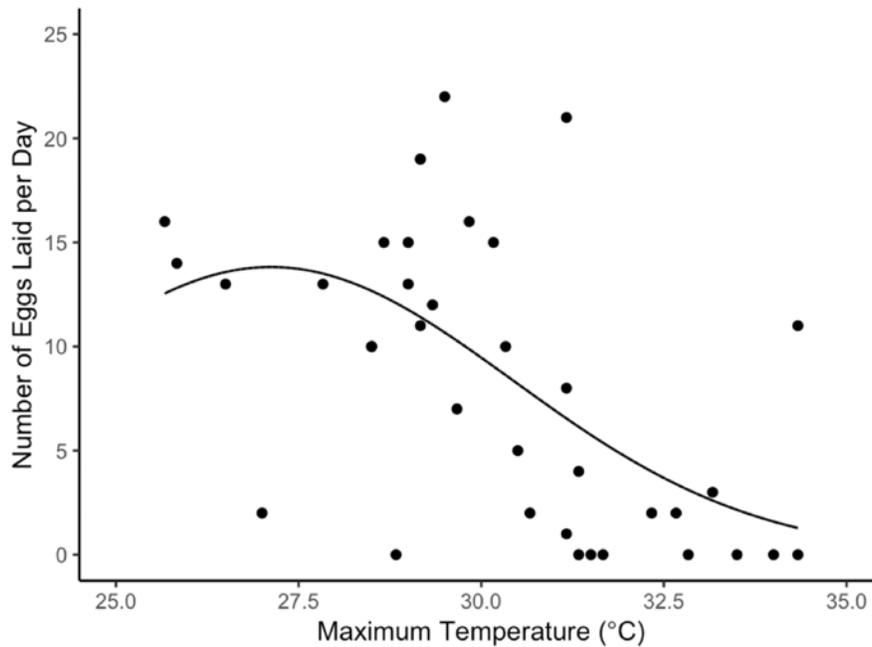
Figure 5.1-5. Effect of average of daily maximum temperatures in oviposition chambers on number of eggs laid per day. Line represents a quasipoisson fit of the highest ranked model, which includes the additive effect of maximum temperature and its square.

We tested for an effect of ordinal date on the probability of undergoing "direct development" (here, the probability of a larva developing into a third generation, rather than undergoing overwinter diapause) (Figure 5.1-6). The point at which 50% of individuals went into

diapause occurred at ordinal date 216, which we used as the critical photoperiod time point for further analyses.

We recorded the timing of first emergence in the first flight period for 62 butterflies in experimental warming enclosures. We found that Appalachian brown butterflies emerged over a range of GDD from 412 to 913 with the average emergence occurring at 582 GDD. We considered 412 GDD to be the lowest thermal accumulation necessary for emergence, and we used this value to project future first emergence dates.
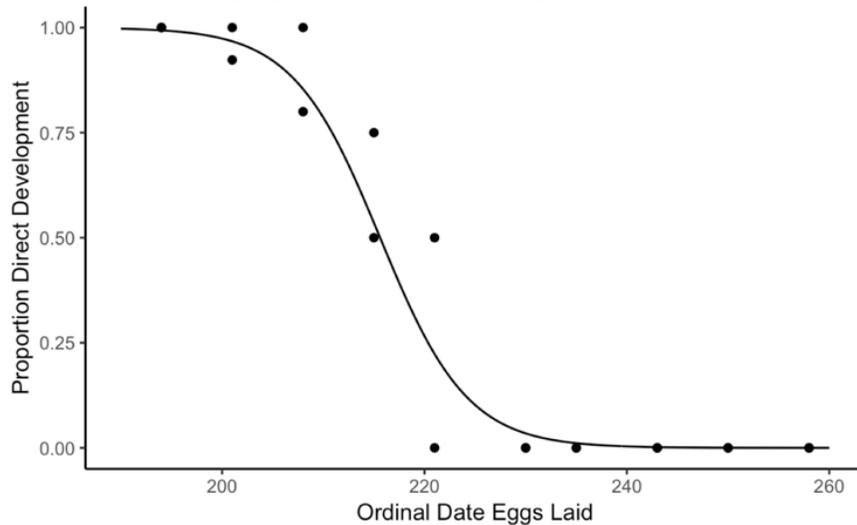
Figure 5.1-6. Changing proportion of individuals developing directly into third flight period adults by ordinal date that eggs were laid. Points represent one or two clutches (always two clutches per date, so single points on one date represent two clutches). Curve represents binomial fit predicting that 50% of eggs are laid on the ordinal date of 216. The critical photoperiod by definition occurs on this date.

Range boundary experiment. As with the Fort Bragg, NC populations, average daily maximum temperatures reduced egg and larval survival (Figure 5.1-7) in the South Carolina and Michigan populations. We found no evidence that site (SC vs. MI) influenced egg or larval survival and highest ranked models included only temperature.

During the Michigan warming experiment we unexpectedly observed adult emergence in September rather than the following spring. This surprised us as *S. appalachia* in Michigan is considered univoltine (Opler 1994). We could not corroborate our finding with observations in the field during 2018 using data from the Michigan Butterfly Network (available at pollardbase.org). However, a second annual generation was also observed for another Satyrine butterfly species during captive rearing the same year (A. Colewick pers. comm. 2018), possibly due to high summer temperatures and/or ideal conditions in greenhouse environments.
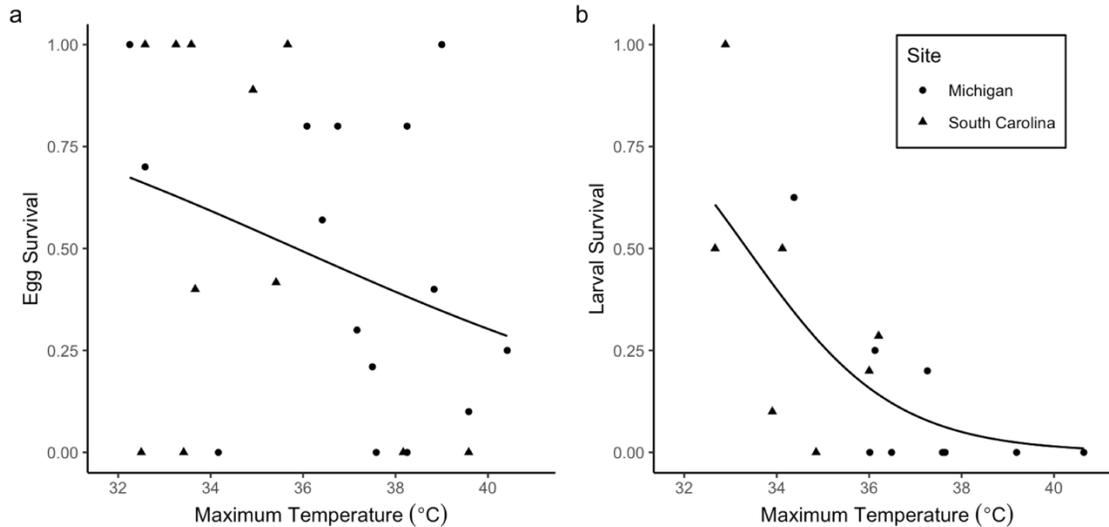
Figure 5.1-7. Relationship between average daily maximum temperature and egg (a) or larval (b) survival. Circles represent data from Michigan and triangles represent data from South Carolina

5.1.3   Western snowy plover (*Charadrius nivosus nivosus*)

Western snowy plovers were negatively impacted by cold temperatures. Warmer winter temperatures were associated with both higher adult survival and higher fecundity (mediated through earlier starts to the breeding season). Prolonged periods of extreme cold had an additional impact on both adult survival and fecundity.

Demographic rates for SEED models: Mark-recapture analysis results highlighted the positive and negative effects of warmer winters and extended cold snaps, respectively, on the western snowy plover's annual survival (Figure 5.1-8). The median $\hat{c}$ procedure detected slight over-dispersion in the global model ($\hat{c} = 1.02$), so we adjusted the model QAICc values accordingly. Four of the seven models considered were competitive, with ΔQAICc < 2 (Table 5.1-4); all these models included maximum daily temperature and duration amplified cold scores (DACS). Two of the top models included a positive trend in survival through time and two included a negative effect of precipitation, but the confidence interval for these parameter estimates overlapped zero in all cases. The magnitude of the effect of maximum daily temperature and DACS effects were similar for the top models. Parameter estimates on the logit scale ranged from 0.153 to 0.176 for maximum temperature, and from -0.033 to -0.046 for DACS. For the SEED model, we used parameter estimates from the second-ranked model including only temperature and DACS. The parameter estimates were 0.1759 (SE=0.0394) and -0.0038 (SE=0.0012), respectively, with an intercept of -1.955 (SE=0.6730).

Table 5.1-4. Top five CJS models for survival of western snowy plovers breeding in the Monterey Bay area, CA and wintering in Recovery Unit 4, which encompasses Monterey Bay. Terms in the models include a trend (T), mean maximum daily temperature for November-February (maxT), duration-amplified cold score (DACS), and precipitation (prec), see section 4.2.1.3 for explanation if variables.We estimated parameters separately for the sexes. Detection is time dependent. K is number of parameters, QDev is Quasi-Deviance. QAICc for the top model is 5172.94.

Model	Delta AQICc	QAICc Weight	Model Likelihood	K	QDev	-2log(L)
φ(T, maxT, DACS)	0.00	0.329	1.000	29	959.90	5216.81
φ (maxT, DACS, prec)	0.69	0.233	0.708	29	960.59	5217.52
φ (maxT, DACS)	0.69	0.233	0.707	28	962.62	5219.59
φ (T, maxT, DACS, prec)	1.14	0.186	0.566	30	959.0	5215.90
φ (T, maxT, prec)	6.56	0.012	0.038	29	966.45	5223.50
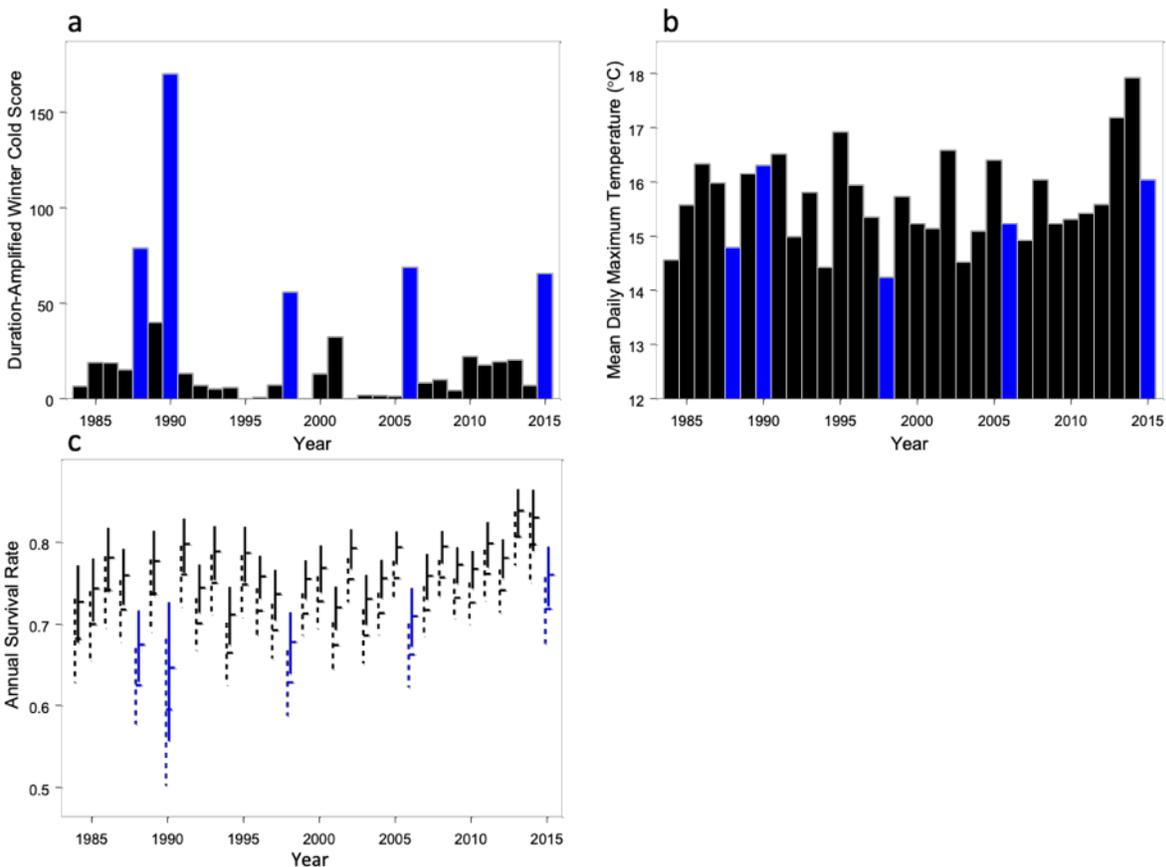
Figure 5.1-8. Cold winters correlated to low western snowy plover survival. a) Annual DACS. b) Annual mean maximum daily temperatures. c) Annual survival of western snowy plover females (dashed lines) and males (solid lines), indicating estimate and 95% CI of estimate. Years of high cold snap scores (DACS) in blue

From 1984-2016, first nests of the year at Monterey Bay were initiated in the 39 days between 21 February and 31 March (mean=15 March); last nests were initiated between 10 and 22 (mean=15) July, a 13 day range. The resulting total period of nest initiations each year was 108-151 days (mean=121 days). In those same years, breeding onset (the first date on which at least three nests are initiated within a three-day period) occurred within 101-135 days (mean =112 days).

Best performing models for both first nest initiation date and breeding onset date identified only temperature variables significantly affecting the start of the breeding season, although key time periods varied between response variables. The single-factor first nest models identified February, late March, and all-March as key periods in which mean temperatures appeared to affect the season start, with marginally significant terms for early and mid-March. Single factor breeding onset date models identified significant temperature effects for all-March, as well as mid- and late month, and a marginally significant effect in early March (Table 5.1-5). Global models for first nests also identified DACS and November-February mean temperatures as significant factors in one or more of the March models, but the global breeding onset models did not identify additional time periods or variables as significant (Table 5.1-6). Where higher DACS were associated with lower annual survival, they were also associated with earlier nesting season starts and a positive effect on fecundity (see next section). Although single-factor breeding onset models performed as well or slightly better than first nest models, first nest global models consistently performed better than corresponding breeding onset models (Table 5.1-5 and Table 5.1-6). Therefore, for SEED model parameter estimates, we used the model predictions for the date of first nest initiation rather than the breeding season onset. Because the three 10-11 day periods of March did not identify a consistent set of significant mean temperature variables, we opted to use the all-March model estimates (First nest, All- March in Table 5.1-6).

Table 5.1-5. Results of single factor temperature models for the start of the breeding season, with adjusted R^2, parameter estimates (Par Est) and standard errors (SE), parameter significance (Par Sig), for November-January (NJ), February (Fb), March (Mr), 1-10 March (M1), 11-21 March (M2), and 22-31 March (M3) mean temperatures (Temp), and November-February duration-amplified cold score (DACS)

Model	First Nest Response			Breeding Onset Response		
	Adj R^2	Par Est (SE)	P-value	Adj R^2	Par Est (SE)	P-value
NJ Temp	0.02		>0.1	-0.01		>0.1
Fb Temp	0.09	-2.01 (0.99)	0.05	-0.02		>0.1
Mr Temp	0.14	-2.13 (0.86)	<0.05	0.23	-2.19 (0.68)	<0.05
M1 Temp	0.06		0.09	0.07		0.07
M2 Temp	0.22		0.07	0.22	-1.55 (0.50)	<0.05
M3 Temp	0.16	-2.35 (0.89)	0.05	0.19	-2.08 (0.72)	<0.05
DACS	0.03		>0.1	-0.03		>0.1

Both male age and clutch initiation date for the first nest of the season affected the number of young males fledged. One-year old (first-time) breeding males fledged fewer chicks than older males and males that started nesting earlier in the season fledged more young than males that started later (Table 5.1-7). Becasue the effect of initiation date was similar for the two age classes, we selected an additive model over the model with an interaction term to parameterize the SEED model.

Table 5.1-6. Results of global model variants using temperature and precipitation data from four March time periods with similar data from November-January (NJ) and February, and the November-February duration-amplified cold score (DACS). Significant (p≤0.05) parameters listed under each of the model variants.

Global model & parameters	Adj R²	First nest response Par Est (SE)	P-value	Adj R²	Breeding onset Par Est (SE)	Par Est (SE)
All of March	0.33			0.2		
Temp.		1.99 (0.99)	0.05		-2.95 (0.90)	<0.05
DACs		-0.12 (0.04)	<0.05			
March 1st-10th	0.2			0.04		
Temp.					-1.67 (0.77)	<0.05
DACs		-0.09 (0.04)	<0.05			
March 11th-21st	0.33			0.17		
Temp.					-1.74 (0.72)	<0.05
Nov-Jan temp.		-3.22 (1.60)	0.05			
DACs		-0.12 (0.04)	<0.05			
March 22nd-31st	0.34			0.12		
Temp.		-2.53 (1.02)	<0.05		-2.69 (0.98)	<0.05
DACs		-0.11 (0.04)	<0.05			

Table 5.1-7. Model selection for the effects of male age (first-time breeder versus older breeder) and date of first clutch initiation on the total number of young fledged in a breeding season. Estimates shown with standard errors (SE). CID1 is the initiation date of the first nest of the season

Model	AIC	Coefficient	Estimate (SE)	p-value
Initiation date	5705	CID1	-0.006 (0.002)	0.01
Male age	5703	Age	0.26 (0.09)	0.004
Initiation date * male age	5703	CID1	-0.001 (0.01)	0.9
		Age	0.36 (0.47)	0.44
		Interaction	-0.003 (0.01)	0.76
Initiation + male age	5702	CID1	-0.004 (0.002)	0.05
		Age	0.22 (0.09)	0.02

5.1.4   Red-legged frog (*Rana aurora* and *R. draytonii*)

We found climate effects on every demographic rate in which we tested for them, as well as independent effects of canopy cover and both native and nonnative predators/competitors. Climate effects on red-legged frog demographic rates were complex. The same climate variable had positive effects on some demographic rates and negative effects on others, and the influence of many climate variables— and non-climate variables— varied from site to site.
Demographic rates for SEED models: We found that the best performing model for the effects of climate on fecundity (eggs per mass) included a positive effect of total precipitation (mm) from October through March of the previous year, and an accelerating positive relationship with female SVL (Figure 5.1-9). The model with SVL outperformed models that included precipitation and site or precipitation and species (*R. aurora* vs. *R. draytonii*; Table 5.1-8).

Table 5.1-8. Model selection table for fecundity (eggs/mass) analyses. Explanatory variables included: total precipitation from the prior breeding season (precip.), a quadratic relationship with average female snout vent length (SVL) by site, site, and species (*R. aurora* vs. *R. draytonii*).

Model	AICc	Δ AICc	Weight
Precip. + SVL + SVL^2	3831.7	0	0.664
Precip. + SVL + SVL^2 + species	3833.6	1.9	0.257
Precip. + site	3837.2	5.5	0.042
SVL + SVL^2 + species	3838.6	6.9	0.021
Precip. + species	3839.7	8	0.012
Site	3842.7	11	0.003
SVL + SVL^2	3846.9	15.2	0.000
Species	3863.6	31.9	0.000
Precip.	3886.8	55.1	0.000
Intercept	3887.8	56.1	0.000
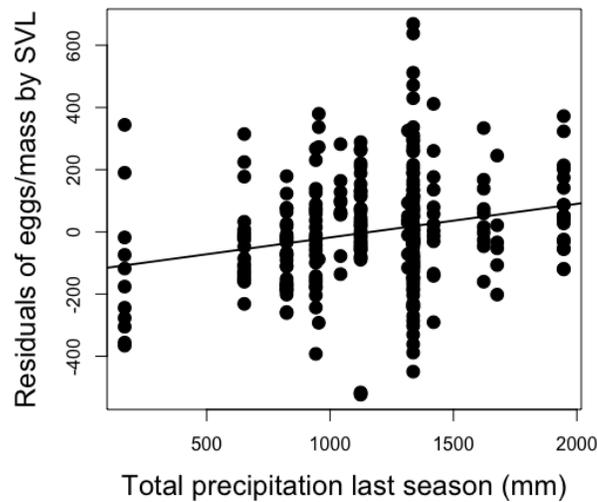
Figure 5.1-9. Relationship between fecundity and total precipitation during the previous breeding season after accounting for the relationship between eggs/mass and SVL (residuals of the relationship shown). Parameter estimates used in the SEED model can be found in Table 4.2-8

Warmer temperatures reduced egg viability, with stronger effects of air temperature (particularly average maximum daily air temperature) than water temperature. The best performing model for explaining egg viability included maximum air temperature and site, although there was weak support for models with temperature or site alone (Table 5.1-9; Figure 5.1-10). Response to temperature did not differ between species (no significant interaction between species and temperature; $P > 0.64$). There was a weak effect of species ($P = 0.04$) in a model that also included temperature (no interaction), however it performed worse than the model with temperature and SVL (Δ DIC = 2.9), suggesting that any apparent species differences in fecundity can be explained by differences in body size. Temperature also influenced egg

77

development rates, with each one °C increase in maximum daily water temperatures reducing the time from egg deposition to hatching by 2.8 days (p = <0.001, $R^2 = 0.77$).

Table 5.1-9. Model selection table for analyses of the effects of temperature on egg viability. Parameter estimates for the top model that were used in the SEED models can be found in Table 4.2-8.

Egg viability models	DIC	Δ DIC	Weight
Site + max temperature	3273.34	0	0.66
Site	3276.01	2.67	0.17
Max temperature	3276.82	3.48	0.12
Intercept (female as random factor)	3278.56	5.22	0.05
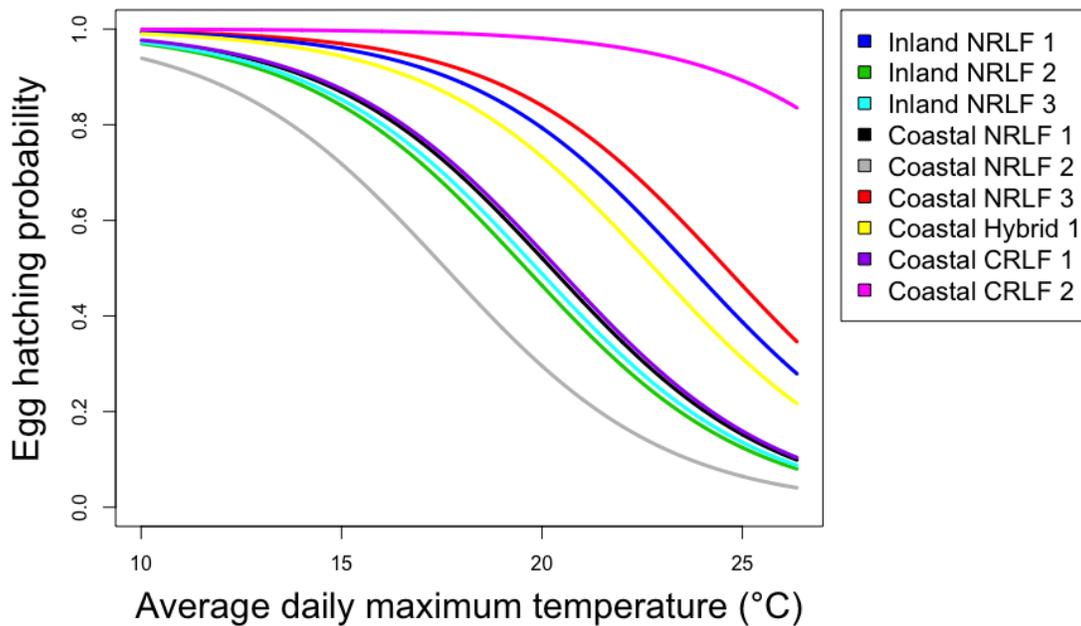
Figure 5.1-10. Predicted relationships between the average daily maximum air temperature and egg viability across all sites from our best performing model. Lines are color coded by site.

Daily survival rates of tadpoles decreased with mean air temperature. However, warmer mean air temperatures were also associated with increased development rates, generally reducing the time spent as a tadpole prior to metamorphosis. Tadpole development rates increased throughout the season, but warmer temperatures had a smaller effect later in the season. These effects meant that faster development through one tadpole stage sometimes resulted in slower development through later stages. Consequently, there was only a weak relationship between temperature and time as a tadpole (Figure 5.1-11).
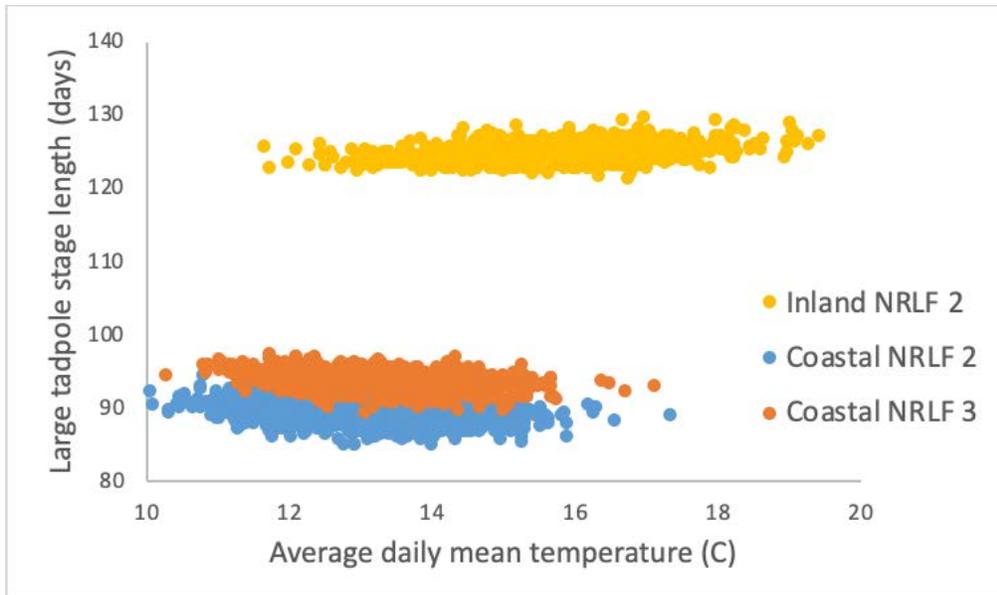
Figure 5.1-11. Average length of time for tadpoles (after reaching 35 mm) to froglet plotted against the average daily mean temperature from the global climate model used to simulate stage progressions at three representative northern red-legged frog breeding sites.

Froglet survival was influenced by temperature both directly and indirectly. Froglet survival increased with average maximum daily temperature and decreased with average minimum daily temperature. Warmer temperatures during tadpole development also produced larger froglets and froglet survival was positively correlated with size. Higher temperatures increased adult survival, but the benefit of additional warming was smaller at warmer temperatures (Figure 5.1-12). The parameter estimates corresponding to the top ranked statistical models for froglet and adult survival are presented in Table 4.2-8.
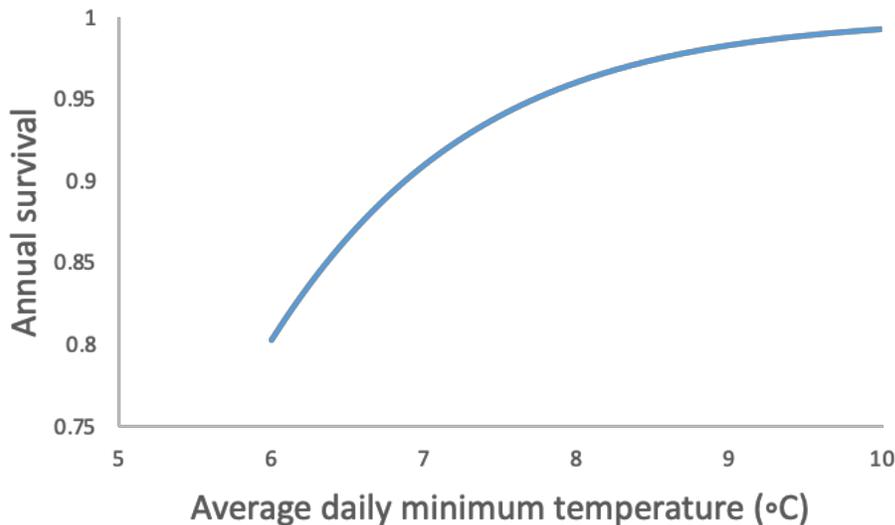
Figure 5.1-12. Projected survival of red-legged frog adults plotted against quarterly mean minimum temperature.

Captive rearing experiment: Shorter hydroperiods reduced survival to metamorphosis and there appeared to be a tipping point where the three shortest hydroperiods had zero tadpoles make it

through metamorphosis (Figure 5.1-13a). The best performing model explaining survival in the only the two longest hydroperiod treatments included food availability (high food treatment having higher survival), however it performed essentially the same as the intercept only model (Table 5.1-10). We found no effect of hydroperiod on froglet size. We did however find interactive effects of bullfrogs and food availability on froglet size. When food availability was high both bullfrog treatments (signal and direct) produced froglets that were similar in size to those that came from control tanks. However, when food availability was low, the froglets that came from either of the bullfrog treatments were significantly smaller than those in control tanks (Figure 5.1-13b). Interestingly, there did not appear to be any differences between the two bullfrog treatments (signal or direct) in their effects on froglet size, suggesting that the effects were likely driven by behavioral changes (e.g. reduced foraging) rather than direct competition for resources.

Table 5.1-10. Model selection table for the effects of hydroperiod length, food availability, and bullfrog treatment on froglet survival when tanks with zero survivorship were excluded.

Model	QAICc	Δ QAICc	Weight
Food	28.4	0	0.387
Intercept	28.9	0.46	0.306
Bullfrog	31	2.58	0.106
Hydro.	31	2.6	0.105
Food + hydro.	32.2	3.8	0.058
Food + Bullfrog	33.5	5.08	0.031
Bullfrog + hydro.	36.5	8.12	0.007
Food + bullfrog +hydro.	43.3	14.93	0

These results show that shortened hydroperiods could have drastic consequences if pools dry completely before tadpoles can metamorphose (Gordon 2020). This suggests that certain climate conditions, like severe drought, could lead to a complete or nearly complete loss of annual reproductive effort for some populations, and that populations that breed in fully ephemeral ponds are more at risk. The interactive effects of bullfrog presence and food availability suggest that the negative impacts of invasive species may be context dependent, leading to the possibility of management actions to facilitate coexistence.
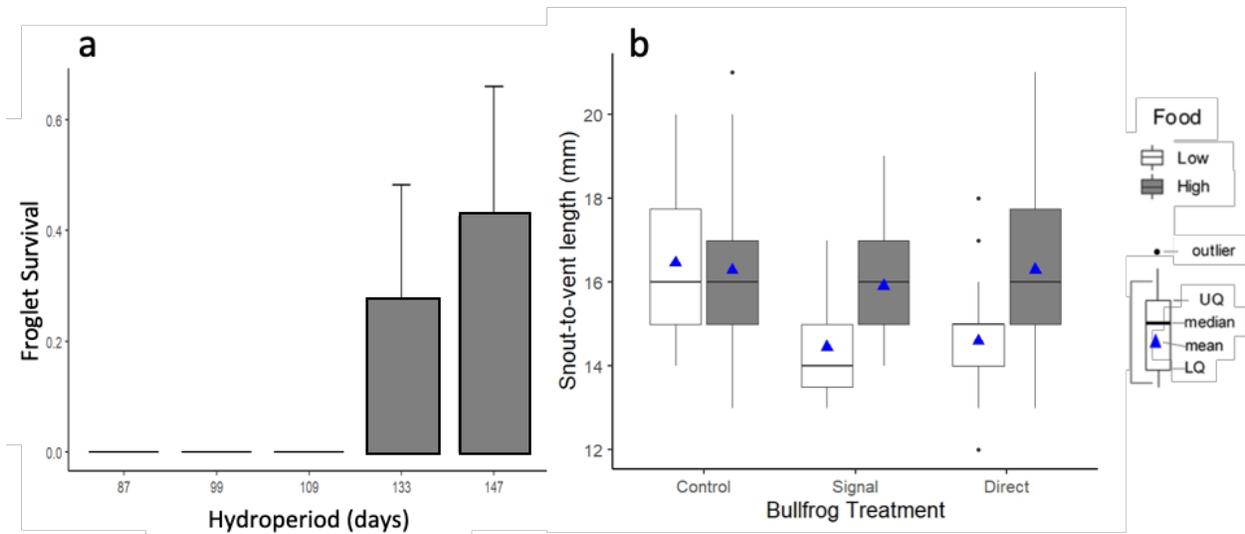
Figure 5.1-13. a) The proportion of tadpoles that completed metamorphosis for each of the five hydroperiod treatments. The three shortest hydroperiod treatments had no tadpoles complete metamorphosis. b) Variation of snout-to-vent lengths from froglets from the two longest hydroperiod lengths grouped by bullfrog and food level treatments in captive experiment. The bold line, triangle, box, whisker, and dots represent the median, mean, 25% and 75% quantiles, 95% confidence interval, and outliers.

We increased the air temperature in tanks with warming lids by just over 3 °C on average over the course of the experiment. In the warming and control tanks, longer hydroperiods increased survival through metamorphosis. The results held regardless of whether all hydroperiods were included or only those hydroperiods that had some froglets survive were included in the model selection process (Figure 5.1-14, Table 5.1-11). There was also some support for the intercept only model (Table 5.1-11). When we excluded the die-off tanks the best performing model was the intercept only model. We found no evidence that temperature influenced froglet survival under experimental conditions even when we included the die-off tanks on our models. However, the die-offs occurred in tanks that had the lowest water level at the time of the heat wave, leading to larger increases in water temperature and likely more UV exposure. If we had used water instead of air temperature in our models, we might have detected an effect of maximum temperature experienced on survival.
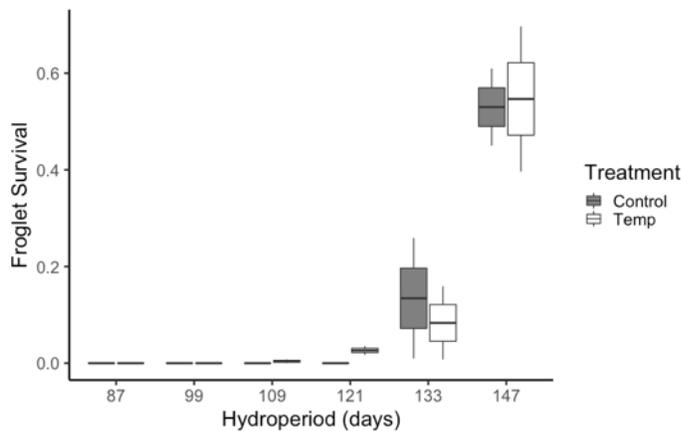
Figure 5.1-14. Variation in survival of froglets from the control and warming lid tanks grouped by hydroperiod treatment. The bold line, triangle, box, whisker, and dots represent the median, mean, 25% and 75% quantiles, 95% confidence interval, and outliers.

81

Table 5.1-11. Model selection table for analyses of the effects of hydroperiod (Hydro), average mean daily temperature (temp), and food availability (food) on froglet survival in the warming and control tanks. Model rankings were the same regardless of which temperature measure was included.

Model	AICc	Δ AICc	Weight
Hydro	11.9	0	0.44
Intercept	13.4	1.5	0.206
Hydro + food	14.6	2.7	0.116
Hydro + temp	15.6	3.7	0.07
Food	15.7	3.8	0.067
Temp	15.8	3.9	0.064
Food + temp	18.3	6.4	0.018
Hydro + food + temp	19.3	7.4	0.011
Hydro*temp	20.3	8.4	0.007
Hydro*temp + Food	25.6	13.7	0.001

The best performing model for explaining differences in froglet SVL from the control and warming tanks included only a quadratic relationship with development time, such that the earliest and latest frogs to metamorphose were the largest, while those with intermediate development times were the smallest (Figure 5.1-15, Table 5.1-12). There was also weak support for models that include the quadratic relationship with development time as well as either GDD, food availability, or hydroperiod, however none of the variables other than development time were significant. The two GDD measures using the two different temperature thresholds were highly correlated ($r = 0.99$) and switching between them did not change the identity of the best performing model.

We found that froglets developed more quickly with shorter hydroperiods, higher food availability, and higher temperatures, although the effects of food and GDD were marginal (hydroperiod: $\beta = 0.52$, $P = 0.001$; low food: $\beta = 3.8$, $P = 0.07$; GDD: $\beta = -0.0095$, $P = 0.11$).
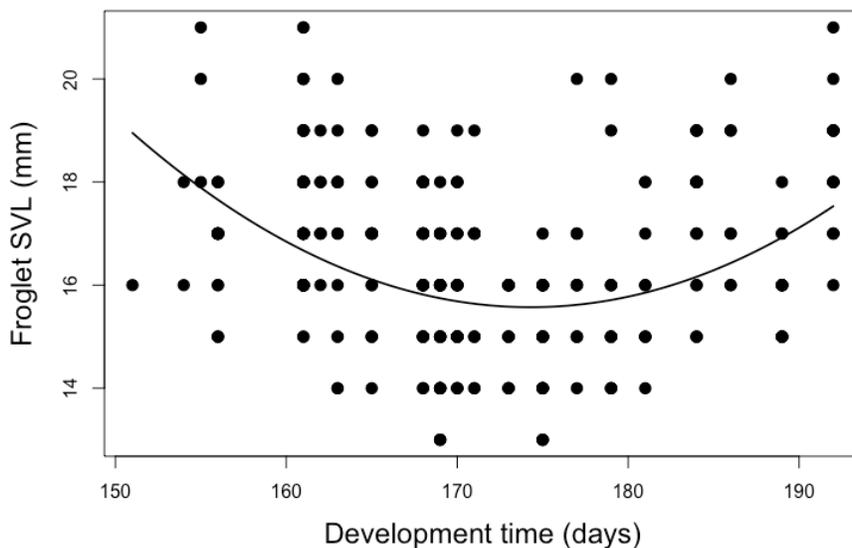
Figure 5.1-15. Relationship between development time and size at metamorphosis for froglets reared in warming and control tanks.

Table 5.1-12. Model selection table for analyses of the effects of development time (Days + days^2), hydroperiod (Hydro), growing degree days (GDD), and food availability (food) on froglet snout vent length (SVL) in the warming and control tank

Model	AIC	Δ AIC	Weight
Days + days^2	1221.34	0	0.3
Days + days^2 + GDD	1222.57	1.23	0.16
Days + days^2 + food	1222.74	1.4	0.15
Days + days^2 + hydro	1223.17	1.84	0.12
Days + days^2 + GDD + food	1223.63	2.29	0.1
Days + days^2 + GDD + hydro	1224.31	2.97	0.07
Days + days^2 + food + hydro	1224.61	3.27	0.06
Days + days^2 + GDD+ food + hydro	1225.4	4.06	0.04
Intercept (tank as random)	1270.54	49.2	0
Food	1271.2	49.86	0
Hydro	1271.96	50.62	0
GDD	1272.47	51.13	0
Food + hydro	1272.61	51.27	0
GDD + food	1273.2	51.86	0
GDD + hydro	1273.86	52.52	0
GDD + food + hydro	1274.6	53.26	0

Effects of canopy cover in the field: The best performing model for egg viability included an interaction between site and canopy cover. At our Coastal NRLF 2 site egg viability was lower in the closed canopy treatment (t-value = 2.5, P = 0.019). None of the other sites showed any effects of canopy cover on egg viability (P>0.35 for the other three sites).

The best performing model for tadpole daily survival also included an interaction between site and canopy treatment (Appendix 8.12). Daily tadpole survival rate in the closed canopy treatment was higher than in the open treatment at two sites but did not differ between canopy treatments at the other three sites (Figure 5.1-16). We found no effect of temperature on tadpole daily survival (Appendix 8.12).
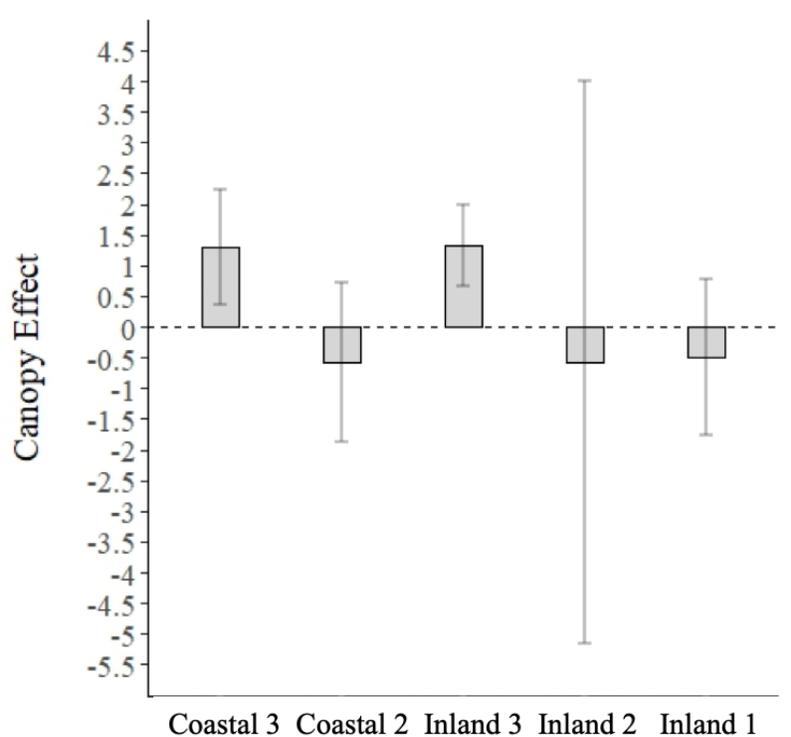
Figure 5.1-16. Canopy cover effect on tadpole survival. Values and error bars are the log odds ratio of estimated tadpole daily survival in the closed mesocosms compared to open mesocosms and associated lower and upper confidence limits. Estimates are from the top performing tadpole survival model.

Our two top performing models explaining tadpole stage duration, a site only effect model and a site plus treatment (closed vs. open canopy) additive effects model, had very similar AIC scores (ΔAIC = 0.33). However, the site and treatment additive model showed little evidence for a treatment effect (z = -1.291, P = 0.197). We therefore used the mean tadpole stage duration of all mesocosms producing froglets within each site in our population growth models.

Despite the elasticity analysis indicating that population growth rates are 2.6 times more sensitive to changes in adult survival than early-stage demographic rates, we found that canopy cover effects on early life stage demographic rates were large enough at three sites to impact population growth rates. The impact of canopy cover on population growth rates mediated through tadpole survival was greater than the impact mediated through egg viability. At Coastal NRLF 2, presence of canopy cover was associated with a 0.22 point reduction in egg viability, leading to 6% decrease in projected population growth rate (λ = 1.11 and 1.04 in the open and closed treatments respectively). At Coastal NRLF 3 and Inland NRLF 3, a 0.07-0.09 point increase in daily survival rates corresponded to a 40-42% increase in projected population growth rates (λ of 0.69 in the open treatments for both sites; λ = 0.97 and 0.98 in the shaded treatments at Coastal NRLF 3 and Inland NRLF 3 respectively).

This works shows that altering canopy cover can be a useful management tool for pool breeding amphibians and can have meaningful population level impacts. However, we caution that canopy alteration is not a one-size-fits-all approach. Our work demonstrates that the influence of canopy cover on early stage demographic rates can vary not only among species, as demonstrated in previous studies, but also across sites within species and can have contrasting effects on different life stages.

5.1.5   Alaskan douglasia (*Douglasia alaskana*)

We found climate effects on every demographic rate in which we tested for them, other than variance in size after one year of growth. Most vital rates were dependent on both temperature and precipitation, with both aspects of climate having positive effects on some demographic rates and negative effects on others.

Demographic rates for SEED models: Coldest month temperature and/or precipitation affected most demographic rates (probability of survival, probability of fruiting, and number of fruits given fruiting), and annual mean temperatures and precipitation affected mean size after one year of growth (Table 5.1-13). We found positive effects of temperature on survival and growth, and negative effects of temperature on reproductive demographic rates. Precipitation had both positive and negative effects on different demographic rates. Higher winter precipitation was associated with lower fruit production, while higher annual precipitation was associated with higher survivorship and growth. Interactions between climate variables and size, as well as effects of prior years' climate were also present, leading to complex effects of some climate variables on some demographic rates (Figure 5.1-17). For example, for probability of survival, the positive interaction between size in the previous time step and the coldest month's temperatures in the year prior suggests that larger plants are more able to capitalize on the positive impact of higher temperatures than are smaller plants (Table 5.1-13). Higher temperatures reduced the probability of fruiting, which then increased survival; these results suggest that it is quite advantageous for larger plants to forgo reproduction in response to high temperatures, but less advantageous for smaller plants.

Table 5.1-13. Coefficient estimates (first row) and standard error (second row) of coefficient estimates for each demographic rate used in this study. Coefficients significant at the 0.05 level are shown in bold; coefficients in italics are marginally significant (P< 0.06). We also show estimates of seedlings per fruit (recruitment) for each population.

Demographic rate	Intercept	Ln(size in previous time step)	Coldest month precip.	Coldest month temp.	Coldest month precip. (year prioir)	Coldest month temp. (year prior)	Coldest month precip. i (year prior) x ln (size in the previous time step)	Temp. (year prior) x ln (size in the previous time step)	Annual precip.	Average annual temp.
p(survival)	**-1.870**	**-0.463**			**-0.007**	**0.076**	**0.005**	**0.036**	**0.003**	
	0.511	**0.105**			**0.003**	**0.024**	**0.001**	**0.015**	**0.001**	
mean size	**1.188**	**0.727**							**0.000**	**0.293**
	0.204	**0.020**							**0.000**	**0.023**
variance in size	**-1.884**	**-0.118**								
	0.102	**0.049**								
p(fruiting)	**-2.629**	**2.067**	**-0.017**	**-0.251**						
	0.404	**0.227**	**0.004**	**0.066**						
# of fruits given fruiting	**0.519**	**-0.218**		**-0.208**						
	0.166	**0.072**		**0.023**						

Population	C	E1	E2	N	S
Estimated seedlings per fruit	0.193	0.333	0.160	0.097	0.196
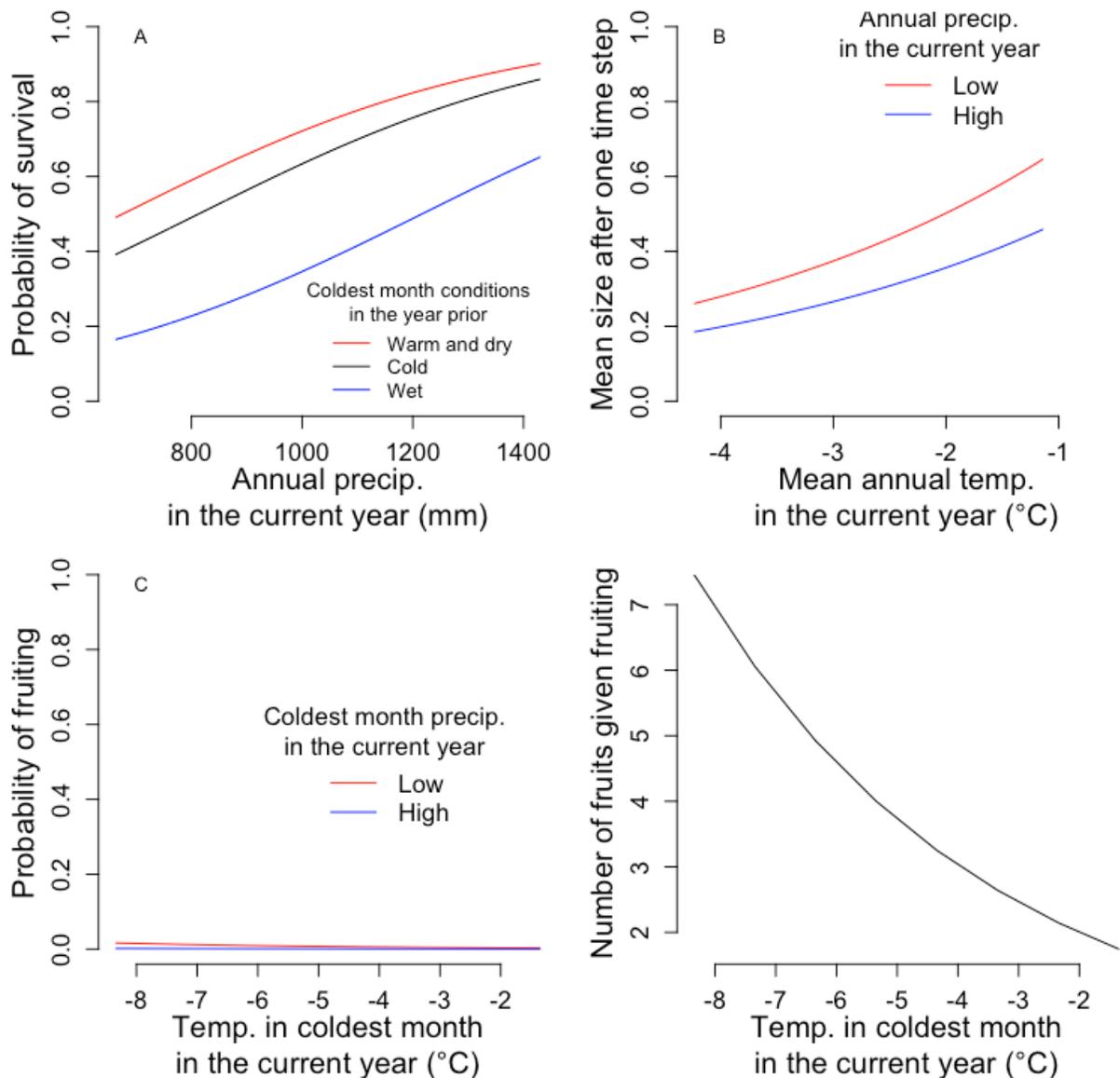
Figure 5.1-17. Demographic rate functions for probability of survival (A), mean size after one year of growth (B), probability of fruiting (C), and number of fruits given fruiting (D) for a plant of median size. For A, we show how the impact of precipitation in the coldest month changes with coldest month conditions in the year prior. For example, if the coldest month in the year prior was warm and dry, then the probability of survival over a given year depends more strongly on precipitation in the coldest month of the current year. For B and C, we show how the impact of temperature varies with the associated precipitation during the same interval.

5.1.6 Venus flytrap (*Dionaea muscipula*)

Some aspect of both climate and fire frequency affected every demographic rate in which we tested for a climate effect. Both climate and fire had complex effects on Venus flytrap demographic rates. In many cases, relationships were nonlinear. In others, the same climate variable had opposing effects on different demographic rates. The magnitude of many observed climate effects on demographic rates both depended on time since fire and varied from site to site.

Demographic rates for SEED models: Both local and regional climate variables were present in the best-supported models, with almost all demographic rates dependent on temperature and/or

precipitation, rather than integrated metrics of water stress (with the exception of probability of fruiting, which depended on water balance) (Table 5.1-14). Both annual climate and monthly extremes were present in the best performing models, with annual, as well as driest, coldest, wettest, and warmest month climate variables all affecting one or more demographic rates. Further, most demographic rates had multiple climate variables present in the top ranked model, and many had quadratic terms or interactions between temperature and precipitation (Table 5.1-14), leading to complex relationships between climate variables and performance (Figure 5.1-18).

Table 5.1-14. Climate variables present in the best performing models for each demographic rate. We show a "1" if a linear term is present, a "2" if a quadratic term is present, "3" if a categorical term is present, and an "x" if an interaction with this term is present (note that we did not find any interactions between annual precipitation^2 and temperature^2). A "+" or a "-" suffix indicates the sign of the effect. "NA" indicates that we did not test for the effect. For climate variables, plain text indicates a local climate variable and italics indicate a regional variable. Note that we were not able to look for an effect of climate on recruitment.

	Years since fire	Annual temp.	Annual precip.	Annual water balance	Warmest month temp.	Warmest month precip.	Warmest month water balance	Driest month temp.	Driest month precip.	Driest month water balance	Coldest month temp.	Wettest month precip.	Wettest month water balance
p(survival)	1+, 2-				1+, 2-, x+	*1-, x+*		1-	*1-*				
Mean plant size after one year of growth	1+	1+			1-			1-, x-	*1-, x-*		1-, 2+	*1-, 2+*	
Variance in plant size after one year of growth	1+	1-	*1+*			*1-*		1+	*1-*		1+		
p(fruiting)	1-			*1-, 2+*			*1+*			*1+, 2-*			*1+, 2-*
Number of fruits	1+, 2-				*1-*	*1+*			*1-*			*1+*	
Recruitment	3-	NA	NA	NA	NA	NA	NA	NA	NA	NA	NA	NA	NA

All demographic rates included terms for years since fire, and some demographic rates also included nonlinear effects of years since fire (Table 5.1-14, Figure 5.1-18). As the number of years since a fire increased, both mean growth and variance in growth were higher, meaning that on average plants grew larger, but there was more heterogeneity in plant growth (perhaps caused by increasing competition, Weiner and Thomas 1986, though see Einum et al. 2012). Similarly, survival and fruit number initially increased with years since fire, but longer intervals between fires reduced performance, leading to an optimum around 6-7 years (fruit number; Figure 5.1-18) or 5-11 years (survival). Finally, probability of fruiting was highest immediately after a fire, as was recruitment.
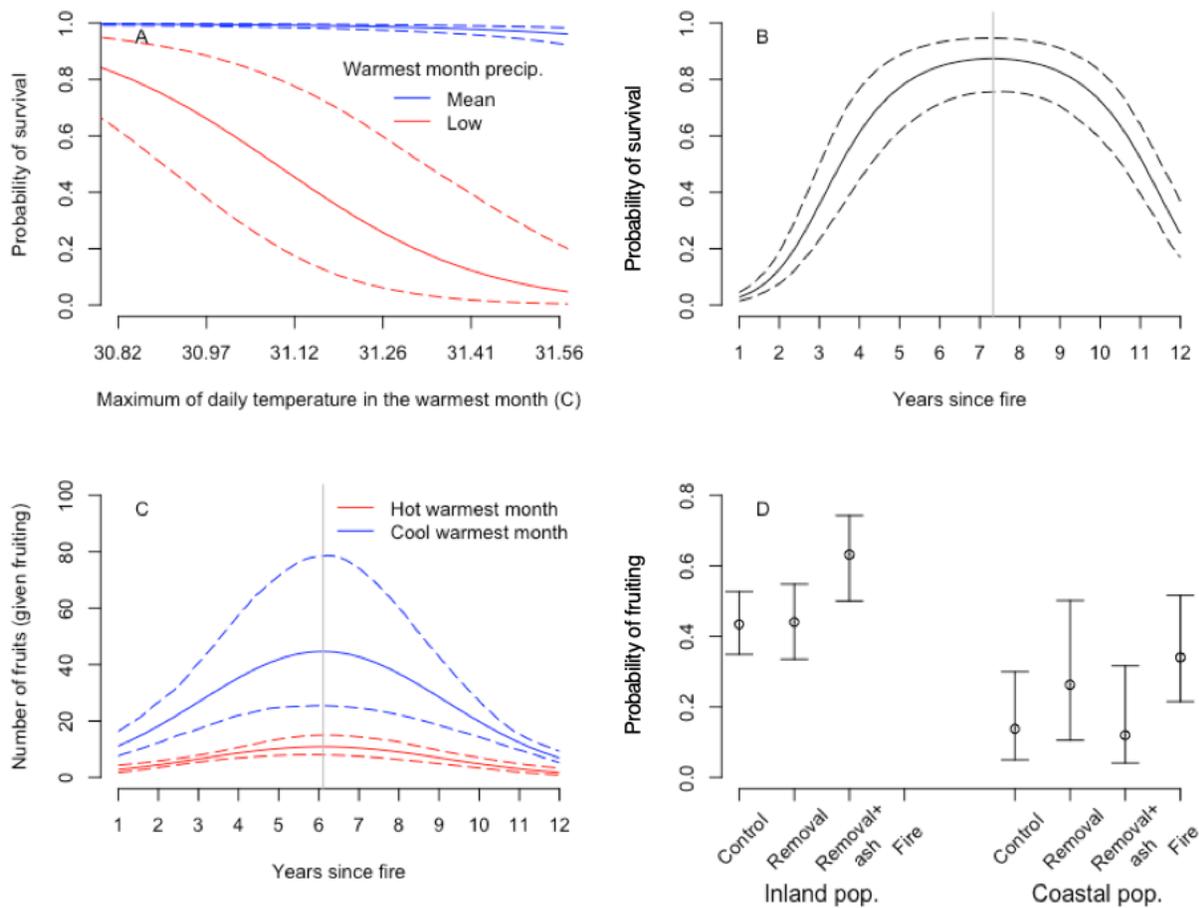
Figure 5.1-18. Examples of effects of climate and years since fire (A, B, C), and of experimental treatments (D) on demographic rates for a plant of mean size. Solid lines show the mean predicted demographic rates while holding all other climate variables or years since fire constant at the mean values. Dashed lines and error bars show 95% confidence intervals calculated across 500 bootstrap replicates. Panel A illustrates an interaction between precipitation and temperature in the warmest month; namely, we show how the effect of temperature in the warmest month differs with precipitation in that month (we show predictions for the 50th and 10th quantiles of driest month precipitation values from 2015-2018). B and C show demographic rate functions with intermediate optima (with the optima shown with grey vertical lines), and C illustrates how these optima differ with temperature in warmest month (we show predictions for the 10th and 90th quantiles of warmest-month temperature). D shows effects of experimental manipulations of fire effects at two populations, and effects of an unanticipated fire at our Coastal population. Note that fire did not occur at the inland population.

Experimental tests of fire effects: Our experimental work showed impacts of all three key fire effects (neighbor removal, ash addition, and tissue damage) on Venus flytrap demographic rates and population growth rate. Experimental conditions affected survival, mean plant size after one year of growth, and probability of fruiting (Figure 5.1-18D, Appendix 8.4). Largely consistent with our observational work, all three manipulated conditions (neighbor removal, neighbor removal plus ash addition, and fire) reduced survival and growth relative to the control, but increased the probability of fruiting (although the impact of condition differed with population for survival and probability of fruiting; Figure 5.1-18D, Appendix 8.4). For example, the effect of the neighbor removal on probability of fruiting was minimal at the inland population, but stronger at the coastal population, but the opposite was true for neighbor removal + ash addition (Figure 5.1-18D). Our results suggest minimal negative impacts of tissue damage at the coastal

89

site. At our inland population, adding ash and removing neighbors significantly increased population growth rate, and removing neighbors resulted in only moderate increases in population growth rate (Figure 5.1-19); these effects are likely driven by reproduction, the only demographic rate consistent with this pattern (Appendix 8.4). Neither removing neighbors nor adding ash and removing neighbors had significant effects on population growth rate at our coastal population. However, we did see a significant positive effect of a fire (Figure 5.1-19), indicating that the positive impacts of ash addition and neighbor removal (at least for an actual fire, which may not have been fully mimicked by our treatments) were substantial enough to compensate for any negative impact of tissue damage.
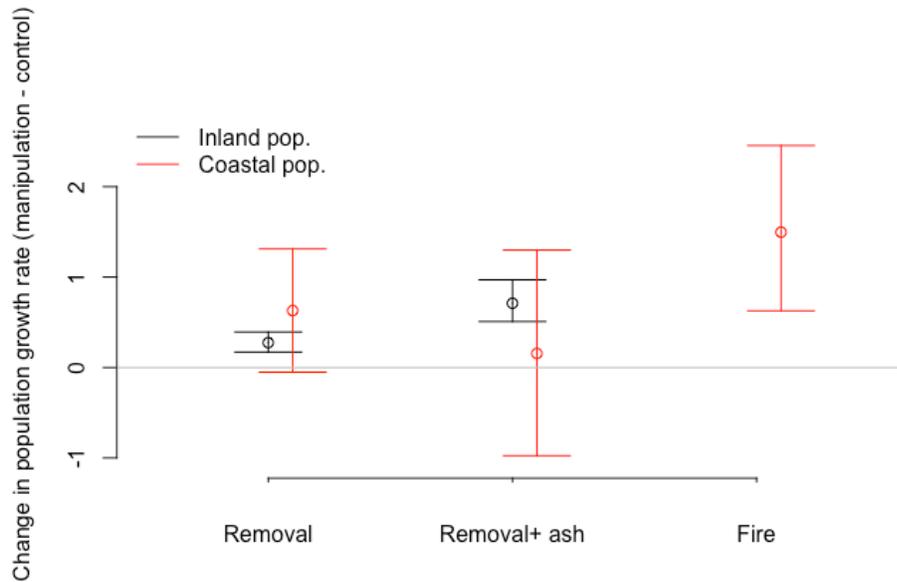
Figure 5.1-19. The effect on Venus flytrap population growth rate of experimental neighbor removal, neighbor removal plus ash addition, and of an accidental fire at the coastal population (which caused neighbor removal, ash addition, and tissue damage). We show the difference in population growth rate between the specified condition and an unmanipulated, unburned control for two separate populations, one inland and one coastal. Error bars indicate 95% confidence intervals, where confidence intervals incorporate parameter uncertainty). A value of zero, indicated by the grey line, indicates no effect of a given condition on population growth.

5.1.7   Red-cockaded woodpecker (*Dryobates borealis*)

Red-cockaded woodpecker demographic rates were influenced by both climate variables and group social status in complex ways. Many demographic rates influenced by climate were sensitive to multiple climate variables. As we observed in other species, some climate variables had positive effects on some demographic rates while having negative effects on others. *Demographic rates for SEED models:* We found support for including non-climate variables as predictors of demographic rates, with the majority of demographic rates dependent on group characteristics, age, and social status. Reproductive performance usually increased with breeders' age, but we found evidence for reproductive senescence: reproductive demographic rates increased and then decreased with both male and female adult age (indicated by negative quadratic terms for paternal and maternal age, Appendix 8.13). Unsurprisingly, more helpers at a given territory improved many reproductive rates (Appendix 8.13). For both adults and fledglings, males had higher survival rates than females. Breeders had the highest survival rates, followed by helpers, then floaters. Similar to reproductive rates, adult survival increased with

number of helpers, and older individuals had lower survival rates (see the negative quadratic term for age, Appendix 8.13).

Climate also strongly influenced demographic rates: both survival rates depended on one or more climate signals, and three of nine reproductive rates were driven by one or more climate signals (all demographic rates controlled by climate signals are shown in Figure 5.1-20). All climate variables besides minimum temperature affected one or more demographic rates, and many different climate windows affected demographic rates. In particular, both short-lag and long-lag climate windows affected reproductive rates, and, similarly, survival rates were dependent on conditions throughout the year.

Survival rates were affected by mean and maximum temperatures, precipitation, and windspeed. The effects of each of these depended on time of year (Figure 5.1-20). Specifically, higher September-March precipitation decreased adult survival (with independent negative effects of October precipitation; Figure 5.1-20). Higher mean temperature in an overlapping time period (November- December) also increased adult survival. The negative effect of wet conditions in the fall, winter, and spring was reduced by higher temperatures, as indicated by a positive mean temperature x precipitation interaction. Higher summer windspeed decreased adult survival, and this negative effect was exacerbated at higher late-summer-to-spring precipitation levels, as indicated by a negative windspeed x precipitation interaction. Post-fledging survival was dependent on quite different climate signals; higher August-October maximum temperature decreased post-fledging survival, but higher March-April windspeed increased post-fledging survival (Figure 5.1-20).

Reproductive demographic rates were affected by maximum temperature, precipitation, and windspeed, with both short-lag climate effects, and, less commonly, long-lag effects (Figure 5.1-20). Specifically, higher February-April maximum temperature increased the probability of initiating a first nest, whereas precipitation had disparate effects: higher February-April precipitation decreased this probability, and higher January precipitation increased this probability. Higher December-March windspeed decreased the probability of initiating a first nest, but this negative effect was reduced when temperatures were high (as indicated by the positive temperature x windspeed interaction). Higher November-April windspeed reduced clutch size. Finally, we found one long-lag climate signal for a reproductive demographic rate: probability of double brooding increased with precipitation during the September through November period before the breeding season in question (Figure 5.1-20).
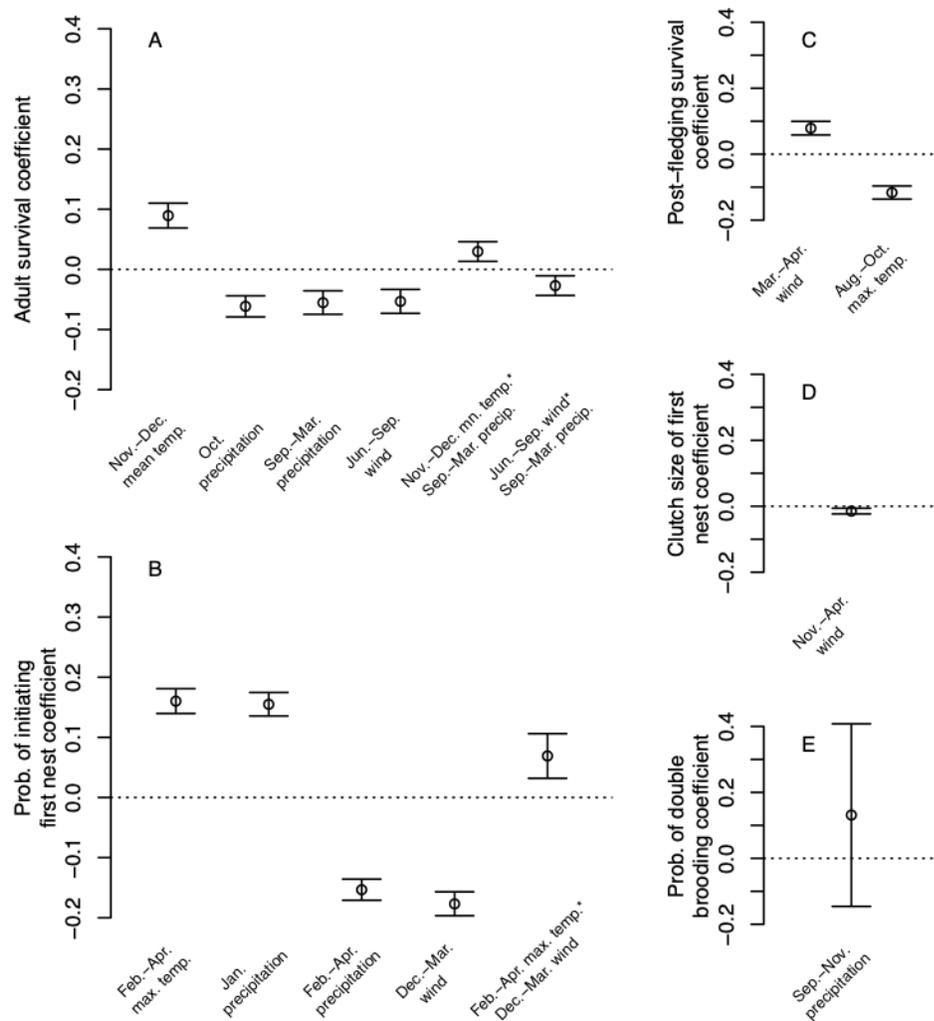
Figure 5.1-20. Coefficients of climate signals in the best performing mixed model for each climate driven demographic rate. Bars indicate standard error (SE) of coefficients. Months include all days in that month. The wide SE in panel E is likely due to relatively few instances of this demographic rate (second and later nests are relatively rare compared to first nests).

5.2   Projecting future population growth rates

In this section, we present the results of SEED models for each of our seven study species. For species with a life history readily described by a few demographic rates, we first present the projected change over the next 20-40 years in the climate variables influencing those demographic rates, followed by the expected change in the demographic rates associated with projected changes in their climate drivers. For all seven species we present the population growth rates over the same time period.

5.2.1   Hydaspe Fritillary Butterfly (*Speyeria hydaspe*)

Both temperature and precipitation are projected to increase at all hydaspe fritillary butterfly study locations between the early 21st century and 2050 (Figure 5.2-1). The median projected increase in temperatures fell within the range of 1.5 ºC to 1.8 ºC. Late spring/summer daily maximum temperatures are projected to rise the most at the Cascades site, and least at the Coast Range sites. Summer daily minimum temperatures are projected to increase the most at the

two upper elevation Sierra Nevada sites. Median projections for annual precipitation gains are as little as 19.8 mm at the lowest Sierra Nevada site to as much as 64 mm at the Cascades site.
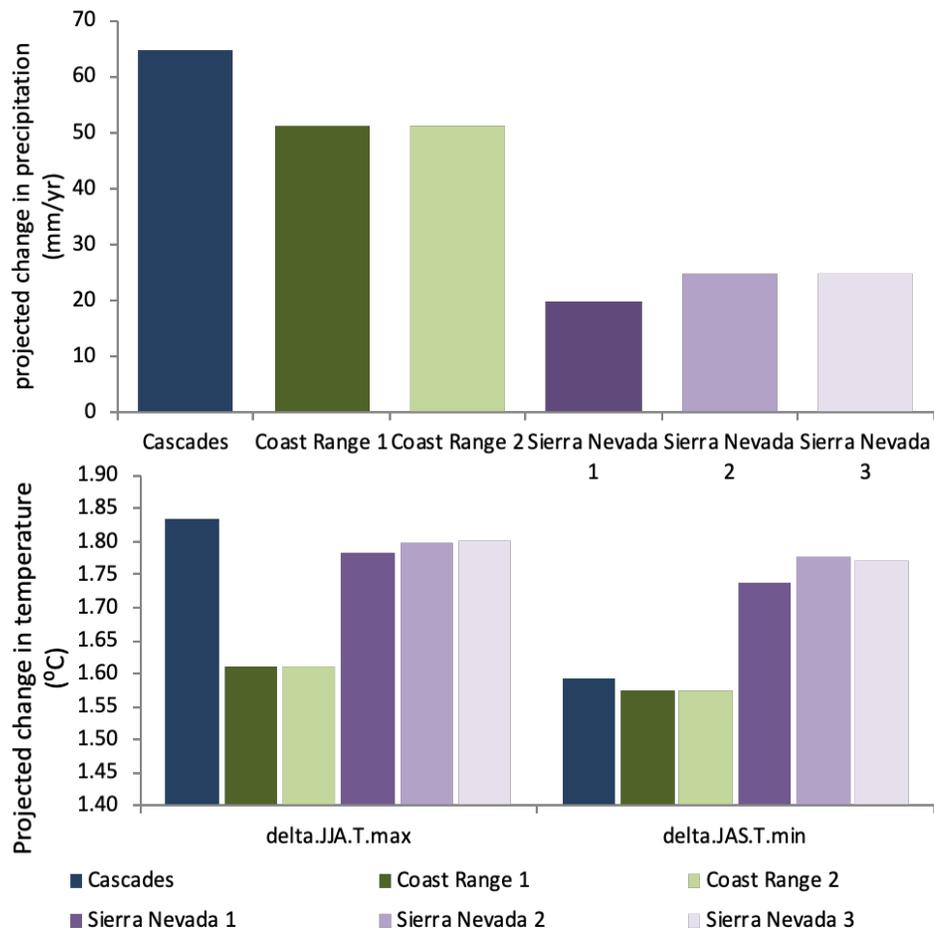
Figure 5.2-1. Projected changes in climate variables impacting hydaspe fritillary butterflies at six sites. Values represent the difference in the median projected climate between 2041-2050 and 2006-2016 from 20 downscaled GCM data sets.

These projected changes would have mixed effects on hydaspe fritillary butterfly demographic rates. Across demographic rates within each site, projected changes in climate would lead to decreased egg hatch rates but increased spring caterpillar survival and adult longevity (Figure 5.2-2). There were no qualitative differences in projected egg hatch rates or population growth rates between SEED models assuming a separate site effect or not. We report results with the site effects on hatch rates included. The magnitude of change in these demographic rates is expected to vary across sites for a variety of reasons. Much of the difference in how larval spring survival responds to warming climate is driven by baseline survival rates. Because survival exhibits a logistic-linear relationship to temperature, and because logistic curves are relatively flat near the boundaries, there is little change with temperature at the lower Sierra Nevada site, where measured present-day larval survival was near zero. Site to site differences in how adult survival is projected to change can be attributed to differences in projected increases in summer temperatures. Both differences in egg predation rates and in how

much summer temperatures are projected to rise cause differences among sites in how much egg hatch rates are projected to decrease.
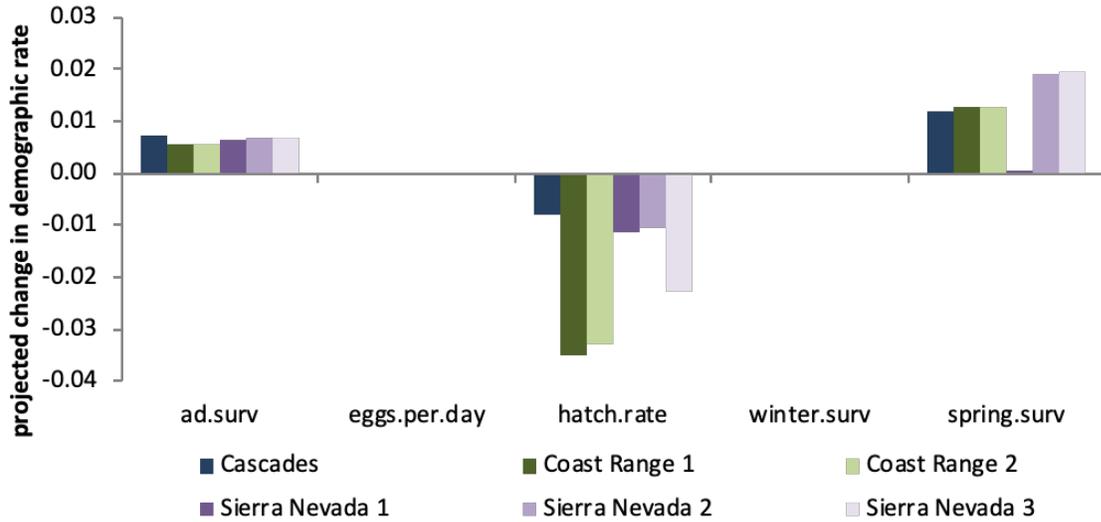
Figure 5.2-2. Projected changes in hydaspe fritillary butterfly demographic rates at six sites. Values represent the difference in the demographic rates between 2041-2050 and 2006-2016 given the mean climate data from 20 downscaled GCM data sets at each site during each period. Two demographic rates, eggs per day and winter larval survival, are not expected to be affected by projected changes in climate conditions.

Two of our study sites, the Cascades and low-elevation Sierra Nevada site, project to be sink populations under current climate conditions. The remaining sites project to be source populations potentially growing at least 50% per year in the absence of density dependence. The difference between source and sink populations was not climate related. One sink population inhabited the warmest, driest site, while the other inhabited the coolest site, which received an intermediate amount of rainfall. In contrast, the highest projected population growth potential under current climate conditions occurred at the two higher elevation Sierra Nevada sites, which were warmer and drier than the two Coast Range source populations.

SEED model results: Our SEED models predicted that projected trends of warmer temperatures and increased annual precipitation at all sites lead to slight increases in hydaspe fritillary butterfly population growth rates across the board (Figure 5.2-3). There was a positive correlation between initial population growth rates and projected increases, with little change expected at the low elevation Sierra Nevada site and the largest gains expected at the two higher elevation Sierra Nevada sites. This widespread species is not likely to require conservation in the coming decades as a result of climate change.
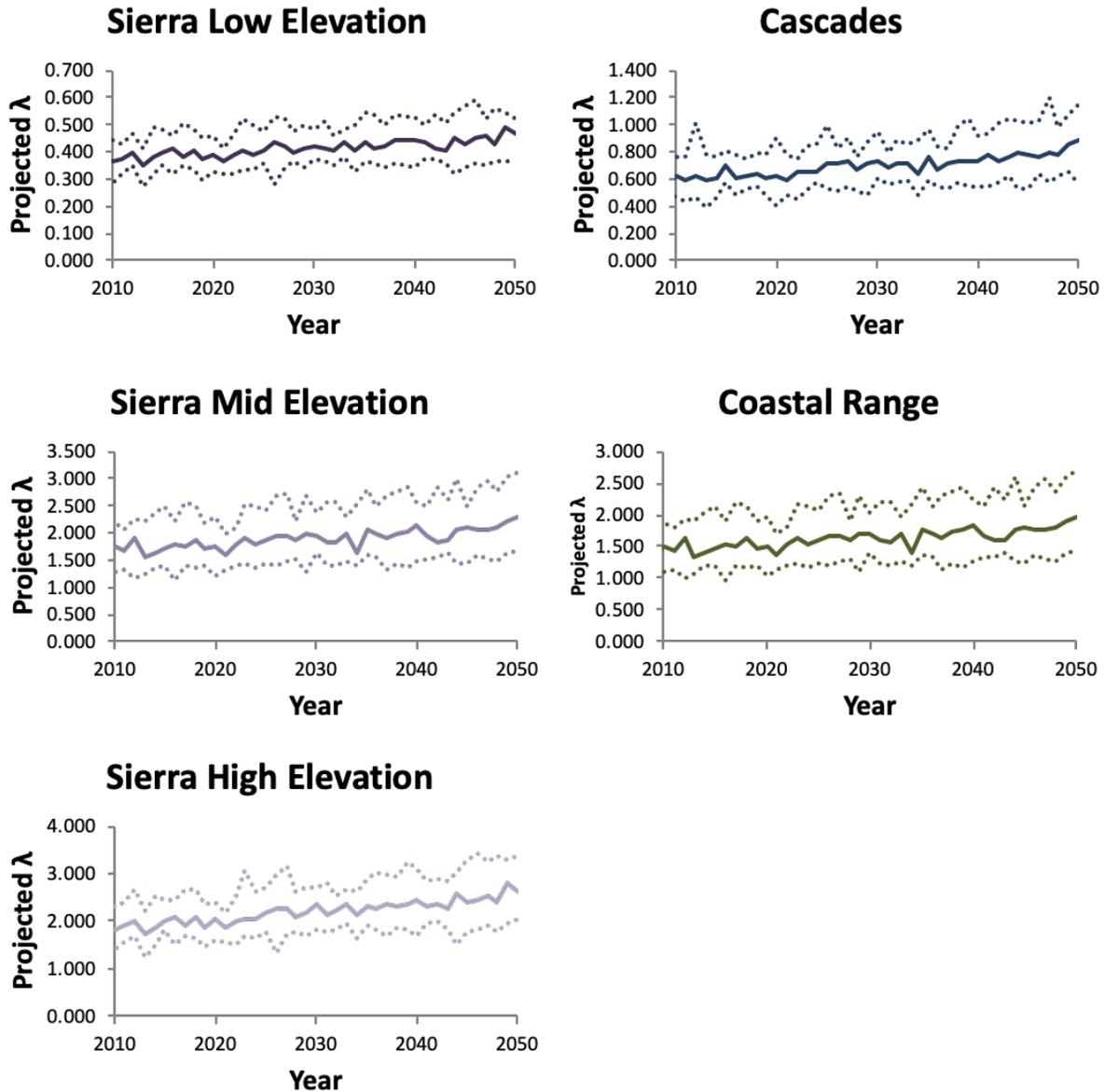
Figure 5.2-3. SEED model projections for annual hydaspe fritillary butterfly population growth rates at six sites from 2007-2050. Dark solid lines show the median projected discrete annual growth rate (λ) from SEED model runs linked to projected climate data from 20 downscaled global climate models. Dashed light lines show the 5th (bottom) and 95th (top) percentile of projected annual growth rates.

5.2.2 Appalachian brown Butterfly (*Satyrodes appalachia*)

Summer temperatures at Fort Bragg, NC, are projected to rise about 1.4–1.8 ℃ by mid-century. This warming would reduce the values of demographic rates of all life stages, with each demographic rate being most sensitive during different times of the year (Figure 5.2-4). Fecundity will be most impacted during the first generation, egg hatch rates during the second generation, and larval survival during the third generation of the year.
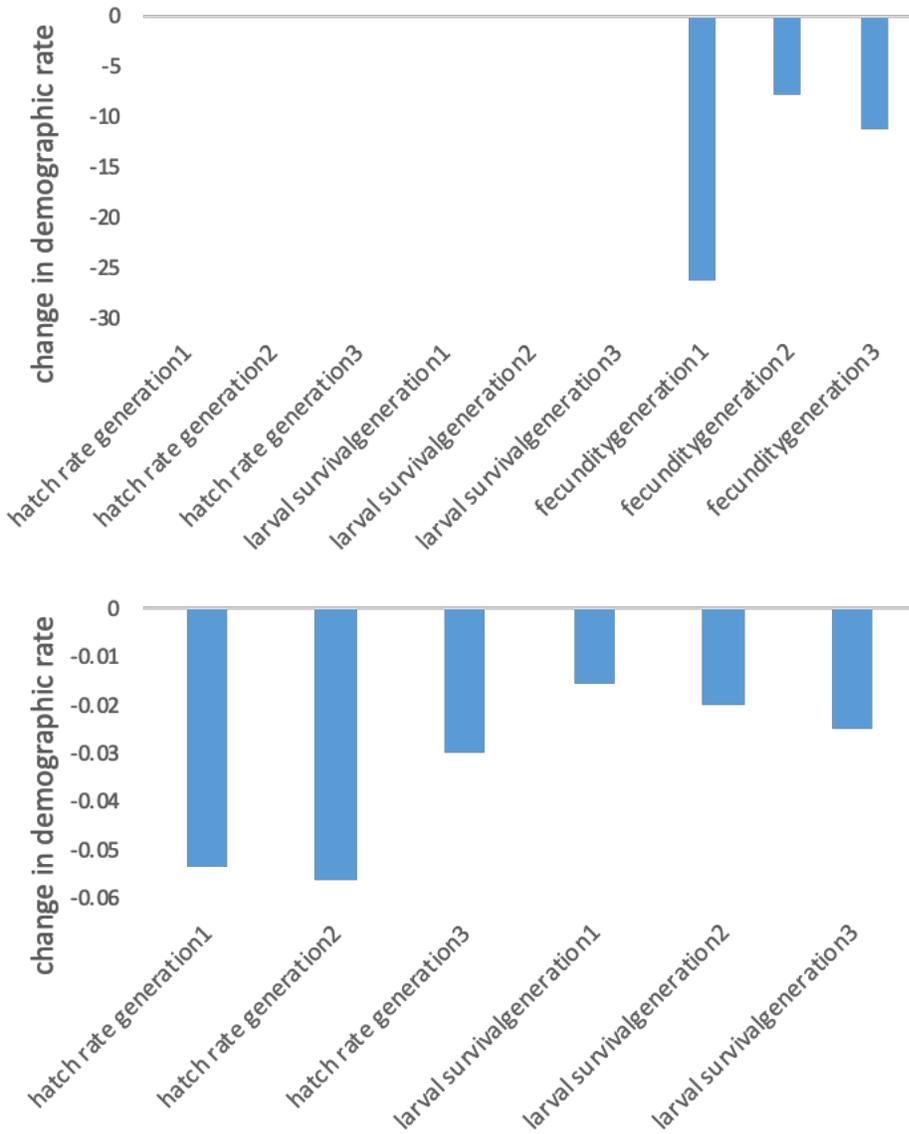
Figure 5.2-4. Projected changes in Appalachian brown butterfly demographic rates. Values represent the difference in the demographic rates between 2051-2060 and 2016-2025 given the mean climate data from 20 downscaled GCM data sets at each site during each period.

SEED model results: The median global climate model projects that annual growth rate for Appalachian brown butterflies will remain under one (shrinking) during the entire period, while the shift from growing to shrinking is projected to occur by the 2050's at the 95th percentile across GCMs (Figure 5.2-5).
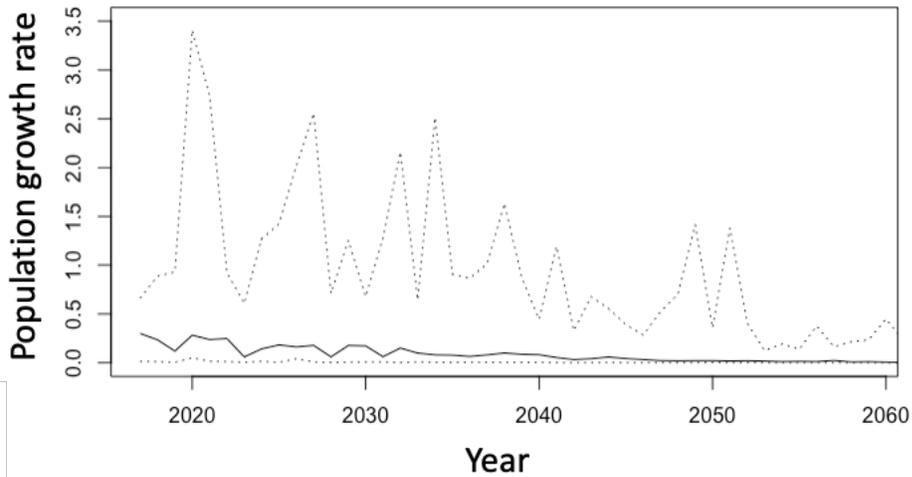
Figure 5.2-5. Projected discrete annual population growth rate (λ) for Appalachian brown butterflies over the years 2016-2100. The solid line represents the median and the dashed lines represent the 5th to 95th percentile range from the output of 20 GCMs.

Evaluating the mitigation potential of additional generations: Increasing the number of generations per year from two to three significantly increased projected growth rates under present day climate conditions (Figure 5.2-6). Fort Bragg would be a clear population sink if Appalachian brown butterflies had only two generations per year but would increase in size by almost 50% per year with three generations per year. However, the additional generation does not provide much of a buffer to climate change, with population growth rates dipping below one well before 2030 even if all larvae in the second generation contribute to the third.
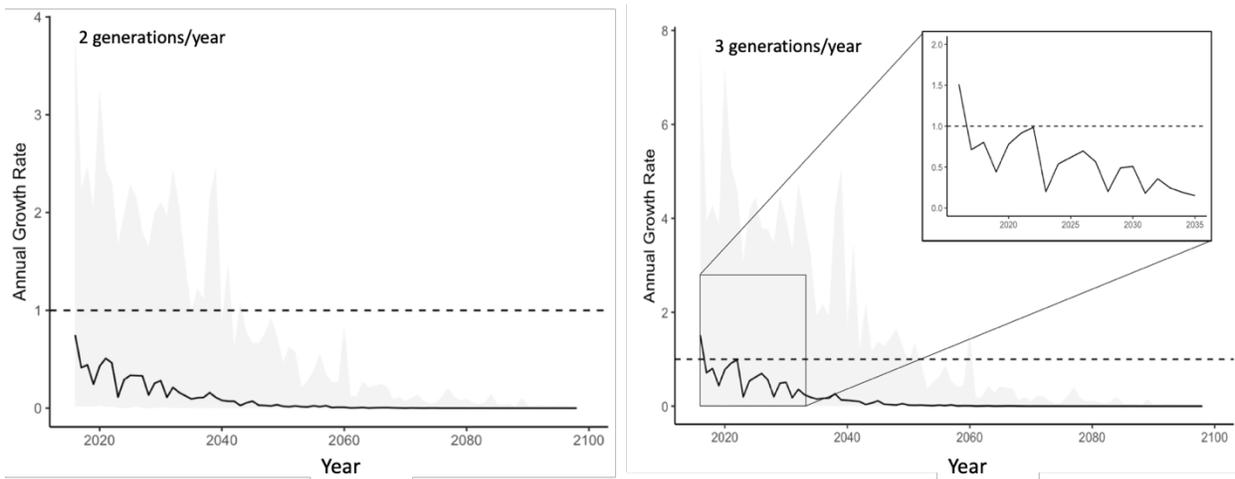
Figure 5.2-6. Projected discrete annual population growth rate (λ) for Appalachian brown butterfly over the years 2016-2100 assuming all caterpillars from second generations undergo diapause (left panel) or direct development (right panel). Solid line shows median projected growth rate and grey shows the range between the 5th and 95th percentile from the output of 20 GCMs.

97

Projected changes in demographic rates in Michigan and South Carolina: Projected warming during egg and larval development is expected to be greater in Michigan than in South Carolina (Figure 5.2-7a and b). However, projected temperatures in Michigan remain cooler than in South Carolina over the 21st century, matching predictions in the literature (Hansen et al. 2006). Using the projected temperature data at each site and the relationships we found between temperature and egg and larval survival, we predict that both egg and larval survival will decrease under future climate conditions (Figure 5.2-7c and d). Both egg and larval survival are expected to be higher in the Michigan compared to South Carolina population under future climates. Sites differences are greatest for larval survival, particularly mid-century when projected temperature differences between Michigan and South Carolina span the steepest part of the larval survival curve (Figure 5.2-7b). Notably, larval survival in the South Carolina population approaches zero by the end of the century, while it drops to just under 25% in the Michigan population. This suggests that populations at the southern end of the range are more likely to extirpated under future climate conditions than populations near the northern range boundary.
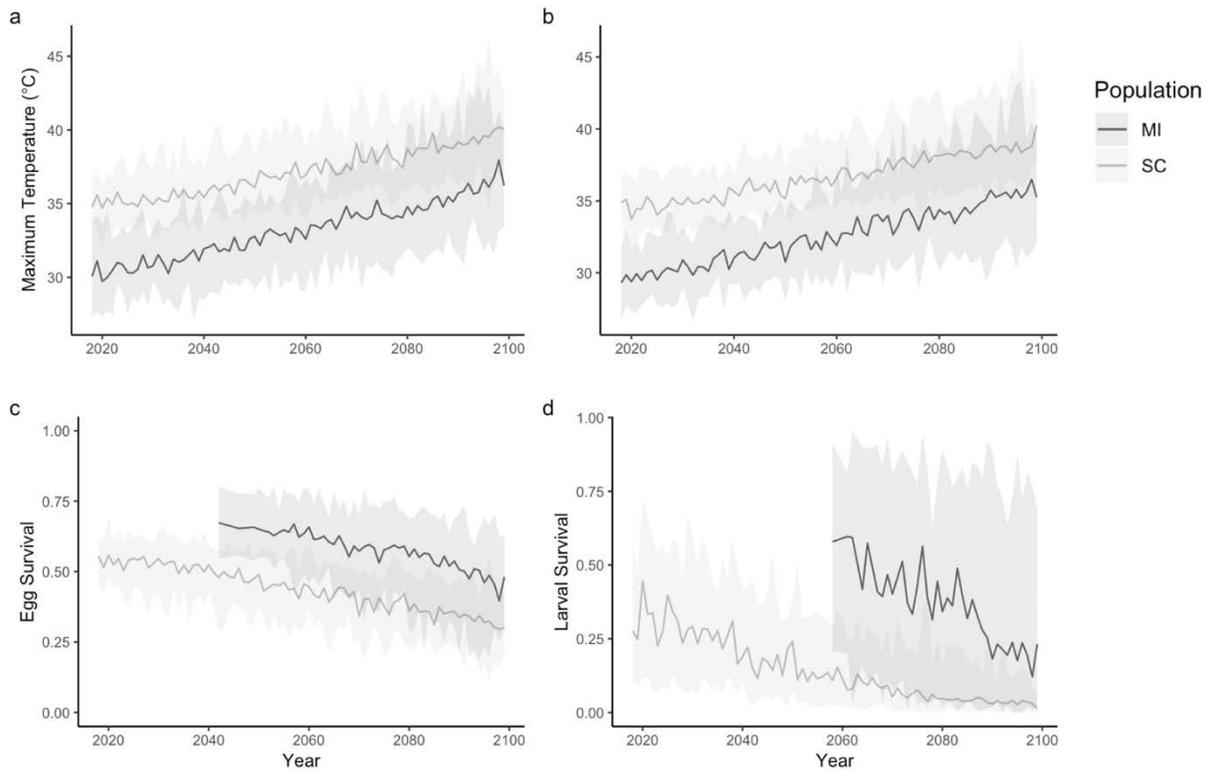
Figure 5.2-7. Projected temperatures for eggs (a) and larvae (b) with projected demographic rates respectively (c, d). Solid lines represent the median and shading represents the 5-95% range from 20 GCMs. Michigan projected egg and larval survival rates are truncated because temperatures ranges occurring before 2058 were not tested in our experiments. In Michigan, our greenhouse temperatures were higher than those recorded in the field during 2018. We only projected demographic rates over temperature ranges that matched our experimental greenhouse temperatures. For the egg survival rates, this began in the 2040s, and for the larval survival rates this began in the 2050s (c and d).

Warming temperatures are likely to make southern populations of this species more conservation reliant over the coming decades. Northern populations may be expected to be observed during more of the summer as warmer temperatures increase the number of flight periods (generations) each year. However, based on trends seen in egg hatch rate and larval

survival, continued warming is likely to cause populations as far north as Michigan to become conservation reliant by the end of the century. This might argue that it makes the most sense to focus conservation efforts on more northern populations that have a greater likelihood of persisting under future climate conditions. Because our results suggest that Appalachian brown adults are unaffected by temperature, one conservation approach would be to rear early life stages under controlled climate conditions and release adults to bolster populations.

5.2.3 Western snowy plover (*Charadrius nivosus nivosus*)

Winter and spring temperatures are expected to warm along the entire western snowy plover coastal range (Figure 5.2-8a). As a consequence, coastal western snowy plover wintering sites that currently experience periodic cold snaps are projected to experience fewer, less severe cold snaps in the coming decades (Figure 5.2-8c). While there was not a spatial pattern in overall winter warming trends (Figure 5.2-8a), there was generally a larger reduction in DACS scores in more northerly sites.
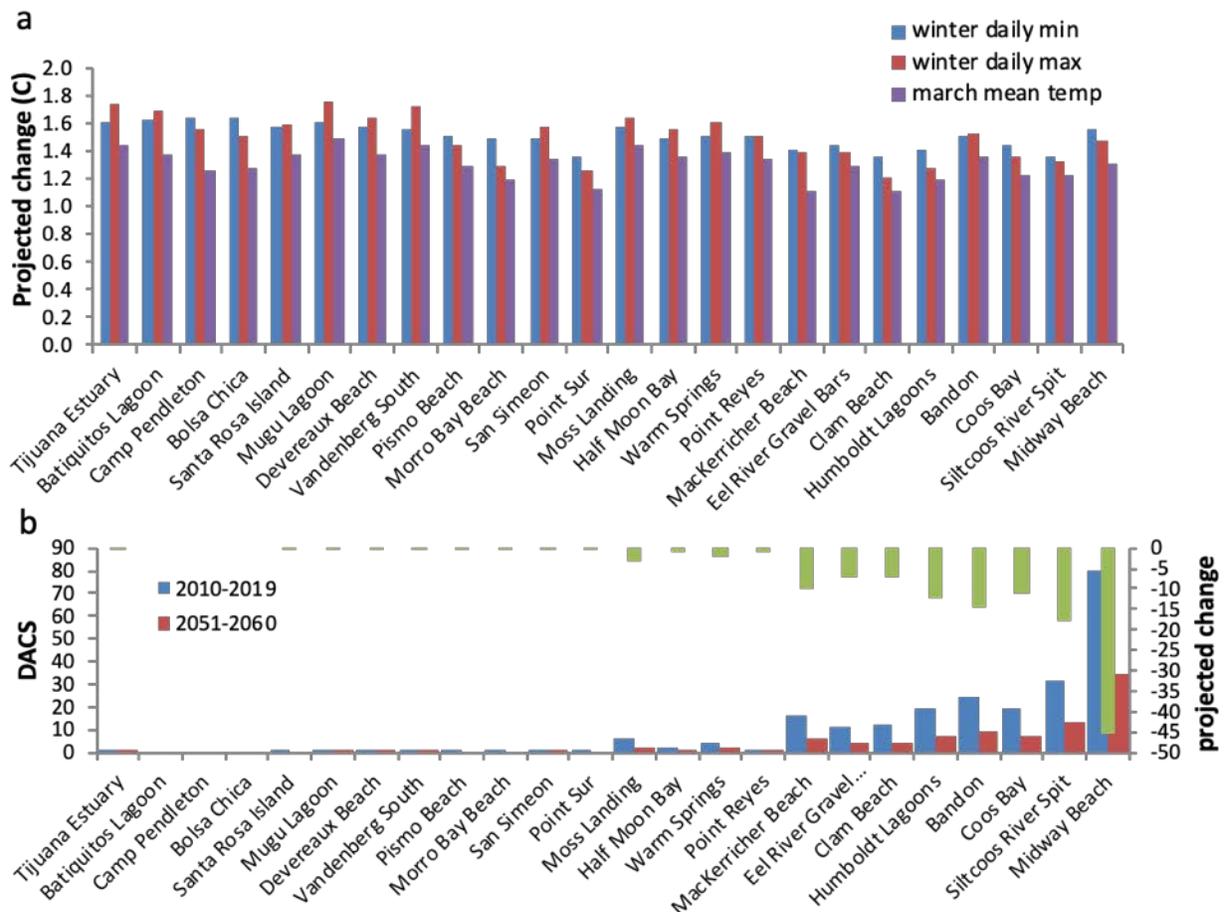
Figure 5.2-8. Projected changes between 2010-2020 and 2051-2060 in climate variables influencing western snowy plover demographic rates. Climate variables include average daily maximum and minimum winter temperatures and average daily mean temperatures during March (a), and duration-amplified cold scores (DACS) (b). Sites are listed in order from south to north (right to left).

Adult survival is projected to increase at all sites in response to warmer winters (Figure 5.2-9). The projected increase is typically greater in more northerly populations, particularly north of Point Sur, where extended cold snaps also contribute to adult mortality. The projected

99

impact of climate change on fecundity was much more variable across sites (Figure 5.2-9b). In the absence of dispersal, there was a general pattern of diminishing benefits of warmer weather moving northward from Batiquitos Lagoon, near San Diego, CA to Point Reyes and increasingly negative impacts moving northward from the mouth of Eel River. However, including the effects of dispersal, which potentially alters local age structures, lead to a more complex spatial pattern of positive and negative changes in fecundity associated with changing climate conditions (Figure 5.2-9b).
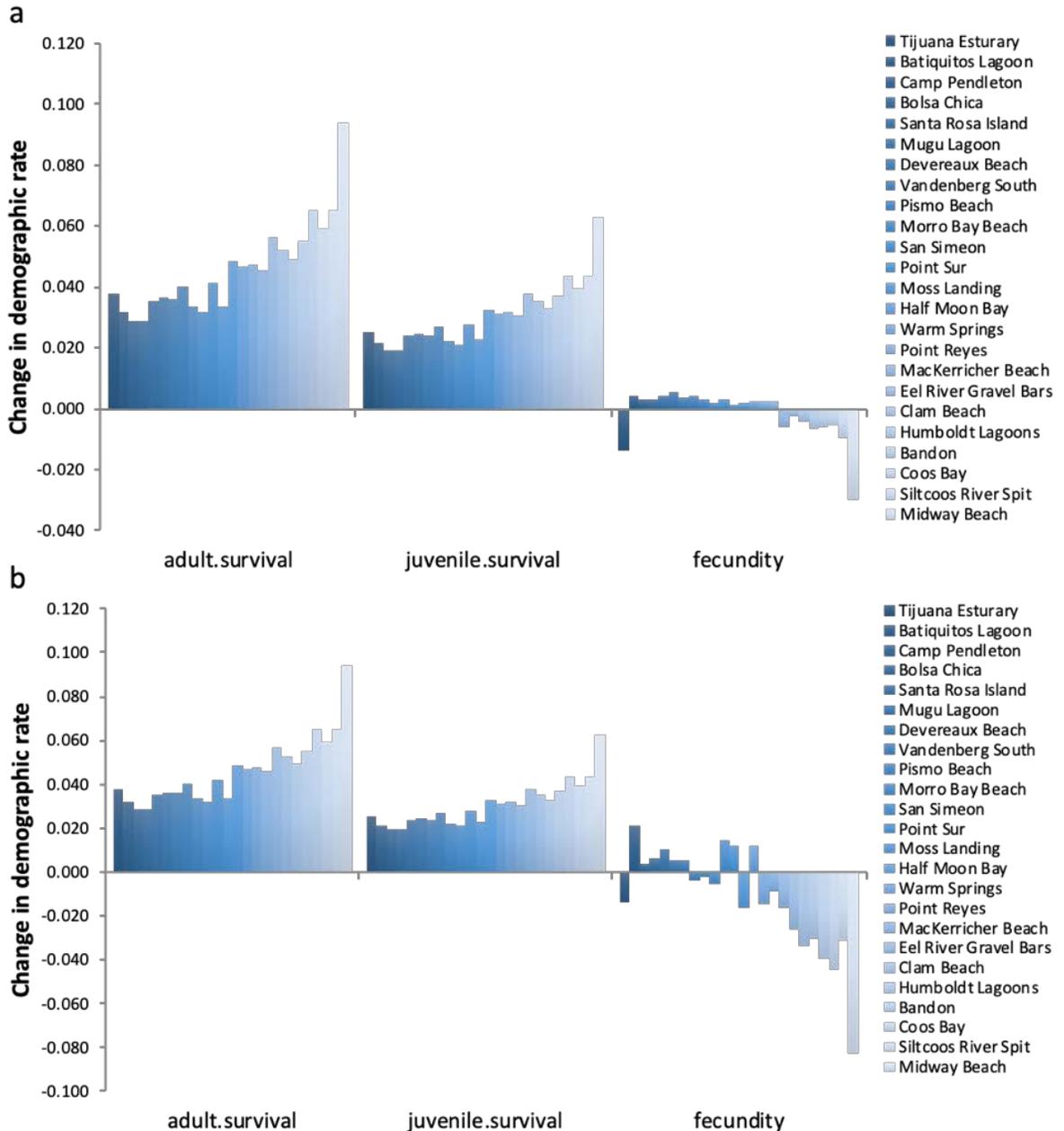
Figure 5.2-9. Projected changes in western snowy plover demographic rates at 24 sites considered in isolation (a) or accounting for dispersal (b). Values represent the difference in the demographic rates between 2051-2060 and 2010-2020 given the mean climate data from 20 downscaled GCM data sets at each site during each period.

All breeding grounds were projected by our SEED models to support increasing western snowy plover populations under current climate conditions (Figure 5.2-10). It is important to note that all non-climate components of demographic rate functions were parameterized for Monterey Bay, which has been characterized by a robust predator control program for the vast majority of the study period. Predator control, at varying levels of effort and success, currently occurs at most major nesting areas from Monterey Bay south and in Oregon, but not in most locations with smaller populations (Eberhart-Phillips et al. 2015). Consequently, the wide variation among sites in predation pressure on eggs, juveniles, and adult western snowy plovers, and in both predator management effort and success, is not captured in our SEED models. Since these factors are widely recognized as important drivers of fecundity for this species, they are likely to have a strong influence on population growth rates.

No dispersal   **With dispersal**
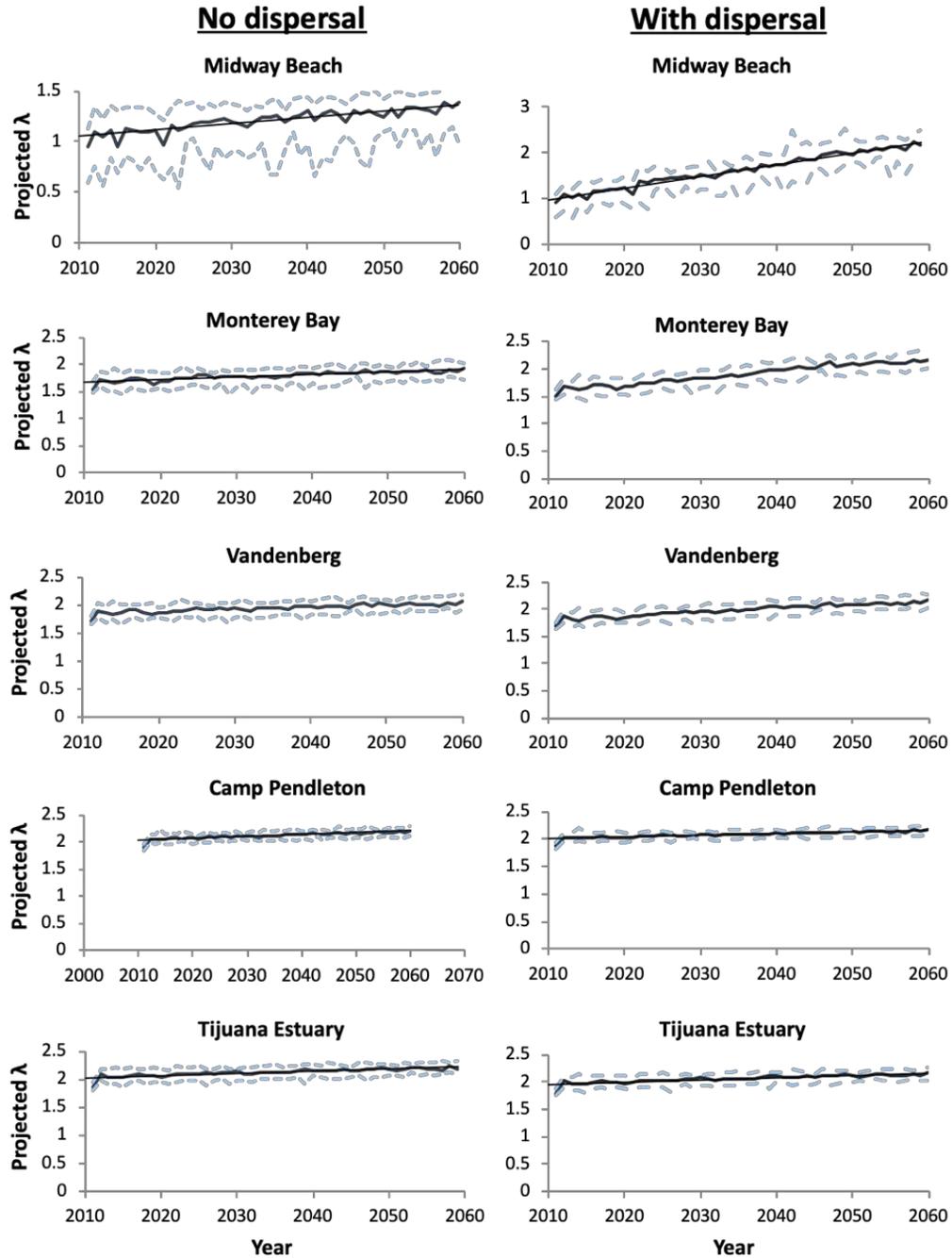
Figure 5.2-10. SEED model projections for annual western snowy plover discrete population growth rates (λ) at four sites from 2010-2060 considered in isolation (left) or accounting for dispersal (right). Dark solid lines show the median projected annual growth rate from SEED model runs linked to projected climate data from 20 downscaled global climate models. Dashed light lines show the 5th (bottom) and 95th (top) percentile of projected annual growth rates. The populations represent the northernmost known breeding site (Midway Beach), our study site (Monterey Bay), and breeding sites on Department of Defense lands (Navy Base Coronado is represented by the Tijuana Estuary).

Population growth rates were projected to remain stable or increase over the coming decades as warmer weather and reductions in the frequency and severity of winter cold snaps

resulted in increased adult survival. There were generally larger gains for more northerly populations, especially for populations north of Point Reyes compared to populations south of Monterey Bay (Moss Landing). The positive effects of warmer winters on western snowy plover population growth rates were amplified by dispersal. Projected average annual increases in population growth rates were always greater when SEED models included both migration and dispersal than when they included only migration. For connected northerly populations dispersal magnified the effect of climate change on western snowy plover populations by up to 450% (Figure 5.2-11).
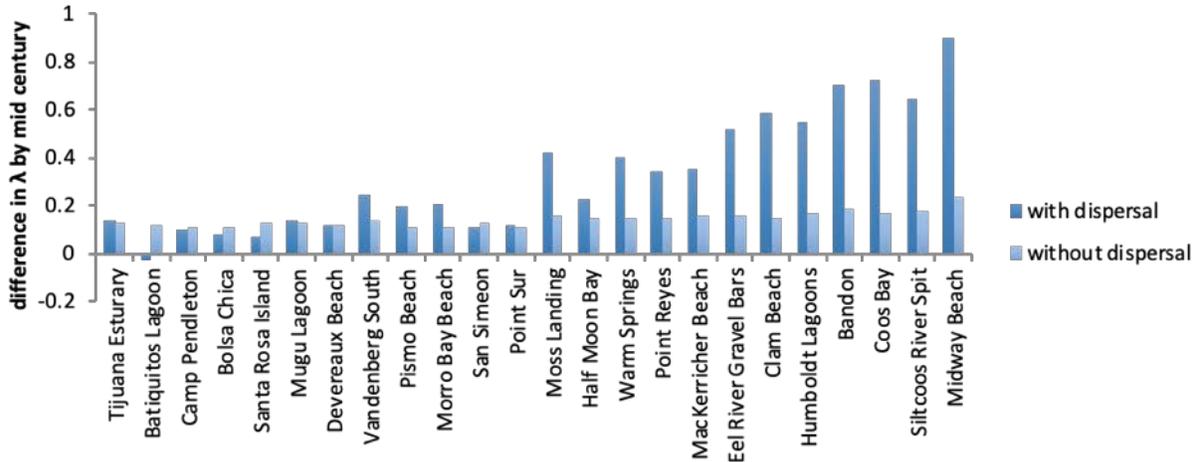
Figure 5.2-11. Projected changes between 2015-2024 and 2051-2060 in discrete annual population growth rates (λ). Bars show the difference in the 10 year average annual growth rate at each site projected from 20 runs of the western snowy plover SEED model, with each run linked to a different global climate model. Light blue bars show projected change when dispersal is not included, and dark blue bars show change with dispersal included in the model.

Warming temperatures along the west coast of the United States will likely make snowy plovers less conservation reliant in the coming decades, particularly at the northern end of their range. However, this conclusion assumes that sea level rise associated with rising temperatures at a global scale does not significantly reduce habitat. Habitat loss due to sea level rise may need to be offset by habitat restoration or improvements. Maintaining high connectivity among northern populations will help mitigate some loss of breeding habitat. Continued prioritization of reducing mortality due to predators associated with human presence along coastal areas is recommended.

5.2.4   Red-legged frog (*Rana aurora* and *R. draytonii*)

Temperatures at all of our study sites are projected to increase over the next several decades (Figure 5.2-12). The three coastal sites occupied by northern red-legged frogs are projected to experience the smallest increases in temperatures, while the three sites occupied by California red-legged frogs are projected to experience the largest temperature increases. Precipitation during the breeding and tadpole seasons (October-June) is projected to increase at all of our study sites. In contrast to temperatures, the three California red-legged frog sites are expected to experience the smallest increase in precipitation (Figure 5.2-12). Summer precipitation is projected to change very little at our study sites over the next few decades (Figure 5.2-12).
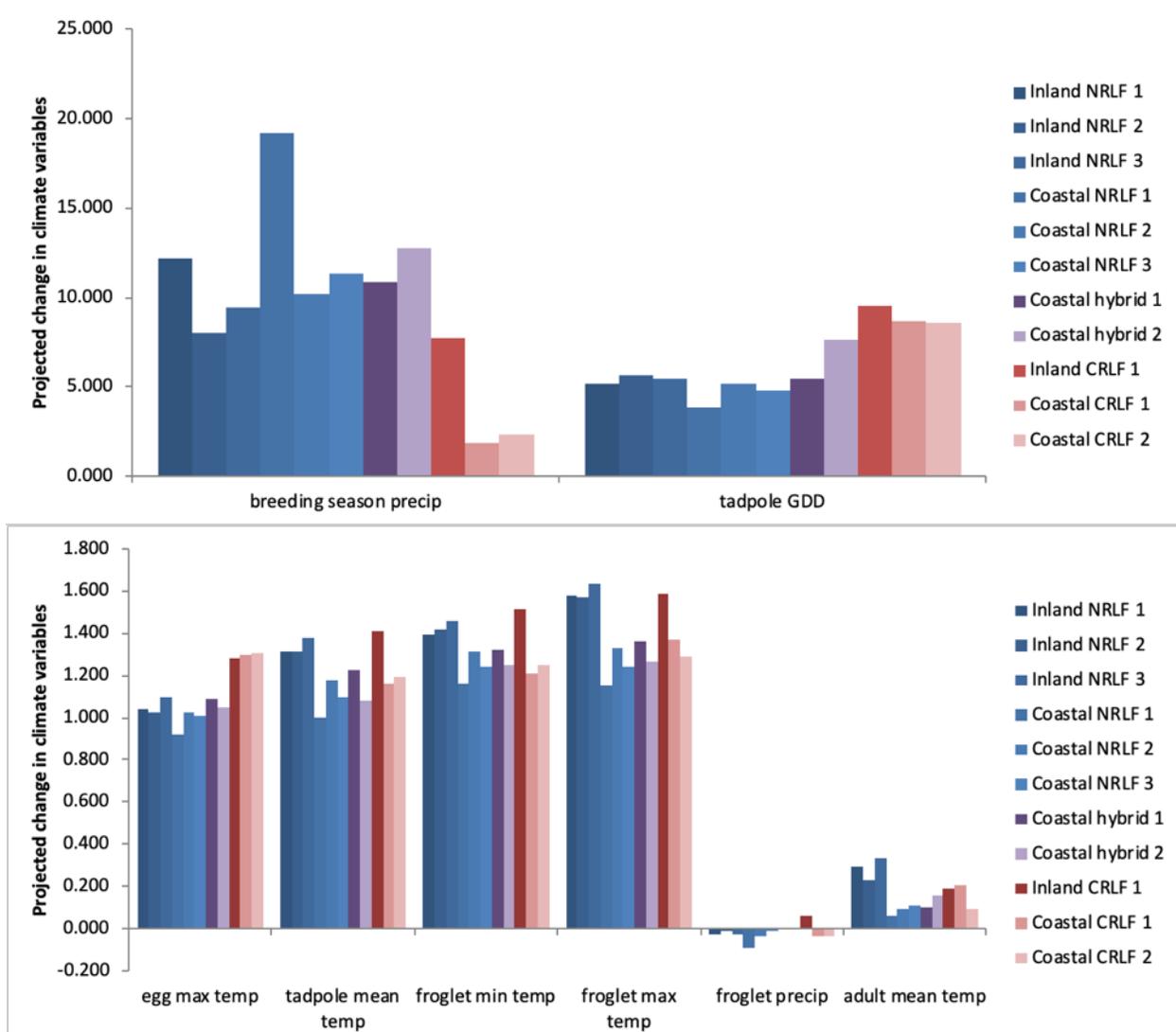
Figure 5.2-12. Projected change in climate drivers of red-legged frog demographic rates. Bars show the difference in the average projected values between 2010-2020 and 2040-2050 from 20 downscaled global climate models for the climate variables indicated on the x-axis. Each bar corresponds to a red-legged frog breeding site included in the study. Left to right position of each site corresponds to its north to south location. Blue bars are northern red-legged frog sites, purple bars are hybrid sites, and red bars are California red-legged frog sites.

These projected changes would have mixed effects on red-legged frog demographic rates (Figure 5.2-13). Higher fall through spring precipitation is expected to increase fecundity. However, warmer winter and spring temperatures are expected to decrease egg viability and tadpole survival. There is little expected change in froglet survival, but relatively large expected increases in adult survival at most of our study sites. The two coastal California red-legged frog sites were projected to experience the smallest increases in adult survival and fecundity, while experiencing relatively large decreases in tadpole survival and, at one of the two sites, egg viability.
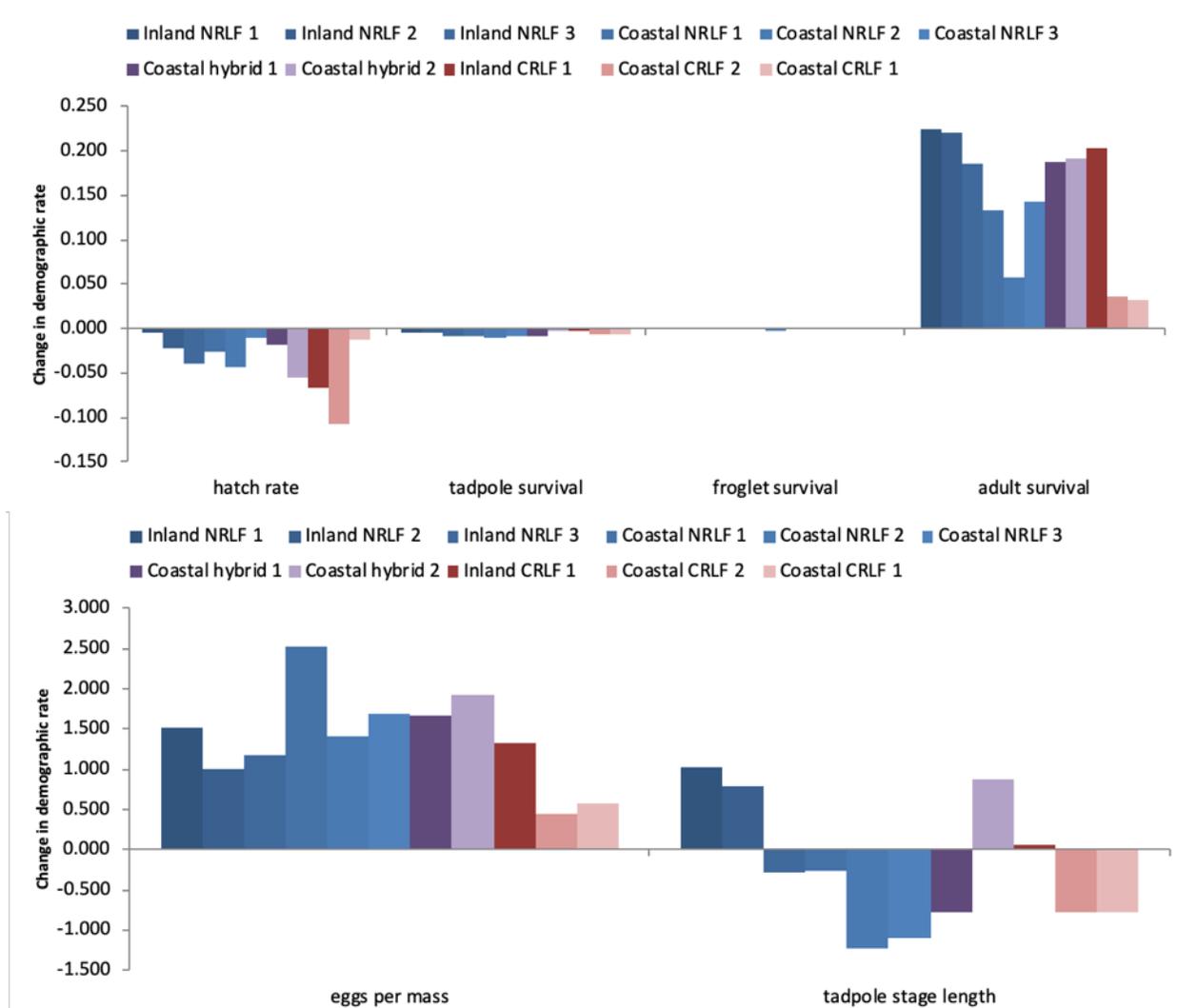
Figure 5.2-13. Projected changes in red-legged frog demographic rates between 2010-2020 and 2040-2050. Bars show the change associated in the average value for each demographic rate assuming the average projected climate conditions during each period from 20 global climate models. Each bar corresponds to a red-legged frog breeding site included in the study. Left to right position of each site corresponds to its north to south location. Blue bars are northern red-legged frog sites, purple bars are hybrid sites, and red bars are California red-legged frog sites

Projected population trajectories were quite different between coastal and inland sites, but not between species (Figure 5.2-14). Coastal sites were projected to be source populations under current climate conditions. Population growth rates at these sites were projected to change very little or have a slightly negative trend in projected population growth rates associated with warming future climates. In contrast, inland sites projected to be sink populations under current conditions with population growth rates increasing relatively sharply with future warming. A surprising result from our SEED model runs was that our inland populations of both species were projected to have sharply declining populations under current climate conditions. This result was not consistent with our observations of robust populations in at least two of those sites. We considered three possible reasons for this discrepancy. First, the climate-demographic rate relationship was mischaracterized. We checked this by comparing annual survival estimates predicted by the top model to annual survival estimates predicted by a model assuming quarterly survival varied independently at each site and was unrelated to climate. Because several quarter

X site combinations were not sampled, the latter model was overparameterized and associated estimates were either imprecise (i.e., had very large confidence intervals) or invalid (i.e., either had no associated error or were equal to 0 or 1). We expected that if our top model did a good job of characterizing the influence of climate on adult survival, within each site years with cooler winters would have lower survival than years with warmer winters, which is what we found. Second, we considered that there might be local adaptation to cold winters at inland sites. If this were the case, we would expect a model including different relationships between temperature and survival at coastal compared to inland sites (i.e., a region X temperature interaction). We redid the analysis including these models, and found that the data were still best described by a model including only temperature.

Finally, we considered that the "current climate conditions" from climate projection models did not reflect realized conditions. In particular, we had reason to suspect warmer temperatures in the years just prior to our study associated with a four-year drought that hit the western United States (Crockett et al. 2018) but not predicted by the global climate projection models we used in our SEED model. We suspected this might be the case because global projection models are designed to show climate patterns and not forecast specific weather events, like the 2011-2015 drought. We checked this by comparing the adult survival estimates predicted for the observed and projected climate conditions at the two inland populations with the largest red-legged frog populations. In both cases, estimated adult survival corresponding to observed temperatures were significantly higher than projected adult survival corresponding to projected temperatures. This finding is consistent with warmer than projected winter temperatures leading to higher than projected population growth rates in recent years at inland breeding sites. It also highlights that, like global climate model projections, our SEED model projections are meant to elucidate general patterns of how frog populations will respond to climate change; they are not predictions about the future trajectories of specific populations.
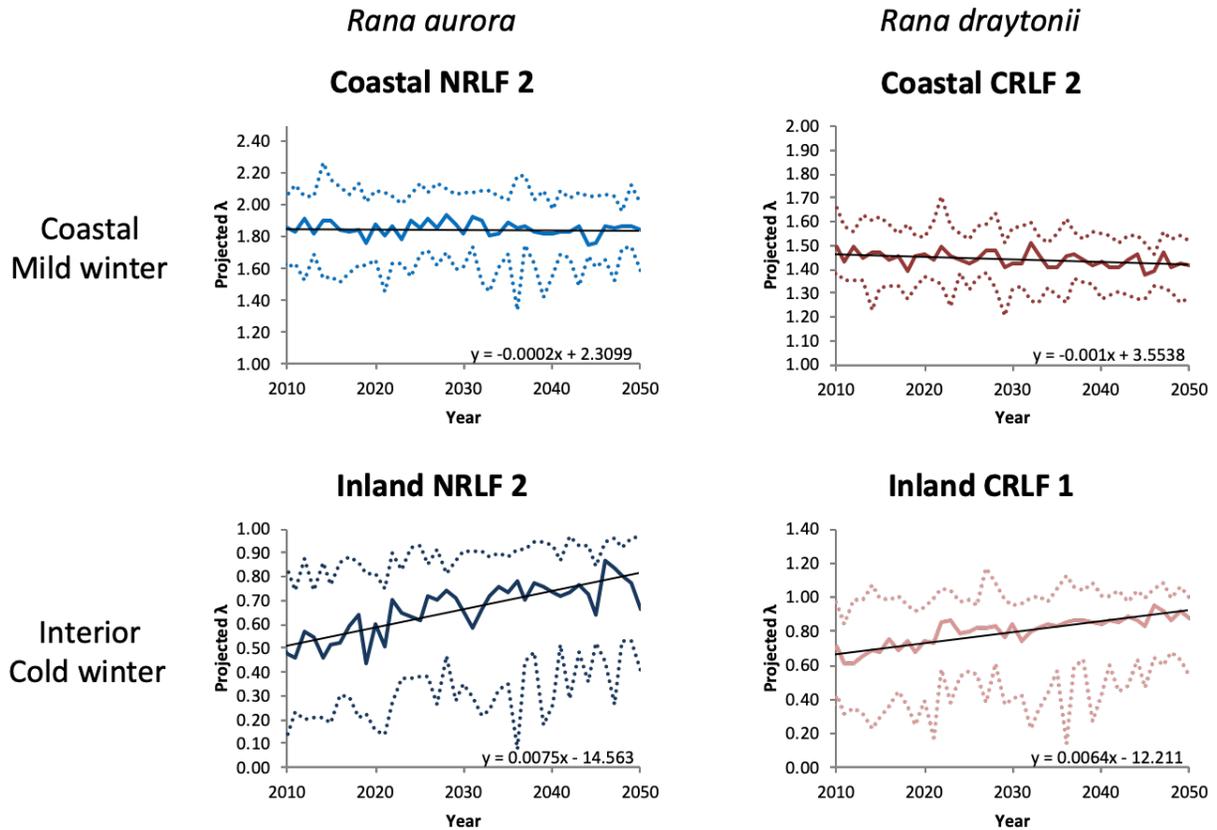
Figure 5.2-14. SEED model projections for annual red-legged population growth rates at four sites from 2010-2050. Dark solid lines show the median projected discrete annual growth rate (λ) from SEED model runs linked to projected climate data from 20 downscaled global climate models. Dashed light lines show the 5th (bottom) and 95th (top) percentile of projected annual growth rates. The four sites were chosen to be representative of the patterns observed across inland vs. coastal sites for the two species.

Southern coastal populations of California red-legged frogs are likely to become more conservation reliant in the coming decades, while populations in the Sierra Nevada foothills and northern red-legged frogs are not. There are a number of management actions, including bullfrog removal, increasing native emergent vegetation, and manipulating breeding site canopy cover, that are effective tools for conserving these species.

5.2.5 Alaskan douglasia (*Douglasia alaskana*)

For the Alaskan douglasia populations studied, we generally saw population growth rates that are below unity, indicating that these populations will decline in size (Figure 5.2-15). Interestingly, we saw somewhat different trends over time at our southern v. northern populations. Namely, annual population growth rate was almost always below one in our northern population, with no trend in population growth rate over time at this population. These predictions suggest that this northern population will almost certainly be extirpated in the future. By contrast, at our southern population, population growth rates were often below one, but increased over time such that annual growth rates after 2045 were often above one. Thus, it appears that if the southern population is able to avoid extirpation until 2045, it may well then experience high enough population growth rates that it will be buffered from extirpation. Most

populations in our study showed dynamics similar to our northern, rather than southern, population.
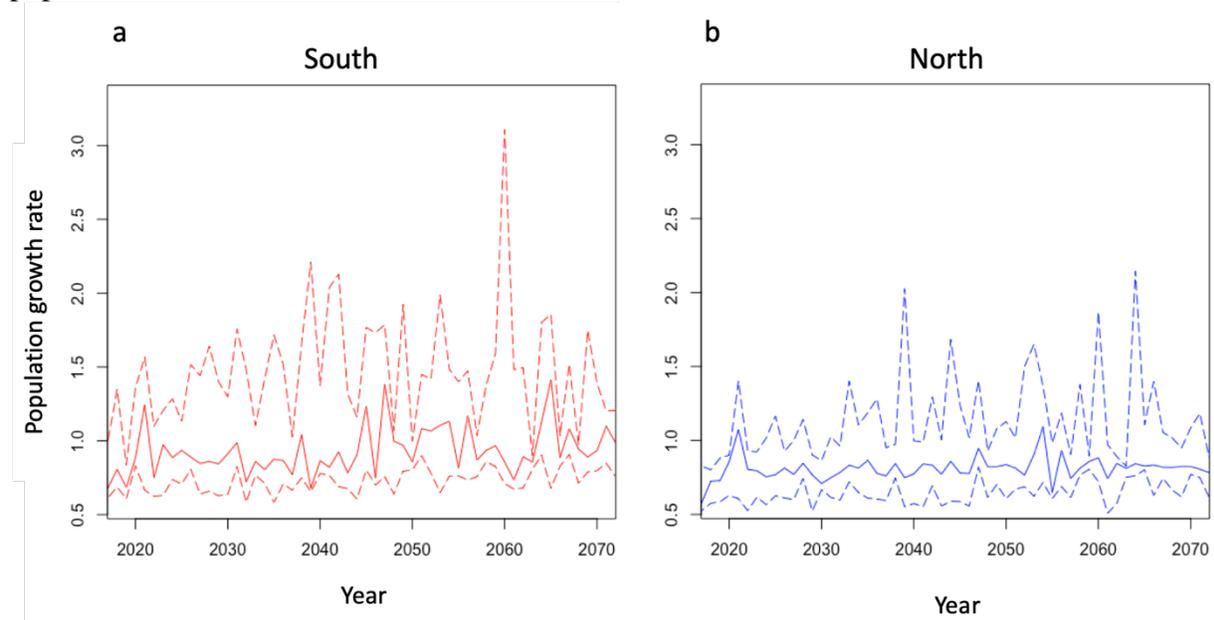
Figure 5.2-15. Projected discrete annual population growth rates (λ) for Alaskan douglassia through 2070 for populations in the southern (a) and northern (b) portion of our study area. The solid line represents the median and the dashed lines represent the 5th to 95th percentile range from the output of 5 GCMs.

5.2.6 Venus flytrap (*Dionaea muscipula*)

For the Venus flytrap metapopulation at Fort Bragg, we simulated the impact of future climate superimposed on a three-year burn cycle (Figure 5.2-16). While there was obviously a strong effect of time since the most recent burn on the population growth rate, we saw no long-term trend in population growth in response to the change in climate over the projection period. Populations grew rapidly ($\lambda \approx 3$) after a fire due to release from the competitive effects of over-growing neighbors, but the population growth rate quickly fell to or slightly below 1 one or two years after a fire as neighbors regrew rapidly. While the results in Figure 5.2-16 do not show the effects of varying the fire return interval (FRI), the rapid decline in population growth after each fire indicates that a FRI much longer than 3 years (the current target of the Fort Bragg burn teams) could pose a much more significant threat to the long-term persistence of populations at Fort Bragg than is represented by climate change.
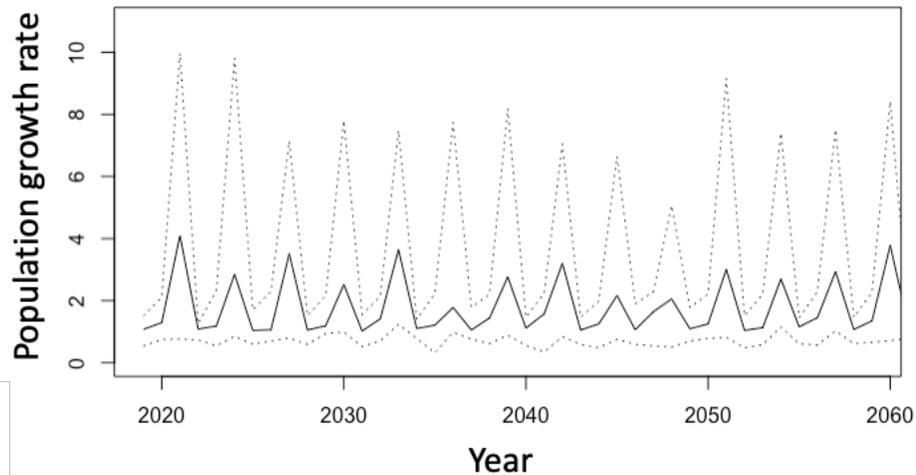
Figure 5.2-16. Projected discrete annual population growth rate (λ) for Venus flytraps through 2100 with a three-year burn cycle. The solid line represents the median and the dashed lines represent the 5th to 95th percentile range from the output of 20 GCMs.

5.2.7 Red-cockaded woodpecker (*Dryobates borealis*)

For the red-cockaded woodpecker, we saw essentially no change in the annual population growth rate for any of the three DoD sites up to the year 2100, the end point of our projections (Figure 5.2-17). Moreover, population growth rates remained close to 1, indicating stable populations. The red-cockaded woodpecker SEED model incorporated density dependence by means of a limit on the number of territories (each containing cavity trees) available to each population (and this limit did not change over the course of each simulation). That growth rates remained near 1, indicates that the future climate over the remainder of this century is predicted to remain suitable enough that the rates of survival and reproduction will remain adequate to ensure that nearly all available territories remain occupied. Red-cockaded woodpecker populations include a large non-breeding adult class consisting of helpers and floaters that buffered breeding population size (territories in our model) against environmental stochasticity. Variation in survival and productivity was reflected in changes in the size of the non-breeding class rather than breeding population size. This likely contributed to the stability of red-cockaded woodpecker populations despite changing climate. Adverse effects of changing climate on red-cockaded woodpecker population growth rates are likely to involve a tipping point or threshold rather than a linear response.

109
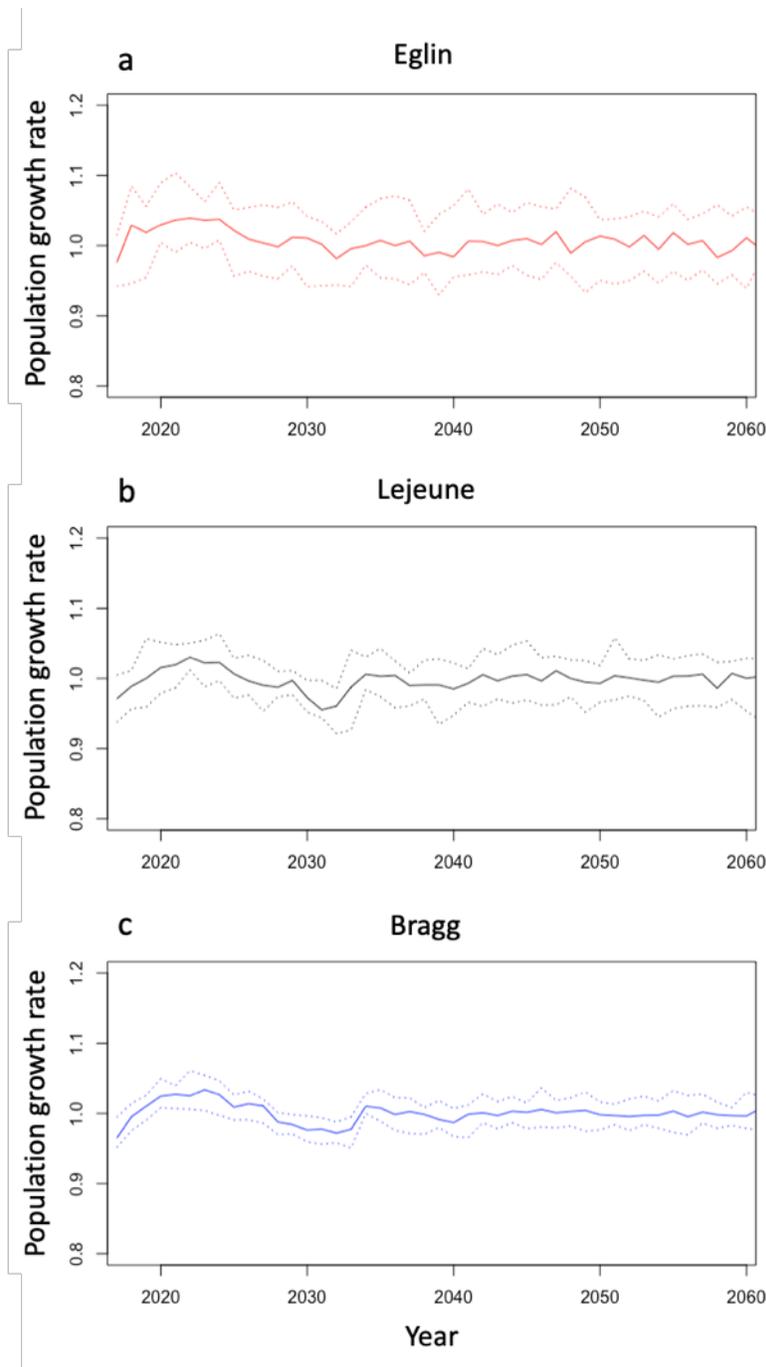
Figure 5.2-17. Projected discrete annual population growth rates (λ) for red-cockaded woodpecker through 2100 for populations in on Eglin Air Force Base (a), Camp Lejeune (b), and Fort Bragg (c). The solid line represents the median and the dashed lines represent the 5th to 95th percentile range from the output of 20 GCMs.

An obvious feature of Figure 5.2-17 is that all three red-cockaded woodpecker focal populations showed fluctuations in the population growth rate in the early years of our projections, which dampened over time. We have not completely pinpointed the cause of these fluctuations. We suspect they arose because the initial social structure (i.e., the among-territory distribution of the number of male and female helpers and floaters of different ages) we used in our simulations is not the equilibrium structure, and as the structure approached an equilibrium,

110

the population growth rate stabilized. These initial fluctuations in population growth could likely be eliminated by starting our simulations a few decades before the present (using historical climate during the recent past to drive demographic rates). However, because these fluctuations dampened out in about two decades, they were unlikely to have any effect on our longer-term projections. Our results suggest that all three red-cockaded woodpecker populations should remain stable in the face of projected climate changes to the end of the current century.

These findings fill an important knowledge gap in red-cockaded woodpecker conservation. The recovery of the red-cockaded woodpecker is a conservation success story. Once likely the most abundant woodpecker in the southeastern coastal plain, by the mid-1980s its numbers had declined two orders of magnitude (Conner et al. 2001; USFWS 2003). Once continuously distributed across the Southeast, it existed only in scattered, isolated populations, most of which were still declining, and none of which were increasing (Costa and Escano 1989). Thanks to the application of new forest and fire management of its habitat (USFWS 2020), and a new species management paradigm that focuses on the role their unique cavities play in their population dynamics (Walters 1991), the species has subsequently made a remarkable recovery. A recent status assessment found that over a twenty-year period (1996-2016), 76% of 79 populations analyzed had increased and were continuing to increase, and five individual populations had been declared recovered (USFWS 2020). The species remains conservation-reliant, and provided the critical management activities continue, its numbers are projected to continue to increase. However, the data available for the species status assessment were insufficient to determine whether or not climate change posed a threat to the otherwise positive outlook for the species (USWFW 2020). Our results suggest that it does not.

5.3 Climate Contribution Index (CCI)
Climate sensitivities of each of the three species for which we calculated CCI scores were greatest for demographic rates corresponding to either fecundity or to survival of pre-reproductive life stages. For hydaspe fritillary butterflies, egg hatch rates showed the greatest climate sensitivity in three of our study populations and larval survival showed the greatest sensitivity at the other three (Figure 5.2-2). Appalachian brown butterfly fecundity during the first generation was the demographic rate most sensitive to climate change (Figure 5.2-4). Although this demographic rate includes adult survival, adult survival was not influenced by climate (section 5.1.2), and the climate sensitivity was driven by the influence of temperature on the egg laying rate. Fecundity, in terms of eggs per egg mass, was the red-legged frog demographic rate with the highest climate sensitivity (Section 5.3.4; Figure 5.2-10).

All three species exhibited spatial variation in climate sensitivities. Hydaspe fritillary butterfly climate sensitivities for hatch rates varied by over four-fold among populations, and larval survival varied by 20 fold among populations (Figure 5.2-2). Appalachian brown butterflies exhibited 1.7 times higher climate sensitivity in egg survival and 11.3 times higher climate sensitivity in larval survival in South Carolina than in Fort Bragg, NC (Figure 5.2-4). Red-legged frog climate sensitivities also varied widely among populations, with nearly a five-fold difference in hatch rate climate sensitivity and eight-fold difference in adult survival climate sensitivity among populations (Figure 5.2-13)

Demographic rate sensitivities did not correspond to climate sensitivities for any of the three species. Hydaspe fritillary butterfly populations were most sensitive to changes in adult survival (Figure 5.3-1a). As with climate sensitivities, there were substantial differences among populations of hydaspe fritillary butterflies demographic rate sensitivities. Appalachian brown butterfly populations were most sensitive to changes in larval survival, especially in the first

111

generation of the year (Figure 5.3-1b). Red-legged frog populations were most sensitive to tadpole survival (Figure 5.3-1c). Note, this result differs from the result of the elasticity analysis reported in section 5.1.3, where we found that adult survival had the biggest influence on population growth rates.
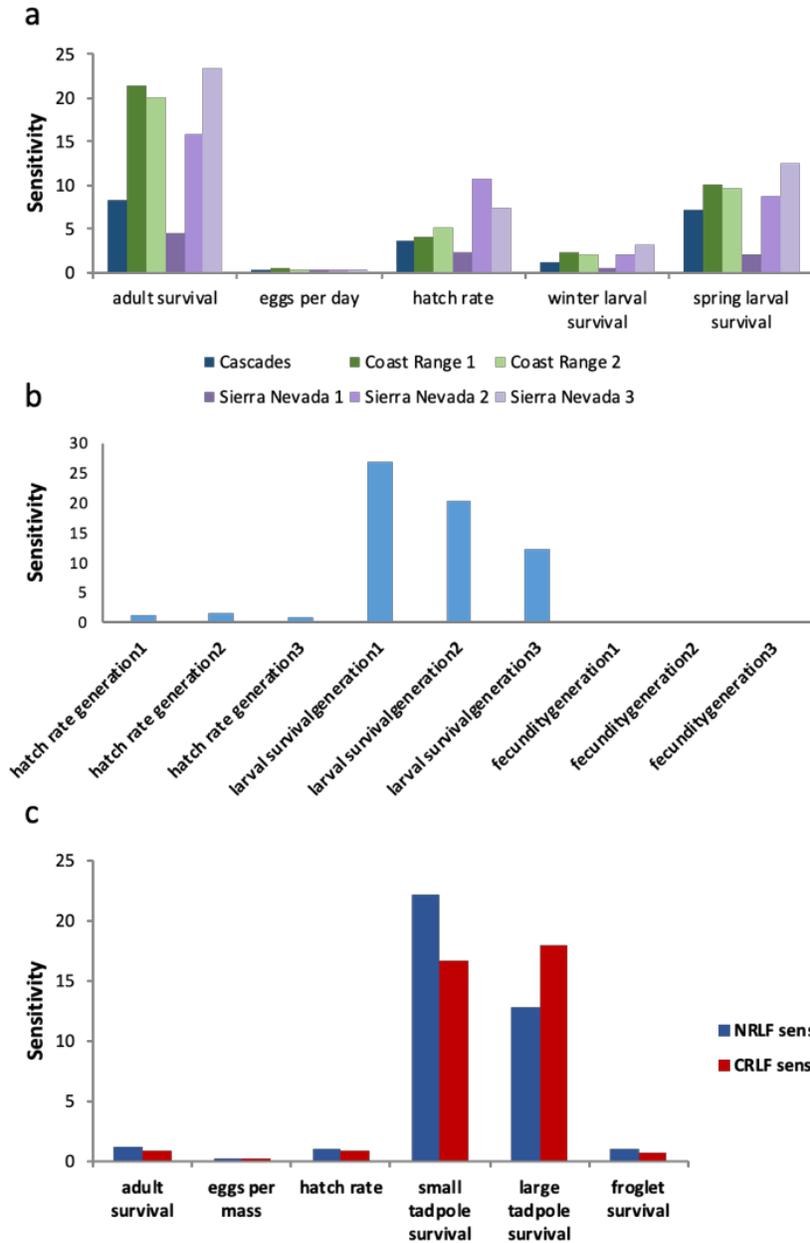
Figure 5.3-1. Demographic rate sensitivities for hydaspe fritillary butterflies (a), Appalachian brown butterflies (b), and red-legged frogs (c). Bars indicate the sensitivity of annual population growth rates to a small change in the demographic rate.

The climate contribution index associated with a demographic rate was not predicted by its climate sensitivity nor by how sensitive population growth rate was to changes in the demographic rate alone. This means that neither how labile a demographic rate is in response to

climate variability nor how much it influences population growth rates can be used alone to predict how much the demographic rate influences population responses to climate change. For example, in Appalachian brown butterflies, fecundity in the second generation had the highest CCI score (i.e. contributed the most to future changes in population growth rates; Figure 5.3-2b) despite demographic rates during the first generation having greater climate sensitivity (Figure 5.2-4), and despite population growth rates being relatively robust to changes in this demographic rate (Figure 5.3-1b). Moreover, we found that the demographic rate associated with the highest CCI was quite variable among taxa. For example, adult survival had the greatest influence on climate-change response for northern red-legged frogs (Figure 5.3-2c), but tadpole survival had the greatest influence on California red-legged frog population growth rates (Figure 5.3-1c). The CCIs for hydaspe fritillary butterflies demonstrated that which demographic rates will have the greatest influence on future population growth rates may even vary among different populations. Spring larval survival had the highest CCI score in two populations, while egg hatch rates had the highest CCI score in three, and the CCI for these two demographic rates and adult survival were essentially equal in one population (Figure 5.3-2a).
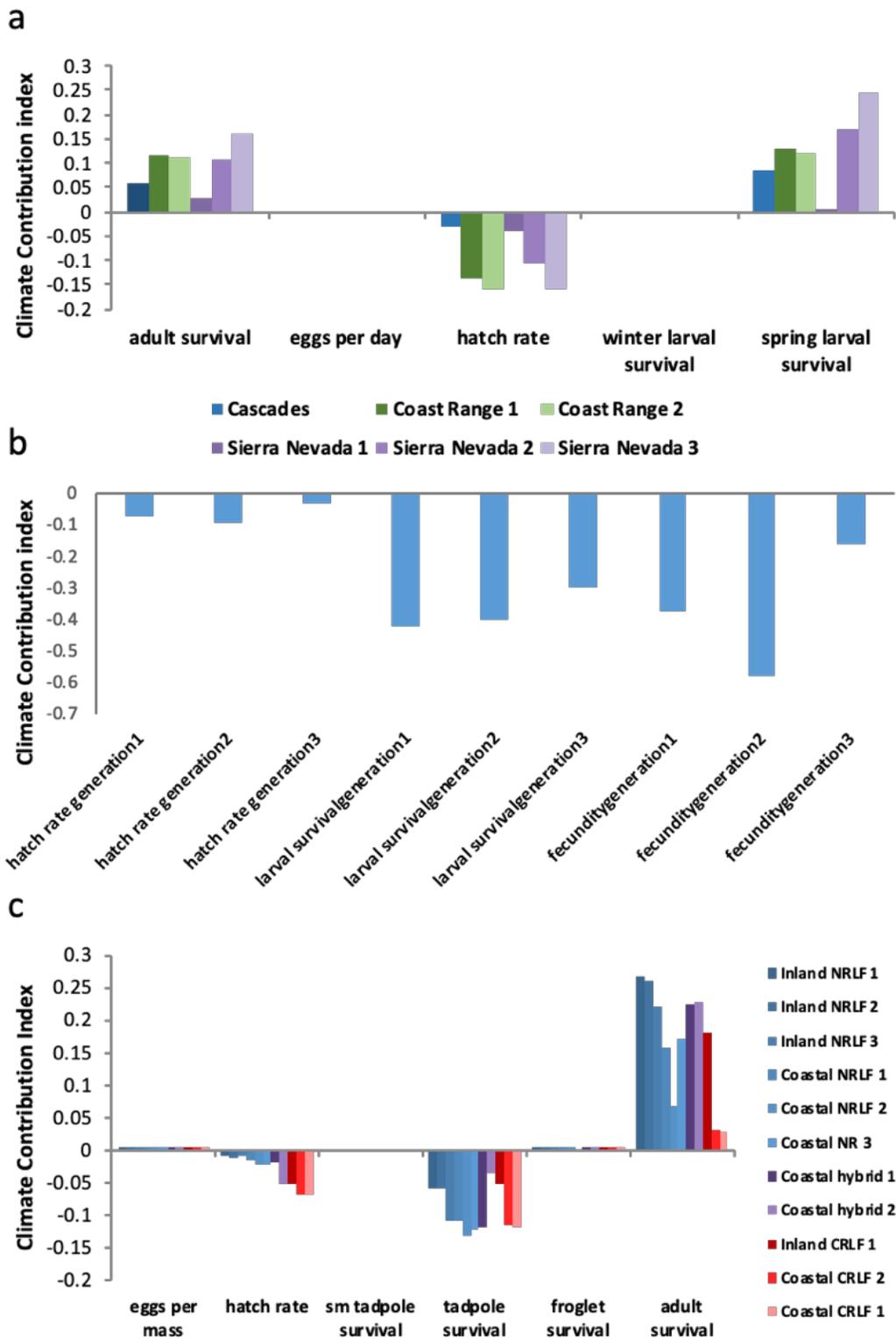
Figure 5.3-2. Climate contribution indices for hydaspe fritillary butterflies (a), Appalachian brown butterflies (b), and red-legged frogs (c).

Several mechanisms underlie the differences in CCI rankings among populations. There was a strong negative correlation in the rank-order of which demographic rates were most sensitive to changes in climate conditions and which contributed the most to population growth. Genereally, fecundity was the most climate-sensitive demographic rate, but also had the lowest demographic rate sensitivity. The hydaspe fritillary butterfly was an exception. For this species, demographic rates that were little impacted by changes in climate conditions (eggs per day, larval winter survival) also had little influence on population growth rates and differences in projected climate change largely explain differences in CCI patterns among populations. The two Coastal Range populations are expected to see the smallest change in spring/early summer temperatures, and correspondingly, have relatively low CCI scores for spring/early summer larval survival compared to the two higher elevation Sierra Nevada sites. The Cascades population is projected to see the largest change in precipitation, leading to a relatively high influence of adult survival on how butterflies there respond to changing climate conditions. The apparently taxonomic difference in CCI scores for red-legged frogs corresponds to size-related differences in fecundity between the two species and projected climate change patterns among different sites. California red-legged frogs are larger and have egg masses with one and half to two times as many eggs. At the same time, the coastal California red-legged frog sites are projected to see a 20% greater increase in breeding season warming than the coastal northern red-legged frog sites, leading to a greater reduction in hatching success. In contrast, because northern red-legged frogs currently experience cooler year-round temperatures, they see a larger benefit in terms of increased adult survival, from projected warming than do California red-legged frogs (Figure 5.2-12).

5.4   Species Integration and Discussion

Two major themes emerge from the studies included in this project. First, climate influenced populations in a wide variety of ways, and for any given species, the relationship between climate and population dynamics was often quite complex. This complexity included not only the impact of numerous different climate variables influencing numerous different demographic rates, but also the potential for strong nonlinearities in climate-demographic rate relationships. Additionally, there were sometimes interactions between different climate variables and between climate and recent life-history events. Nonetheless, some patterns did emerge. Namely, offspring production and younger life stage survival tended to be more vulnerable to projected changes in climate. The second theme is that most populations appeared to be robust to the direct effects of climate change. Populations most at risk tended to be those already at the warmest edge of a large latitudinal (or elevational) range. In contrast, populations at the coolest edge of their species distributions were most likely to see the greatest benefits from projected changes in climate conditions, while species with relatively narrow latitudinal and elevational distributions were generally unaffected by climate change.

Most species were affected by multiple climate drivers, with strong nonlinear effects in some cases. Our study species with the most complex life histories had no fewer than nine different climate variables impacting demographic rates. Only Appalachian brown butterflies were influenced by a single climate variable (mean temperature during the life-stage), but there was a threshold effect in both egg hatch rates and larval survival. In fact, without experimentally elevating temperatures above those experienced at Fort Bragg during our study, we would not have detected these thresholds. As a consequence, we would not have been able to predict the reduction in egg or larval survival under the non-analogue climate conditions projected to be the new normal within the next decade. Another kind of nonlinear climate effect, interactions

between climate variables or between climate and recent life-history events, were also common in species with complex life histories.

We found contrasting effects of climate across different life stages for most of our study species. Only for the Appalachian brown butterfly and the western snowy plover were the effects of climate on demographic rates all in the same direction. Opposing effects of climate across demographic rates could serve as a buffer, reducing the overall impacts of climate change on population growth rates (Doak and Morris 2010). This buffering effect likely contributed to the lack of projected effects of climate on population growth rates we observed for some of our study species. For example, in red-cockaded woodpeckers increasing temperatures decreased post-fledging survival but increased adult survival. Likewise, in Alaskan douglasia increasing temperatures negatively affected reproductive demographic rates while increasing survival and growth.

Temperature-driven phenological shifts can also act to buffer the effects of climate change. For example, we found that warming temperatures advanced the timing of the flight periods of both butterfly species. For the Appalachian brown butterfly this shift led to an additional generation. Adding this generation into our SEED models improved population growth rates, although not enough to prevent future population declines. While we did not include phenology in the Hydaspe fritillary butterfly SEED model, the predicted shift to earlier flight periods under warmer conditions could buffer post-diapause larvae, adults, and eggs from experiencing the full extent of warming associated with climate change. However, reducing the amount of warming experienced would have mixed effects on different life stages, benefiting egg survival, but reducing larval and adult survival. Unlike the Appalachian Brown, hydaspe fritillaries are univoltine throughout their range and are less likely to increase voltinism with warming. Earlier flight periods have the potential to impact hydaspe larval survival by exposing newly hatched larvae to a longer period of hot and dry conditions before the cool temperatures and first rains in the fall, which exposes them to greater desiccation risk. In contrast, for multi-voltine butterfly species, warming and the associated phenology shifts have been found to prolong flight periods and increase voltinism, potentially increasing population growth rates (Roy and Sparks 2000, Altermatt 2010, Wepprich 2017, Kerr et al. 2019).

We found temperature to be a factor in almost every demographic rate that was sensitive to climate except for the clutch size of the first nest and probability of double brooding in red-cockaded woodpeckers and fecundity in red-legged frogs. In general, we found more negative impacts of warming on early life stages. For example, with red-legged frogs and hydaspe fritillary butterflies the only negative effects of increasing temperature were on early life stages (egg viability for both species and tadpole survival for the frogs). Warming reduced post-fledging survival in red-cockaded woodpeckers, and in Appalachian brown butterflies the only demographic rate not negatively impacted by temperature was adult survival. With the exception of Venus flytraps, survival of the reproductively mature life stage of all the species we studied either benefited or was unaffected by increased temperatures.

We did not find a general pattern relating climate effects on any particular life stage to climate change effects on future population growth. For example, negative effects of warming temperatures on tadpole survival rates had a strong influence on the coastal California red-legged frog populations, contributing to future declines in projected population growth at these sites. In contrast, reduced tadpole survival in northern red-legged frogs is more than offset by gains in adult survival, leading to increasing projected population growth rates. The demographic rate contributing the most to a population's response to climate change did not necessarily

correspond to the rate most heavily affected by climate nor to the rate with the greatest influence population growth rates. Instead, the demographic rates that tended to be the best predictors of population responses were those that were both relatively sensitive to climate conditions and had a relatively large influence on population dynamics. Identifying these demographic rates *a priori* is problematic, because there is an inherent tradeoff between the demographic rate variability and elasticity (Pfister 1998, Morris and Doak 2004).

Most projected population growth rates were unaffected or positively influenced by future climate change. Of the 49 different populations we evaluated, only 3 (6.1%) are projected to have lower future population growth rates due to climate change. Positive effects of climate change on growth rates may seem unexpected, but this result is consistent with predictions for ectotherms in temperate regions, where species typically have broad thermal tolerances and often experience temperatures that are below their thermal optimum. Warming is generally expected to increase fitness of ectotherms living at higher latitudes, while for ectotherms living near their thermal optimum at lower latitudes, even moderate warming could have negative impacts on population growth as fitness typically drops steeply at temperatures above the thermal optimum (Deutsch et al. 2008, Angilletta 2009). This suggests that populations closer to the southern periphery of their range would be most at risk from warming temperatures, which is what we observed. All three populations projected to be adversely affected by climate change, Appalachian brown butterflies at Fort Bragg, NC and the two California red-legged frog populations at Vandenberg Air Force Base, are at the southern end of their species ranges. Even among the remaining populations, there was a general trend for populations at warmer locations to respond less favorably to projected warming conditions than populations at cooler locations. This pattern held true not only for the ectotherm animals in our study, but also for snowy plovers. It is not obvious for Alaskan douglasia whether the southern or northern population currently experiences warmer conditions, as the southern population is more coastal, potentially buffering it from temperature extremes. Our results are consistent with other work that has shown that populations at the southernmost or lowest elevation extent of their range are more likely to be negatively impacted by climate change (Parmesan 1996).

Based on our SEED model results, two of our study species, Venus flytrap and red-cockaded woodpecker, appear to be exceptions to this pattern, showing little difference in predictions for northern vs. southern populations. Both of these species occupy a smaller latitudinal range (spanning approximately 10° or less) than the butterflies, red-legged frogs, or snowy plover, each of which have species ranges spanning at least 15° of latitude. The narrow distribution of the Venus flytrap and red-cockaded woodpecker is clearly linked to specialized habitat requirements unrelated to climate. While our SEED models suggested little difference between the response of red-cockaded woodpeckers to climate change in the northern and southern portions of their range, previous work has found evidence that this species may be more susceptible to climate change at the southern end of its range. Garcia 2014 and DeMay and Walters 2019 found that red-cockaded woodpecker productivity was high and increasing in the northeastern portion of the range, but low and decreasing in the southwestern portion. Improving conditions, often accompanied by range expansion, at the northern edge of the range and deteriorating conditions accompanied by range contraction at the southern edge of the range is a widespread response to climate change in north temperate birds.

Two of the red-cockaded woodpecker populations we analyzed for the SEED model are located at the northeastern edge of the species' range (Lejeune, Sandhills), and one is located in the southwestern portion of the range (Eglin). Our modeling of the relationships between

demography and climate in red-cockaded woodpeckers was driven more by the large samples available from the two northern populations than the small samples from the southern one. Therefore, if climate in the southwestern portion of the range represents the most adverse limit of the range encountered by the species, we may have failed to fully capture climate effects on demography operating at that limit of current conditions. If true, this would cause us to underestimate future effects of climate on red-cockaded woodpecker populations. More study of climate effects in this portion of the range are needed to assess this possibility.

We found evidence of indirect effects of climate mediated through interactions with other species. Temperature strongly influenced hydaspe fritillary butterfly egg survival by increasing daily egg predation rates by 46% per one ºC of warming. While we did not measure it directly, we suspect that the quality of both host and nectar plants could influence hydaspe fritillary demographic rates. Nectar availability has been linked to fecundity in related species (Boggs and Ross 1993), and host plant quality likely influences larval survival. Early snow melt can reduce floral resources (Inouye 2008), and violets, the hydaspe fritillary's host plants, require moist conditions and thus are negatively impacted by droughts. We also found evidence to suggest that the effects of temperature on the timing of the end of the flight period may be mediated through the influence of temperature on nectar plant phenology. We found a tight correlation between temperature and both flight period end and senescence of the primary nectar plant used at each site. The date recorded as the end of the flight period and the date recorded for full senescence of the primary nectar plant differed by more than a week on only one occasion across all sites and years. Given that we only surveyed nectar plant blooming progression every two weeks, this suggests a tight association between preferred nectar resources disappearing and the end of the flight period.

Temperature driven changes in phenology and development rates also have the potential to impact population growth rates through interactions with other species or processes. For example, the increased development rates we found with warming for hydaspe fritillary and red-legged frog eggs and larvae could reduce predation rates by reducing the amount of exposure. In hydaspe fritillaries this reduced exposure time could mitigate some of the effects of warmer temperatures increasing the daily egg predation rates. Red-legged frog breeding phenology and egg/larvae development rates might also interact with canopy cover to affect the amount of shading to which these early life stages are exposed.

Many of these potential indirect effects of climate were not captured in our SEED models and could alter population trajectories. For example, while future annual precipitation is expected to increase slightly at all of our hydaspe fritillary butterfly sites, projected warmer temperatures could mean that more of the precipitation will fall in the form of rain rather than snow. Reduced snowpack and warmer temperatures could lead to both earlier snow melt and a higher likelihood of drought conditions during the late spring and summer. These conditions could strongly influence nectar and host plant availability and quality, which in turn could influence hydaspe fecundity and larval and adult survival. Indeed, at the beginning of our study hydaspe fritillary butterfly population sizes were extremely low at our Sierra Nevada sites, less than one 10th the size of any of our other populations. The Sierra Nevada sites were also hit the hardest of any of our sites by the severe drought in CA from 2012-2016 (NOAA 2015), just prior to our study. An exceptionally wet year in 2017 ended the drought and the Sierra Nevada hydaspe fritillary populations grew by more than 450% between 2017 and 2018, while the other sites grew by less than 80%. These patterns are reflected in our analysis of the effects of climate on observed population growth rates, where we saw clear evidence of density dependence and a strong

positive effect of precipitation, but no effects of temperature. For red-cockaded woodpeckers, hurricanes can lead to population declines by destroying all cavity trees within a territory. This suggests that extreme weather events can have pronounced impacts on population growth rates, and that those effects may be mediated through impacts on other species/resources (Dobkin et al. 1987, Singer and Ehrlich 1979, Ehrlich et al. 1980, Singer and Thomas 1996, Parmesan et al. 2000 Piessens et al. 2008). Predicting the effects of extreme weather events on population trajectories is challenging both because measuring the effects of extreme events on demography is challenging (we cannot control when extreme events will occur and the effects of extreme events are often indirect) and because accurately predicting extreme weather events at local scales is impractical (Fischer et al. 2013).

Another pattern that emerged when comparing results across species is the potential for managing non-climate drivers to benefit almost all species. For example, fire frequency strongly influenced Venus flytrap population growth rates. In the coastal plain and Sandhills of the Carolinas where Venus flytraps are found, the fire regime is typically managed through controlled burns, suggesting that management actions could have significant effects on Venus flytrap populations. Climate change could impact the frequency of non-controlled wildfires in the region, setting up another possible indirect effect of climate change. Fire frequency also affects the fecundity of red-cockaded woodpeckers, as does the availability of nest cavities, many of which are manmade. Controlled burning is a critical management tool used on DoD lands for red-cockaded woodpecker conservation. Canopy cover impacted red-legged frog tadpole survival at some sites and these impacts were strong enough to have meaningful impacts on population growth rates. Canopy cover management has also been proposed as a tool to benefit rare frogs in the Southeast (Thurgate and Pechmann 2007). We also saw interactive effects of invasive bullfrog presence and food availability on froglet body condition. Removal of bullfrogs and other nonnative predators from breeding ponds is a commonly used tool to help special status amphibians throughout the Western U.S. (e.g., Govindarajulu et al. 2005, Knapp et al. 2007). Predator management is also a critical part of western snowy plover conservation efforts (e.g., Peterson and Colwell 2014, Brinkman 2018). As with the effects of climate, the effects of non-climate drivers often varied across populations. Canopy cover influenced demographic rates at some red-legged frog sites but not others, and the outcomes of experimental tests of fire effects on Venus flytrap demography showed differed between the inland vs coastal populations. This highlights the need for population rather than species specific management plans for many special status species.

6   Conclusions

Given the numerous and often highly complex ways that climate influences populations, we find that predicting species' responses to climate change will require a holistic approach focusing on demographic processes. Tools that explicitly consider climate-demographic rate relationships, such as SEED models, provide a significant advantage over more commonly used occupancy based approaches for planning future conservation needs.

The most common approach to measuring a species response to climate change is to use bioclimatic envelope models, also known as ecological niche or species distribution models, to use current and/or historic associations between climate and a species distribution to predict the persistence of populations and distribution shifts in the future (e.g. Araújo and Peterson 2012, Warren et al. 2014). These models have the advantage of being able to account for the integrated direct and indirect effects of climate on the species distribution and the data needed for these

models is relatively easy to obtain (not labor intensive nor expensive) compared to demographic studies. However, bioclimatic envelope models have been criticized for relying on faulty assumptions and being contradicted by empirical evidence, and there has been much debate about their usefulness (e.g. Hampe 2004, Akçakaya et al. 2006, Botkin et al. 2007, Dormann 2007, Sinclair et al. 2010, Araújo and Peterson 2012, Ehrlén and Morris 2015).

One reason bioclimatic envelope models may fail to make accurate predictions is that many species distributions are not limited by climate factors. For example, one study of 144 plant species native to the US that occur outside their native range found that 86% of the species studied were found to occur in areas predicted to be climatically unsuitable based on the climate in their native range (Bocsi et al. 2016). There are several other factors that might limit species distributions besides climate, including species interactions (Case et al. 2005, Louthan et al. 2015), resource availability (John et al. 2007, Endara and Jaramillo 2011), and dispersal limitation (Ozinga et al. 2005). The red-cockaded woodpecker is a habitat specialist dependent on mature (i.e., > 100 years old) pine trees for nesting. Because the pace of climate change is faster than the change in the distribution of such habitat, bioclimatic envelope models will not be able to predict changes in the distribution of red-cockaded woodpeckers.

Another issue with bioclimatic envelope models is that climate factors may be obscured by source-sink population dynamics (Pulliam 2002). Areas that appear to be suitable climatically based on occupancy, might actually have climates that would lead to population declines without immigration. Similarly, individuals may be present in areas that are no longer suitable, as population declines may be lagged compared to changing conditions (i.e. "living dead" populations - Ehrlen and Morris 2015), complicating predictions based on current occupancy (Sinclair et al. 2010). Overall, occupancy data provides limited insight into how population growth rates vary annually in response to climate and non-climate factors. Since neither climate nor population growth rates are static, simply using occurrence data may miss important impacts of climate on population growth rates or lead to spurious correlations.

Furthermore, predicting species responses to conditions that they have not yet experienced is non-trivial. For example, evolutionary adaptation and phenotypic plasticity may allow some species to persist under climate conditions outside the range that they currently experience (Bush et al. 2016). Phenological shifts might also serve to buffer species from experiencing the full extent of predicted warming (Cormont et. al 2012). Warming may also accelerate development rates, as seen in red-legged frog and hydaspe fritillary butterfly eggs and larvae in our study, which can reduce the length of time when vulnerable life stages are exposed to predators. For some species, behavioral changes provide another buffer against effects of climate change as well. For example, some butterfly larvae actively select microhabitats, switching to different host plants or levels of openness, to stay within a preferred temperature range (Aston et al. 2009). Bioclimatic envelope models provide little information about the underlying mechanisms driving the effects of climate on population dynamics. Understanding the underlying mechanisms may be critical for accurately predicting how populations will change in the future or for targeting management efforts to mitigate any negative impacts of climate change.

Demographic models provide tools for overcoming most of these limitations provided that the model 1) includes environmental drivers for demographic rates, and 2) integrates across the life-cycle of the species being modeled. The main benefit of using demographic models is that individual demographic rates typically respond quickly to changes in environmental drivers. Consequently, year to year variation in climate conditions makes it easier to measure the effect

of climate on demographic rates rather than obscuring long-term population trends. It is also easier to link demographic rates, compared to population size or occupancy, to local conditions in well-connected populations, and thus to detect source-sink dynamics that might make niche model predictions unreliable.

While measuring changes in single demographic rates in response to variable climate conditions represents a sensitive tool for detecting climate drivers, integrating across the full spectrum of climate drivers and demographic rates is critical for predicting population level impacts of climate trends for many reasons. First, climate generally influences population growth rates through many different mechanisms, with different climate variables acting on different life stages. A focus on only one climate variable or one demographic rate (or even a few) may reveal strong links that fail to translate into effects on population growth. This may be especially true when, as is often the case (e.g., Hydaspe fritillary butterfly, red-legged frog, red-cockaded woodpecker in this study; Doak and Morris 2010), demographic rates respond in opposing ways to changes in climate conditions. Furthermore, because there is a tradeoff between sensitivity of a demographic rate to environmental drivers and its contribution to population growth (Gaillard et al. 1998, Pfister 1998, Morris and Doak 2004), it is difficult to predict which climate-demographic rate relationship will have the biggest role in shaping future population trajectories. Indeed, we find that the contribution of a demographic rate to future population trajectories is predicted by neither the sensitivity of a demographic rate to climate variability nor by the ranking of sensitivity of population growth alone.

There are, of course, limitations to SEED models. Identifying and quantifying each of the climate-demographic rate relationships needed to parameterize a SEED model requires large amounts of data, which are expensive to collect compared to occupancy data. Because models are only as good as the data used to build them, careful consideration of what observational and experimental data to collect is important at the outset. Care must be taken to consider how non-climate variables, such as local densities at the time of study, and habitat features that vary among populations might influence climate-demographic rate relationships in those populations. Accounting for these sources of spatial variation is especially important when interpreting space-for-time studies. Likewise, temporally variable non-climate drivers, such as time since fire or predator management, must be accounted for when using time-series data to fit climate-demographic rate relationships. Nonlinearities in demographic rate sensitivities to climate variables must also be kept in mind. We recommend measuring apparently climate-insensitive demographic rates under climate conditions experimentally forced outside of current conditions to detect thresholds whenever practical.

While we did not explicitly account for simultaneous climate effects on interacting species, such effects are likely to influence population growth rates of managed species. Because there may be a lag between the change in climate and significant population change of an important prey, mutualist, competitor, or enemy species, the indirect effects of climate mediated through these types of species interactions will often lag behind observed changes in relevant climate variables and direct effects. However, individual species responses to changing environmental conditions can predict changes in ecological communities even when species interactions are not directly accounted for (Lytle et al. 2017). Moreover, multi-species SEED models can accommodate species interactions, albeit with even greater data requirements than single species SEED models. Indeed, accounting for climate-driven phenological mismatches between interacting species in multi-species SEED models may be a powerful tool for

identifying the impacts of phenological changes on the population growth of multiple species, and thus on the future composition of entire ecological communities.

General Management Implications: SEED models and Contribution Index are useful tools for predicting whether expected changes in future climate conditions will exacerbate or mitigate threats to special status species managed on DoD lands. These predictions provide useful information for planning future management needs. For example, our study included two military bases, Fort Bragg, NC and Vandenberg Air Force Base, CA, with managed species predicted to have very different responses to projected climate change in the coming decades. On Fort Bragg, both red-cockaded woodpecker and Venus flytrap populations are expected to be buffered from changing climate conditions, whereas warming temperatures are expected to cause Appalachian brown butterfly populations there to switch from sources to sinks. At Vandenberg Air Force Base, snowy plover populations are predicted to benefit from warming spring temperatures and milder winters along the west coast, while California red-legged frogs are predicted to do worse. Looking ahead, this means that Fort Bragg may want to plan now for mitigation projects to reduce the impacts of expected warming on Appalachian brown butterflies. Such mitigation may come in the form of habitat restoration focused on providing greater shade coverage while continuing to support robust host-plant coverage, or ways to reduce predation on eggs and larvae to offset reduced survival during these stages associated with warmer temperatures. For Vandenberg Air Force Base, this means potentially devoting more resources to California red-legged frog protection (e.g., through bullfrog removal at breeding sites). In contrast, future budgeting needs for snowy plovers, or for red-cockaded woodpeckers and Venus flytraps, should be determined by mitigation requirements for non-climate threats. We note here that climate does play a role in critical management issues for all three species, fire frequency for red-cockaded woodpeckers and Venus flytraps and sea-level rise for snowy plovers.

The populations of special status species most likely to be vulnerable to climate change in our study were wide-ranging species at the climatic edges of their ranges. We note that climatic edges are not necessarily the same as the geographic periphery of a species range, as is evidenced by multi-directional shifts both in avian species ranges in Britain (Gillings et al. 2015) and in presumed bioclimatic envelopes in the United States (Bateman et al. 2016). The mismatch between climatic edges and geographic periphery may be due to landforms influencing temperatures or precipitation patterns, differences in the latitudinal and longitudinal directionality of temperature and precipitation patterns, and spatial patterns of extreme climate events. Another important climatic edge may be where winter precipitation occurs primarily as snow versus rain. For example, even though red-legged frogs occupy habitats with and without significant snowfall, we found that the relationship between adult survival and temperatures observed in populations without snowfall was not consistent with sustainable populations in places with snowfall. Differences in the timing of breeding between inland and coastal sites likely reflect strategies for avoiding colder winter weather by inland populations; similar patterns have been observed for populations of marble and tiger salamanders breeding in Massachusetts vs North Carolina (Petranka 1989). The transition from winter snow to rain has been shown to increase thermal stress and even to lead to complete reproductive failure in some winter breeding birds (Wingfield et al. 2017, 2011; Shipley et al. 2019). Changes in the timing of snowmelt are also associated with different coping strategies in mammals (Sheriff et al. 2017) and flowering phenology of nectar plants, which can affect floral resources and the length of butterfly flight periods (Section 5.1.1).

We were surprised at the rarity of climate-related reductions in population growth rates predicted by our SEED models. Only three of the 49 populations we evaluated from seven different species included in our study were predicted to do worse because of projected changes in climate over the next few decades. In contrast, seven populations were projected sinks under current climate conditions, not including snowy plover populations without active predator management known to be populations sinks (Colwell 2017) but predicted by our SEED models to be sources given fecundity and survival rates associated with active predator management. We interpret this result to reflect that for temperate special status species, climate-related threats are probably less prevalent than non-climate related threats, such as habitat loss, degradation and fragmentation, altered disturbance regimes, or competition with and predation by invasive species.

7   Literature Cited

Abatzoglou, J. T. 2013. Development of gridded surface meteorological data for ecological applications and modelling. International Journal of Climatology. 33: 121–131. doi:10.1002/joc.3413

Abatzoglou J. T. and Brown, T. J. 2012. A comparison of statistical downscaling methods suited for wildfire applications. International Journal of Climatology. 32: 772–780. doi:10.1002/joc.2312

Aiello-Lammens, M. E., Chu-Agor, M., Convertino, M., Fischer, R. A., Linkov, I., and Resit Akcakaya, H. 2011. The impact of sea-level rise on Snowy Plovers in Florida: integrating geomorphological, habitat, and metapopulation models. Global Change Biology, 17: 3644-3654.

Akaike, H. 1973. Information theory as an extension of the maximum likelihood principle. Pages 267–281 in Petrov, B.N., and F. Csaki, (eds.) Second International Symposium on Information Theory. Akademiai Kiado, Budapest.

Akçakaya H. R., Butchart, S. H. M., Mace, G. M., Stuart, S. N., and Hilton-Taylor, C. 2006. Use and misuse of the IUCN Red List Criteria in projecting climate change impacts on biodiversity. Global Change Biology 12:2037–2043.

Altermatt, F. 2010. Tell me what you eat and I'll tell you when you fly: diet can predict phenological changes in response to climate change. Ecology Letters, 13: 1475-1484. doi:10.1111/j.1461-0248.2010.01534.x

Anderson, B. J., Akcakaya, H. R., Araujo, M. B., Fordham, D. A., Martinez-Meyer, E., Thuiller, W., and Brook, B. W. 2009. Dynamics of range margins for metapopulations under climate change. Proceedings of the Royal Society B: Biological Sciences. 276: 1415-1420; DOI: 10.1098/rspb.2008.1681.

Angilletta Jr., M.J. 2009. Thermal Adaptation: A Theoretical and Empirical Synthesis. Oxford University Press, Oxford, U.K.

Anholt, B. R., Negovetic, S., and Som, C.1998. Methods for anaesthetizing and marking larval anurans. Herpetological Review 29:153–154.

Araújo, M. B. and Peterson, A. T. 2012. Uses and misuses of bioclimatic envelope modeling. Ecology, 93: 1527-1539. doi:10.1890/11-1930.1

Aschehoug, E.T., Sivakoff, F. S., Cayton, H. L., Morris, W. F., and Haddad, N. M. 2015. Habitat Restoration Affects Immature Stages of a Wetland Butterfly through Indirect Effects on Predation. Ecology 96: 1761–67. https://doi.org/10.1890/14-2403.1.

Ashton, S., Gutiérrez, D. and Wilson, R. J. 2009. Effects of temperature and elevation on habitat use by a rare mountain butterfly: implications for species responses to climate change. Ecological Entomology, 34: 437-446. doi:10.1111/j.1365-2311.2008.01068.x

Atkinson, D. 1994. Temperature and organism size — a biological law for ectotherms? Advances in Ecological Restoration 25: 1–58.

Bailey L. D., van de Pol, M. 2016. climwin: An R Toolbox for Climate Window Analysis. PLoS ONE 11: e0167980.

Bartel, R. A., Haddad, N. M., and Wright, J. P. 2010. Ecosystem engineers maintain a rare species of butterfly and increase plant diversity. Oikos, 119: 883–890.

Bartoń, K. 2017. MuMIn: Multi-Model Inference. R package version 1.40.0.

Bateman, B. L., Pidgeon, A. M., Radeloff, V. C., VanDerWal, J., Thogmartin, W. E., Vavrus, S. J. and Heglund, P. J. 2016. The pace of past climate change vs. potential bird distributions and land use in the United States. Global Change Biology 22: 1130-1144.

Bates, D., Maechler, M., Bolker, B., and Walker, S. 2015. Fitting Linear Mixed-Effects Models Using lme4. Journal of Statistical Software, 67: 1-48. doi:10.18637/jss.v067.i01.

Birch, L.C. 1953. Experimental Background to the Study of the Distribution and Abundance of Insects: I. The Influence of Temperature, Moisture and Food on the Innate Capacity for Increase of Three Grain Beetles. Ecology, 34: 698-711. doi:10.2307/1931333

Blaustein, A. R., Walls, S. C., Bancroft, B. A., Lawler, J. J., Searle, C. L., and Gervasi, S. S. 2010. Direct and indirect effects of climate change on amphibian populations. Diversity 2: 281-313.

Boggs, C. L. and Ross, C. L. (1993). The effect of adult food limitation on life history traits in *Speyeria mormonia* (Lepidoptera: Nymphalidae). Ecology 74: 433–441.

Bonhomme, R. 2000. Bases and limits to using 'degree.day' units. European Journal of Agronomy 13: 1–10.

Bocsi, T., Allen, J. M., Bellemare, J., Kartesz, J., Nishino, M. and Bradley, B. A. 2016. Plants' native distributions do not reflect climatic tolerance. Diversity and Distributions 22: 615-624. doi:10.1111/ddi.12432

Botkin, D., Saxe, H., Araújo, M. B., Betts, R., Bradshaw, R., Cedhagen, T., Chesson, P., Davis, M. B., Dawson, T., Etterson, J., Faith, D. P., Guisan, A., Ferrier, S., Hansen, A. S., Hilbert, D., Kareiva, P., Margules, C., New, M., Skov, F., Sobel, M. J., and Stockwell, D. 2007. Forecasting effects of global warming on biodiversity. BioScience 57: 227–236.

Brinkman, M.P., Garcelon, D.K. and Colwell, M.A. 2018. Evaluating the efficacy of carbachol at reducing corvid predation on artificial nests. Wildlife Society Bulletin, 42: 84-93.

Bryant, S. R., Thomas, C. D., and Bale, J. S. 2002. The influence of thermal ecology on the distribution of three nymphalid butterflies. Journal of Applied Ecology, 39: 43–55.

Burnham, K. P. and Anderson, D. R. 2002. Model Selection and Multimodel Inference: A Practical Information-theoretic Approach, 2nd edn. New York: Springer.

Burrell, N. S., and Colwell, M. A. 2012. Direct and indirect evidence that productivity of snowy plovers *Charadrius nivosus* varies with occurrence of a nest predator. Wildfowl 62: 204–223.

Bush, A., Mokany, K., Catullo, R., Hoffmann, A., Kellermann, V., Sgrò, C., McEvey, S. and Ferrier, S. 2016. Incorporating evolutionary adaptation in species distribution modelling reduces projected vulnerability to climate change. Ecology Letters 19: 1468-1478. doi:10.1111/ele.12696

Case, T. J., Holt, R. D., McPeek, M. A. and Keitt, T. H. 2005. The community context of species' borders: ecological and evolutionary perspectives. Oikos, 108: 28-46. doi:10.1111/j.0030-1299.2005.13148.x

Capinera J. L. 2008. Encyclopedia of Entomology. 2nd edn. Dordrecht, the Netherlands: Springer.

Cardé, R. T., Shapiro, A. M. and Clench, H. K. 1970. Sibling species in the *eurydice* group of *Lethe* (Lepidoptera: Satryidae). Psyche: A Journal of Entomology 77: 70–103.

Caswell, H. 2000. Matrix Population Models: Construction, Analysis and Interpretation, Second Edition. Sinauer, Sunderland, Massachusetts, USA

Cayton, H. L., Haddad, N. M., Gross, K., Diamond, S. E., and Ries, L. 2015. Do growing degree days predict phenology across butterfly species? Ecology, 96: 1473–1479.

Cecala, K. K., Price, S. J., and Dorcas, M. E. 2007. A comparison of the Effectiveness of Recommended Doses of MS-222 (tricaine methanesulfonate) and Orajel® (benzocaine) for Amphibian Anesthesia. Herpetological Review 38: 63-66.

Chen, I. C., Hill, J. K., Ohlemüller, R., Roy, D. B., and Thomas, C. D. 2011. Rapid range shifts of species associated with high levels of climate warming. Science 333: 1024-1026.

Colwell, M. A., McAllister, S. E., Millett, C. B., Transou, A. N., Mullin, S. M., Nelson, Z. J., Wilson, C. A., and LeValley, R. R. 2007. Philopatry and natal dispersal of the Western snowy plover. The Wilson Journal of Ornithology 119: 378-385

Conner, R. N., Rudolph, D. C., and Walters, J. R. 2001. The red-cockaded woodpecker, surviving in a fire-maintained ecosystem. University of Texas Press, Austin, TX.

Cormont, A., Jochem, R., Malinowska, A., Verboom, J., WallisDeVries, M.F., and Opdam, P. 2012. Can phenological shifts compensate for adverse effects of climate change on butterfly metapopulation viability? Ecological Modeling 227: 72-81 https://doi.org/10.1016/j.ecolmodel.2011.12.003

Costa, R. and Escano, E. F. 1989. Red-cockaded woodpecker: status and management in the southern region in 1986. USDA Forest Service, Atlanta, GA.

Colwell, M. A., Feucht, E. J., Lau, M. J., Orluck, D. J., McAllister, S. E. and Transou, A. N. 2017. Recent Snowy Plover population increase arises from high immigration rate in coastal northern California. Wader Study 124: 000-000.

Cross, H. Z., Zuber, M. S. 1972. Prediction of flowering dates in maize based on different methods of estimating thermal units. Agronomy Journal 64: 351-355.

Crozier, L., and Dwyer, G. 2006. Combining population-dynamic and ecophysiological models to predict climate-induced insect range shifts. The American Naturalist 167: 853–866.

Daniels, S. J. and Walters, J. R. 2000. Between-year breeding dispersal in red-cockaded woodpeckers: multiple causes and estimated cost. Ecology 81:2473-2484.

Davidson, J., and Andrewartha, H. G. 1948. The influence of rainfall, evaporation and atmospheric temperature on fluctuations in the size of a natural population of *Thrips imaginis* (Thysanoptera). The Journal of Animal Ecology: 200-222.

Davidson, C., Bradley Shaffer, H. and Jennings, M.R., 2001. Declines of the California red-legged frog: Climate, UV-B, habitat, and pesticides hypotheses. Ecological Applications, 11:464-479.

de Kroon, H., Plaisier, A., van Groenendael, J. and Caswell, H. 1986. Elasticity: The Relative Contribution of Demographic Parameters to Population Growth Rate. Ecology 67:1427–1431.

DeMay, S. M. and Walters, J. R. 2019. Variable effects of a changing climate on lay dates and productivity across the range of the Red-cockaded Woodpecker. The Condor: Ornithological Applications 121:1-14.

Dethier, B. E., and Vittum, M. T. 1967. Growing degree days in New York State. Cornell University Agricultural Experiment Station, Geneva, New York, USA.

Deutsch, C. A., Tewksbury, J. J., Huey, R. B., Sheldon, K. S., Ghalambor, C. K., Haak, D. C., and Martin, P. R. 2008. Impacts of climate warming on terrestrial ectotherms across latitude. Proceedings of the National Academy of Sciences of the United States of America 105: 6668-6672.

Doak, D. F., and Morris, W. F. 2010. Demographic compensation and tipping points in climate-induced range shifts. Nature 467: 959-962.

Dobkin, D. S., Olivieri, I., and Ehrlich, P. R.1987: Rainfall and the interaction of microclimate with larval resources in the population dynamics of checkerspot butterflies (*Euphydryas editha*) inhabiting serpentine grassland. Oecologia, 71, 161-166

Dormann, C. F. 2007. Promising the future? Global change projections of species distributions. Basic and Applied Ecology 8:387–397.

Eberhart-Phillips, L. J., Hudgens, B. R., and Colwell, M. A. 2015. Spatial synchrony of a threatened shorebird: Regional roles of climate, dispersal and management. Bird Conservation International 26: 119-135. doi:10.1017/S0959270914000379

Ehrlén, J., and Morris, W. F. 2015. Predicting changes in the distribution and abundance of species under environmental change. Ecology Letters 18: 303–314.

Einum, S., Forseth, T., and Finstad, A. G. 2012. Individual variation in response to intraspecific competition: problems with inference from growth variation measures. Methods in Ecology and Evolution, 3: 438–444. doi: 10.1111/j.2041-210X.2011.00167.x

Ellner, S. P., and Rees, M. 2006. Integral Projection Models for Species with Complex Demography. American Naturalist 167: 410–28. http://www.journals.uchicago.edu/doi/10.1086/499438

Endara, M., and Jaramillo, J. 201). The Influence of Microtopography and Soil Properties on the Distribution of the Speciose Genus of Trees, *Inga* (Fabaceae:Mimosoidea), in Ecuadorian Amazonia. Biotropica 43: 157-164.

Ehrlich , P. R., Murphy, D. D., Singer, M. C., Sherwood, C. B., White, R. R., and Brown, I. L. 1980. Extinction, reduction, stability and increase: The responses of checkerspot butterfly (*Euphydryas*) populations to the California drought**.** Oecologia 46: 101. https://doi.org/10.1007/BF00346973

Freckleton, R. P. 2011. Dealing with collinearity in behavioural and ecological data: Model averaging and the problems of measurement error. Behavioral Ecology and Sociobiology 65: 91–101. Available from: http://webhome.auburn.edu/~tds0009/PDFs/Freckleton 2011 collinearity.pdf

Feng, X., Nielsen, L. L., and Simpson, M. L. 2007. Responses of soil organic matter and microorganisms to freeze–thaw cycles. Soil Biology and Biochemistry 39: 2027-2037. https://doi.org/10.1016/j.soilbio.2007.03.003

Fischer, E., Beyerle, U. and Knutti, R. 2013. Robust spatially aggregated projections of climate extremes. Nature Climate Change 3: 1033–1038 doi:10.1038/nclimate205

Fournier, D., Skaug, H., Ancheta, J., Ianelli, J., Magnusson, A., Maunder, M., Nielsen, A, and Sibert, J. 2012. AD Model Builder: using automatic differentiation for statistical inference of highly parameterized complex nonlinear models. Optimization Methods and

Software, 27: 233-249. doi: 10.1080/10556788.2011.597854

Fox, J. 2002. Cox proportional-hazards regression for survival data. In J. Fox (Ed.), An R and S-PLUS companion to applied regression (pp. 1–18). Thousand Oaks, CA: Sage.

Freppaz, M., Williams, B. L., Edwards, A. C., Scalenghe, R. and Zanini, E. 2007. Simulating soil freeze/thaw cycles typical of winter alpine conditions: Implications for N and P availability. Applied Soil Ecology. 35: 247-255. https://doi.org/10.1016/j.apsoil.2006.03.012

Frost, C. C. 1998. Presettlement fire frequency regimes of the United States: a first approximation. Tall Timbers Fire Ecology Conference Proceedings. No. 20. Retrieved from https://talltimbers.org/wp-content/uploads/2018/09/70-Frost1998_op.pdf

Gaillard, J.M., Festa-Bianchet, M. and Yoccoz, N.G. 1998. Population dynamics of large herbivores: variable recruitment with constant adult survival. Trends in ecology & evolution, 13: 58-63.

Garcia, V. 2014. Lifetime fitness and changing life history traits in Red-cockaded Woodpeckers. Ph.D. dissertation, Virginia Tech University, Blacksburg, VA, USA.

Gillings, S., Balmer, D. E. and Fuller, R. J. 2015. Directionality of recent bird distribution shifts and climate change in Great Britain. Global Change Biology 21: 2155-2168. doi:10.1111/gcb.12823

Girvetz, E. H., Zganjar, C., Raber, G. T., Maurer, E. P., Kareiva, P., and Lawler, J. J. 2009. Applied climate-change analysis: the climate wizard tool. PLoS One 4: e8320.

Gompertz, B. 1825. On the nature of the function expressive of the law of human mortality, and on a new mode of determining life contingencies. Philosophical Transactions of the Royal Society B 115:513–583

Gordon, L. L. 2020. Effects of multiple stressors: hydroperiod, introduced bullfrogs, and food limitation on northern red-legged frogs (*Rana aurora*). Masters Thesis Humboldt State University.

Gosner, K. L. 1960. A simplified table for staging anuran embryos and larvae with notes on identification. Herpetologica 16: 183–190.

Govindarajulu, P., Altwegg, R, and Anholdt, B. R. 2005. Matrix model investigation of invasive speceis control: bullfrogs on Vancouver Island. Ecological Applications 15: 2161-2170.

Grant, E. H. C. 2008. Visual implant elastomer mark retention through metamorphosis in amphibian larvae. Journal of Wildlife Management 72: 1247–1252.

Hadfield, J. D. 2010. MCMC methods for multi-response generalized linear mixed models: the MCMCglmm R package. Journal of Statistical Software, 33: 1-22.

Hall, D., Riggs, G. 2016. MODIS/Terra Snow Cover Daily L3 Global 500m Grid, Version 6. Boulder, Colorado USA. NASA National Snow and Ice Data Center Distributed Active Archive Center. doi: 10.5067/MODIS/MOD10A1.006. Accessed August 4, 2019.

Hampe, A. 2004. Bioclimate envelope models: what they detect and what they hide. Global Ecology and Biogeography 13: 469–471.

Hansen, J., Sato, M., Ruedy, R., Lo, K., Lea, D. W., and Medina-Elizade, M. 2006. Global temperature change. Proceedings of the National Academy of Sciences, 103: 14288–14293.

Harley, C. D. C., and Paine, R. T. 2009. Contingencies and compounded rare perturbations dictate sudden distributional shifts during periods of gradual climate change, Proceedings of the National Academy of Sciences 106: 11172–11176

Hölldobler, B. and Wilson, E. O. 1990. The Ants. Cambridge, MA: Harvard University, The

Belknap Press

Hudgens, B., Eberhart-Phillips, L., Stenzel. L., Burns, C., Colwell, M., and Page, G. 2014. Population Viability Analysis of the Western Snowy Plover. Report prepared for the U.S. Fish and Wildlife Service. Arcata, CA.

Hudgens, B. and Harbert, M. 2019. Amphipod predation on northern red-legged frogs, *Rana aurora*, embryos. Northwestern Naturalist 100:126-131.

Hurvich, C. M., and Tsai, C.-L. 1989. Regression and time series model selection in small samples. Biometrika, 76: 297–307.

Inouye, D. W. 2008. Effects of climate change on phenology, frost damage, and floral abundance of montane wildflowers. Ecology 89: 353–362.

IPCC, 2013: Summary for Policymakers. In: Climate Change 2013: The Physical Science Basis. Contribution of Working Group I to the Fifth Assessment Report of the Intergovernmental Panel On Climate Change [Stocker, T.F., D. Qin, G.-K. Plattner, M. Tignor, S. K. Allen, J. Boschung, A. Nauels, Y. Xia, V. Bex and P.M. Midgley (eds.)]. Cambridge University Press, Cambridge, United Kingdom and New York, NY, USA.

Jackman, S. 2017. pscl: Classes and Methods for R Developed in the Political Science Computational Laboratory. United States Studies Centre, University of Sydney. Sydney, New South Wales, Australia. R package version 1.5.2. UR https://github.com/atahk/pscl/

Jenouvrier, S., Caswell, H., Barbraud, C., Holland, M., Stroeve, J., and Weimerskirch, H. 2009. Demographic models and IPCC climate projections predict the decline of an emperor penguin population. Proceedings of the National Academy of Sciences 106: 1844-1847.

John, R., Dalling, J. W., Harms, K. E., Yavitt, J. B., Stallard, R. F., Mirabello, M., Hubbell, S. P., Valencia, R., Navarrete, H., Vallejo, M., and Foster, R. B. 2007. Soil nutrients influence spatial distributions of tropical tree species. Proceedings of the National Academy of Sciences 104: 864 LP - 869. doi:10.1073/pnas.0604666104. http://www.pnas.org/content/104/3/864.abstract.

Kats, L. B. and Ferrer, R. P. 2003. Alien predators and amphibian declines: review of two decades of science and the transition to conservation. Diversity and Distributions 9: 99–110.

Kesler, D. C., Walters, J. R., and Kappes Jr., J. J. 2010. Social influences on dispersal and the fat-tailed dispersal distribution in red-cockaded woodpeckers. Behavioral Ecology 21: 1337-1343.

Kerr, N. Z., Wepprich, T., Grevstad, F. S., Dopman, E.B., Chew, F.S,, and Crone, E. E. 2020 Developmental trap or demographic bonanza? Opposing consequences of earlier phenology in a changing climate for a multivoltine butterfly. Global Change Biology 26: 2014– 2027. https://doi.org/10.1111/gcb.14959

Kiekebusch, E. 2020. Effects of temperature, phenology, and geography on butterfly population dynamics under climate change. North Carolina State University.

Kiesecker, J. M., and Blaustein, A. R. 1997. Population differences in responses of red-legged frogs (*Rana aurora*) to introduced bullfrogs. Ecology 78:1752–1760.

Kiesecker, J. M., Blaustein, A. R., and Miller, C. L. 2001. Potential mechanisms underlying the displacement of native red-legged frogs by introduced Bullfrogs. Ecology 82: 1964–1970.

Knapp, R.A., Boiano, D.M. and Vredenburg, V.T. 2007. Removal of nonnative fish results in population expansion of a declining amphibian (mountain yellow-legged frog, *Rana muscosa*). Biological Conservation 135: 11-20.

Kudo, G. and Ida, T. Y. 2013. Early onset of spring increases the phenological mismatch

between plants and pollinators. Ecology 94: 2311–2320

Kuefler, D., Haddad, N. M., Hall, S., Hudgens, B., Bartel, B. and Hoffman, E. 2008. Distribution, population structure and habitat use of the endangered Saint Francis Satyr butterfly, *Neonympha mitchellii francisci*. The American Midland Naturalist 159: 298-320.

Kuefler, D., Hudgens, B., Haddad, N. M., Morris, W. F. and Thurgate, N. 2010. The conflicting role of matrix habitats as conduits and barriers for dispersal. Ecology, 91: 944-950. doi:10.1890/09-0614.1

Laake, J. L. 2013. RMark: An R Interface for analysis of capture-recapture data with MARK. AFSC Processed Rep. 2013-01, 25 p. Alaska Fisheries Science Center, NOAA, National Marine Fisheries Servive, 7600 Sand Point Way NE, Seattle WA 98115.

Lawler, J. J., Shafer, S. L., White, D., Kareiva, P., Maurer, E. P., Blaustein, A. R., and Bartlein, P. J. 2009. Projected climate-induced faunal change in the Western Hemisphere. Ecology. 90: 588-597.

Lebeau, J., Wesselingh, R. A. and Van Dyck, H. 2016. Floral resource limitation severely reduces butterfly survival, condition and flight activity in simplified agricultural landscapes. Oecologia 180: 421–427. https://doi.org/10.1007/s00442-015-3492-2

Lefkovitch, L. P. 1965. The study of population growth in organisms grouped by stages. Biometrics 21: 1–18.

Licht, L. E. 1974. Survival of embryos, tadpoles, and adults of the frogs *Rana aurora aurora* and *Rana pretiosa pretiosa* sympatric in southwestern British Columbia. Canadian Journal of Zoology 52: 613-627.

Louthan, A. M., Doak, D. F., and Angert, A. L. 2015. Where and when do species interactions set range limits? Trends in Ecology and Evolution 30: 780-792.

Lowe, S., Browne, M., Boudjelas, S., and De Poorter, M. 2000. 100 of the World's Worst Invasive Alien Species A selection from the Global Invasive Species Database. Published by The Invasive Species Specialist Group (ISSG) a specialist group of the Species Survival Commission (SSC) of the World Conservation Union (IUCN), 12pp. First published as special lift-out in Aliens 12, December 2000. Updated and reprinted version: November 2004.

Lytle, D.A., Merritt, D.M., Tonkin, J.D., Olden, J.D. and Reynolds, L.V. 2017. Linking river flow regimes to riparian plant guilds: A community-wide modeling approach. Ecological Applications 27: 1338-1350.

McHarry, K. 2017. Influence of canopy cover and climate on early life-stage vital rates for Northern red-legged frogs (*Rana aurora*), and implications for population growth rates. Masters Thesis Humboldt State University.

McHarry, K.W., Abbott, J. A., van Hattem, M. G., and Hudgens, B. 2018. Efficacy of visible implant elastomer tags with photographic assist for identifying individuals in capture-mark-recapture studies using larval frogs. Herpetological Conservation and Biology 13: 576–585.

McMaster, G. S., and Smika, D. E. 1988. Estimation and evaluation of winter wheat phenology in the central Great Plains. Agriculture and Forest Meteorology 43: 1-18.

Memmott, J., Craze, P. G., Waser, N. M., and Price, M. V. 2007. Global warming and the disruption of plant–pollinator interactions. Ecology Letters 10: 710–717.

Moore, J. L., and Remais, J. V. 2014. Developmental Models for Estimating Ecological Responses to Environmental Variability: Structural, Parametric, and Experimental Issues.

Acta Biotheoretica 62: 69–90.

Morris, W.F. and Doak, D.F. 2004. Buffering of life histories against environmental stochasticity: accounting for a spurious correlation between the variabilities of vital rates and their contributions to fitness. The American Naturalist, 163: 579-590.

Moussus, J. P., Julliard, R., and Jiguet, F. 2010. Featuring 10 phenological estimators using simulated data. Methods in Ecology and Evolution 1:140–150.

Network for Alaska and Arctic Planning, University of Alaska. 2019. Projected Monthly Temperature Products- 10 min CMIP5/AR5. Retrieved 5/2/2019 from http://ckan.snap.uaf.edu/dataset/projected-monthly-temperature-products-10-min-cmip5-ar5

Neuman, K. K., Page, G. W., Stenzel, L. E., Warriner, J. C., and Warriner, J. S. 2004. Effect of mammalian predatory management on Snowy Plover breeding success. Waterbirds 27: 257-263.

NOAA National Centers for Environmental Information, State of the Climate: Drought for October 2015, published online November 2015, retrieved on December 12, 2019 from https://www.ncdc.noaa.gov/sotc/drought/201510.

Nufio, C. R., McGuire, C. R., Bowers, M. D., and Guralnick. R. P. 2010. Grasshopper community response to climatic change: variation along an elevational gradient. PLoS ONE 5:e12977.

Odum, R. A. and Zippel, K. C. 2008. Amphibian water quality: approaches to an essential environmental parameter. International Zoo Yearbook 42: 40-52. doi:10.1111/j.1748-1090.2008.00053.x

Opler, P. 1994. Peterson first guide to butterflies and moths. Houghton Mifflin Company, New York, New York.

Ozinga, W. A., Schaminée, J. H. J., Bekker, R. M., Bonn, S., Poschlod, P., Tackenberg, O., Bakker, J., and Groenendael, J. M. v. 2005. Predictability of plant species composition from environmental conditions is constrained by dispersal limitation. Oikos 108: 555-561. doi:10.1111/j.0030-1299.2005.13632.x

Page, G. W., Stenzel, L. E., Page, G. W., Warriner, J. S., Warriner, J. C., and Paton, P. W. 2009. Snowy Plover (*Charadrius alexandrinus*), the Birds of North American Online (A. Poole, Ed.) Ithaca. Cornell Lab of Ornithology. Retrieved from the Birds of North America Online: http://bna.birds.cornell.edu/bna/species/154 doi:10.2173/bna.154

Parmesan, C. 1996. Climate and species' range. Nature 382: 765–766. https://doi.org/10.1038/382765a0

Parmesan, C., Root, T. L., and Willig, M. 2000. Impacts of extreme weather and climate on terrestrial biota. Bullentin of the American Meteorological Society 81:443–450.

Parmesan, C., Ryrholm, N., Stefanescu, C., Hill, J. K., Thomas, C. D., Descimon, H., and Warren, M. 1999. Poleward shifts in geographical ranges of butterfly species associated with regional warming. Nature 399: 579-583.

Parmesan, C., and Yohe, G. 2003. A globally coherent fingerprint of climate change impacts across natural systems. Nature 421: 37-42.

Parry, D., Spence, J. R., and Volney, W. A. 1998. Budbreak phenology and natural enemies mediate survival of first-instar forest tent caterpillar (Lepidoptera: Lasiocampidae). Environmental Entomology. 27: 1368–1374.

Peterson, S.A. and Colwell, M.A., 2014. Experimental evidence that scare tactics and effigies reduce corvid occurrence. Northwestern Naturalist 95: 103-112.

Petranka, J.W.1998. Salamanders of the United States and Canada. Smithsonian Institution Press, Washington, District of Columbia.

Pfister, C.A. 1998. Patterns of variance in stage-structured populations: evolutionary predictions and ecological implications. Proceedings of the National Academy of Sciences, 95: 213-218.

Picó, F. X. 2012. Demographic fate of *Arabidopsis thaliana* cohorts of autumn-and spring-germinated plants along an altitudinal gradient. Journal of Ecology 100: 1009-1018.

Piessens, K., Adriaens, D., Jacquemyn, H., and Honnay, O. 2009. Synergistic effects of an extreme weather and habitat fragmentation on a specialist herbivore. Oecologia 159:117–126

Pollard, E. 1979. Population ecology and change in range of the white admiral butterfly *Ladoga camilla* L. in England. Ecological Entomology 4: 61-74.

Pulliam, H. 2000. On the relationship between niche and distribution. Ecology Letters 3: 349-361. doi:10.1046/j.1461-0248.2000.00143.x

Prysby, M. D. 2004. Natural enemies and survival of monarch eggs and larvae. Pages 27–38 in K. Oberhauser and M. Solensky, editors. The monarch butterfly. Biology and conservation. Cornell University Press, Ithaca, New York, USA.

Radchuk, V., Turlure. C., and Schtickzelle, N. 2013. Each Life Stage Matters: The importance of assessing the response to climate change over the complete life cycle in butterflies. Journal of Animal Ecology 82: 275–85.

R Core Team. 2017. R: A language and environment for statistical computing. R Foundation for Statistical Computing, Vienna, Austria. URL https://www.R-project.org/.

RStudio Team. 2015. RStudio: Integrated Development for R. RStudio, Inc., Boston, MA URL http://www.rstudio.com/.

Redmond, M. D. 2019. mirandaredmond/cwd_function: CWD and AET function V1.0.0 [Internet]. 2019 [cited 2019 Sep 11]. Available from: https://zenodo.org/record/2530955#.XXlWP5NKh24.

Reynolds, R., Lambert, J., Flather, C., White, G., Bird, B., Baggett, L., Lambert, C., and Bayard de Volo, S. 2017. Long-term demography of the Northern Goshawk in a variable environment. Wildlife Monographs 197: 1-40. doi: 10.1002/wmon.1023

Robinson, G. S., Ackery, P. R., Kitching, I. J., Beccaloni, G. W., and Hernàndez, L. M. 2002. Hostplants of the moth and butterfly caterpillars of America north of Mexico. Memoirs of the American Entomological Institute vol. 69. Gainesville, FL. 824 pp.

Roy, D. B. and Sparks, T. H. 2000. Phenology of British butterflies and climate change. Global Change Biology 6: 407–416.

Russelle, M. P., Wilhelm, W. W., Olson, R. A., and Power, J. F. 1984. Growth analysis based on degree days. Crop Science 24: 28-32.

Seamster, A. P. 1950. Developmental studies concerning the eggs of *Ascaris lumbricoides* var. suum. The American Midland Naturalist 43: 450–470.

Sæther, B. E., Tufto, J., Engen, S., Jerstad, K., Røstad, O. W., and Skåtan, J. E. 2000. Population dynamical consequences of climate change for a small temperate songbird. Science 287: 854-856.

Scenarios Network for Alaska and Arctic Planning, University of Alaska. 2019. Projected Monthly Temperature Products- 10 min CMIP5/AR5. Retrieved 5/2/2019 from http://ckan.snap.uaf.edu/dataset/projected-monthly-temperature-products-10-min-cmip5-ar5

Scott, J. A. 1986. The Butterflies of North America: A Natural History and Field Guide. Stanford University Press, Stanford, California.

Scott, J. M., Goble, D. D., Haines, A. M., Wiens, J. A., and Neel, M. C. 2010. Conservation-reliant species and the future of conservation. Conservation Letters 3: 91-97.

Shaffer, H. B., Fellers, G. M., Voss, S. R., Oliver, J. C., and Pauly, G. B. 2004. Species boundaries, phylogeography and conservation genetics of the red-legged frog (*Rana aurora/draytonii*) complex. Molecular Ecology 13: 2667.

Sheriff, M.J., Boonstra, R., Palme, R., Buck, C.L., and Barnes, B.M. 2017. Coping with differences in snow cover: the impact on the condition, physiology and fitness of an arctic hibernator. Conservation Physiology 5: cox065 https://doi.org/10.1093/conphys/cox065

Sherwood, J. A., Debinski, D. M., Caragea, P. C., and Germino, M. J. 2017. Effects of experimentally reduced snowpack and passive warming on montane meadow plant phenology and floral resources. Ecosphere 8: e01745. 10.1002/ecs2.1745

Shipley, A. A., Sheriff, M. J., Pauli, J. N., and Zuckerberg, B. 2019. Snow roosting reduces temperature-associated stress in a wintering bird. Oecologia 190: 309-321.

Sinclair, S. J., White, M. D., and Newell, G. R. 2010. How useful are species distribution models for managing biodiversity under future climates? Ecology and Society 15: 8. http://www.ecologyandsociety.org/vol15/iss1/art8

Singer, M. C. and Parmesan, C. 2010. Phenological asynchrony between herbivorous insects and their hosts: signal of climate change or pre-existing adaptive strategy? Philosophical Transactions of the Royal Society B. 365: 3161-3176 doi:10.1098/rstb.2010.0144

Singer, M. C., and Thomas, C. D.1996. Evolutionary responses of a butterfly metapopulation to human- and climate-caused environmental variation. The American Naturalist 148: S9–S39. www.jstor.org/stable/2463046

Sivakoff, F., Morris, W., Aschehoug, E., Hudgens, B., and Haddad, N. 2016. Habitat restoration alters adult butterfly morphology and potential fecundity through effects on host plant quality. Ecosphere 7:1-12.

Skaug, H., Fournier, D., Bolker, B., Magnusson, A., and Nielsen, A. 2016. Generalized Linear Mixed Models using 'AD Model Builder'. R package version 0.8.3.3.

Skelly, D. K., Freidenburg, L. K., and Kiesecker, J. M. 2002. Forest canopy and the performance of larval amphibians. Ecology 83: 983–992.

Spiegelhalter, D. J., Best, N. G., Bradley, C.P., and van der Linde, A. 2002. Bayesian measures of model complexity and fit. Journal of the Royal Statistical Society, Series B 64: 583–639.

Stenzel, L., Page, G. W., Warriner, J. C., George, D. E., Eyster, C. R., Ramer, B. A., and Neuman, K. K. 2007. Survival and natal dispersal of juvenile snowy plovers (*Charadrius alexandrinus*) in central coastal California. The Auk 124: 1023-1036.

Stenzel, L. E., Page, G. W., Warriner, J. C., Warriner, J. S., Neuman, K. K., George, D. E., Eyster, C. E., and Bidstrup, F. C. 2011. Male-skewed adult sex ratio, survival, mating opportunity and annual productivity in the Snowy Plover *Charadrius alexandrinus*. Ibis 153: 312-322.

Stenzel, L., Warriner, J., Warriner, J., Wilson, K., Bidstrup, F., and Page, G. 1994. Long-Distance Breeding Dispersal of Snowy Plovers in Western North America. Journal of Animal Ecology 63: 887-902.

Thurgate, N. Y., and Pechmann, J. H. K. 2007. Canopy closure, competition, and the endangered Dusky Gopher Frog. Journal of Wildlife Management 71:1845–1852.

United States Department of Agriculture, NRCS. 2019b. The PLANTS Database (http://plants.usda.gov, 1 August 2019). National Plant Data Team, Greensboro, NC 27401-4901 USA.

United States Fish and Wildlife Service. 2003. Recovery plan for the Red-cockaded Woodpecker (*Picoides borealis*): Second revision. U.S. Fish and Wildlife Service, Atlanta, GA, USA.

United States Fish and Wildlife Service. 2007. Recovery Plan for the Pacific Coast Population of the Western Snowy Plover (*Charadrius alexandrinus nivosus*). In 2 volumes. Sacramento, California. xiv + 751 pages. Available at: http://www.fws.gov/cno/es/recoveryplans.html

United States Fish and Wildlife Service. 2020. Species Status Assessment Report for the Red-cockaded Woodpecker (*Picoides borealis*). U.S. Fish and Wildlife Service, Atlanta, GA, USA.

Urban, M. C. 2015. Accelerating extinction risk from climate change. Science 348: 571-573.

Urban, M. C., Bocedi, G., Hendry, A. P., Mihoub, J. B., Pe'er, G., Singer, A., Bridle, J. R., Crozier, L. G., De Meester, L., Godsoe, W. Gonzalez, A., Hellman, J. J., Holt, R. D., Huth, A., Johst, K., Krug, C. B., Leadley, P. W., Palmer, S. C., Pantel, J. H., Schmitz, A., Zollner, P. A., and Travis, J. M. 2016. Improving the forecast for biodiversity under climate change. Science 353: p.aad8466.

van de Pol. M., Bailey, L. D., McLean, N., Rijsdijk, L., Lawson, C. R., and Brouwer, L. 2016. Identifying the best climatic predictors in ecology and evolution. Methods in Ecology and Evolution 7: 1246-1257.

Van Tienhoven, A. M., Den Hartog, J. E., Reijns, R. A., and Peddemors, V. M. 2007: A computer-aided program for pattern-matching of natural marks on the spotted raggedtooth shark, *Carcharias taurus*. Journal of Applied Ecology 44: 273-280. https://doi.org/10.1111/j.1365-2664.2006.01273.x

Walters, J. R., Doerr, P. D., and Carter, III, J. H. 1988. The cooperative breeding system of the red-cockaded woodpecker. Ethology 78: 275-305.

Walters, J. R. 1991. Application of ecological principles to the management of endangered species: the case of the red cockaded woodpecker. Annual Review of Ecology and Systematics 22: 505 523.

Walther, G. R., Post, E., Convey, P., Menzel, A., Parmesan, C., Beebee, T. J., and Bairlein, F. 2002. Ecological responses to recent climate change. Nature 416: 389-395.

Wepprich, T. 2017. Effects of climatic variability on a statewide butterfly community. North Carolina State University.

Warren, D. L., Wright, A. N., Seifert, S. N. and Shaffer, H. B. 2014. Incorporating model complexity and spatial sampling bias into ecological niche models of climate change risks faced by 90 California vertebrate species of concern. Diversity and Distributions 20: 334-343. doi:10.1111/ddi.12160

Warriner, J. S., Warriner, J. C., Page, G. W., and Stenzel, L. E. 1986. Mating system and reproductive success of a small population of polygamous Snowy Plovers. Wilson Bulletin 98: 15-37.

Warton, D. I. and Hui, F. K. C. 2011. The arcsine is asinine: the analysis of proportions in ecology. Ecology 92: 3-10. doi:10.1890/10-0340.1

Weiner, J., and Thomas, S. C. 1986. Size Variability and Competition in Plant Monocultures. Oikos, 47: 211. doi: 10.2307/3566048

Werner, E. E., and Glennemeier, K. S. 1999. Influence of forest canopy cover on the breeding pond distributions of several amphibian species. Copeia 1999:1–12.

White, G. C., and Burnham, K. P. 1999. Program MARK: survival estimation from populations of marked animals. Bird Study 46(Suppl.): 120–138.

Wilensky, U., NetLogo. http://ccl.northwestern.edu/netlogo/. Center for Connected Learning and Computer-Based Modeling, Northwestern University, Evanston, IL, 1999.

Williams, J.L., Miller, T. E. X., and Ellner. S. P. 2012. Avoiding unintentional eviction from integral projection models. Ecology 93: 2008–14. http://www.ncbi.nlm.nih.gov/pubmed/23094372

Wilson, J. W., Sexton, J. O, Jobe, R. T., and Haddad, N. M. 2013. The relative contribution of terrain, land cover, and vegetation structure indices to species distribution models. Biological Conservation 164: 170– 176. https://doi.org/10.1016/j.biocon.2013.04.021.

Wingfield, J. C., Kelley, J. P., and Angelier, F. 2011. What are extreme environmental conditions and how do organisms cope with them? Current Zoolology 57: 363–374. (doi:10.1093/czoolo/57.3.363)

Wingfield, J. C., Perez, J. H., Krause, J. S., Word, K. R., Gonzalez-Gomes, P. L., Lisovski, S., and Chmura, H. E. 2017. How birds cope physiologically and behaviourally with extreme climatic events. Philosophical Transactions of the Royal Society B: Biological Sciences, 372: 1723. https://doi.org/10.1098/rstb.2016.0140.

Xue, F.-S., Kallenborn, H. G., and Wei, H.-Y. 1997. Summer and winter diapause in pupae of the cabbage butterfly, *Pieris melete* Ménétriés. Journal of Insect Physiology 43: 701–707. https://doi.org/10.1016/S0022-1910(97)00053-X

Yap, T. A., Koo, M. S., Ambrose, R. F., and Vredenburg, V. T. 2018. Introduced bullfrog facilitates pathogen invasion in the western United States. PLOS ONE 13: e0188384. https://doi.org/10.1371/journal.pone.0188384

Youngsteadt, E., Irwin, R. E., Fowler, A., Bertone, M. A., Giacomini, S. J., Kunz, M., Suiter, D., and Sorenson, C. E. 2018. Venus flytrap rarely traps its pollinators. The American Naturalist 191: 539–46. https://www.journals.uchicago.edu/doi/10.1086/696124

Zalom, F. G., Goodell, P. B., Wilson, L. T., Barnett, W. W., and Bentley, W. J. 1983. Degree-days: The calculation and use of heat units in pest management. UC DANR Leaflet 21373.

8 Appendices

8.1 **Appendix 8.1.** GCM projections used in this manuscript for future climate correlations, downscaled to a 4 km x 4 km grid using the MACA method.

	GCM name
1	bcc-csm1-1
2	bcc-csm1-1-m
3	BNU-ESM
4	CanESM2
5	CCSM4
6	CNRM-CM5
7	CSIRO-Mk3-6-0
8	GFDL.ESM2M
9	GFDL-ESM2G
10	HadGEM2-CC365
11	HadGEM2-ES365
12	inmcm4
13	IPSL-CM5A-LR
14	IPSL-CM5A-MR
15	IPSL-CM5B-LR
16	MIROC-ESM
17	MIROC-ESM-CHEM
18	MIROC5
19	MRI-CGCM3
20	NorESM1-M

8.2   **Appendix 8.2** Observed nectar plant usage by adult hydaspe fritillary butterflies during mark-recapture surveys at each site. Nectar plant species are listed in order of usage by site.

Site and nectar plant species	# of observations each year				
Cascades	**2016**	**2017**	**2018**	**Total**	**% usage**
Subalpine Daisy (*Erigeron peregrinus*)	17	93	41	151	0.57
Goldenrod (*Solidago sp.*)	4	23	0	27	0.1
Bull Thistle (*Cirsium vulgare*)	0	23	0	23	0.09
Pearly Everlasting (*Anaphalis margaritacea*)	6	4	8	18	0.07
Cascade Aster (*Aster ledophyllus*) and other *Aster spp.*	8	6	3	17	0.06
Gray's Licorice-root (*Ligusticum grayi*)	0	4	1	5	0.02
Valerian (*valeriana sp.*)	0	3	2	5	0.02
Cow Parsnip (*Heracleum lanatum*)	0	0	2	2	0.01
Oxeye Daisy (*Leucanthemum vulgare*)	3	0	0	3	0.01
Hawkbit (*Leontodon sp.*)	3	0	0	3	0.01
Mountain Owl's-clover (*Orthocarpus imbricatus*)	0	0	3	3	0.01
Tansy Ragwort (*Senecio jacobaea*)	2	0	0	2	0.01
Arrowleaf Groundsel (*Senecio triangularis*)	0	0	1	1	0.004
Few leaved thistle (*Cirsium remotifolium*)	1	0	0	1	0.004
Lupine (*Lupinus sp.*)	0	0	1	1	0.004
St. John's Wort (*Hypericum perforatum*)	1	0	0	1	0.004
Coast Range 1	**2016**	**2017**	**2018**	**Total**	**% usage**
Douglas' Thistle (*Cirsium douglasii*)	83	334	114	531	0.79
Angelica sp.	40	28	22	90	0.13
Golden Chinquapin Tree (*Chrysolepis chrysophylla*)	6	18	11	35	0.05
Naked Buckwheat (*Eriogonum nudum*)	0	3	1	4	0.01
Monardella sp	0	3	2	5	0.01
Huckleberry Oak (*Quercus vacciniifolia*)	0	3	0	3	0.004
Western False Asphodel (*Triantha occidentalis*)	0	0	1	1	0.001
Coast Range 2	**2016**	**2017**	**2018**	**Total**	**% usage**
Spreading Dogbane (*Apocynum androsaemifolium*)	32	75	11	118	0.66
Canada Thistle (*Cirsium arvense*)	8	18	0	26	0.15
Bull Thistle (*Cirsium vulgare*)	4	7	2	13	0.07
Common Yarrow (*Achillea millefolium*)	1	9	1	11	0.06
Wild Teasel (*Dipsacus fullonum*)	4	0	0	4	0.02
Golden Chinquapin Tree (*Chrysolepis chrysophylla*)	0	3	0	3	0.02
Arrowleaf Groundsel (*Senecio triangularis*)	0	0	1	1	0.01
Harsh Checker Mallow (*Sidalcea asprella*)	0	1	0	1	0.01
Naked Buckwheat (*Eriogonum nudum*)	1	0	0	1	0.01

Sierra Nevada 1	2016	2017	2018	Total	% usage
Coyote Mint (*Monardella villosa*)	3	11	53	67	0.71
Wallflower (*Erysimum capitatum*)	0	0	18	18	0.19
Sanborn's Onion (*Allium sanbornii*)	0	0	4	4	0.04
Bull Thistle (*Cirsium vulgare*)	0	3	0	3	0.03
Naked Buckwheat (*Eriogonum nudum*)	0	0	1	1	0.01
Blackberry (*Rubus sp.*)	0	0	1	1	0.01
Yellow Star-thistle (*Centaurea solstitialis*)	0	1	0	1	0.01
Sierra Nevada 2	**2016**	**2017**	**2018**	**Total**	**% usage**
Horsemint Giant Hyssop (*Agastache urticifolia*)	19	34	394	447	0.87
Aster spp.	16	1	21	38	0.07
Bull thistle (*Cirsium vulgare*)	0	0	10	10	0.02
Goldenrod (*Solidago sp.*)	1	2	7	10	0.02
Angelica sp.	0	1	1	2	0.004
Cinquefoil (*Potentilla sp.*)	0	0	1	1	0.002
Common Yarrow (*Achillea millefolium*)	0	1	1	2	0.004
Milk Thistle (*Silybum marianum*)	2	0	0	2	0.004
Sierra Nevada 1	**2016**	**2017**	**2018**	**Total**	**% usage**
Bull thistle (*Cirsium vulgare*)	NA	NA	269	269	0.98
Coyote Mint (*Monardella villosa*)	NA	NA	2	2	0.01
Harsh Checker Mallow (*Sidalcea asprella*)	NA	NA	1	1	0.004
California harebell (*Asyneuma prenanthoides*)	NA	NA	1	1	0.004
Goldenrod (*Solidago sp.*)	NA	NA	1	1	0.004

8.3 **Appendix 8.3** Relationship between the metric of size used in our demographic rate functions and IPMs (length of longest leaf x number of leaves) v. total leaf area. Here, total leaf area is calculated using the measured length and width of each leaf and assuming it is elliptical. *R2* is 0.8334, and the correlation between the variables is large (rho= 0.91) and significant (*P* = 2.2e-16).
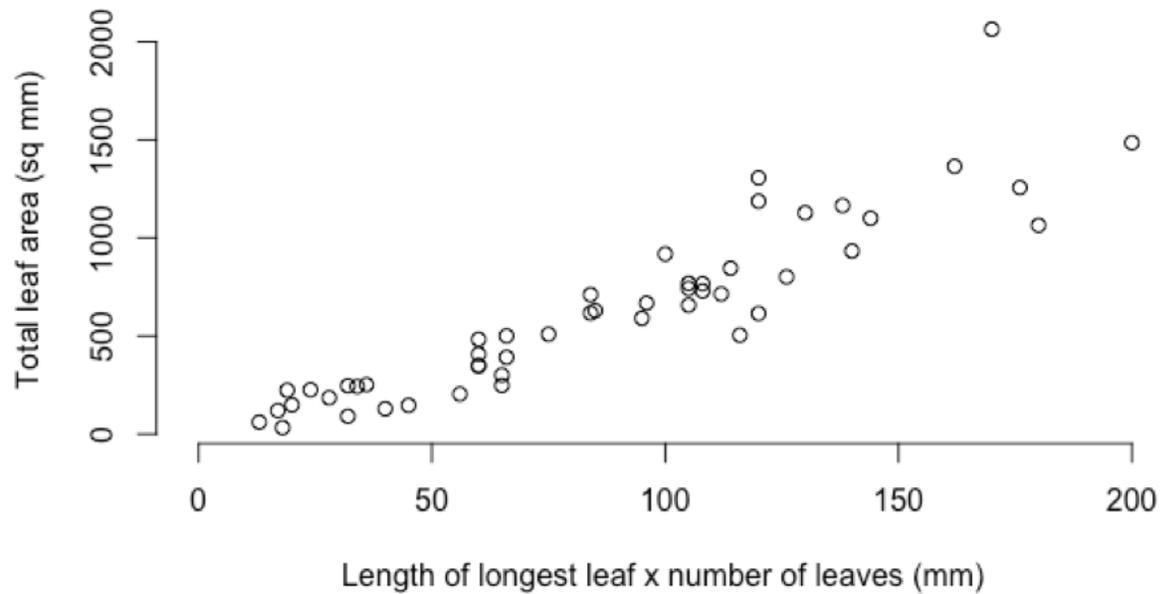
Appendix 8.4 Parameter estimates (in first row) and standard error of parameter estimates (in second row) for best-fit models for each demographic rate from the Venus flytrap experimental tests of fire effects. Parameter estimates significant at the alpha = 0.05 level are shown in bold. The absence of a parameter estimate indicates the parameter was not present in the best-fit model for the demographic rate. The last column shows the results of an ANCOVA testing for overall effect of condition on each demographic rate, using plant size as a covariate; the first row is the chi-square value (for binomial models) or the F-value (for linear models) for the condition effect, and the second row is the associated p-value. Condition effects significant at the alpha = 0.05 level are shown in bold. For recruitment, we show the difference between observed values for the indicated condition and the value of the control condition.

	(Intercept)	Size in previous time step	Coastal population	Neighbor removal condition	Neighbor removal +ash condition	Fire	2018 year	Neighbor removal condition x coastal population	Neighbor removal + ash condition x coastal	ANCOVA results (chi-square or F- value and p-value)
survival	**4.353**	**0.347**	14.146	-0.684	-0.711	-13.93	**-1.847**	-15.63	0.671	2.469
	0.564	**0.129**	915.81	0.36	0.438	915.81	**0.519**	915.81	1383.2	0.481
Mean size after one year of growth	**4.650**	**0.188**		**-0.209**	**-0.157**	**-0.183**	**-0.221**			**68.588**
	0.057	**0.023**		**0.066**	**0.075**	**0.063**	**0.059**			**0.000**
Variance in size after one year of growth	**-1.779**						**-0.393**			**2.715**
	0.126						**0.154**			**0.044**
p(fruit)	-0.768	**0.882**	**-2.196**	0.031	**0.780**	1.161	**-1.254**	0.793	-0.953	**47.270**
	0.242	**0.112**	**0.588**	0.270	**0.289**	0.641	**0.234**	0.793	0.867	**0.000**
No. fruit	**-2.801**									0.568
	0.068									0.637
Recruitment	N/A	N/A	N/A	0.338	0.531	1.567	N/A	N/A	N/A	N/A

8.5   **Appendix 8.5** Generalized SEED model code

Generalized Spatially Explicit Environmentally Driven (SEED) Model to Evaluate Potential Response
to Climate Change by Species Managed on Department of Defense Properties.
Prepared by: Brian Hudgens
Institute for Wildlife Studies

OVERVIEW:
The primary tool we are using in this project to evaluate which species will become more, or
less, conservation reliant because of a changing climate is the Spatially Explicit
Environmentally Driven (SEED) population model. These models integrate functions describing the
relationship between vital rates and variation in different climate variables over the life cycle
of a species to project population growth given a set of climate conditions. By linking these
models to climate projection models, we are able to make predictions about how population growth
of a species at one or more specific locations is likely to change over the coming decades. The
goal of this document is to provide a general outline for how SEED models are designed.
Our original idea for the generalized SEED model was to provide R-code that served as the core
code underlying the SEED models developed for the seven species studied as part of this project.
We imagined that we would modify this code with relatively minor tweaks to account for
differences in species life histories and how climate influenced population growth. However, our
work to date has revealed that climate influences different species through vastly different
mechanisms that often take very different approaches to describe within a simulation. These
complications include climate-driven changes in phenology that interact with climate effects on
vital rates or require that different time windows of climate data be used during different years
of a simulation. We found that the SEED models that worked best for the species we studied shared
only the most general framework.
In order to provide a product that had greater potential to be useful to a broader range of
Department of Defense managers and cooperators we decided to provide that general framework along
with examples of functions or programming code used to address some of the scenarios we have
encountered. The code is heavily commented with an eye towards guiding readers through the kinds
of practical coding decisions that have to be made when developing a SEED model.
The general framework corresponds to the broad steps assigned a Roman numeral. Alternative code
snippets or functions are placed within that framework where they would appear in the SEED codes
developed for the species included in this project; with comments provided to explain what
conditions each alternative is meant to apply to. We also use comments within the code to
describe assumptions about datasets read into the model, including variable names and order.

```
################################# OUTLINE ##############################################
# I.    Read in landscape matrix                                                       #
# II.   Create distance and dispersal probability matrices
# III.  Define tracking variables                                                      #
# IV.   Define life history functions                                                  #
# V.    Read in projected future climate conditions                                    #
# VI.   Loop through population dynamics for present day and future climates            #
# VII.  Output                                                                          #
#######################################################################################


#######################################################################################
###########              I. Read in landscape matrix                     ###########
#######################################################################################
Landscape=read.csv('Drive:/Directory/Sub_Directory/LandscapeFile.csv',header=T, sep=",")
pop.count=length(Landscape$site.id)  #counts the number of populations in the landscape
#File should be a data frame with the following columns:
#site.id; UTM.Easting; UTM.Northing; Max.population.size; Demographic.Rate1-Demographic.RateX;
N1-Nx
#site.id is a unique identifier assigned to each site used to:
#       -link site to correct climate projections
#       -link site to site-specific vital rates and max population size
#       -properly assign dispersal probabilities
#       -if different links use different site names, additional columns should be included with
#        alternative site names
#UTM.Easting and UTM.Northing are location coordinates used to determine distance between sites
#       -These columns are not necessary if a previously calculated dispersal matrix is imported
as well

#Max.populaiton.size is the maximum number of adults that can live at the site
#       -used to restrict population growth to a finite number
#       -may not be needed, or replaced with other variable if better information is used to
#        determine density dependence within a population

#Demographic.Rate1,... Demographic.RateX are site specific parameters unrelated to climate
variables
#     Examples include:
#       -month when breeding typically begins at a site,
#       -site specific modifications to vital rates,
#       -site specific modifications to distance based dispersal rates
#Initial population size N1-Nx correspond to the number of individuals in each stage in year 1
#       - For populations without stage structure only a single column for initial population
size is required
#       - In most cases, there will not be columns corresponding to stages that last < 1 year
#       - Unoccupied sites are indicated by N1-Nx=0


#######################################################################################
###########    II. Create distance and dispersal probability matrices     ###########
#######################################################################################

# Alternative 1: read in previously calculated dispersal matrix
#       This alternative is preferred under most circumstances

disp.matrix=read.csv('Drive:/Directory/Sub_Directory/DispersalFile.csv',header=T, sep=",")

# Alternative 2: calculate dispersal based on distance between site locations
#       This alternative is justified for landscapes with small patches
#       relative to distances between them and a uniform landscape between patches.
#       It may also be a useful approximation when there is little information about dispersal.

#create empty matrices with rows and columns for each site in the landscape
dist.matrix= disp.matrix=matrix(0,nrow=pop.count, ncol=pop.count)
#       creates the matrix variable: disp.matrix[from, to]

#calculate Euclidean distances between sites and feed into dispersal formula
for(i in 1:pop.count){
  for (ii in 1:pop.count){
    dist.matrix[i,ii]=sqrt((Landscape$UTME[i]-Landscape$UTME[ii])^2 + (Landscape$UTMN[i]-
Landscape$UTMN[ii])^2)
}}

#Translate distances into dispersal likelihood using exponential decay model
# with decay parameter alpha
disp.matrix=exp(-alpha*dist.matrix)
# Divide dispersal formula results by sum to get destination probabilities.
#       This step results in the  home site being the most likely destination so that emigration
rates
#       are determined implicitly depending on patch arrangement
for(i in 1:pop.count){
disp.matrix[i,]=disp.matrix[i,]/sum(disp.matrix[i,])}
```

```
# Optional additional for loop if only emigrants considered
for(i in 1:pop.count){
disp.matrix[i,i]=0
disp.matrix[i,]=disp.matrix[i,]/sum(disp.matrix[i,])}
# Replace NaN that may arise for extremely isolated sites do not send migrants to other patches
disp.matrix[disp.matrix=="NaN"]=0

# Create cumulative probability matrix to facilitate random draw
c.disp.matrix=disp.matrix
for(i in 2:pop.count){
 c.disp.matrix[,i]=c.disp.matrix[,i-1]+c.disp.matrix[,i]
} # end for(i)
# Migration rates to different nonbreeding sites may be estimated using the same techniques.
Because
# nonbreeding sites will typically be different than breeding sites it may be easier to calculate
# migration rates outside of the SEED model and read in a migration matrix using the read.csv
function.
###########################################################################################
############# III. Define tracking variables                          ############
###########################################################################################
# Create data frame with 4 columns corresponding to gcm index, year, site.id, and population N.
If multiple
# stages are being censused then the fourth column would be the number of individuals in the
first tracked stage
# and additional columns will be needed corresponding to the additional stages N2-Nx.
gcm.count=20                              #of gcm models included
yr.count=45                               #of years projected to get to 2050
pop.count=length(Landscape$site.id)   #counts the number of populations in the landscape
GCM=rep(1:gcm.count, each=yr.count*pop.count)

YR=rep(2006: 2006+yr.count-1, each=pop.count)
POP=rep(Landscape$site.id, gcm.count*yr.count)
SEED.OUTPUT=data.frame(GCM,YR, POP)
SEED.OUTPUT$N=0                           #This would be N1 and repeated for N1-Nx if multiple stages
tracked
# Record initial population size (by stage if appropriate) in the tracking data frame
for(i in 1:pop.count){
 SEED.OUTPUT$N[SEED.OUTPUT$YR==2006 & SEED.OUTPUT$POP==Landscape$site.id[i]]=Landscape$N[i]
# repeat this line as necessary if multiple stages are to be tracked
} # end for(i)

###########################################################################################
#############                IV. Define life history functions            ############
###########################################################################################
#This section will look different for each species, depending on the species life history,
# how it responds to variation in climate variables, social structure, density dependence etc.
# The section comprises several functions that calculate those vital rates that are climate-
dependent
# or that change from year to year or site to site for non-climate reasons (e.g., density
dependence).
#Generalized examples follow, assuming each vital rate is a linear function of:
#       - 2 site-specific parameters: ncvar1, ncvar2
#       - 2 climate variables: clim.var1, clim.var2 (e.g., annual rainfall, mean temperature
during relevant time)
#       - one general climate relationship where the climate variable is multiplied by alpha
#       - one site-specific relationship where the climate variable is multiplied by ncvar2
#The lines of each function are:
#       -Function name and input variables ending in opening bracket {
#       -Linear equation using the input variables
#       -(Optional) Multi-step functions
#       -(Optional) Inverse transformation yielding real vital rate
#       -Closing bracket }
###### Fecundity (seeds/plant; eggs/female; young/litter)
fecundity.function=function(ncvar1, ncvar2, clim.var1, clim.var2){
   fecundity=ncvar1+alpha*clim.var1+ncvar2*clim.var2
}
#Alternative fecundity function for stage-based fecundity
#       This function first calculates the fecundity for each stage class as a linear function
#       of the climate variable clim.var1 with stage-specific link parameters class.var.vector.
#       The stage specific fecundity values are then weighted by the proportion of the population
#       in each class (p_class_vector), and the weights are summed to yield a weighted average
fecundity for
#       the population.
fecundity.function=function(p.class.vector, ncvar1, class.var.vector, clim.var1){
   fec.vector=rep(0,length(class.var.vector))
   for(i in 1:length(class.var.vector)){
     fec.vector[i]=ncvar1+class.var.vector*clim.var1
   } #end for(i)
   weight.vector=fec.vector*p.class.vector
   fecundity=sum(weight.vector)
```

142

```
}

#Imposes logistic-like reduction in fecundity with increasing population size
fecundity.density.dependence=function(fecundity, N, K){
    fecundity=fecundity*(max(0, 1-N/K))
}
###### Survival of first stage (e.g., seed germination rates, egg hatch rates)
stage1.surv.function=function(ncvar1, ncvar2, clim.var1, clim.var2){
    stage1.surv= ncvar1+ alpha*clim.var1+ncvar2*clim.var2
    stage1.surv=exp(stage1.surv)/(1+exp(stage1.surv)) #inverse logistic transformation for
survival rates
}

###### Survival of time-dependent second stage (e.g., caterpillar or tadpole survival)
#Part 1: Climate-dependent timing (e.g., temperature dependent development rate)
#        In this example, the day of year that an event occurs is modeled as a linear function of
some climate
#        climate variable, with a site-specific baseline (baseline.day + ncvar1).
phenol.function=function(ncvar1, climate.var.1)
    phenology.var=baseline.day+ncvar1+alpha*climate.var.1
}
#Part2: Vital rate function of climate and phenology.
#        In this example, we assume the phenology variable is the stage length in days for which
survival is
#        calculated
stage2.surv.function=function(ncvar1, phenology.var, clim.var1){
    daily.surv= ncvar1+alpha*clim.var1
    daily.surv=exp(daily.surv)/(1+exp(daily.surv)) #inverse logistic transformation for survival
rates
    stage2.surv=daily.surv^phenology.var
}
###### In this example we assume that the phenology variable determines the week of the year in
which a stage
#        starts and that climate variables clim.var1, clim.var2 etc. are weekly values of the
        relevant climate
#        variable
stage3.surv.function=function(ncvar1, phenology.var, clim.var1, clim.var2, clim.var3, clim.var4,
clim.var5, clim.var6){
climate.vector=c(clim.var1, clim.var2, clim.var3, clim.var4, clim.var5, clim.var6)
start.week=base.week+floor(phenology.var/7)
run.s=1
for(i in start.week:6){
  week.surv=ncvar+alpha*climate.vector[i]
  week.surv=exp(week.surv)/(1+exp(week.surv))
  run.s=run.s*week.surv
} #end for(i)
stage3.surv=run.s
}
###### In this example we assume that the phenology.var.1 determines the week of the year in
which a stage
#        starts and that phenology.var.2 determines the week of the year in which a stage ends.
Both variables
#        are assumed to already be in units of one week. As above, climate variables clim.var1,
clim.var2 etc. #        are weekly values of the relevant climate variable.
stage3.surv.function=function(ncvar1, phenology.var.1, phenology.var.2, clim.var1, clim.var2,
clim.var3, clim.var4, clim.var5, clim.var6){
climate.vector=c(clim.var1, clim.var2, clim.var3, clim.var4, clim.var5, clim.var6)
start.week=base.week+phenology.var.1
end.week=start.week+phenlogy.var.2
run.s=1
for(i in start.week:end.week){
  week.surv=ncvar1, alpha*climate.vector[i]
  week.surv=exp(week.surv)/(1+exp(week.surv))
  run.s=run.s*week.surv
} #end for(i)
stage3.surv=run.s
}
###### Survival of adults
#        Here we assume only a single adult stage. For species with multiple adult stages (e.g.,
size classes),
#        the appropriate alternative(s) may be repeated using stage-specific parameters.
#Alternative 1: Survival estimated on annual scale
 adult.surv.function=function(ncvar1, ncvar2, clim.var1, clim.var2){
    adult.surv= ncvar1+ alpha*clim.var1+ncvar2*clim.var2
    adult.surv=exp(adult.surv)/(1+exp(adult.surv)) #inverse logistic transformation for survival
rates
}

#Alternative 2: Survival estimated on quarterly scale
adult.surv.function=function(ncvar1, clim.var.q1, clim.var.q2, clim.var.q3, clim.var.q4){
climate.vector=c(clim.var.q1, clim.var.q2, clim.var.q3, clim.var.q4)
```

```
run.s=1
for(i in 1:4)
    quarterly.s=ncvar1+alpha*climate.vector[i]
    quarterly.s=exp(quarterly.s)/(1+exp(quarterly.s))
    run.s=run.s*quarterly.s
} #end for(i)
adult.surv=run.s
}
#Alternative 3: Survival of (partially) migratory species
#       -In this alternative we assume that some proportion of animals spend part of the year
#        at other, known, locations, and that the climate at these locations affects their
survival.
#        As in previous functions, ncvar1 relates to site-specific nonclimate
#        influences on survival and clim.var1 is a climate variable at the breeding site. The
#        ncvar2.vector and clim.var2.vector variables are assumed to be vectors with each entry
corresponding
#        to site specific nonclimate and climate related influences on survival at each potential
nonbreeding
#        site and the variable p.migrate.vector is the proportion of animals from the breeding
site being
#        evaluated when the function is called that spends the nonbreeding season at the
corresponding
#        nonbreeding site. The population level adult survival during the nonbreeding season is
taken as the
#        weighted average of the nonbreeding season survival at each nonbreeding site, weighted
by the
#        proportion migrating to each nonbreeding site.
adult.surv.function=function(ncvar1, ncvar2.vector, clim.var1, clim.var2.vector,
p.migrate.vector){
    breeding.s=ncvar1+alpha1*clim.var1
    breeding.s=exp(breeding.s)/(1+exp(breeding.s))
    nonbreeding.s.vector=ncvar2.vector+alpha2*clim.var2.vector
    nonbreeding.s.vector=exp(nonbreeding.s.vector)/(1+exp(nonbreeding.s.vector))
    nonbreeding.s.vector=p.migrate.vector*nonbreeding.s.vector
    nonbreeding.s=sum(nonbreeding.s)
    adult.s=breeding.s*nonbreeding.s
}

#Stage transitions (e.g., plant growth)
#       -This example assumes that individuals only move up stage-classes (e.g., they grow but
don't shrink)
#        with the probability of growing 0, 1,...K classes described by a negative exponential
distribution.
#        The probability distribution for growth from each stage to larger stages is calculated
in a separate
#        function, prob.function, called by the main growth.function. An alternative strategy
would be to use
#        a multinomial probability distribution with transition rates calculated outside of the
SEED model. The
#        vector p.class.vector contains the proportion of the population in each stage at the
start of the year.
#        The vectors ncvar1.vector and alpha.vector are used to calculate the stage-specific
transition rates
#        given the projected value of the single climate variable, clim1.var. The return variable
contains the
#        proportion of the population in each class after growth. New individuals entering the
smallest class
#        should be accounted for after the growth function is called.

prob.function=function(alpha, ncvar1, clim.var1, start.class, max.class){
    like=rep(0,max.class)
    for(i in start.class:max.class){
    like[i]=exp(-(ncvar1+alpha*clim.var1)*(i-start.class))}
    prob.vect=like/sum(like)
    } #end for(i)
}

growth.function=function(p.class.vector, ncvar1.vector, alpha.vector, clim1.var)
    new.p.class.vector=rep(0,length(p.class.vector))
    for(i in 1:length(p.class.vector){
    prob.vect=prob.function(alpha1[i],ncvar.vector[i], clim1.var, i, length(p.class.vector))
    for(ii in 1:length(p.class.vector){
    new.p.class.vector[ii]=new.p.class.vector[ii]+p.class.vector[i]*prob.vect[ii]
    } #end for(ii)
    } #end for(i)
    new.p.class.vector= new.p.class.vector/sum(new.p.class.vector)    #ensures new proportions sum
to 1
}
################################################################################
####            V.    Read in projected future climate conditions          ##########
################################################################################
```

```
# Use a separate .csv file for each climate variable used. In the examples below, we assume that
each
# pre-adult life stage is modeled as a function of two climate variables at the breeding site and
that adult
# survival is modeled as a function of two climate variables at the breeding site and one at the
nonbreeding
# site. Each file should contain the following columns: site.id, year, (optional)
quarter/month/week, climate
# data. There should be as many climate data columns as gcm projections used. Time labels are
assumed here to
# correspond to the period being predicted. That is, climate values for 2050 are used to
calculate vital rates
# that determine the population in 2050.
fecundity.clim.var1.data=read.csv('Drive:/Directory/Sub_Directory/Fecund.Climate.File1.csv',heade
r=T, sep=",")
fecundity.clim.var2.data=read.csv('Drive:/Directory/Sub_Directory/Fecund.Climate.File2.csv',heade
r=T, sep=",")
stage1.clim.var1.data= read.csv('Drive:/Directory/Sub_Directory/S1.Clim.var1.data.csv',header=T,
sep=",")
stage1.clim.var2.data= read.csv('Drive:/Directory/Sub_Directory/S1.Clim.var2.data.csv',header=T,
sep=",")
stage2.clim.var1.data= read.csv('Drive:/Directory/Sub_Directory/S2.Clim.var1.data.csv',header=T,
sep=",")
stage2.phenol.clim.var1.data=
read.csv('Drive:/Directory/Sub_Directory/S2.Clim.var2.data.csv',header=T, sep=",")
stage3.clim.var1.data= read.csv('Drive:/Directory/Sub_Directory/S3.Clim.var1.data.csv',header=T,
sep=",")
stage3.clim.var2.data= read.csv('Drive:/Directory/Sub_Directory/S3.Clim.var2.data.csv',header=T,
sep=",")
adult.breed.clim.var1.data=
read.csv('Drive:/Directory/Sub_Directory/AdBr.Clim.var1.data.csv',header=T, sep=",")
adult.breed.clim.var2.data=
read.csv('Drive:/Directory/Sub_Directory/AdBr.Clim.var2.data.csv',header=T, sep=",")
adult.nonbreed.clmate.data1=
read.csv('Drive:/Directory/Sub_Directory/AdNB.Climate.data.csv',header=T, sep=",")

###############################################################################################
#IV.    Loop through 45 years of population dynamics for present day and future climates    ######
###############################################################################################
#Intitiate loops to cycle through projections, years and populations
for(gcm.i in 1:20){                          #Start climate projection loop
for(time in 1:44) {                          #Start time loop with time=1 corresponding to 2007
Ad1.vector=rep(0,pop.count)    #Initialize or clear vector of young adults each year
for(pop in 1:pop.count){       #Start population (site) loop
# The inner loop runs through each population and updates population size from year to year.
There are a
# few decisions that have to be made here based on the life history of the species being modeled:
#     - What life stage(s) are counted? Often the youngest life stages are not included in
population
#       counts because they are hard to census (often true for seeds), exhibit the greatest
variability
#       from year to year due to high sensitivity of fecundity and juvenile survival to climate
and other
#       factors that tend to vary from year to year making it difficult to track population
trends or changes
#       in long term population growth trajectories, and/or have little reproductive value.
#     - When do population counts occur relative to breeding, migration, and dispersal? This
question is
#       related to the previous question as the timing of a population census may preclude the
inclusion
#       of the youngest life stage(s). SEED model output for specific populations will be most
useful to
#       managers if counts coincide with the most practical time to conduct population surveys
in the field,
#       but other factors need to be considered as well, such as which life stages are
influenced by
#       density dependence.
#     - When do life history events such as reproduction, dispersal, migration, and mortality
take place
#       relative to each other? This determines the order in which the life history functions
are called
#       and from which locations climate projections need to cover for each life stage.
#
# The example that follows corresponds to a long-lived species with two pre-adult life stages
occurring in
# the first year. Population censuses occur just prior to breeding. Dispersal happens after the
second
# stage, and individuals do not breed until they are second year of life. Consequently two adult
stages are
# tracked, one year olds, which do not breed, and >1 year old adults which breed. The example is
a single-sex
```

145

```
# model, which assumes that individuals of one sex (typically males) are capable of mating with
multiple members
# of the other sex to such a degree that their numbers never limit population-level reproduction.
Single-sex
# models also apply to self-pollinating plants and organisms that reproduce asexually.

# Calculate new individuals entering population due to reproduction as per-capita birth-rates*N2
adults
# Pull out site-specific variables ncvar1, ncvar2 from Landscape data frame, and site/year/gcm
specific
# climate variables clim.var1, clim.var2 from fecundity.clim.var1.data and
fecundity.clim.var2.data,
# respectively. In this example, we assume that the two climate variables have a single value for
each
# year (e.g., January precipitation, or the mean daily temperature averaged from June through
August)
# so that the columns of the corresponding data frames are: site.id, year, gcm1, gcm2... gcm.20.
ncvar1=Landscape$fec.ncvar1[pop]
ncvar2=Landacape$fec.ncvar2[pop]
clim.var1= fecundity.clim.var1.data[fecundity.clim.var1$site.id==Landscape$site.id[pop] &
fecundity.clim.var1$year==(time+2006), gcm.i+2]
clim.var2= fecundity.clim.var1.data[fecundity.clim.var2$site.id==Landscape$site.id[pop] &
fecundity.clim.var2$year==(time+2006), gcm.i+2]
Fecundity=fecundity.function(ncvar1, ncvar2, clim.var1, clim.var2)
S1=Fecundity*SEED.OUTPUT$N2[SEED.OUTPUT$GCM==gcm.i & SEED.OUPUT$POP==Landscape$site.id[pop] &
SEED.OUPUT$YR==(time+2005)]
# Calculate stage 1 survival, pulling the site-specific variables and climate variables as
described for
# fecundity.
ncvar1=Landscape$S1.ncvar1[pop]
ncvar2=Landacape$S1.ncvar2[pop]
clim.var1= stage1.clim.var1.data[stage1.clim.var1$site.id==Landscape$site.id[pop] &
stage1.clim.var1$year==(time+2006), gcm.i+2]
clim.var2= stage1.clim.var1.data[stage1.clim.var2$site.id==Landscape$site.id[pop] &
stage1.clim.var2$year==(time+2006), gcm.i+2]
S1.surv= stage1.surv.function(ncvar1, ncvar2, clim.var1, clim.var2)
S2=S1*S1.surv

# Calculate stage 2 phenology, pulling the site-specific variables and climate variables
# as described for fecundity.
ncvar1=Landscape$S2.phenol.ncvar1[pop]
clim.var1= stage2.phenol.clim.var1.data[stage1.clim.var1$site.id==Landscape$site.id[pop] &
stage2.phenol clim.var1$year==(time+2006), gcm.i+2]
stage.length=phenol.function(ncvar1, clim.var1)

# Calculate stage 2 survival, pulling the site-specific variables and climate variables
# as described for fecundity.
ncvar1=Landscape$S2.ncvar1[pop]
clim.var1= stage2.clim.var1.data[stage1.clim.var1$site.id==Landscape$site.id[pop] &
stage2.clim.var1$year==(time+2006), gcm.i+2]
S2.surv=stage2.surv.function(ncvar1, stage.length, clim.var1)
Ad1=S2*S2.surv
# Calculate adult survival, pulling the site-specific variables and climate variables
# as described for fecundity except that survival is tracked quarterly, so there the
# climate variables have a value for each quarter, and the projected values for the first
# gcm are in the fourth column (the third column indicating the corresponding quarter). This call
matches
# Alternative 2 for the adult survival functions.
# Create vector of adults in each stage from recorded population size in SEED.OUT in previous
time step
adults.start=(SEED.OUTPUT$N1[SEED.OUTPUT$GCM==gcm.i & SEED.OUPUT$POP==Landscape$site.id[pop] &
SEED.OUPUT$YR==(time+2005)], SEED.OUTPUT$N2[SEED.OUTPUT$GCM==gcm.i &
SEED.OUPUT$POP==Landscape$site.id[pop] & SEED.OUPUT$YR==(time+2005)])
ncvar1=Landscape$Ad.ncvar1[pop]
clim.var.q1=adult.breed.clim.var1.data[adult.breed.clim.var1$site.id==Landscape$site.id[pop] &
adult.breed.clim.var1$year==(time+2006) & adult.breed.clim.var1$quarter==1, gcm.i+3]
clim.var.q2=adult.breed.clim.var1.data[adult.breed.clim.var1$site.id==Landscape$site.id[pop] &
adult.breed.clim.var1$year==(time+2006) & adult.breed.clim.var1$quarter==2, gcm.i+3]
clim.var.q3=adult.breed.clim.var1.data[adult.breed.clim.var1$site.id==Landscape$site.id[pop] &
adult.breed.clim.var1$year==(time+2006) & adult.breed.clim.var1$quarter==3, gcm.i+3]
clim.var.q4=adult.breed.clim.var1.data[adult.breed.clim.var1$site.id==Landscape$site.id[pop] &
adult.breed.clim.var1$year==(time+2006) & adult.breed.clim.var1$quarter==4, gcm.i+3]
adult.surv=adult.surv.function(ncvar1, clim.var.q1, clim.var.q2, clim.var.q3, clim.var.q4)
adults=adults.start*adult.surv
# Number of >1 yr old adults is set to number adults in both stages that survive rounded to
nearest integer
# and recorded in appropriate entry of SEED.OUTPUT
SEED.OUTPUT$N2[SEED.OUTPUT$GCM==gcm.i & SEED.OUPUT$POP==Landscape$site.id[pop] &
SEED.OUPUT$YR==(time+2005)]=round(sum(adults))
# Number of 1 yr old adults depends on dispersal, so the next step is to record the number of Ad1
adults
```

146

```
# for each population.
Ad1.vector[pop]=Ad1
} #end for(pop)
# Track dispersal. In this example we assume dispersal Alternative 1.
Disp.matrix=Ad1*disp.matrix
# Sum over each source population the number of immigrants (or remaining 1 yr old adults) to get the
# total 1 yr old adults for each population and record in the appropriate entry of SEED.OUTPUT
for(i in 1:pop.count){
    tot.ad1=round(sum(Disp.matrix))
    SEED.OUTPUT$N2[SEED.OUTPUT$GCM==gcm.i & SEED.OUPUT$POP==Landscape$site.id[pop] &
SEED.OUPUT$YR==(time+2005)]=tot.ad1
} #end for(i)
} #end for(time)
} #end for(gcm)

#write output to file
write.csv(SEED.OUTPUT, "C:/directory/sub-directory/filename.csv")
```

8.6 **Appendix 8.6** Snowy plover migration table. Values are the expected proportion of individuals migrating from a given site to each potential overwinter site. Site abbreviations listed below table.

From \to	TE	BL	CP	BC	SRI	ML	DB	VS	PB	MBB	SS	PS	ML	HMB	WS	PR	MB	ER	CB	HL	B	CoB	SRS	MiB
TE	0.837	0.019	0.018	0.015	0.014	0.014	0.012	0.011	0.010	0.009	0.008	0.006	0.006	0.004	0.004	0.004	0.002	0.002	0.001	0.001	0.001	0.001	0.001	0.000
BL	0.016	0.837	0.018	0.016	0.014	0.014	0.012	0.011	0.010	0.009	0.008	0.007	0.006	0.004	0.004	0.004	0.002	0.002	0.001	0.001	0.001	0.001	0.001	0.000
CP	0.014	0.017	0.837	0.016	0.015	0.014	0.013	0.012	0.010	0.009	0.008	0.007	0.006	0.005	0.005	0.004	0.002	0.002	0.001	0.001	0.001	0.001	0.001	0.000
BC	0.012	0.014	0.015	0.837	0.015	0.015	0.013	0.012	0.011	0.010	0.009	0.007	0.006	0.005	0.005	0.004	0.003	0.002	0.001	0.001	0.001	0.001	0.001	0.000
SRI	0.010	0.012	0.013	0.015	0.837	0.016	0.014	0.013	0.012	0.010	0.009	0.008	0.007	0.005	0.005	0.004	0.003	0.002	0.002	0.001	0.001	0.001	0.001	0.000
ML	0.010	0.012	0.012	0.014	0.016	0.837	0.015	0.013	0.012	0.011	0.010	0.008	0.007	0.005	0.005	0.004	0.003	0.002	0.002	0.001	0.001	0.001	0.001	0.000
DB	0.009	0.010	0.011	0.013	0.014	0.014	0.837	0.015	0.013	0.012	0.010	0.008	0.007	0.006	0.006	0.005	0.003	0.002	0.002	0.002	0.001	0.001	0.001	0.000
VS	0.008	0.009	0.010	0.011	0.013	0.013	0.014	0.837	0.014	0.013	0.011	0.009	0.008	0.006	0.006	0.005	0.003	0.002	0.002	0.002	0.001	0.001	0.001	V.000
PB	0.007	0.008	0.009	0.010	0.011	0.012	0.013	0.014	0.837	0.014	0.013	0.010	0.009	0.007	0.007	0.006	0.004	0.002	0.002	0.002	0.001	0.001	0.001	0.000
MBB	0.006	0.008	0.008	0.009	0.010	0.011	0.012	0.013	0.014	0.837	0.014	0.011	0.010	0.008	0.008	0.006	0.004	0.003	0.002	0.002	0.001	0.001	0.001	0.000
SS	0.006	0.007	0.007	0.008	0.009	0.010	0.011	0.012	0.013	0.014	0.837	0.013	0.011	0.009	0.009	0.007	0.005	0.003	0.003	0.003	0.001	0.001	0.001	0.000
PS	0.005	0.006	0.006	0.007	0.008	0.008	0.009	0.010	0.011	0.012	0.014	0.837	0.015	0.011	0.011	0.009	0.006	0.004	0.003	0.003	0.002	0.002	0.001	0.001
ML	0.004	0.005	0.006	0.006	0.007	0.007	0.008	0.009	0.010	0.011	0.012	0.015	0.837	0.013	0.013	0.011	0.007	0.005	0.004	0.004	0.002	0.002	0.002	0.001
HMB	0.004	0.004	0.004	0.005	0.006	0.006	0.006	0.007	0.008	0.009	0.010	0.012	0.014	0.837	0.018	0.015	0.010	0.006	0.005	0.005	0.003	0.002	0.002	0.001
WS	0.004	0.004	0.004	0.005	0.006	0.006	0.006	0.007	0.008	0.009	0.010	0.012	0.014	0.018	0.837	0.015	0.010	0.006	0.005	0.005	0.003	0.002	0.002	0.001
PR	0.003	0.004	0.004	0.005	0.005	0.005	0.006	0.006	0.007	0.008	0.009	0.011	0.012	0.016	0.016	0.837	0.013	0.008	0.007	0.007	0.004	0.003	0.003	0.001
MB	0.002	0.003	0.003	0.003	0.004	0.004	0.004	0.005	0.005	0.006	0.007	0.008	0.009	0.012	0.012	0.015	0.837	0.015	0.013	0.012	0.007	0.006	0.005	0.002
ER	0.002	0.002	0.002	0.002	0.003	0.003	0.003	0.003	0.004	0.004	0.005	0.006	0.007	0.009	0.009	0.011	0.016	0.837	0.021	0.020	0.011	0.010	0.008	0.003
CB	0.001	0.002	0.002	0.002	0.002	0.002	0.003	0.003	0.003	0.004	0.004	0.005	0.006	0.008	0.008	0.009	0.014	0.022	0.837	0.024	0.013	0.011	0.010	0.004
HL	0.001	0.002	0.002	0.002	0.002	0.002	0.003	0.003	0.003	0.004	0.004	0.005	0.006	0.007	0.007	0.009	0.014	0.021	0.024	0.837	0.014	0.012	0.011	0.004
B	0.001	0.001	0.001	0.001	0.002	0.002	0.002	0.002	0.002	0.002	0.003	0.003	0.004	0.005	0.005	0.006	0.009	0.014	0.017	0.018	0.837	0.028	0.024	0.009
CoB	0.001	0.001	0.001	0.001	0.001	0.002	0.002	0.002	0.002	0.002	0.003	0.003	0.004	0.005	0.005	0.006	0.009	0.013	0.015	0.016	0.030	0.837	0.029	0.011
SRS	0.001	0.001	0.001	0.001	0.001	0.001	0.002	0.002	0.002	0.002	0.002	0.003	0.003	0.004	0.004	0.005	0.008	0.013	0.015	0.015	0.028	0.032	0.837	0.014
MiB	0.001	0.001	0.001	0.001	0.001	0.001	0.001	0.002	0.002	0.002	0.002	0.003	0.003	0.004	0.004	0.005	0.007	0.011	0.013	0.014	0.025	0.028	0.033	0.837

Abrev.	Site
TE	Tijuana Estuary
BL	Batiquitos Lagoon
CP	Camp Pendleton
BC	Bolsa Chica
SRI	Santa Rosa Island
ML	Mugu Lagoon
DB	Devereaux Beach
VS	Vandenberg South
PB	Pismo Beach
MBB	Morro Bay Beach
SS	San Simeon
PS	Point Sur
ML	Moss Landing
HMB	Half Moon Bay
WS	Warm Springs
PR	Point Reyes
MB	MacKerricher Beach
ER	Eel River Gravel Bars
CB	Clam Beach
HL	Humboldt Lagoons
B	Bandon
CoB	Coos Bay
SRS	Siltcoos River Spit
MiB	Midway Beach

8.7   Appendix 8.7 Tadpole stage lengths (days from hatching to metamorphosis) predicted at each site each year for the 20 climate projection models (see Appendix 8.1). Site labels are abbreviated as follows, first letter: C = coastal, I = inland; second letter; C = CRLF, H = Hybrid, N = NRLF.

		Climate Models																		
sites	year	1	2	3	4	5	6	7	8	9	10	11	12	13	14	15	16	17	18	19	20
CN3	2006	93.5	93.5	90.6	91.8	92.9	92.0	93.5	91.1	92.8	93.6	93.7	95.3	90.4	94.1	92.9	94.0	96.2	94.9	94.5	94.0
CN3	2007	90.9	95.6	91.0	93.4	93.8	94.2	93.1	94.8	95.9	95.3	95.1	94.4	93.4	91.6	94.2	94.7	93.8	94.8	94.4	93.5
CN3	2008	94.0	95.2	93.0	94.4	96.4	93.8	93.5	94.5	93.8	96.2	92.6	95.4	94.7	95.9	95.5	94.5	94.4	95.4	94.4	93.3
CN3	2009	92.0	91.1	91.4	92.8	93.7	92.6	93.8	94.1	94.7	92.6	93.2	94.8	93.1	95.5	94.2	92.2	93.1	94.7	94.9	93.2
CN3	2010	94.7	94.2	93.3	91.4	92.4	92.6	95.0	94.8	94.9	93.9	92.9	94.8	92.5	94.6	94.1	94.0	93.4	95.2	94.2	93.5
CN3	2011	95.0	93.0	93.7	91.7	94.3	93.1	94.7	93.2	96.3	94.3	93.8	94.8	94.1	95.2	94.2	95.5	95.0	94.2	94.2	93.3
CN3	2012	89.4	93.9	92.2	92.5	94.8	93.0	93.6	94.2	94.0	92.2	92.4	94.4	95.2	95.1	94.2	92.6	94.6	95.3	95.6	93.3
CN3	2013	95.3	92.1	93.0	93.7	94.5	93.9	93.5	93.5	92.5	90.3	94.5	93.6	93.6	93.9	94.0	93.9	91.9	93.7	93.2	94.1
CN3	2014	91.3	94.3	93.1	94.2	91.4	90.9	93.2	92.5	93.6	92.9	94.1	94.0	95.0	93.8	92.8	94.9	95.9	94.2	95.1	94.4
CN3	2015	95.3	94.4	91.0	92.4	89.4	95.6	94.3	92.6	92.8	91.4	93.8	95.3	94.9	92.5	94.2	96.6	94.7	96.2	94.3	93.1
CN3	2016	91.7	93.2	91.8	94.3	93.8	94.4	93.1	95.6	93.8	92.6	94.7	95.1	93.1	92.5	95.4	95.3	93.2	93.9	92.8	93.5
CN3	2017	92.2	92.8	92.5	93.5	90.9	92.4	95.9	94.5	93.7	95.2	92.2	93.6	92.8	93.3	92.7	93.9	91.1	93.4	93.7	95.0
CN3	2018	93.0	93.6	91.5	92.2	93.6	94.6	92.8	95.1	93.9	95.5	92.9	92.9	92.4	94.2	95.1	93.4	94.0	93.0	95.5	93.6
CN3	2019	93.8	93.5	95.0	92.1	91.3	94.4	93.2	94.1	95.6	94.0	94.5	94.3	92.2	94.3	94.4	92.3	95.3	92.6	94.6	94.9
CN3	2020	92.3	93.3	92.3	93.4	95.1	93.5	92.3	94.0	93.4	94.7	93.0	94.4	93.9	92.1	95.0	91.5	93.7	95.2	94.1	92.3
CN3	2021	94.0	95.4	90.2	92.1	95.1	95.7	93.7	92.7	94.5	93.5	96.1	92.7	92.4	93.8	92.9	93.8	94.2	93.5	95.7	92.9
CN3	2022	95.2	91.6	91.9	93.1	92.6	94.2	93.3	93.3	92.9	94.6	91.7	93.9	94.3	93.3	94.2	94.0	93.5	93.5	94.4	94.0
CN3	2023	92.4	92.3	91.5	92.6	92.4	92.2	93.7	92.7	93.1	91.6	91.9	92.0	93.1	93.3	93.0	95.7	91.1	93.9	94.9	95.3
CN3	2024	95.2	94.1	90.4	90.9	96.0	93.4	94.0	93.6	95.5	94.0	91.0	94.5	92.8	93.7	93.0	94.4	95.6	94.6	92.2	93.1
CN3	2025	92.2	93.9	90.8	92.4	92.5	91.1	92.4	92.6	94.0	92.4	93.7	93.9	94.1	91.7	94.2	94.5	94.1	89.8	94.3	94.0
CN3	2026	92.1	93.7	93.3	93.2	92.8	93.3	94.3	94.6	94.5	93.7	92.6	95.3	92.3	92.9	91.6	94.9	94.3	91.8	93.9	91.3
CN3	2027	93.0	93.1	91.9	93.7	95.9	93.2	93.8	95.2	93.5	93.4	91.5	93.7	93.5	92.3	93.9	94.9	94.3	92.4	94.5	93.8
CN3	2028	93.5	92.5	92.3	93.4	95.2	94.6	93.7	94.0	92.6	94.7	93.8	94.8	92.2	89.8	94.7	92.2	90.7	93.0	95.4	92.9
CN3	2029	91.9	91.1	93.8	93.1	91.8	92.0	93.7	94.5	94.3	95.6	94.5	93.7	91.7	92.3	95.0	93.9	93.2	92.4	92.5	94.0
CN3	2030	93.0	94.7	93.2	91.3	92.7	93.0	94.4	90.8	92.7	94.4	93.7	94.6	93.1	92.5	96.1	94.5	92.4	93.7	95.2	93.5
CN3	2031	93.0	92.3	93.7	91.3	95.1	93.0	94.3	93.4	93.1	93.3	95.8	93.9	93.6	92.2	95.0	94.6	92.7	92.3	91.9	92.3
CN3	2032	94.6	96.5	91.7	93.5	93.7	94.2	95.9	94.3	93.3	93.4	90.3	93.3	91.5	92.8	91.4	94.8	95.2	92.3	94.3	92.4
CN3	2033	93.8	94.0	95.5	92.2	92.5	94.0	95.3	97.0	93.0	92.8	93.6	93.7	91.0	93.0	94.6	93.6	92.9	94.1	93.9	94.5
CN3	2034	91.2	90.8	90.4	92.6	95.5	92.2	94.2	92.9	94.2	94.2	91.2	94.0	93.5	93.1	91.3	93.2	92.2	92.6	95.2	94.9
CN3	2035	92.3	92.2	90.9	94.3	94.0	93.5	94.0	91.5	94.7	93.0	91.4	93.8	92.5	92.6	93.1	93.9	93.5	93.4	94.5	91.7
CN3	2036	93.2	90.2	89.0	93.7	93.0	92.6	93.2	95.7	90.5	93.9	91.9	94.6	95.6	91.5	93.1	93.5	93.8	94.1	94.0	91.6
CN3	2037	93.2	94.7	92.7	91.3	91.9	91.8	92.8	94.3	92.9	94.2	92.8	93.4	92.3	93.2	94.9	93.6	91.4	91.8	91.4	93.6
CN3	2038	93.1	93.8	91.6	93.3	94.1	93.1	92.9	94.1	94.2	91.8	91.9	94.5	93.3	90.5	92.4	92.3	92.7	95.1	93.1	92.1
CN3	2039	91.8	96.0	92.1	93.0	93.6	93.1	93.8	94.1	96.6	91.3	92.3	93.7	93.7	93.5	93.4	94.1	89.9	93.3	93.9	93.6
CN3	2040	93.7	93.1	92.0	92.7	91.8	93.8	93.4	94.0	91.4	92.2	92.2	94.4	93.1	92.8	91.9	92.8	90.9	92.0	95.8	93.8
CN3	2041	92.7	92.3	93.7	91.2	93.9	93.0	93.2	92.8	90.2	93.1	94.1	93.5	91.7	92.9	93.6	92.1	90.9	94.5	94.2	
CN3	2042	92.8	92.1	90.0	91.4	91.7	93.6	91.7	93.3	93.6	92.7	95.2	93.6	94.9	90.6	92.9	93.0	92.6	91.1	93.6	94.4
CN3	2043	93.4	91.6	90.4	93.1	92.9	95.2	92.0	92.2	93.0	90.6	93.0	94.2	92.1	92.1	93.4	92.7	92.3	93.2	94.8	94.0
CN3	2044	92.6	92.8	93.8	93.8	91.5	94.4	94.4	92.0	91.4	94.3	94.2	93.7	91.4	93.0	93.8	92.3	93.0	93.0	94.1	93.9
CN3	2045	91.7	93.8	93.9	92.2	92.7	92.0	91.1	91.0	92.0	92.2	93.7	92.9	92.2	92.3	92.2	93.0	92.5	92.9	94.7	91.8

CN3	2046	92.6	91.1	92.5	91.1	93.1	92.4	92.2	92.1	92.6	93.5	91.9	94.0	91.4	92.2	92.7	93.4	91.9	93.8	94.2	93.7
CN3	2047	91.4	91.7	90.8	90.7	92.9	92.3	89.8	95.1	92.6	92.4	92.3	93.1	91.3	92.0	93.9	91.8	92.1	92.5	92.9	94.5
CN3	2048	92.8	93.0	91.0	91.7	90.6	94.0	92.4	91.8	92.7	93.2	91.7	93.0	92.0	93.2	92.4	92.9	93.4	92.9	93.9	94.5
CN3	2049	90.4	93.6	92.3	91.3	93.5	92.3	94.9	91.6	92.0	93.7	91.8	93.6	90.8	92.5	91.8	93.4	90.8	92.4	93.7	92.9
CN3	2050	94.8	93.3	91.7	92.0	91.5	94.5	93.4	93.5	92.7	92.9	92.4	93.0	90.6	92.5	92.6	93.7	92.9	93.4	95.0	93.2
IN2	2006	125.0	123.6	124.7	124.9	125.0	124.7	125.8	125.4	122.9	124.5	124.7	123.5	123.8	125.2	123.8	124.1	124.2	122.8	126.3	124.7
IN2	2007	124.1	122.5	122.6	124.5	125.7	124.2	123.6	122.7	123.9	124.8	126.1	123.1	125.2	123.1	124.2	125.1	126.5	124.4	123.2	123.6
IN2	2008	123.7	123.6	124.3	124.2	124.0	124.4	125.2	123.9	125.3	122.7	124.2	124.2	124.1	124.1	124.7	122.5	124.4	123.8	123.6	123.0
IN2	2009	124.1	124.9	126.6	123.9	124.6	124.6	125.3	122.7	123.0	123.8	123.8	124.4	123.3	123.1	126.0	123.8	122.9	124.9	124.1	122.4
IN2	2010	124.6	125.0	125.2	123.8	124.7	125.8	123.6	125.5	123.4	122.9	124.8	123.5	123.4	123.6	123.3	123.9	124.3	124.5	122.5	123.2
IN2	2011	125.3	123.1	124.6	123.9	124.8	124.3	122.2	123.2	122.2	124.8	123.0	125.0	123.9	123.5	123.4	124.2	123.5	123.3	122.6	122.9
IN2	2012	125.6	124.2	127.1	122.9	125.9	123.3	122.9	124.4	124.4	126.0	123.4	123.3	124.3	125.7	124.3	122.4	124.5	122.6	125.8	123.9
IN2	2013	124.0	124.8	123.2	124.1	125.5	123.9	124.3	123.4	123.7	125.7	124.8	125.1	124.6	122.9	125.7	124.9	122.5	123.9	124.2	125.1
IN2	2014	122.2	123.9	124.6	124.6	123.5	123.7	123.9	123.0	123.6	123.1	125.9	124.0	123.5	127.8	122.2	123.5	125.3	123.5	123.7	122.9
IN2	2015	123.3	123.5	125.0	123.6	124.5	124.0	123.0	124.5	123.4	124.7	123.1	123.4	126.1	125.8	124.7	125.5	122.6	124.1	122.4	123.8
IN2	2016	122.7	123.1	121.8	123.6	123.7	123.4	123.0	122.4	125.2	124.2	123.5	124.7	123.6	126.4	126.0	123.5	125.1	126.1	123.9	124.1
IN2	2017	124.6	124.1	123.8	122.7	124.0	124.4	123.7	122.6	125.5	124.7	124.1	124.0	125.7	123.8	124.3	126.2	124.5	126.0	124.7	123.5
IN2	2018	124.2	124.1	123.5	125.2	124.9	124.8	122.0	123.4	124.0	125.1	123.4	126.7	122.4	122.8	124.0	124.4	125.0	123.7	125.8	125.2
IN2	2019	126.7	123.2	125.1	124.1	123.7	125.3	126.6	123.3	123.3	122.2	125.7	123.9	124.9	125.1	123.0	123.4	124.4	124.7	125.1	123.5
IN2	2020	124.2	123.7	124.9	125.9	124.9	126.2	123.4	122.8	124.2	122.4	124.8	123.4	123.4	124.1	122.9	124.3	125.8	126.2	124.4	122.8
IN2	2021	125.0	121.7	124.5	124.4	123.7	123.6	125.1	125.3	124.1	123.7	125.4	123.5	124.3	123.7	124.3	123.1	124.7	126.1	123.5	125.5
IN2	2022	122.5	124.7	122.0	123.5	124.3	123.8	125.8	123.8	126.6	123.7	123.7	122.0	124.6	122.5	125.6	123.0	123.4	124.7	122.4	124.5
IN2	2023	124.4	124.5	128.9	125.2	125.8	124.9	123.3	124.0	125.8	125.0	124.6	123.2	124.3	126.8	125.4	124.9	124.3	126.4	123.3	124.3
IN2	2024	124.2	123.1	124.0	124.7	126.4	124.6	124.3	124.9	125.6	126.1	123.2	125.4	125.0	123.1	123.1	125.4	124.0	122.6	123.4	123.0
IN2	2025	122.7	126.6	123.9	123.8	124.1	123.6	124.3	123.4	123.5	123.9	126.7	123.9	126.2	122.1	125.1	124.5	123.0	124.7	122.5	123.1
IN2	2026	124.1	122.6	125.1	125.7	124.5	124.6	125.1	123.6	124.0	124.4	127.0	124.8	125.8	123.2	123.6	124.5	125.4	125.9	123.7	123.0
IN2	2027	123.8	124.2	126.6	124.3	126.3	124.1	124.4	124.9	124.1	122.3	123.5	124.4	123.5	122.8	123.8	123.8	126.0	125.8	123.8	124.8
IN2	2028	124.7	124.9	124.4	124.1	124.6	123.2	123.8	123.5	124.6	122.6	125.7	124.6	122.9	122.3	124.1	124.3	124.6	122.2	124.1	124.3
IN2	2029	127.6	123.9	128.8	125.5	126.8	124.6	126.0	123.6	123.1	124.0	124.0	123.8	126.6	125.4	124.1	123.2	125.3	123.9	123.2	123.8
IN2	2030	122.7	124.1	124.8	124.9	121.9	125.0	125.4	122.7	126.2	126.0	122.8	125.9	123.9	125.8	124.1	123.6	125.2	124.4	124.1	123.6
IN2	2031	123.3	123.7	123.9	125.0	123.2	125.6	124.1	123.6	122.4	123.3	123.7	123.8	126.2	125.8	123.1	123.3	125.9	124.5	124.1	123.9
IN2	2032	123.9	125.6	123.2	125.5	127.4	123.9	122.4	125.1	124.2	123.4	122.4	123.7	124.1	125.1	124.0	124.5	125.1	123.8	126.5	123.3
IN2	2033	123.5	122.5	125.7	122.6	122.7	126.0	122.6	122.5	125.7	125.9	123.9	123.2	123.8	126.6	123.8	123.8	124.8	126.2	123.5	123.5
IN2	2034	124.6	123.2	125.2	125.2	123.3	123.3	123.0	124.3	127.0	126.0	124.4	122.8	125.2	125.4	123.5	124.2	127.3	124.4	124.4	125.8
IN2	2035	124.2	124.7	125.4	122.7	125.3	127.4	124.6	123.1	123.9	124.3	123.9	124.4	123.2	125.4	124.7	124.9	124.7	124.0	123.7	125.1
IN2	2036	125.9	124.5	122.2	125.8	124.5	128.3	126.6	123.2	121.4	123.5	124.4	122.8	127.2	123.7	122.7	125.4	124.7	124.2	124.4	124.5
IN2	2037	127.1	123.5	125.6	123.4	124.1	125.5	124.3	123.8	123.8	123.4	123.7	123.5	126.0	124.7	124.0	122.9	124.4	123.4	125.6	124.6
IN2	2038	124.4	125.3	126.1	123.8	124.4	125.4	123.9	126.9	125.2	126.7	124.6	122.4	124.1	123.6	124.8	126.5	129.5	124.4	124.0	123.8
IN2	2039	124.4	123.8	125.2	125.6	125.7	125.8	125.2	124.1	126.2	124.7	124.6	122.8	124.8	124.1	126.4	126.1	124.4	122.9	124.5	124.5
IN2	2040	125.2	123.6	123.9	124.6	124.6	124.2	124.6	124.0	123.6	124.6	123.3	125.5	126.9	126.6	125.9	125.3	123.3	125.0	124.8	125.8
IN2	2041	125.1	124.5	124.9	123.7	124.3	123.7	126.1	121.7	125.8	127.3	124.7	123.7	124.5	123.1	123.7	123.6	124.4	126.7	123.6	124.9
IN2	2042	125.2	124.4	122.5	123.7	126.1	125.5	125.1	123.5	124.5	125.7	124.3	124.6	124.6	125.3	125.5	128.4	124.2	122.9	123.3	
IN2	2043	124.8	124.4	124.2	124.5	125.1	125.3	124.8	122.9	123.9	122.8	125.8	124.6	124.1	123.9	125.8	124.9	125.3	126.0	125.0	124.3
IN2	2044	124.4	123.3	124.9	124.4	124.2	124.5	124.6	125.0	125.2	126.0	123.6	123.5	126.3	127.5	124.9	123.5	125.1	124.1	123.9	125.1
IN2	2045	124.5	126.6	125.3	123.3	124.8	124.6	126.8	125.3	123.6	127.8	127.9	122.6	123.7	123.6	126.1	122.8	124.4	126.5	124.7	124.9
IN2	2046	124.4	123.7	124.2	126.1	126.7	125.0	125.9	124.4	124.0	124.5	123.0	124.3	124.3	125.0	126.2	126.7	125.1	125.3	124.7	125.8
IN2	2047	123.4	124.8	126.1	124.4	124.2	126.7	124.9	126.0	125.5	125.3	124.3	123.1	126.3	124.6	126.8	123.6	123.1	126.4	124.1	123.8
IN2	2048	127.9	124.4	128.2	125.1	124.1	124.7	125.5	125.9	124.9	123.5	124.8	124.4	124.8	125.1	122.7	125.5	125.9	124.7	124.6	123.9
IN2	2049	123.2	125.3	126.6	124.7	124.7	122.8	126.7	122.5	126.4	125.2	125.2	123.2	125.4	125.3	125.0	125.3	126.4	125.1	125.1	124.8
IN2	2050	124.5	126.2	127.9	124.7	123.7	125.7	123.8	126.2	123.7	125.6	124.4	123.2	124.9	129.1	121.0	125.2	126.5	123.5	123.3	122.2

IN1	2006	126.9	125.5	126.6	127.6	126.6	126.7	128.5	126.9	124.5	126.6	126.1	125.8	126.1	127.4	125.5	126.6	126.1	125.4	127.9	126.3
IN1	2007	124.8	124.5	124.9	127.1	127.3	126.5	125.0	125.0	126.6	126.6	128.0	125.2	126.7	124.9	126.4	126.9	127.7	126.4	125.7	125.0
IN1	2008	124.8	125.3	126.3	126.0	124.9	126.1	127.3	125.4	127.6	125.0	126.2	125.8	125.4	125.5	126.4	124.0	126.2	125.7	125.4	125.3
IN1	2009	126.5	128.4	129.8	125.9	126.6	125.9	127.4	124.2	123.9	125.5	125.6	126.3	125.7	124.3	127.6	125.7	125.1	126.3	125.9	124.1
IN1	2010	126.3	126.9	127.2	125.5	125.9	128.0	125.8	127.2	124.9	124.6	126.2	126.2	125.2	125.5	125.3	125.6	126.4	126.2	124.5	125.1
IN1	2011	126.9	124.6	126.3	126.0	127.3	126.6	124.7	125.3	123.3	127.1	125.0	127.2	125.9	124.2	125.7	125.4	125.7	125.2	124.5	125.2
IN1	2012	127.6	126.8	128.9	124.1	128.0	124.7	124.9	126.4	126.4	128.0	124.5	125.2	126.2	128.9	127.0	124.4	126.1	124.5	128.9	127.2
IN1	2013	125.4	126.5	125.7	125.8	127.8	125.3	126.0	125.2	126.5	128.1	126.5	125.8	126.3	125.0	128.0	126.6	123.7	126.4	125.3	126.9
IN1	2014	124.5	125.9	127.0	126.0	125.3	125.6	126.3	124.8	126.2	125.0	128.1	125.0	124.4	129.9	124.0	126.0	126.9	125.2	125.3	123.9
IN1	2015	124.4	124.5	127.0	125.3	126.9	125.6	125.6	124.7	127.3	125.3	126.6	123.6	125.4	128.4	127.4	127.4	127.0	124.3	125.0	126.2
IN1	2016	124.4	125.4	124.1	125.7	125.9	126.0	124.7	124.6	127.8	126.8	125.1	125.7	126.2	128.7	127.6	124.7	127.6	128.5	126.2	125.6
IN1	2017	127.0	126.0	126.3	124.9	125.7	127.7	125.6	125.1	127.8	127.0	126.6	125.2	128.0	125.6	126.5	128.2	126.8	128.4	126.6	125.5
IN1	2018	126.7	125.6	125.4	127.6	127.1	127.1	124.6	125.5	126.6	125.7	129.1	125.6	124.3	125.7	126.4	127.9	125.5	128.8	124.4	127.1
IN1	2019	128.2	125.7	126.8	126.8	124.9	127.6	128.5	125.2	124.9	123.6	127.9	126.0	127.0	127.8	124.4	125.9	126.1	127.0	127.9	125.6
IN1	2020	126.3	125.7	126.9	129.0	126.4	128.3	125.4	124.3	126.7	124.1	126.5	125.5	124.8	126.0	124.4	126.9	128.4	127.3	126.4	125.0
IN1	2021	127.5	123.7	126.5	126.5	125.8	125.9	126.6	127.7	126.0	125.3	127.7	125.6	126.6	126.3	126.3	124.6	126.6	128.7	124.4	127.5
IN1	2022	124.5	126.8	124.0	126.3	126.2	125.6	128.0	125.5	129.1	126.1	125.5	123.2	126.0	123.6	127.8	124.3	125.8	127.0	124.2	126.8
IN1	2023	126.5	127.2	131.5	125.4	127.3	127.3	126.5	126.5	127.4	127.7	126.9	124.2	126.6	130.1	127.3	127.1	125.7	129.5	125.8	126.3
IN1	2024	126.0	124.8	127.2	127.6	128.8	127.1	125.8	126.0	127.0	128.3	126.0	127.2	127.1	125.5	124.6	126.9	125.9	124.5	125.8	124.9
IN1	2025	124.7	128.5	126.9	126.2	127.3	126.1	127.4	125.3	125.3	126.3	128.7	125.3	128.1	124.3	127.1	127.3	125.4	126.8	123.9	124.5
IN1	2026	126.9	124.0	126.8	128.1	125.8	126.0	126.5	125.6	125.7	126.3	128.5	127.1	128.5	125.4	125.9	126.5	127.3	128.2	124.4	125.3
IN1	2027	126.1	127.2	130.1	127.1	128.4	126.3	126.2	126.5	125.9	123.9	124.9	127.0	126.0	124.5	126.1	125.8	128.1	127.1	125.0	127.6
IN1	2028	126.1	126.7	126.6	125.9	126.9	125.5	126.2	125.5	127.0	124.1	127.7	126.8	124.8	124.2	125.5	126.3	127.0	124.5	126.5	126.0
IN1	2029	132.5	125.9	131.5	127.1	128.7	126.3	127.6	125.8	125.1	125.8	125.9	125.1	128.8	127.8	126.6	125.3	127.7	126.5	125.1	124.9
IN1	2030	124.4	125.9	126.7	127.2	124.2	127.0	127.8	125.5	127.9	128.2	125.0	127.5	126.6	128.0	126.4	126.4	127.2	126.1	125.5	125.7
IN1	2031	125.1	125.8	125.7	126.7	124.9	127.4	126.0	125.6	126.5	124.5	125.1	125.1	128.1	128.5	124.7	124.6	128.2	126.4	126.2	126.7
IN1	2032	126.4	127.1	125.6	128.2	128.7	125.5	123.6	126.7	126.3	125.9	125.4	125.4	126.9	127.2	125.8	126.2	127.3	126.1	129.3	125.0
IN1	2033	124.9	123.5	127.1	124.4	125.0	127.4	124.5	123.8	128.1	126.9	125.8	124.6	125.6	128.3	126.5	125.5	125.9	128.2	125.9	126.5
IN1	2034	127.0	125.9	126.5	128.0	125.7	124.8	125.4	126.4	127.8	127.7	127.8	124.9	128.1	127.8	125.2	126.5	130.1	127.3	126.8	127.2
IN1	2035	127.0	126.8	127.3	125.0	127.2	129.7	125.7	125.2	125.2	126.1	125.5	126.5	125.6	127.5	127.1	126.5	125.9	125.8	125.9	127.1
IN1	2036	128.1	127.0	124.8	128.0	126.1	130.4	128.7	125.0	123.3	125.9	126.7	125.1	129.5	126.0	124.8	127.6	126.6	126.6	126.2	126.4
IN1	2037	129.2	125.3	127.3	125.4	126.4	127.0	126.8	125.5	125.9	125.4	125.8	124.4	128.5	126.4	125.6	125.1	126.3	124.6	127.7	126.0
IN1	2038	125.6	127.4	128.8	125.3	126.5	127.7	125.9	129.3	126.5	129.3	127.1	124.9	126.7	126.0	127.3	129.2	131.3	126.7	125.4	125.7
IN1	2039	126.2	125.6	127.3	127.3	127.8	127.6	126.9	126.0	128.5	126.5	127.0	123.9	126.5	126.5	127.4	127.0	124.6	126.1
IN1	2040	126.8	126.0	126.3	126.9	126.7	125.9	125.8	126.0	125.7	126.4	125.6	127.3	128.7	128.7	127.8	128.2	124.9	127.3	126.4	127.2
IN1	2041	126.7	127.4	127.4	126.3	125.7	124.9	128.4	123.3	127.5	130.1	126.3	125.9	125.9	126.0	126.5	124.8	125.9	128.6	125.4	126.7
IN1	2042	128.3	126.4	124.1	126.3	127.8	128.7	126.6	124.7	125.8	128.7	125.3	127.3	127.4	129.1	127.0	127.4	131.6	126.3	125.1	124.8
IN1	2043	126.2	126.8	126.6	126.3	126.8	127.0	127.7	124.7	126.0	124.1	128.7	126.4	126.0	126.1	127.8	125.9	128.0	127.7	126.3	126.2
IN1	2044	126.8	125.3	126.2	126.2	125.4	126.0	126.8	127.7	126.8	127.9	125.6	125.1	129.4	129.5	126.9	125.8	126.9	125.6	125.9	127.2
IN1	2045	126.4	128.9	128.3	124.9	127.6	125.7	129.2	128.0	126.2	128.5	129.1	123.9	127.1	125.2	127.9	124.7	127.2	129.8	127.2	127.7
IN1	2046	126.3	125.5	126.4	128.4	128.7	127.1	129.4	126.1	125.8	126.9	125.9	125.6	126.6	126.6	127.6	127.7	128.3	127.2	127.5	127.4
IN1	2047	125.2	127.5	129.8	126.2	126.6	128.9	126.7	128.5	129.2	127.7	126.3	125.5	129.1	126.2	129.1	124.7	125.3	128.7	126.3	126.3
IN1	2048	130.1	125.8	131.0	127.9	125.7	127.2	127.4	129.0	127.1	125.1	127.8	127.3	126.8	127.4	124.4	127.5	128.4	126.5	127.4	125.7
IN1	2049	125.8	127.1	128.5	126.6	126.5	125.0	130.3	124.4	128.6	127.7	127.0	125.1	127.7	126.7	127.5	127.0	128.6	128.4	127.4	127.7
IN1	2050	126.0	127.9	129.5	127.2	126.1	126.9	124.8	128.6	125.7	128.5	126.9	125.5	126.8	131.7	123.1	127.5	128.9	125.0	125.4	124.2
IN3	2006	108.0	108.4	106.7	108.2	107.9	108.1	108.1	107.4	108.2	108.0	109.1	108.8	107.2	108.4	108.6	108.7	109.3	109.3	109.4	109.2
IN3	2007	107.5	108.1	105.8	107.9	109.5	109.1	109.0	108.4	110.1	109.9	108.7	108.2	108.8	106.3	108.1	108.9	109.6	108.6	108.7	107.9
IN3	2008	108.4	107.6	107.9	108.4	110.1	109.6	108.6	109.0	109.2	109.2	108.9	108.8	109.1	108.9	109.7	108.6	108.5	109.6	108.7	108.1
IN3	2009	107.4	107.3	107.4	107.9	109.6	107.9	109.3	108.1	108.9	107.6	107.2	109.1	108.1	108.4	110.0	106.5	108.0	109.9	109.1	108.3
IN3	2010	108.7	108.4	108.3	107.4	107.6	107.9	109.1	109.7	109.4	108.1	108.4	109.4	107.1	109.2	108.4	109.1	108.6	109.2	109.1	107.7

IN3	2011	109.7	107.9	108.8	107.3	108.6	108.4	108.8	108.6	109.5	109.0	108.4	109.0	108.5	109.3	108.8	110.0	109.0	109.1	108.9	108.1
IN3	2012	107.3	108.9	108.2	107.7	109.1	108.0	109.0	109.8	109.1	106.4	108.3	109.0	109.6	109.2	109.0	107.1	108.7	109.4	110.4	108.6
IN3	2013	109.1	107.5	108.4	108.6	108.6	108.4	108.5	108.1	108.0	106.0	108.8	108.2	108.0	108.2	108.5	108.7	107.7	108.6	108.2	108.5
IN3	2014	107.6	108.5	108.6	108.5	107.1	107.0	108.1	108.1	109.1	108.9	108.4	108.9	109.5	110.1	108.5	108.8	110.1	108.3	109.3	109.0
IN3	2015	109.1	107.6	107.4	107.8	107.6	109.6	108.3	108.2	107.7	107.8	107.5	109.4	110.2	108.6	109.1	110.5	108.9	110.7	108.4	107.8
IN3	2016	106.7	109.6	107.5	109.1	108.4	108.7	108.6	109.3	108.6	108.0	108.9	109.4	107.6	108.6	110.0	109.6	108.9	108.7	107.6	107.4
IN3	2017	107.2	108.4	107.5	107.8	107.3	107.7	108.4	108.1	109.0	109.4	107.4	108.5	107.7	108.7	108.1	108.3	107.5	108.7	108.8	108.8
IN3	2018	108.2	108.9	107.4	107.7	108.9	110.0	108.4	109.2	108.5	109.1	109.2	108.3	107.7	108.7	109.0	108.9	108.3	108.9	109.4	109.4
IN3	2019	108.7	109.2	109.7	107.4	107.8	110.0	109.6	108.9	109.2	107.9	109.1	108.4	107.9	108.8	108.9	106.9	109.4	108.9	109.2	109.1
IN3	2020	108.4	108.0	107.7	109.1	109.5	109.0	108.2	109.0	107.5	107.7	107.2	108.8	108.1	108.6	108.2	107.6	109.2	109.4	107.4	107.2
IN3	2021	108.8	108.2	106.9	108.0	108.3	109.0	108.3	108.2	109.1	108.4	110.3	107.6	108.2	108.4	107.7	108.7	108.9	109.4	109.6	107.8
IN3	2022	108.9	108.0	106.9	108.1	107.5	108.4	108.5	107.5	108.3	108.1	107.6	107.7	108.8	107.8	108.0	108.2	108.8	109.2	108.3	108.9
IN3	2023	109.7	108.7	109.0	107.6	109.6	108.5	108.3	108.2	108.1	108.5	107.5	108.0	107.9	109.3	108.1	109.2	106.3	110.0	108.7	109.3
IN3	2024	108.5	108.4	107.1	106.7	110.5	108.1	108.3	109.1	109.4	108.0	105.6	109.4	108.4	108.6	107.8	108.5	109.6	109.1	107.7	108.1
IN3	2025	107.6	108.7	107.1	107.5	108.4	106.6	108.4	107.9	108.1	108.4	109.6	108.1	108.9	107.4	109.2	109.2	108.4	105.6	108.9	108.0
IN3	2026	107.9	108.2	108.8	109.7	109.0	108.5	109.5	109.0	109.4	108.8	108.6	109.2	108.6	108.2	107.7	109.5	109.3	108.2	108.4	107.7
IN3	2027	108.2	108.4	108.4	108.1	110.7	108.3	108.4	110.2	108.5	108.4	107.2	108.4	108.6	107.3	108.3	109.3	109.6	108.9	108.4	108.7
IN3	2028	107.9	108.8	107.4	107.9	109.1	108.0	108.3	108.3	107.5	108.6	108.6	109.0	107.8	106.7	109.3	108.0	105.8	106.9	109.3	107.7
IN3	2029	107.8	108.1	110.6	109.0	108.9	108.1	109.2	108.7	109.3	108.7	108.3	107.9	107.8	108.4	108.9	107.9	107.4	108.7	107.9	109.1
IN3	2030	107.9	109.2	107.7	107.2	107.7	108.4	109.1	107.6	107.4	109.8	107.7	109.8	107.6	108.3	109.3	109.1	107.6	108.3	109.3	108.6
IN3	2031	108.0	108.6	108.5	107.0	109.4	107.8	108.3	108.9	108.6	108.1	109.9	108.9	109.0	108.1	109.3	108.7	108.0	108.5	107.6	109.4
IN3	2032	109.0	109.6	106.4	108.1	110.0	108.5	109.1	108.2	108.1	108.3	106.7	108.1	107.1	108.8	106.3	109.4	110.4	106.9	109.4	108.1
IN3	2033	107.6	107.8	110.1	106.8	107.8	108.4	108.5	109.8	109.3	108.4	108.2	108.3	107.3	109.5	108.8	108.2	108.6	108.8	108.8	108.8
IN3	2034	107.0	106.1	106.7	108.2	108.8	107.8	107.8	108.9	108.9	109.3	107.4	108.2	108.7	109.0	108.0	107.3	108.5	108.2	109.7	109.9
IN3	2035	107.3	109.0	107.0	108.7	108.0	108.9	108.6	107.1	109.4	107.8	108.1	109.3	106.9	108.6	107.3	109.5	109.2	108.1	109.0	107.5
IN3	2036	108.7	106.9	106.5	109.1	108.0	107.7	108.5	109.2	106.5	108.4	108.2	109.1	109.5	107.2	107.6	109.5	108.3	108.9	108.1	107.1
IN3	2037	109.7	107.8	108.4	107.8	107.7	106.7	108.1	108.4	107.3	108.8	108.9	107.8	108.1	109.1	109.3	108.6	107.2	105.9	106.5	109.1
IN3	2038	108.7	108.8	108.5	108.5	109.8	108.4	108.6	109.2	109.2	107.9	108.0	108.1	107.9	107.9	107.7	107.8	108.7	109.7	107.4	108.2
IN3	2039	107.8	109.3	108.3	108.3	109.4	107.6	109.6	108.4	110.6	106.6	108.0	108.1	109.6	109.8	108.4	108.0	107.4	107.6	108.5	108.1
IN3	2040	109.2	108.1	107.2	108.5	108.4	108.9	108.4	109.4	106.3	108.7	108.1	109.3	108.8	108.7	108.1	108.9	108.6	108.7	110.0	109.4
IN3	2041	108.6	107.3	108.3	106.6	108.7	106.7	109.3	108.8	108.1	107.9	108.3	107.7	108.4	107.0	108.5	108.2	107.7	106.9	108.4	109.5
IN3	2042	108.6	108.7	105.6	107.1	108.3	108.5	108.4	108.2	109.1	108.1	108.5	108.4	109.6	107.4	109.2	109.3	108.7	106.5	108.3	108.9
IN3	2043	108.9	107.3	106.3	108.1	109.0	109.3	106.4	107.6	107.7	106.7	107.9	109.4	108.4	107.8	107.8	108.3	108.1	109.0	108.6	109.4
IN3	2044	108.1	108.9	108.9	108.2	106.6	109.4	108.8	108.1	107.1	109.3	109.0	107.7	106.6	108.5	108.8	108.8	109.4	107.7	109.0	109.2
IN3	2045	107.8	109.6	109.1	108.0	108.0	108.2	107.9	107.2	107.6	109.9	110.4	108.1	107.3	108.6	108.7	107.3	107.9	109.1	109.5	107.9
IN3	2046	108.2	107.0	109.2	107.9	108.6	107.6	109.4	107.6	107.1	108.6	107.3	108.8	106.4	107.2	108.1	109.0	107.3	109.6	108.9	109.1
IN3	2047	108.0	108.4	107.8	106.7	108.0	108.8	108.0	109.5	107.8	108.7	107.4	107.9	107.4	107.7	108.2	107.5	107.7	108.5	107.1	108.7
IN3	2048	109.1	108.2	108.6	107.3	107.1	109.4	108.8	107.7	107.5	107.7	108.3	108.4	107.3	109.8	108.0	108.4	109.8	108.8	108.9	108.4
IN3	2049	106.6	109.2	108.9	108.9	109.0	108.3	108.6	107.1	107.7	109.3	109.1	108.7	106.6	109.2	107.2	109.8	107.1	108.0	109.0	108.8
IN3	2050	109.6	109.2	109.3	107.3	106.9	110.0	108.6	109.2	107.8	109.0	107.6	108.3	107.2	108.9	107.4	108.3	109.3	108.5	108.7	107.6
CH2	2006	125.2	123.4	123.8	123.7	123.9	124.5	126.5	123.7	122.6	124.8	124.7	123.4	125.1	124.1	123.3	124.6	124.2	124.5	124.7	124.0
CH2	2007	122.1	123.1	123.9	125.0	124.1	124.4	123.8	123.3	124.0	123.9	125.0	123.1	124.4	122.9	124.0	125.0	125.5	123.4	123.3	124.4
CH2	2008	123.2	123.5	122.7	124.2	124.3	123.7	125.4	124.4	125.0	124.0	124.2	123.7	123.0	123.7	125.1	123.3	123.5	123.8	123.8	124.3
CH2	2009	123.1	125.0	124.5	123.6	124.1	124.5	124.1	122.6	122.5	124.3	123.3	123.8	122.9	123.1	123.7	123.9	122.6	123.6	123.9	122.0
CH2	2010	124.2	124.1	124.4	124.6	125.2	124.1	123.8	124.9	123.1	124.0	123.7	123.5	124.2	123.5	123.2	122.5	123.8	124.0	121.9	122.9
CH2	2011	125.4	123.2	125.3	125.3	123.7	124.7	123.4	123.5	122.6	125.1	123.6	123.7	124.6	123.7	123.9	122.8	122.8	124.3	122.9	123.6
CH2	2012	125.4	124.5	126.9	123.0	123.6	123.4	123.8	123.8	123.2	124.4	124.0	123.4	122.8	125.5	123.7	123.1	124.9	123.1	124.7	124.3
CH2	2013	124.5	123.2	123.3	125.6	125.2	124.6	123.1	122.8	123.1	125.2	124.9	124.9	124.6	123.1	124.1	124.6	121.9	124.3	123.1	124.3
CH2	2014	122.9	123.3	125.3	123.7	122.8	123.3	123.5	122.7	125.1	122.5	125.1	123.4	123.1	125.5	121.9	123.7	124.5	121.4	122.7	123.3
CH2	2015	122.4	123.1	125.2	124.3	124.9	124.3	123.0	123.7	123.5	123.5	122.4	124.3	124.6	123.8	124.0	125.0	122.2	123.5	122.4	123.7

CH2	2016	123.5	123.7	122.6	124.0	123.1	123.1	122.9	123.1	124.5	123.6	123.4	125.3	123.2	124.8	124.1	123.2	124.1	124.2	124.0	124.2
CH2	2017	125.3	124.5	124.3	123.6	123.5	124.7	123.7	123.9	127.0	122.9	124.9	123.5	124.9	123.6	123.9	126.4	123.3	124.9	125.1	125.4
CH2	2018	124.6	124.8	123.5	125.6	124.5	124.4	122.3	124.0	124.7	124.0	125.3	123.6	124.2	123.7	124.1	125.5	123.9	124.7	121.9	126.1
CH2	2019	126.4	123.5	125.6	124.4	123.1	124.5	125.0	124.6	124.2	122.2	124.5	123.4	124.4	125.0	122.8	123.3	124.3	123.9	125.0	123.5
CH2	2020	125.1	123.6	125.7	126.0	124.3	124.9	123.5	124.2	123.3	122.8	124.7	124.2	123.7	124.8	122.7	125.4	124.9	124.4	123.5	123.2
CH2	2021	124.5	122.1	123.6	124.0	126.0	124.4	124.8	123.7	123.8	123.5	124.2	124.0	123.8	124.2	122.8	122.7	123.9	124.7	124.6	124.3
CH2	2022	122.5	126.1	122.1	123.4	124.1	123.3	125.8	123.9	124.9	123.4	124.0	122.5	123.6	123.3	124.1	123.1	123.6	123.9	124.0	125.8
CH2	2023	124.5	123.5	126.1	124.7	124.0	124.5	123.4	125.1	124.8	125.4	125.6	122.8	124.3	125.3	124.0	124.4	124.0	125.8	123.3	124.9
CH2	2024	124.5	123.7	125.6	124.9	125.6	123.9	124.2	124.4	125.1	126.2	123.8	124.5	125.8	122.9	123.5	124.2	123.8	122.6	123.5	122.9
CH2	2025	122.5	126.1	124.3	124.2	123.5	123.2	123.2	123.9	124.3	125.3	126.6	124.1	125.6	123.1	125.6	124.5	122.9	124.8	123.3	124.0
CH2	2026	124.9	123.3	125.0	126.1	123.6	123.9	124.8	124.6	124.8	122.9	125.1	124.3	126.3	124.8	124.5	124.0	124.3	124.4	123.6	124.3
CH2	2027	123.5	125.4	127.4	124.0	125.4	123.5	123.6	125.3	124.9	122.2	123.3	124.3	123.2	122.3	122.7	124.0	125.2	124.7	123.6	124.7
CH2	2028	125.1	125.4	123.4	124.5	124.1	123.6	124.1	124.3	123.4	122.7	125.4	123.7	122.6	122.1	122.5	124.7	124.2	123.4	123.8	124.2
CH2	2029	127.1	123.2	126.1	125.5	126.1	123.3	125.3	124.6	123.6	123.3	125.0	123.5	125.0	125.4	125.3	123.6	124.3	123.6	124.2	123.3
CH2	2030	122.2	123.6	124.8	124.9	122.9	123.3	125.8	123.3	126.2	124.4	124.1	124.8	123.7	124.4	124.9	125.0	124.8	125.1	123.3	124.7
CH2	2031	123.6	124.8	123.0	123.3	123.6	125.0	123.9	123.7	123.2	124.6	122.8	123.9	124.9	124.5	123.3	122.4	125.0	124.3	122.8	124.5
CH2	2032	125.5	124.2	123.7	124.9	127.1	123.2	123.3	124.7	123.4	123.6	123.5	122.8	124.4	124.9	124.7	123.6	125.7	125.3	125.3	123.4
CH2	2033	122.5	122.9	123.8	122.4	122.9	125.1	123.3	123.0	125.9	124.0	123.9	122.6	123.1	126.2	124.5	123.9	122.8	125.8	125.8	123.5
CH2	2034	123.8	126.0	123.4	124.7	124.6	122.2	124.8	124.4	125.8	124.6	125.3	123.1	124.8	126.5	122.9	124.4	126.0	124.8	124.7	125.9
CH2	2035	124.9	124.4	124.0	124.3	125.1	126.7	124.0	123.8	124.1	124.4	125.0	125.7	123.8	126.1	124.2	124.5	124.1	124.7	123.6	124.4
CH2	2036	127.8	124.0	122.6	125.2	123.3	125.6	125.4	123.2	122.5	123.0	122.8	123.4	126.8	124.8	124.8	125.2	124.9	125.1	123.5	122.9
CH2	2037	127.0	124.4	125.2	123.5	123.8	123.7	123.4	124.0	122.2	123.9	123.9	123.6	126.8	125.5	122.7	123.1	123.2	122.4	124.4	123.9
CH2	2038	124.6	125.5	125.2	123.3	125.8	124.3	123.3	124.8	125.4	124.7	125.0	122.6	125.0	123.6	124.7	125.4	126.7	124.6	123.2	124.0
CH2	2039	124.1	123.0	125.2	125.6	124.3	124.3	124.6	122.9	127.7	124.7	125.6	123.7	124.4	124.0	124.7	125.1	123.0	122.9	123.6	125.0
CH2	2040	126.3	123.7	123.8	125.7	124.8	124.9	124.2	124.0	124.6	124.0	124.0	124.4	126.6	125.2	124.4	125.4	124.2	125.3	124.5	125.3
CH2	2041	123.8	124.4	124.5	124.6	123.6	122.8	126.7	122.3	126.8	125.5	125.6	124.1	126.2	123.1	124.4	123.5	123.7	125.4	123.9	125.6
CH2	2042	124.5	124.3	123.8	123.6	125.8	125.0	124.9	124.4	124.6	126.1	122.9	123.9	125.0	125.8	124.5	124.9	126.6	123.3	123.7	123.6
CH2	2043	123.7	126.4	124.0	124.3	124.2	126.0	124.5	123.5	123.3	123.5	127.0	126.0	123.4	124.7	124.9	125.9	124.6	124.7	125.5	124.0
CH2	2044	125.0	123.2	122.8	123.7	123.8	123.9	124.5	123.8	124.1	126.2	123.3	123.1	124.5	125.9	124.2	124.0	126.1	124.6	124.1	125.2
CH2	2045	124.5	127.2	125.3	123.6	125.5	123.7	126.5	124.3	124.2	125.1	125.9	123.2	123.6	123.8	127.7	123.6	124.5	127.3	125.7	127.1
CH2	2046	124.6	124.8	124.0	126.2	125.9	122.9	126.7	125.4	125.1	124.9	123.4	123.6	123.9	124.1	124.4	126.2	124.8	124.4	125.6	124.0
CH2	2047	123.4	124.3	124.6	124.1	126.2	125.8	124.9	127.3	125.3	124.3	125.0	124.0	125.1	124.7	124.3	123.8	123.0	127.1	124.1	124.2
CH2	2048	126.5	123.8	125.7	125.4	124.2	123.9	124.5	123.5	127.3	124.0	126.7	123.5	124.3	125.7	122.7	124.8	124.3	123.8	124.8	124.0
CH2	2049	124.1	125.5	126.1	124.9	125.0	123.5	126.6	122.4	124.9	125.2	124.2	124.2	124.9	126.4	124.1	124.3	125.0	124.7	124.3	123.9
CH2	2050	123.3	124.9	128.1	124.3	124.1	124.2	122.5	126.2	123.5	126.0	123.6	123.2	124.6	128.0	122.3	126.1	127.6	124.4	123.6	122.7
CH1	2006	102.2	102.1	99.8	101.4	101.2	101.8	102.6	100.0	101.7	102.3	102.2	103.5	99.7	102.8	101.8	102.6	104.2	103.5	103.4	102.5
CH1	2007	99.5	103.7	99.5	101.8	103.6	103.3	101.8	103.3	104.1	104.1	103.7	103.6	102.8	100.0	101.6	103.6	103.6	102.9	103.3	102.6
CH1	2008	103.1	103.6	101.6	103.5	104.6	102.2	101.9	103.1	102.8	104.8	101.4	103.2	103.6	103.9	104.1	103.1	103.4	104.2	102.8	102.5
CH1	2009	100.4	99.7	100.6	101.4	103.0	101.6	103.3	102.0	103.3	101.4	102.4	104.2	102.4	103.4	103.6	101.8	102.0	103.4	103.1	102.4
CH1	2010	103.2	102.8	101.7	101.2	100.5	101.8	102.9	103.8	103.5	102.9	102.5	103.3	102.8	103.1	102.0	102.6	101.7	103.4	102.9	102.3
CH1	2011	103.7	101.4	102.9	101.0	102.9	102.9	103.4	102.0	104.4	103.2	102.7	103.3	103.0	104.1	103.1	104.2	103.9	103.7	102.9	102.1
CH1	2012	99.4	102.3	100.6	101.4	103.9	101.9	103.3	103.5	103.2	100.2	101.8	102.6	104.6	103.7	102.9	102.6	103.3	103.7	104.4	102.0
CH1	2013	103.5	101.3	103.1	102.7	102.6	102.5	103.3	102.6	101.2	99.8	103.1	102.2	102.4	101.8	102.3	102.1	100.9	102.6	101.5	102.8
CH1	2014	101.1	103.0	102.3	103.2	100.0	100.0	101.9	101.3	102.8	102.8	102.9	102.7	104.1	103.5	102.0	103.7	103.9	102.8	104.1	103.4
CH1	2015	104.3	102.6	99.4	101.0	99.0	104.0	102.6	101.8	101.1	101.0	102.3	103.8	103.0	101.5	102.7	104.9	103.4	105.1	102.8	101.4
CH1	2016	100.4	102.8	101.6	103.4	102.5	102.9	102.1	104.1	102.4	101.3	103.2	104.3	102.4	101.8	103.9	103.9	101.7	102.6	102.3	102.1
CH1	2017	100.7	101.8	101.8	102.5	100.7	101.1	104.1	103.5	103.0	103.9	101.9	102.3	102.2	102.8	101.2	102.9	99.7	102.6	103.1	103.8
CH1	2018	102.8	102.5	99.9	101.3	102.5	103.0	101.8	102.9	102.6	103.7	102.1	101.1	102.0	103.0	103.1	102.9	103.3	101.9	104.2	102.9
CH1	2019	103.0	103.1	104.0	101.3	100.2	103.4	102.1	102.9	104.3	102.0	104.1	102.6	101.2	103.0	103.2	101.4	104.1	102.0	104.1	103.0
CH1	2020	101.2	101.7	101.4	103.2	104.0	102.7	102.0	101.8	102.5	102.9	100.9	102.9	102.5	101.3	103.1	100.1	103.0	103.7	101.9	101.4

CH1	2021	102.2	103.7	99.4	101.4	103.5	103.8	102.6	101.9	103.5	102.8	104.6	101.3	101.4	102.7	100.9	102.3	103.3	102.7	103.4	101.4
CH1	2022	104.3	102.2	100.5	102.3	100.7	102.6	101.2	101.9	101.9	103.6	101.0	102.4	102.5	102.4	103.1	102.4	102.1	102.8	102.3	103.0
CH1	2023	102.7	101.8	101.9	102.1	101.4	101.3	102.1	101.6	102.5	102.1	101.2	101.1	101.9	103.5	101.6	104.0	99.8	103.4	103.0	104.4
CH1	2024	103.5	103.2	100.1	99.4	104.5	101.6	102.7	102.1	104.1	102.3	100.3	103.5	102.7	101.9	102.1	102.6	104.0	104.1	100.9	102.7
CH1	2025	101.0	103.6	100.5	100.7	102.1	100.4	101.7	101.4	102.8	102.1	103.1	103.2	102.3	101.4	102.9	102.8	102.6	99.1	102.8	103.0
CH1	2026	101.6	103.0	103.1	103.0	102.3	102.5	102.8	103.4	103.1	102.8	101.2	103.5	101.0	102.1	101.3	103.2	103.2	101.1	102.9	100.5
CH1	2027	101.9	102.6	101.8	102.7	103.8	102.7	102.4	104.1	102.7	102.5	100.4	102.9	102.7	101.5	103.1	102.9	103.3	101.8	104.0	102.6
CH1	2028	102.5	101.8	100.9	102.1	103.7	102.6	103.1	102.8	101.8	103.4	101.7	103.2	100.2	99.8	103.1	101.2	100.6	101.4	104.1	102.1
CH1	2029	101.6	100.8	102.9	102.8	100.9	100.8	102.9	103.3	103.1	104.1	102.8	102.1	100.3	102.3	104.1	103.5	101.7	102.1	101.6	102.5
CH1	2030	102.0	103.6	102.0	100.4	100.1	102.0	103.9	99.1	101.1	103.3	102.2	103.2	102.1	102.6	104.4	103.0	101.8	102.1	103.3	102.3
CH1	2031	102.2	101.8	103.3	100.8	103.8	101.2	103.3	103.0	101.9	102.7	104.5	103.0	102.5	101.5	103.8	103.4	101.5	101.4	100.9	101.1
CH1	2032	103.2	104.5	100.7	102.5	103.1	102.9	104.0	102.5	102.5	101.9	98.1	102.1	100.6	101.7	99.8	103.9	104.3	101.2	103.1	101.7
CH1	2033	102.4	103.4	104.3	101.3	101.0	103.0	103.5	105.1	101.9	102.4	102.6	102.8	100.1	102.7	102.9	102.9	101.6	103.1	103.1	102.9
CH1	2034	100.3	99.1	100.4	101.1	104.5	100.6	103.2	102.1	103.0	103.4	100.1	103.2	102.1	102.5	100.0	102.7	102.2	101.9	103.8	103.6
CH1	2035	101.6	101.1	99.8	103.7	102.7	102.8	103.2	100.6	103.0	101.7	100.6	103.2	101.1	102.0	100.7	103.2	103.2	102.6	102.8	100.8
CH1	2036	102.8	99.0	97.6	102.7	101.7	101.7	101.9	104.3	99.0	103.5	102.2	103.3	103.9	100.7	101.9	102.3	102.7	102.6	102.7	100.7
CH1	2037	103.1	102.9	101.7	101.2	100.3	100.2	102.5	103.1	102.1	102.7	102.1	102.7	101.1	102.6	103.2	102.8	100.0	100.1	100.2	102.3
CH1	2038	101.3	103.1	101.3	102.0	102.8	102.3	101.0	102.9	103.0	100.8	101.5	102.8	102.3	100.4	101.4	100.6	102.4	103.5	101.1	101.0
CH1	2039	101.2	104.3	101.9	102.9	103.1	102.4	103.0	102.8	105.0	100.2	101.2	102.2	102.5	102.9	102.4	102.9	99.4	101.8	103.1	102.7
CH1	2040	102.7	102.3	101.7	102.7	100.7	102.4	102.5	103.4	100.8	102.8	101.2	103.5	101.5	101.7	100.6	102.1	100.6	102.1	104.6	103.1
CH1	2041	101.3	101.7	102.3	100.1	103.5	102.4	102.7	103.5	101.8	99.9	103.0	103.0	102.0	100.9	102.2	102.5	101.3	100.3	103.0	103.3
CH1	2042	101.5	100.3	99.3	101.1	100.9	102.9	101.8	102.8	102.7	102.3	103.6	102.5	103.7	99.7	102.3	102.3	101.8	100.6	102.4	102.5
CH1	2043	102.9	100.6	98.8	102.1	102.6	103.9	100.3	101.1	101.9	99.5	101.8	103.3	101.0	102.0	101.8	101.9	101.4	102.4	103.8	102.9
CH1	2044	101.8	101.8	103.0	102.6	100.7	103.1	103.4	101.5	99.9	103.1	103.6	101.8	101.6	102.8	102.6	101.5	101.9	102.1	103.6	102.8
CH1	2045	100.6	102.6	103.5	100.9	101.6	101.7	100.2	100.6	101.0	102.0	103.8	102.2	101.2	101.8	100.7	101.7	101.9	102.2	104.2	101.5
CH1	2046	101.5	100.2	102.0	101.0	101.5	101.3	100.9	101.5	101.3	103.0	101.4	102.9	100.2	101.6	101.5	102.9	100.6	102.7	102.8	103.2
CH1	2047	100.2	101.7	100.9	99.6	102.2	101.4	99.5	104.0	101.3	101.7	101.9	101.8	101.0	101.2	102.6	100.1	101.2	101.6	101.3	103.0
CH1	2048	102.7	101.9	101.1	101.1	98.6	103.2	100.6	101.8	101.4	102.3	102.3	101.9	101.9	103.5	101.5	101.8	102.7	102.0	103.0	102.5
CH1	2049	99.5	102.9	102.0	101.6	102.6	102.0	103.8	100.2	101.6	103.6	101.4	102.6	100.5	101.7	100.5	101.8	99.2	101.5	102.9	102.3
CH1	2050	103.9	102.5	101.6	100.4	100.5	103.1	102.0	102.3	102.0	102.5	102.2	101.4	100.5	101.9	101.3	102.4	101.9	102.3	103.6	102.3
CN2	2006	88.6	89.0	86.3	87.6	88.8	87.0	88.8	87.5	89.3	88.6	89.6	90.5	85.9	90.2	89.4	90.2	92.2	91.1	90.3	89.6
CN2	2007	86.8	91.1	86.4	88.3	89.9	91.3	89.5	90.1	92.0	91.2	89.9	90.0	89.6	85.8	88.8	91.0	90.0	90.3	90.3	89.5
CN2	2008	90.4	91.0	87.9	90.8	92.7	89.7	89.4	91.0	89.7	92.6	89.0	90.9	91.6	91.8	91.9	90.1	90.8	91.5	90.5	89.1
CN2	2009	88.6	87.2	86.7	88.9	89.8	88.6	90.3	89.8	89.9	88.4	88.9	90.3	88.7	91.3	91.2	88.2	89.7	90.2	91.0	89.8
CN2	2010	90.5	90.1	87.7	87.3	87.2	87.7	90.8	90.4	91.8	89.9	88.8	90.9	89.1	90.1	89.5	89.5	88.8	90.7	91.1	88.8
CN2	2011	90.9	88.5	89.0	86.7	89.9	88.7	89.8	89.6	92.4	89.9	88.9	90.4	90.5	90.8	90.2	92.0	91.4	90.3	90.1	87.8
CN2	2012	84.9	88.4	87.8	88.4	91.1	88.3	90.3	90.1	89.3	87.3	88.6	90.4	91.9	90.5	90.4	88.7	91.6	90.3	92.2	89.5
CN2	2013	91.7	88.0	89.0	90.3	89.4	89.4	89.7	88.8	88.2	84.6	90.8	89.4	89.4	89.4	89.5	89.2	88.2	89.1	89.0	90.7
CN2	2014	87.6	90.2	89.4	89.7	86.1	86.4	88.8	87.6	90.1	89.1	89.1	90.1	91.0	89.3	89.0	90.9	91.7	90.3	90.9	90.7
CN2	2015	90.4	90.2	86.6	87.0	86.3	91.3	90.3	88.4	88.7	85.2	89.3	91.4	90.0	88.9	89.9	93.7	91.0	92.7	90.7	88.5
CN2	2016	87.2	89.6	87.1	90.2	89.1	91.2	88.0	92.1	89.7	88.8	89.7	91.0	89.4	87.9	92.2	92.4	89.3	89.7	88.2	88.5
CN2	2017	86.8	88.8	88.0	88.9	86.6	87.6	91.5	90.4	90.4	91.2	88.1	89.7	88.0	89.8	88.6	89.8	86.1	89.2	89.0	91.6
CN2	2018	88.0	89.1	87.3	87.7	89.8	90.3	88.8	90.9	90.6	90.5	88.6	88.8	88.2	90.1	90.8	89.9	90.0	89.0	92.1	89.9
CN2	2019	89.6	89.9	91.9	87.9	87.4	91.5	89.0	90.8	91.9	89.3	90.1	90.4	87.9	90.2	90.4	88.4	92.0	88.2	90.1	90.6
CN2	2020	87.2	88.2	87.7	89.8	92.2	88.8	88.6	89.3	88.3	90.3	87.8	90.3	89.4	89.0	91.1	86.8	89.3	91.6	89.3	87.0
CN2	2021	89.8	90.6	86.1	87.7	90.6	91.9	89.8	87.8	91.0	89.7	92.3	88.8	88.6	89.6	88.5	90.2	90.4	89.3	91.4	88.0
CN2	2022	91.9	87.1	87.1	88.6	88.3	89.8	88.6	89.1	88.8	90.7	86.3	90.0	89.9	89.3	90.3	90.2	89.2	89.5	90.3	89.5
CN2	2023	88.6	88.9	87.4	88.4	89.2	87.9	89.0	89.9	89.4	87.4	87.2	88.8	88.4	90.0	88.9	91.1	86.0	90.1	90.3	91.8
CN2	2024	91.0	90.0	85.6	85.9	92.6	88.3	89.2	89.5	91.5	89.1	85.8	90.3	89.1	89.8	88.7	89.9	92.3	91.2	87.4	89.4
CN2	2025	87.9	90.3	86.7	87.8	88.2	86.2	89.8	87.8	89.5	88.6	90.0	89.6	89.6	87.3	90.4	90.3	90.4	85.4	89.7	90.0

CN2	2026	87.3	89.9	88.5	89.4	89.4	88.0	90.3	91.0	90.5	89.6	87.1	91.3	88.6	88.5	87.4	91.1	90.1	87.4	89.9	86.9
CN2	2027	87.8	89.5	86.9	88.5	92.5	88.7	89.6	90.9	88.8	89.6	87.6	89.3	89.7	88.7	90.5	91.1	90.5	87.7	91.0	89.5
CN2	2028	89.4	87.6	88.1	89.0	91.0	89.3	89.5	89.6	88.1	90.1	89.1	90.5	88.0	85.7	90.7	88.1	85.6	88.1	91.4	88.6
CN2	2029	87.8	86.7	88.8	88.6	88.3	87.1	90.0	89.4	90.8	91.3	89.8	89.5	87.5	87.7	90.9	90.0	89.2	88.3	88.5	90.2
CN2	2030	88.7	90.9	88.2	86.6	88.6	89.5	90.9	87.0	87.4	89.4	89.3	91.0	88.6	89.0	92.4	90.2	87.5	88.6	90.8	89.9
CN2	2031	89.1	88.4	89.6	87.0	91.5	88.6	90.1	90.5	88.9	89.1	91.3	89.8	89.6	87.3	91.5	90.5	88.0	88.2	87.2	87.4
CN2	2032	90.2	92.1	87.0	88.8	89.3	89.9	91.6	90.5	88.5	88.6	85.7	89.2	86.5	88.1	86.4	90.4	91.7	87.5	89.6	87.9
CN2	2033	89.5	89.7	91.9	88.2	88.3	89.4	90.9	94.1	88.5	89.1	88.7	89.7	86.3	89.1	90.7	89.1	87.5	89.4	90.4	89.7
CN2	2034	86.6	86.3	84.5	88.5	92.0	88.3	89.9	88.5	89.8	89.5	86.7	90.6	89.6	89.0	86.4	88.7	87.9	88.0	91.2	91.2
CN2	2035	87.1	87.4	85.4	90.5	89.7	89.5	89.6	87.7	90.2	88.2	87.7	90.1	87.8	88.1	89.2	90.1	90.0	89.0	89.7	87.3
CN2	2036	89.7	85.9	84.4	89.2	89.0	87.6	88.6	91.8	86.0	89.6	88.0	90.0	91.3	86.8	88.5	89.7	89.0	90.1	89.8	87.0
CN2	2037	89.7	90.2	88.8	86.4	87.0	86.6	88.3	90.0	89.2	89.3	88.0	89.5	87.6	90.0	90.6	89.6	87.4	86.5	87.7	88.8
CN2	2038	88.6	89.6	86.8	89.0	89.7	88.7	88.5	89.3	89.6	87.8	87.2	90.6	89.3	85.9	88.0	87.5	88.8	90.8	89.2	88.5
CN2	2039	86.8	92.1	87.9	88.3	89.5	88.3	89.0	89.8	93.4	87.3	87.1	89.1	89.8	90.1	89.3	89.3	84.7	88.4	89.6	89.7
CN2	2040	89.5	89.2	87.1	89.4	88.2	89.9	89.1	90.4	86.6	88.4	88.1	90.2	89.0	88.6	87.6	89.4	87.3	88.2	91.6	89.0
CN2	2041	88.5	87.9	89.4	86.3	90.5	87.8	88.8	90.9	88.3	85.7	88.6	89.4	89.0	87.5	88.7	90.2	88.3	86.3	90.3	90.0
CN2	2042	88.2	86.9	85.2	86.5	87.8	89.5	87.8	88.5	89.4	88.6	91.2	89.4	91.4	86.7	89.4	88.4	88.5	86.2	89.8	89.7
CN2	2043	89.5	87.6	85.9	88.7	88.7	92.1	86.8	87.4	88.4	85.8	88.3	90.4	87.9	87.9	88.8	89.0	88.3	88.1	89.2	89.9
CN2	2044	88.1	88.6	89.3	88.7	87.6	89.9	89.9	87.4	86.4	89.6	90.0	89.5	86.9	89.4	89.6	87.8	88.6	89.1	90.6	90.5
CN2	2045	87.2	89.9	90.1	87.0	88.3	88.1	87.3	86.8	88.1	86.8	89.8	88.3	88.3	87.8	87.9	89.2	88.5	89.7	91.0	87.3
CN2	2046	88.5	86.9	88.0	87.1	88.5	88.1	87.1	87.0	88.6	89.9	87.1	90.0	87.6	87.0	89.1	89.3	87.0	89.5	90.5	89.2
CN2	2047	86.9	87.8	86.7	85.9	88.7	87.1	86.4	91.9	88.7	87.2	87.5	88.9	87.5	86.4	89.5	88.1	87.2	87.4	88.3	90.2
CN2	2048	88.4	88.8	85.4	87.0	87.4	90.3	87.6	87.1	88.4	88.4	87.3	88.6	88.2	89.7	88.5	88.6	89.6	89.4	90.2	90.1
CN2	2049	85.5	88.8	88.1	86.1	88.8	87.4	91.0	87.4	87.3	88.9	88.3	89.5	86.4	87.5	88.0	89.1	85.7	87.6	90.2	89.1
CN2	2050	90.9	88.6	86.5	87.1	87.2	90.8	88.7	89.6	88.4	88.8	87.3	88.7	86.0	88.4	87.6	89.2	89.0	89.8	90.4	89.4

8.8 **Appendix 8.8** Model selections table for the analyses of the effects of climate on hydaspe fritillary butterfly egg laying rate. Climate variables include average maximum daily temperature while females were in the oviposition containers and snow melt date at each site/year. Other measures of temperature (daily mean and minimum) were correlated with maximum temperature and performed similarly. Neither climate variable was significant in a model that included site.

Model	AICc	Delta AICc	Weight
Site	805.6072	0	0.319534
Site + max temp.	805.6667	0.0595	0.310168
Site + max temp. + melt date	806.13	0.5228	0.246033
Site + melt date	807.7765	2.1693	0.108009
Intercept	811.5641	5.9569	0.016255

8.9 **Appendix 8.9** Model selection table for the analyses of the effects of climate on hydaspe fritillary butterfly egg predation rate over the entire course of the predation trials. All models included female as random effect. While all models performed similarly, maximum temperature was never significant in any model (P>0.3).

Model	DIC	Delta DIC	Weight
Site	555.0612	0	0.29820315
Site + max temperature	555.2816	0.22047	0.267078235
intercept	555.5097	0.448533	0.238294737
Max temperature	555.8962	0.835000	0.196423878

8.10 **Appendix 8.10** Model selection table for analyses of the effects of climate variables and site differences on hydaspe fritillary overwinter larval survival. The climate variables tested include: average daily minimum, maximum, and mean temperature recorded in larval cups between larvae being placed in the duff and first snow fall, the coldest winter temperature recorded in the cups, and snow melt date in the spring. All climate measures were correlated ($|r|>0.5$) and each site included only a single value for each climate measure, so we only included one variable at a time in the models. While many of the temperature measures performed similarly or even very slightly better than the intercept only model, the p-values for temperature were always greater than 0.1.

Model	DIC	Delta DIC	Weight
Mean temp. prior to snow	574.8113	0	0.179035401
Min temp. prior to snow	574.8827	0.071367	0.17275946
Min temp. experienced	574.8877	0.076433	0.172322357
Intercept (female and cup as random)	575.4067	0.5954	0.132938093
Snow melt date	575.4116	0.600333	0.132610583
Max temp. prior to snow	575.5754	0.7641	0.122184666
Site	576.2284	1.4171	0.08814944

8.11 Appendix 8.11 Model selection table for analyses of the effects of climate variables and site differences on hydaspe fritillary adult survival. The climate variables tested include: average daily minimum, maximum, and mean temperature recorded between sample occasions, and total annual (water year) precipitation.

Model	AIC	Δ AIC	Weight
Minimum temp. + precipitation	5353.62	0.00	0.806
Site + mean temp. + precipitation	5358.80	5.18	0.060
Minimum temp.	5358.90	5.29	0.057
Site + precipitation	5359.99	6.37	0.033
Site + maximum temp.	5360.57	6.95	0.025
Site	5362.65	9.03	0.009
Site + minimum temp.	5363.48	9.87	0.006
Precipitation	5364.51	10.89	0.003
Intercept	5375.91	22.29	0.000

8.12 Appendix 8.12 Table showing model results from tadpole survival analysis in the canopy cover experiment.

Model	N(k)	AICc	ΔAICc	weight	Deviance
S(site * treatment)	30	3869.73	0.000	9.81E-01	694.715
S(site + treatment)	26	3877.84	9.105	1.03E-02	712.005
S(site + treatment * temp)	28	3878.96	10.226	5.90E-03	709.037
S(site)	25	3882.22	13.485	1.15E-03	718.427
S(temp)	22	3883.97	15.239	4.81E-04	726.297
S(site + temp)	26	3884.14	15.407	4.42E-04	718.307
S(treatment + temp)	23	3885.09	16.358	2.75E-04	725.379
S(treatment + temp + temp^2)	24	3886.27	17.535	1.52E-04	724.517
S(treatment * temp)	24	3887.11	18.379	1.00E-04	725.361
S(.)	21	3888.33	19.601	5.43E-05	732.695
S(treatment)	22	3889.69	20.961	2.75E-05	732.019

Appendix 8.13 Non-climate drivers of demographic rates. For fixed effect categorical variables, we indicate the coefficient for each categorical variable (note that the missing categorical variable's coefficient is estimated at zero), and for fixed effect numeric variables, we indicate the magnitude of the coefficient. For random effects, we show the standard deviation of the random effect. All numeric predictor variables are scaled, such that the magnitudes of the coefficients are comparable.

Survival rates	Fixed effects						Random effects
	Intercept	Sex	Status	No. helpers	Age	Age^2	Site
post-fledging survival	-0.5140	0.5347 (male)					0.1282
adult survival	0.983	0.5389 (male)	-0.7080 (floater), -0.2696 (helper)	0.0403	0.3351	-0.4145	0.1583

Reproductive rates	Fixed effects						Random effects
	Intercept	No. helpers	Maternal age	Maternal age^2	Paternal age	Paternal age^2	Site
probability of initiating a first nest	1.569	0.2636	2.4662	-1.6603	1.442	-1.2382	0.2276
clutch size of first nest	1.1554623		0.188215	-0.1206764			0.0003352
total clutch size of second and later nests	1.236297						0.0003706
fraction of eggs surviving to fledge from first nest	0.42465	0.21728		-0.03182	0.35093	-0.30796	0.1282
fraction of eggs surviving to fledge from second and later nests	0.1505	0.1632					0
probability of initiating second and later nests given failure of first nest	-0.9981		1.8325	-1.4913	0.7651	-0.574	0
probability of double brooding	-7.2369		0.6983		5.0427	-5.0709	0
probability of first nest success	0.9799	0.3129	0.6699	-0.4947	0.6261	-0.6241	0.2989
probability of second and later nest success	0.8971	0.4		-0.1859	-0.7794	1.0023	0.06136

8.14 Appendix 8.14 List of publications and conference abstracts.

Publications:

Gordon, L. L. 2020. Effects of multiple stressors: hydroperiod, introduced bullfrogs, and food limitation on northern red-legged frogs (*Rana aurora*). (Master's Thesis, Humboldt State University, Arcata, California).

Hudgens, B. and Harbert, M. 2019. Amphipod predation on northern red-legged frogs, *Rana aurora*, embryos. Northwestern Naturalist 100:126-131.

Kiekebusch, E. 2020. Effects of temperature, phenology, and geography on butterfly population dynamics under climate change. North Carolina State University

Louthan, A. M., Pringle, R. M., Goheen, J. R., Palmer, T. M., Morris, W. F., and Doak, D. F. 2018. Aridity weakens population-level effects of multiple species interactions on *Hibiscus meyeri*. Proceedings of the National Academy of Sciences USA 115: 543-548. DOI: 10.1073/pnas.1708436115

McHarry, K. 2017. Influence of canopy cover and climate on early life-stage vital rates for Northern red-legged frogs (*Rana aurora*), and implications for population growth rates. Masters Thesis Humboldt State University.

McHarry, K. W., Abbott, J. A., van Hattem, M. G., and Hudgens, B. 2018. Efficacy of visible implant elastomer tags with photographic assist for identifying individuals in capture-mark-recapture studies using larval frogs. Herpetological Conservation and Biology 13: 576–585.

Morris, W. F., Ehrlén, J., Dahlgren, J. P., Loomis, A.K., and Louthan, A. M. 2019. Biotic and anthropogenic forces rival climatic/abiotic factors in determining global plant population growth and fitness. Proceedings of the National Academy of Sciences USA, www.pnas.org/cgi/doi/10.1073/pnas.1918363117

Schultz, C. B., Haddad, N. M., Henry, E. H., and Crone, E. E. 2019. Movement and demography of at-risk butterflies: building blocks for conservation. Annual Review of Entomology 64:167-184

Conference abstracts:

Abbott, J.M., B. Hudgens, M. Harbert, K. McHarry, and L. Gordon. Climate influences the phenology, abundance, and demographic rates of hydaspe fritillary butterflies. Ecological Society of America, Louisville, KY, August 2019.

Abbott, J.M., B. Hudgens, and K. McHarry. Effects of temperature on Northern red-legged frog tadpole survival. Society for Northwestern Vertebrate Biology, Blue Lake, CA, March 2017.

Gordon, L. L., Hudgens, B. H., Abbott, J. M., McHarry, K., and M. Harbert. Effects of temperature and hydroperiod on northern red-legged frogs at Humboldt Bay National Wildlife Refuge. The Wildlife Society Western Section, Yosemite, February 2019.

Gordon, L. L., Hudgens, B. H., Abbott, J. M., McHarry, K., and M. Harbert. Effects of climate change and biological invasions on northern red-legged frogs. International Congress for Conservation Biology, Kuala Lumpur, Malaysia, July 2019.

Harbert, M., and Hudgens, B. Amphipod Predation on Northern Red-Legged Frog, Rana Aurora, Embryos. The Wildlife Society Western Section, Yosemite, February 2019

Hudgens, B.H., J.M. Abbott, E. Kiekebusch, & K. McHarry. Detecting climate effects on survival in space-for-time studies. The Strategic Environmental Research and

Development Program and Environmental Security Technology Certification Program Symposium, Washington, D.C., November 2017

Hudgens, B., J. Abbott, E. Kiekebusch and K. McHarry. 2017. Detecting climate effects on survival in space-for-time studies. SERDP-ESTCP Symposium, Washington, D.C. November 2017.

Hudgens, B., J. Abbott, E. Kiekebusch, A. Louthan, W. Morris, N. Haddad, J. Walters, L. Stenzel. 2018 Predicting Species Stewardship Priorities in a Changing World I. SERDP-ESTCP Symposium, Washington, D.C. November 2018.

Hudgens, B., A. Louthan, J. Abbott, E. Kiekebusch, W. Morris, N. Haddad, J. Walters, L. Stenzel Predicting Species Stewardship Priorities in a Changing World II. SERDP-ESTCP Symposium, Washington, D.C. December 2019.

Louthan A.. "Species interactions exert stronger effects on plant populations in abiotically stressful areas." Department of Botany, University of Hawai'i-Manoa,

Louthan A. 2019. "Effects of climate and fire return interval on Venus flytrap (Dionaea muscipula)." North Carolina Rare Plant Discussion Meeting, North Carolina Zoological Park. March 6, 2019.

Kiekebusch, E., Louthan, A., Morris, W., Hudgens, B. and N. Haddad. 2019. Measuring population responses to temperature across the annual lifecycle of a butterfly. 2019. Oral Presentation. International Congress for Conservation Biology, Kuala Lumpur, Malaysia

Kiekebusch, E., Louthan, A., Morris, W., Hudgens, B. and N. Haddad. 2018. Measuring demographic rates and phenology at cryptic life stages of a locally rare wetland butterfly. Poster. Ecological Society of America, New Orleans LA

Kiekebusch, E., Hudgens, B. and N. Haddad. 2017. Population dynamics of Appalachian Brown butterflies under increased temperatures. Poster. Ecological Society of America, Portland, OR

Hickey, C., Reiter, M., Stenzel, L., and Hudgens, B. Average and extreme climate conditions both affect annual survival in Western Snowy Plovers. Western Hemisphere Shorebird Group Meeting, Panama City, Panama, October 2019.

Stenzel, L., Page, G., and Hudgens, B. Average and extreme climate conditions both affect annual survival in Western Snowy Plovers. Range-wide Snowy Plover Meeting, Moss Landing, CA, January 2020.